

# **Regulation of microglial cell function by corticosteroids and disruption by organotins**

## **Inauguraldissertation**

zur

Erlangung der Würde eines Doktors der Philosophie

vorgelegt der

Philosophisch-Naturwissenschaftlichen Fakultät

der Universität Basel

von

Boonrat Chantong

aus Bangkok, Thailand



Basel, 2014

**Genehmigt von der Philosophisch-Naturwissenschaftlichen Fakultät  
auf Antrag von**

**Prof. Dr. Alex Odermatt**

A handwritten signature in black ink, appearing to read 'A. Odermatt', written in a cursive style.

**PD. Dr. F. Tschudi-Monnet**

**Basel, den 17.09.2013**

**Prof. Dr. Jörg Schibler**

**Dekan**

# TABLE OF CONTENT

<b>Content</b>	<b>Page</b>
<b>1. ACKNOWLEDGEMENTS</b>	1
<b>2. LIST OF ABBREVIATIONS</b>	2-3
<b>3. LIST OF FIGURES</b>	4
<b>4. SUMMARY</b>	5-7
<b>5. CHAPER 1</b>	
Introduction	8-18
Hypotheses and Aims	19
List of papers	20
<b>6. CHAPER 2</b>	21-35
Mineralocorticoid and glucocorticoid receptors differentially regulate NF-kappaB activity and pro-inflammatory cytokine production in murine BV-2 microglial cells	
<b>7. CHAPER 3</b>	36-47
Virtual screening as a strategy for the identification of xenobiotics disrupting corticosteroid action	
<b>8. CHAPER 4</b>	48-89
Dibutyltin promotes oxidative stress and increases inflammatory mediators in BV-2 microglia cells	
<b>9. CHAPER 5</b>	90-137
Metabotropic glutamate receptor 5 modulates ER stress through pertussis toxin-sensitive G proteins	

<b>Content</b>	<b>Page</b>
<b>10. CHAPER 6</b>	138-179
Corticosterone potentiates trimethyltin induced inflammatory responses mediated by mineralocorticoid receptor in BV-2 cells	
<b>11. CHAPER 7</b>	180-186
Conclusion and outlook	
<b>12. REFERENCES</b>	187-192
<b>13. CURRICULUM VITAE</b>	193-194

## ACKNOWLEDGEMENTS

This work was supported by the Swiss National Science Foundation and Swiss Center for Applied Human Toxicology. The Royal Thai Government Scholarship is responsible for my educational expense at University of Basel during PhD program.

I would like to thank my principal supervisor, Professor Alex Odermatt, who has made my studies in this PhD program possible. I am exceedingly grateful to his continual inspiration and guidance since the beginning of this research project. Who shared his knowledge and encouraged my independence to pursue my own research and scientific communications.

I am sincerely grateful to all of my colleges, I have learned so much from their expertise and refinement in areas of laboratory techniques, experimental design, and data interpretation.

Finally, I am sincerely appreciative of all the opportunities which I have been given throughout my life in PhD study.

## LIST OF ABBREVIATIONS

[Ca <sup>2+</sup> ] <sub>i</sub>	Free intracellular Ca <sup>2+</sup>
11β-HSD1	11β-hydroxysteroid dehydrogenase type 1
11β-HSDs	11β-hydroxysteroid dehydrogenases
4-PBA	4-phenyl butyric acid
AD	Alzheimer's disease
AICAR	5-amino-1-β-D-ribofuranosyl-imidazole-4-carboxamide
Akt	Protein kinase B
AMPK	AMP-dependent protein kinase
ATF6	Activating transcription factor 6
CHOP	C/EBP homologous protein
CHPG	(RS)-2-chloro-5-hydroxyphenylglycine
DBT	Dibutyltin
ER	Endoplasmic reticulum
ERK1/2	Extracellular signal-regulated protein kinase1/2
GITR	Glucocorticoid-induced TNFR family related gene
GPCR	G protein-coupled receptor
GR	Glucocorticoid receptors
GRP78	Glucose-regulated protein 78
GRP96	Glucose-regulated protein 96
HPA	Hypothalamic–pituitary-adrenal
IL-1β	Interleukin-1β
IL-6	Interleukin-6
iNOS	Inducible nitric oxide synthase
IP <sub>3</sub> R	1,4,5-trisphosphate receptor
IRE1	Inositol-requiring enzyme-1
JAK	Janus kinase
JNK	c-Jun NH(2)-terminal kinase
LPS	Lipopolysaccharide
MAPKs	Mitogen-activated protein kinases

MBT	Monobutyltin
mGluR5	Metabotropic glutamate receptor 5
mGluRs	Metabotropic glutamate receptors
MPEP	2-methyl-6-(phenylethynyl)-pyridine
MPTP	1-methyl-4-phenyl-1,2,3,6-tetrahydropyridine
MR	Mineralocorticoid receptors
NADPH oxidase	NOX
NF- $\kappa$ B	Nuclear factor kappa B
NO	Nitric oxide
NOX-2	NADPH oxidase-2
p38 MAPK	p38 mitogen-activated protein kinase
PD	Parkinson's disease
PERK	PKR-like ER kinase
PI3K	Phosphatidylinositol 3-kinase
PKC	protein kinase C
PLC	Phospholipase C
PTX	Pertussis toxin
PVC	Polyvinyl chloride
ROS	Reactive oxygen species
RyR	Ryanodine receptor
Sn	Tin
TBT	Tributyltin
TMT	Trimethyltin
TNFR2	Tumor necrosis receptor 2
TNF- $\alpha$	Tumor necrosis factor- $\alpha$
UPR	Unfolded protein response

## LIST OF FIGURES

	<b>Content</b>	<b>Page</b>
<b>Figure 1.</b>	Structures of organotins	<b>18</b>
<b>Figure 2.</b>	Model for the role of MR and GR in regulating neuroinflammation in BV-2 cells.	<b>183</b>
<b>Figure 3.</b>	Proposed model of signaling pathway of mGluR5 regulation in BV-2 cells	<b>184</b>
<b>Figure 4.</b>	Model of the inflammatory mechanism of dibutyltin (DBT) in BV-2 cells	<b>185</b>
<b>Figure 5.</b>	Model of the inflammatory mechanism of trimethyltin (TMT) in BV-2 cells	<b>186</b>

## SUMMARY

Microglia cells are the resident brain macrophages regulating in the initiation and maintenance of neuroinflammation. Chronic or exacerbated activation of microglia can contribute to neurodegenerative diseases. In the present thesis, mechanism of endogenous corticosteroids and xenobiotics on microglia function were investigated using the mouse BV-2 microglia cell line.

Corticosteroids are potent modulators of inflammation and mediate their effects by binding to mineralocorticoid receptors (MR) and glucocorticoid receptors (GR). MR and GR are suggested to regulate microglia activation and suppression, respectively. We showed that GR and MR differentially regulate on nuclear factor kappaB (NF- $\kappa$ B) activation and neuroinflammatory parameters, including interleukin-6 (IL-6) and tumor necrosis factor- $\alpha$  (TNF- $\alpha$ ). 11 $\beta$ -hydroxysteroid dehydrogenase type 1 (11 $\beta$ -HSD1), converting inactive 11-dehydrocorticosterone to active corticosterone, is involved in the action of GR and MR. Both 11-dehydrocorticosterone and corticosterone showed biphasic effects with low/moderate concentrations potentiating IL-6 and TNF- $\alpha$  expression and NF- $\kappa$ B activation through MR. At high concentrations, corticosteroids suppressed these mediators through GR. We also showed that the silane AB110873, identified by a MR pharmacophore, stimulates mitochondrial reactive oxygen species (ROS) generation and the production of the IL-6 by activating MR.

Metabotropic glutamate receptor 5 (mGluR5) has been documented to modulate microglia function. Microglial activation induced by (RS)-2-chloro-5-hydroxyphenylglycine (CHPG), a mGluR5 agonist, has been shown to decrease microglia activation and release of associated pro-inflammatory factors. Additionally, oxidative stress and inflammatory response of microglia cells are associated with AMP-dependent protein kinase (AMPK) and calcium-mediated signaling. Here, we investigated the relationship between oxidative stress and inflammation and AMPK and calcium-mediated pathways in the antagonism of mGluR5 with 2-methyl-6-(phenylethynyl)-pyridine (MPEP). MPEP significantly increased oxidative stress parameters and inflammatory mediators in a concentration-dependent manner. MPEP reduced ATP production and changed the phosphorylation state of AMPK. MPEP increased the elevation of free intracellular Ca<sup>2+</sup> ([Ca<sup>2+</sup>]<sub>i</sub>) from endoplasmic reticulum (ER) through IP<sub>3</sub> receptor. ER stress markers were induced by MPEP and blocked by a chemical chaperone (4-phenyl butyric acid, 4-PBA) and a calcium chelator (BAPTA-AM). AMPK activation abolished and inhibition potentiated ER

stress induced by MPEP. The effect of MPEP on phospholipase C (PLC)-associated pathways was also investigated. A PLC inhibitor (U73122), and a Gi protein inhibitor (pertussis toxin, PTX) blocked MPEP-induced increase of  $[Ca^{2+}]_i$ . MPEP also significantly increased PLC activity. Furthermore, AICAR, BAPTA-AM, U73122, and PTX prevented oxidative stress and inflammatory response induced by MPEP.

Excessive and chronic exposure to organotin compounds has been associated with neurotoxicity and neuroinflammation. Dibutyltin (DBT) is an organotin widely used as a stabilizer in polyvinyl chloride plastics. In the present study, we found that DBT promotes mitochondrial oxidative stress and induces ATP depletion, leading to AMPK activation in a time-dependent manner. DBT induced concentration-dependent increases in IL-6, NADPH oxidase-2 (NOX-2), TNF- $\alpha$  expression. NOX-2 inhibitor, apocynin inhibited the action of DBT, not only on IL-6 up-regulation but also an intracellular ROS production. DBT induced the nuclear translocation of NF- $\kappa$ B and NF- $\kappa$ B inhibitor Cay10512 blocked IL-6 expression induced by DBT. Furthermore, we showed a role for phosphatidylinositol 3-kinase (PI3K)/ protein kinase B (Akt), extracellular signal-regulated protein kinase1/2 (ERK1/2), p38 mitogen-activated protein kinase (p38 MAPK), c-Jun NH(2)-terminal kinase (JNK), protein kinase C (PKC), PLC, and  $[Ca^{2+}]_i$  in the DBT-mediated toxicity.

Trimethyltin (TMT) is an organotin with potent neurotoxic effects, characterized by neuronal destruction and neuroinflammation, which involves microglia activation as a consequence of neuronal damaged. In the present study, we found that TMT induces the expression of IL-6 and inducible nitric oxide synthase (iNOS). Cay10512 blocked TMT-induced translocation of NF- $\kappa$ B into nucleus. PD98059 and SB20190, inhibitors of ERK1/2 and p38 MAPK, respectively, inhibited the ability of TMT to induce IL-6 and iNOS expression. The proinflammatory action of TMT was substantially enhanced by low/moderate corticosterone and 11-dehydrocorticosterone but suppressed by dexamethasone. Spironolactone suppressed the effects of TMT and the potentiation by corticosterone on proinflammatory mediator expression. Similarly, the potentiation of corticosterone was inhibited by PD98059 and SB20190.

In conclusion, a tightly coordinated activity of GR and MR regulates the NF- $\kappa$ B pathway and the control of inflammatory mediators in microglia cells. The balance of GR and MR activity is locally modulated by the action of 11 $\beta$ -HSD1, which is upregulated by pro-inflammatory mediators. This study

highlights the role of mGluR5 antagonism in mediating oxidative stress, ER stress and inflammation in microglial cells. The calcium dependent pathways are mediated through Gi protein-coupled receptors, PLC, and PI<sub>3</sub> receptors. AMPK also may play a role in the regulation of mGluR5 by disturbing the energy balance. TMT and corticosterone influence the same signaling pathways to exert inflammatory responses. TMT also directly disturbed the local corticosteroid balance.

# CHAPTER 1

## Introduction

Microglia are CNS resident macrophage-like cells that have been implicated as possible contributors to neuroinflammation in the brain. These cells become readily activated in response to a wide variety of stimuli, such as injuries, axotomy, and inflammation (1). Microglia play an important role in both innate and adaptive immune responses in the brain (2). The number of microglia cells represents the increasing response to CNS insults such as restraint induced chronic stress in mice (3). The activated microglia work to restore homeostasis and are characterized by proliferation and morphological change from the ramified resting state to the motile amoeboid morphology that is accompanied by an increase in production of pro-inflammatory cytokines (4). The rapid up-regulation of pro-inflammatory products aids in the defense against the immune challenge but also potentially contributes to neurological damage under conditions of chronic inflammation.

Increasing evidence suggests that inflammation involving microglia activation through the release of pro-inflammatory mediators underlies many neurodegenerative diseases such as Parkinson's disease (PD), Alzheimer disease (AD) and multiple sclerosis (MS) (5-8). The expression of proinflammatory cytokines in the pathogenesis of various neurodegenerative diseases has been demonstrated (9-13). Proinflammatory cytokines released from microglia such as interleukin-6 (IL-6), interleukin-1 $\beta$  (IL-1 $\beta$ ), and tumor necrosis factor- $\alpha$  (TNF- $\alpha$ ) play critical roles in microglia-mediated neurodegeneration (14-16). Moreover, an inflammatory response in the injured brain also elicits pro-inflammatory cytokines (17,18). In addition to cytokines, nitric oxide (NO), produced by inducible nitric oxide synthase (iNOS) in microglia, is one of the characterized pro-inflammatory factors that induces neuronal death (19-21). Moreover, glucocorticoid-induced TNFR family related gene (GITR) was also suggested to play a role in the inflammatory response in microglia cells which contribute to inflammatory diseases (22-25). Tumor necrosis receptor2 (TNFR2) is highly expressed on microglia cells and plays an important role in the regulation of innate immune response following brain injury on infection (26).

In the CNS, glucocorticoids including corticosterone in the case of rodents or cortisol in humans have profound effects on brain development and adult CNS function. Excess or insufficient glucocorticoids cause abnormalities in neuronal and glial structure and function. In mammals, the mechanisms for responding to stress are regulated by the hypothalamic-pituitary-adrenal (HPA) axis, which results in

the releases of glucocorticoids. Glucocorticoids at basal levels have been shown to increase synaptic plasticity, and facilitate the maintenance of hippocampus-dependent cognition. In terms of neuroinflammation, however, the effects of glucocorticoids in the brain are controversial. Some studies showed that glucocorticoids caused an increase in the number of inflammatory cells, such as granulocytes, monocytes/macrophages, and microglia in the hippocampus (27,28). While synthetic glucocorticoids have long been used as an anti-inflammatory therapy when administered after injury, there is increasing evidence that glucocorticoids, a major hormone released during periods of stress, acts as a priming event resulting in potentiation of both central and peripheral proinflammatory cytokine production following a subsequent systemic immune challenge (29,30). In particular, glucocorticoids potentiated the expression of proinflammatory cytokines in cultured neurons (31), suggested that glucocorticoids may have a proinflammatory role (29). It has been demonstrated that the administration of a single dose of corticosterone that leads to blood levels similar to those observed during an acute stressor potentiates the proinflammatory cytokine response to a subsequent systemic inflammatory challenge (32). Prior exposure to glucocorticoids potentiated the lipopolysaccharide (LPS)-induced production of the pro-inflammatory cytokines IL-1 $\beta$  and IL-6 in spinal neuroinflammation and enhanced LPS-induced fever and sickness behaviors in rats (33). Stress-induced glucocorticoids function to sensitize the microglial proinflammatory response in the hippocampus to immunologic challenges (34). Acute and chronic stress has been found to sensitize or prime the neuroinflammatory response to immunologic challenges (28,35).

At the cellular level, the effects of glucocorticoids are largely a consequence of their transcriptional effects mediated via binding to Type I mineralocorticoid receptors (MR) and Type II GC receptors (GR) which are members of nuclear receptors. The MR has a higher affinity for corticosterone (Kd, 0.5 nM) than does GR (Kd, 2.5–5 nM) (36). *In vitro* binding studies indicated that naturally produced steroid hormones such as corticosterone and cortisol preferentially bind to MR as compared to synthetic glucocorticoids like dexamethasone, which showed higher affinity for GR (37). These results were confirmed by experiments performed with hippocampal tissue indicating that the MR exhibits increased binding with ten-fold higher affinity for endogenous glucocorticoids than GR (38). The high affinity of MR for glucocorticoids suggests that at basal levels the MR is mostly occupied whereas the GR is only partially bound by glucocorticoids (38). This results in continuous activation of MR at most times, even in between bursts of hormone secretion. The GR, however, has a lower affinity for the hormone and appears to be primarily activated during times of stress and circadian rhythm induced elevations of

corticosteroid concentrations (39). Differential binding by the two receptors in the brain plays an important role in the various effects of glucocorticoids observed in the CNS (40).

Both MR and GR have been identified in cell types that are responsible for the regulation of inflammatory responses including dendritic cells, macrophage, lymphocytes, and microglia cells (41). The MR is highly enriched in granule cells of the dentate gyrus and in the pyramidal cells of the hippocampal CA1 and CA2 regions and to a lesser extent in the hypothalamus, cerebellum, and brainstem (42). The GR is more widely distributed throughout the brain than the MR, and it is strongly expressed in the hippocampal formation and certain hypothalamic nuclei (43). The GR density is highest in the paraventricular nucleus and structures of the limbic system, making it readily accessible to the actions of the HPA axis (44). The limbic structures also express a significant amount of MR and there are a number of regions, especially the hippocampus, that show co-expression of MR and GR, which can be seen across many species (45).

In addition to the direct effects of corticosteroids on neuronal cells, corticosteroids may modulate brain functions through their actions on astrocytes, oligodendrocytes, and microglia because these glial cells express GR and MR (43). GR and MR are expressed *ex vivo* in microglia and GR is the most abundant steroid hormone receptor transcript *ex vivo* in microglia. These receptors have been suggested to regulate inflammatory response in microglia cells (41). MR expressed on microglia might play a role in the activation of microglia activity (46). Spironolactone, an MR antagonist, inhibited production of several pro-inflammatory cytokines via MR mechanisms and showed positive effects in patients with inflammatory diseases (47-49). Microglia activation induced by corticosterone and aldosterone was decreased by spironolactone (50). However, GR expressed in microglia cells showed suppressive effects. The inhibitory effect of corticosterone on proliferation of microglia cells is mediated by GR, but not MR (51). In mice, microglial GR protected dopaminergic neurons after acute 1-methyl-4-phenyl-1,2,3,6-tetrahydropyridine (MPTP) intoxication and microglial GR gene inactivation exacerbated both microglial and astroglia reactivity after acute MPTP treatment (52). Both MR and GR differentially regulate the function of mitogen-activated protein kinases (MAPKs) and nuclear factor kappa B (NF- $\kappa$ B) (53-56).

For the functions of microglia, several studies demonstrated that corticosterone inhibits microglia cells, reducing inflammatory reactions in the brain (57,58). Microglia activation induced by acute stress was reversed by corticosterone administration (59). Triamcinolone inhibited microglia activation and protected neuronal cells from death induced by microglia activation (60). Glucocorticoids inhibited

proliferation of microglia cells (61). *In vivo* experiments have shown that glucocorticoid injection alters the density and morphology of microglia cells in immature rats (62). Low concentrations of corticosterone decreased the expression of the proinflammatory cytokines IL-1 $\beta$  and TNF- $\alpha$  in the rat hippocampus following kainic acid stimulus (31), while chronic administration of corticosterone increased the level of LPS-induced NF- $\kappa$ B activity in the hippocampus of stressed rats (28).

The local glucocorticoid bioavailability is regulated by intracellular metabolism by 11 $\beta$ -hydroxysteroid dehydrogenases (11 $\beta$ -HSDs), which alter the exposure of glucocorticoid receptors to their ligands. 11 $\beta$ -HSD1 regenerates active glucocorticoids from their inactive 11-keto derivatives and is widely expressed throughout the adult CNS (63). Elevated hippocampal and neocortical 11 $\beta$ -HSD1 is observed with ageing and causes cognitive decline; its deficiency prevents the emergence of cognitive defects with age (64). Microglia also express functional 11 $\beta$ -HSD1 which is suggest to control proinflammatory mediator production and inflammation, (65).

Metabotropic glutamate receptors (mGluRs) are expressed in many different cell types throughout the brain and spinal cord (66). Recently, mGluRs have been considered to be promising targets for neuro-protective agents in both acute and chronic neurodegenerative disorders (67,68). mGluRs are G-protein-coupled receptors of which there are eight subtypes divided into three groups (I–III) based on their sequence homology, signal transduction pathways and pharmacological profiles (67,69). Metabotropic glutamate receptor subtype 5 (mGluR5) belongs to the group I receptors, which are typically postsynaptic and mediate their signaling through G $\alpha$ q-proteins. This results in the stimulation of phospholipase C (PLC), leading to phosphoinositide hydrolysis and intracellular Ca<sup>2+</sup> mobilization and also activation of extracellular signal-regulated protein kinases (ERK1/2) downstream signaling pathways (67). mGluR5 is expressed in microglia (66,70) and the mGluR5 specific agonist (R,S)-2-chloro-5-hydroxyphenylglycine (CHPG) inhibits microglia activation, oxidative stress, and the release of inflammatory mediators both *in vitro* and *in vivo* (71-76). Moreover, mGluR5 activation reduced fibrinogen-induced microglia activation, which resulted in neuronal protection (77). mGluR5 activation reduced  $\beta$ -amyloid-induced cell death in primary neuronal cultures (78). It has been reported that mGluR5 is significantly expressed in activated microglia which surround the site of injury following traumatic brain injury in rats. This observation may support the idea that pharmacological manipulation of the mGluR5 may be beneficial in neuroinflammatory diseases (79,80). The use of mGluR5 agonists as a therapy for chronically injured spinal cord has been proposed (68). Therefore, the dysregulation of mGluR5 may result in initiation or progression of neurodegenerative disorders.

Among the transcription factors that activate the inflammatory genes, NF- $\kappa$ B is perhaps the most relevant in microglia cells. Activation of NF- $\kappa$ B is triggered by phosphorylation, which subsequently leads to the translocation of the free NF- $\kappa$ B into the nucleus where it promotes the expression of proinflammatory genes (81,82). NF- $\kappa$ B transcription is activated by various kinases as well as reactive oxygen species (ROS) (83). Phosphatidylinositol 3-kinase (PI3K)/ protein kinase B (Akt) are also known to regulate the expression of inflammatory mediators in microglia (82,84,85). MAPKs, including p38 MAPK, ERK1/2, and c-Jun NH(2)-terminal kinase (JNK) have been suggested to be critical regulators of oxidative stress and proinflammatory signaling cascades (86). Several reports have shown that NF- $\kappa$ B, PI3K/Akt, and MAPKs are regulated by intracellular calcium levels and consequently influence cytokine expression and release in inflammation responsive-cells (87-93). In addition, it has been shown that activation of MAPKs or NF- $\kappa$ B is mediated via the activation of PLC and stimulation of protein kinase C (PKC) in various cell types (89,94,95).

In addition to microglial inflammatory response, accumulating evidence also supports the concept that oxidative imbalance and subsequent oxidative stress play an important role in the pathophysiology of neurodegenerative diseases (96). Under physiological conditions, cellular redox balance is maintained by the equilibrium between the formation and elimination of free radicals such as ROS and NO. Excessive generation of ROS/NO or inadequate antioxidant defense can result in damage to cellular structures. The CNS appears to be especially vulnerable to oxidative stress due to its high rate of oxygen consumption, low levels of molecular antioxidants and the susceptibility of neurons or oligodendrocytes due to their specific metabolic properties. ROS have been recognized as an activator to the chronic progression of neurodegenerative diseases (8,97,98). ROS plays a key role in microglial response in neurodegeneration (99-102). Microglial intracellular ROS generation facilitates pro-inflammatory pathways by activating MAPKs and NF- $\kappa$ B signaling (103-106). The NADPH oxidase (NOX) family is a series of enzymes involved in producing ROS. NOX-2 is highly expressed in innate immune cells including microglia cells. NOX-2 has been implicated in persistent microglial activation, ROS formation, and neurodegeneration in substantia nigra (14). iNOS expression plays a prominent role in the mechanism of oxidative stress in various cell types. NF- $\kappa$ B, MAPKs, and Janus kinase (JAK)/STAT-dependent signal transduction play an important role in iNOS expression. mGluR5 modulates cellular oxidative status by affecting ROS and NO production through inhibition of NOX-2 activity (71,74-76).

The CNS strongly depends on efficient mitochondrial function, because the brain has a high energy demand. Defects in mitochondrial dynamics, generation of ROS, and environmental factors especially oxidative stress may have an influence on energy metabolism and contribute to the pathogenesis of

several neurodegenerative diseases (107,108). The mitochondria generate ATP through oxidative phosphorylation. Under conditions of low ATP levels, the cellular energy sensor AMP-dependent protein kinase (AMPK) positively regulates signaling pathways which replenish ATP (109-111). Alternatively, AMPK is directly targeted and activated by pro-oxidant species or intracellular calcium levels (112,113). Although AMPK is considered to be a pro-survival kinase, it has been reported that prolonged activation can induce cell damage including endoplasmic reticulum (ER) stress (113-116). AMPK can also interact with the MAPK signaling cascade to mediate apoptosis, a process elicited by both energetic imbalance and pro-oxidant conditions, such as treatment with H<sub>2</sub>O<sub>2</sub> or UV (117).

The energy balance also influences oxidative stress and inflammatory responses in microglia, which contributes to disease progression (118-121). AMPK has been suggested to play a role in the regulation of metabolic homeostasis and cytokine release (122,123). Once activated, AMPK, in parallel, decreases ATP consuming pathways whilst activating pathways to enhance ATP production. If conditions are particularly stressful, AMPK affects cell viability by activating apoptosis and/or autophagy. AMPK was commonly recognized as a pivotal sensor of cellular energy balance. Disturbance of the AMPK pathway has been implicated in several neuroinflammatory-related diseases and neurodegenerative disorders (124-127).

Changes in Ca<sup>2+</sup> levels have been implicated to regulate several activities of microglia including cytokine release, migration, ROS generation, and proliferation (128-131). Calcium also serves as the key link coupling cellular energy balance and mitochondrial ATP production. Mitochondrial calcium uptake is associated with an increase in mitochondrial bioenergetics and inflammatory response. However, a consequence of mitochondrial calcium uptake is the production of ROS, which plays a major role in neurodegenerative diseases. In response to different stimuli, intracellular free Ca<sup>2+</sup> levels ([Ca<sup>2+</sup>]<sub>i</sub>) are increased either by the release of Ca<sup>2+</sup> from the ER or by entry across the plasma membrane (132,133). The ER also serves as a Ca<sup>2+</sup> reservoir regulated by two major Ca<sup>2+</sup> release channels, the 1,4,5-trisphosphate receptor (IP<sub>3</sub>R) (134,135) and the ryanodine receptor (RyR) (135), as well as by Ca<sup>2+</sup> ATPases, which control Ca<sup>2+</sup> transport into the ER (135). The prolonged depletion of Ca<sup>2+</sup> in the ER and Ca<sup>2+</sup> overload in the cytoplasm are main causes of ER stress (136,137). ER stress is generally caused by an overload of unfolded proteins in the ER, which activates the unfolded protein response (UPR), involving the transcriptional up-regulation of ER-chaperones, attenuation of protein translation and ER-associated degradation of misfolded proteins (137,138). Inositol-requiring enzyme-1 (IRE1), activating transcription factor 6 (ATF6), and PKR-like ER kinase (PERK) act as transducers in

the UPR signaling pathway. The ER-resident molecular chaperones including glucose-regulated protein 78 (GRP78) and glucose-regulated protein 94 (GRP94) as well as the transcriptional factor C/EBP homologous protein (CHOP) are induced by the UPR and they increase ER protein-folding capacity and maintain storage of ER  $\text{Ca}^{2+}$  (138,139). In addition, perturbation of ER integrity and increased ROS production are induced by an accumulation misfolded proteins in the ER, leading to the activation of the UPR (140). Prolonged ER stress results in cell death by the apoptotic pathway mediated by caspase-12, an ER localized cysteine protease (138). In addition to calcium homeostasis, impairment of mitochondrial function and AMPK signaling have been considered to modulate the ER stress response (117,141-145). Specifically, mitochondrial dysfunction activated AMPK, leading to ER stress through NO production, resulting in apoptosis of pancreatic  $\beta$ -cells (143). Activation of AMPK resulted in ER stress in several cell types (117,142,145). Conversely, AMPK activation by AICAR attenuated ER stress and protected SH-SY5Y neuroblastoma cells against homocysteine-induced neurotoxicity (141). The elevation of intracellular calcium is mediated by PLC-mediated  $\text{IP}_3$  formation, which is a well-established downstream signaling effector of G protein-coupled receptor (GPCR) activation. Stimulation of GPCRs activates the Gq protein, promoting its dissociation into  $\text{Gq}\alpha$  and  $\text{G}\beta\gamma$  and the exchange of guanosine diphosphate bound to  $\text{G}\alpha\text{q}$  for GTP. The resulting GTP- $\text{G}\alpha\text{q}$  complex activates the  $\beta$  isoforms of PLC (146). mGluR5 activation in microglia has been suggested to be involved in the  $\text{G}\alpha\text{q}$ -protein signal transduction pathway through PLC, PKC and  $\text{Ca}^{2+}$  (72). However, pertussis toxin (PTX)-sensitive  $\text{G}_i$  proteins and  $\text{IP}_3$  signaling resulting in  $[\text{Ca}^{2+}]_i$  increase has been reported (147-150). Taken together, the evidence suggests that not only Gq-coupled receptors but also  $\text{G}_i$ -coupled receptors can contribute to increase  $[\text{Ca}^{2+}]_i$  by release from the ER. In addition, many reports indicate that the synthesis of  $\text{IP}_3$  and  $[\text{Ca}^{2+}]_i$  signaling by one type of G-protein-coupled receptor can be influenced by the stimulation of a different type of GPCR (151-153).

In the past several decades, organotins have been widely used as polyvinyl chloride (PVC) stabilizers, industrial catalysts, agricultural biocides, wood preservatives, and antifouling agents in paints (154). The major sources of organotin intake for humans are dietary sources, such as seafood and shellfish, food crops, and drinking water. A serious problem is that organotins can accumulate in fish, animals and plants (155), exposing humans who are in further up in the food chain, to these substances (156). Most organotins have been reported to be toxic in humans (157). Several animal experiments have suggested that the spectrum of potential adverse chronic systemic effects of organotins in humans is quite broad including immune suppression, endocrine disruption, neurotoxicity, and metabolic toxicity. Organotins affect many organs and disrupt multiple physiological functions causing reproductive

disturbance, teratogenicity, developmental disorders, and possibly carcinogenicity (158,159). Therefore, there is an increasing concern that their widespread use may cause adverse effects within environmental and biological systems.

Organotin compounds are characterized by a tetravalent structure with at least one carbon–tin bond, and they are classified as mono-, di-, tri- and tetra-alkyltins, depending on the number of added alkyl groups (**Figure1**). Triorganotins including tributyltin, triphenyltin, and trimethyltin possess a high specificity of action and are cytotoxic in several test systems (158,160,161). Particularly, studies on the toxicity of triorganotins, especially trimethyltin (TMT), have been mainly focused on neurotoxicity. TMT intoxication in animals exhibited a variety of adverse effects on the CNS including seizures, self-mutilation, vocalization, hyperactivity and aggressive behavior, because of extensive neuronal damage (162,163). Accidental human exposure to TMT has resulted in similar adversities including weakness, aggressive behavior, depression, disorientation, seizures, severe memory loss and death in severe cases (164). Due to their high toxicity, triorganotins have been banned for industrial or agricultural applications. However, dialkyltins are still widely used.

TMT has been known as a classic neurotoxicant. TMT can accumulate in the body and pose a risk for workers chronically exposed to a low dose of TMT. Neurobehavioral changes were observed in rats and mice treated with TMT (165). TMT induced neurotoxicity by interfering with synaptic and neurodegeneration-related networks and protein processing and degradation pathway (166). One of the proposed mechanisms for the neurotoxicity of TMT is the induction of inflammation. Memory dysfunction induced by TMT in rats was observed with up-regulation of the mRNA expression levels of reactive microglia marker and proinflammatory cytokines (167). The inflammatory responses by increasing cytokine expression after TMT treatment in adipocytes were reported (168). In addition, *in vitro* experiments, TMT-induced apoptosis in human neuroblastoma cells through activation of NF- $\kappa$ B, JNK, ERK, and p38 was observed (169). Although the potential neurotoxicity of TMT has been widely reported, the critical target molecules for the mechanisms of induction of inflammation in microglia remain unclear.

Many reports exhibited a significant involvement of endogenous corticosterone in the pathological phenomena related to TMT toxicity. Particularly, the plasma corticosterone concentration transiently increased in TMT-treated rats (170) together with alterations of neuropathological and behavioral features (171) and induced hippocampal necrosis (172). Time- and concentration-dependent changes of plasma corticosterone after TMT injection were also observed in mice (173). Both endogenous and

exogenous glucocorticoids prevented neuronal degeneration induced by TMT in mouse brain (174). In addition, TMT cytotoxicity seems to be oppositely regulated by GR and MR activity. Spironolactone protected neurons in dentate granule cells from TMT cytotoxicity whereas, the GR antagonist mifepristone potentiated the TMT cytotoxicity (173). However, the role of corticosterone in TMT-induced inflammation is still unclear whether it acts as a protective or deleterious factor and it needs to be determined.

Dibutyltin (DBT) is found in the environment and in dietary sources (175-177). DBT is used as biocide or as stabilizer in a wide range of industrial and agricultural applications (178). DBT has been detected in drinking water supplied via PVC pipes (179). Importantly, DBT is a degradation product of tributyltin (TBT), which has been used as a fungicide, wood preservative, and antifoulant (180). In human tissues, DBT was detected in human liver (181-183). Concentrations of DBT in the range of 3–100 nM were observed (184,185). DBT is found in human blood at concentrations ranging as high as 300 nM (184,186). TBT shows toxicity in various cell types including; neurons (187-189), hepatocytes (190,191), T-lymphocytes (192) and osteoblasts (193). A number of studies suggested that DBT may be neurotoxic. For example, DBT has proven as a developmental neurotoxicant *in vitro* and *in vivo* (194). DBT significantly inhibited neurite outgrowth and was found to be even more toxic than TMT *in vitro* (195). In primary cultures of cerebellar granule cells, DBT showed potent neurotoxicity through induction of apoptosis (179). DBT neurotoxicity in aggregating brain cell cultures affected the myelin content in cholinergic neurons. In addition, markers for astrocytes and oligodendrocytes were diminished (195). DBT at concentrations of 0.25-100  $\mu$ M caused a decrease in cell viability, mitochondrial potential and cell proliferation in neuroblastoma cells (196). DBT significantly inhibited neurite outgrowth and caused cell apoptosis in PC12 cells (197). Developmental neurotoxicity of DBT and the distribution of total tin (Sn) in the brain after DBT exposure was documented (198). DBT was consistently present in the brain in a two-generation reproductive toxicity study of TBT (183). In addition, DBT caused *in vivo* neurotoxicity with increasing apoptotic cell death in the neocortex and hippocampus of offspring (194). DBT interfered with the secretion of TNF- $\alpha$  in natural killer cells and the effects were concentration dependent (199).

However, the neuroinflammatory action of DBT is still not well investigated. Several studies explored the inflammatory responses following DBT exposure in *in vitro* and *in vivo*. In human natural killer cells, several transcription factors were induced by DBT, mediated by MAPKs (200,201). Necrosis induced by DBT was observed in T-lymphocytes contributing the thymic atrophy in rats (192).

Although DBT toxicity in the nervous system has been extensively studied, the focus was mainly on neuronal cells.

BV-2 microglia cells have been successfully used to study functions of microglia including inflammatory responses, oxidative stress, ER stress, and intracellular regulation triggered by toxic compounds (162,202,203). In the present studies, we used BV-2 cells as a model to investigate the effects of glucocorticoids and xenobiotic compounds such as organotins on the inflammatory mediators and oxidative stress at the cellular and molecular levels. The effects of the endogenous glucocorticoids 11-dehydrocorticosterone and corticosterone, the mineralocorticoid aldosterone and the synthetic glucocorticoid dexamethasone on NF- $\kappa$ B activation and IL-6 expression in the presence or absence of MR and GR antagonists were investigated. Further, the impact of proinflammatory cytokines and corticosteroids on the expression of TNFR2 and 11 $\beta$ -HSD1 was studied. The direct effect of mGluR5 inhibition on  $[Ca^{2+}]_i$  and the receptors involved were tested. The key signaling pathways of increased calcium including oxidative stress, mitochondrial function, the release of proinflammatory cytokines, and ER stress induced by blockage of mGluR5 were investigated. Moreover, the action of the xenobiotics, silane AB110873 which has MR agonist properties, on the induction of IL-6 release and oxidative stress was elucidated. The effects of DBT on AMPK, NF- $\kappa$ B, PI3K/Akt, MAPKs,  $Ca^{2+}$ , PLC, and PKC contributing to oxidative stress and cytokine release were investigated. Furthermore, the role of NF- $\kappa$ B and MAPKs and their influence on the TMT-mediated induction of iNOS and/or IL-6 expression in microglia cells was examined. The role and regulation of glucocorticoids on TMT action was also investigated.

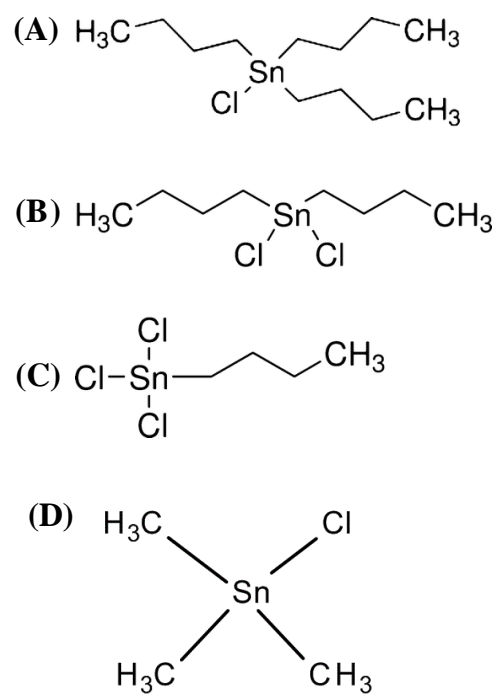


**Figure 1:** Structures of organotins. (A) tributyltin (TBT) chloride, (B) dibutyltin (DBT) dichloride, (C) monobutyltin (MBT) trichloride, and (D) trimethyltin chloride (TMT) modified from (196).

## Hypotheses and aims

Microglia are implicated in the pathogenesis of neuroinflammatory conditions such as Alzheimer disease, Parkinson disease, and multiple sclerosis. Therefore, factors influencing microglia functions may contribute to the development of diseases. In order to better understand the mechanisms of endogenous corticosteroids and xenobiotic compounds on microglia activation, further research is needed. Therefore, in this thesis addressed the following hypotheses and tasks:

1. The balance of local corticosteroids regulated by  $11\beta$ -HSD1 and its regulation by signaling pathways such as NF- $\kappa$ B and MAPKs in microglia is yet to be fully understood. Glucocorticoids impacts on microglia inflammatory activity and the exact mechanism need to be uncovered.
2. The metabotropic glutamate receptors (mGluRs) modulate microglia function through inhibition of intracellular calcium regulation.
3. Xenobiotic compounds disturb microglia functions by induction of oxidative stress, ER stress, and inflammatory responses.
4. Xenobiotic compounds disturb glucocorticoid functions in microglia resulting in enhanced microglia activity and susceptibility.

More specifically the aims were to:

1. Characterize if glucocorticoids alter the inflammatory responses of microglia cells
2. Characterize if xenobiotic compounds alter microglia functions including inflammatory response, oxidative stress, and ER stress.
3. Elucidate the involvement of metabotropic glutamate receptors and intracellular calcium on microglia functions
4. Elucidate the importance of NF- $\kappa$ B, MAPKs, AMPK, and PI3K/Akt pathways in microglia cells during exposure to xenobiotic compounds and/or glucocorticoids.

## List of papers

This thesis includes the following manuscripts (referred to in the text by Roman numeral)

- I. Mineralocorticoid and glucocorticoid receptors differentially regulate NF-kappaB activity and pro-inflammatory cytokine production in murine BV-2 microglial cells. Chantong B, Kratschmar DV, Nashev LG, Balazs Z, Odermatt A. *J Neuroinflammation*. 2012. 9.
- II. Virtual screening as a strategy for the identification of xenobiotics disrupting corticosteroid action. Nashev LG, Vuorinen A, Praxmarer L, Chantong B, Cereghetti D, Winiger R, Schuster D, Odermatt A. *PLoS One*. 2012;7(10).
- III. Dibutyltin promotes oxidative stress and increases inflammatory mediators in BV-2 microglia cells. (Manuscript in submission).
- IV. Corticosterone potentiates trimethyltin-induced inflammatory responses mediated by mineralocorticoid receptor in BV-2 cells (Manuscript in preparation).
- V. Metabotropic glutamate receptor 5 modulates ER stress through pertussis toxin-sensitive heterotrimeric G proteins (Manuscript in preparation).

## CHAPTER 2

**Mineralocorticoid and glucocorticoid receptors differentially regulate NF-kappaB activity and pro-inflammatory cytokine production in murine BV-2 microglial cells**

## RESEARCH

## Open Access

## Mineralocorticoid and glucocorticoid receptors differentially regulate NF-kappaB activity and pro-inflammatory cytokine production in murine BV-2 microglial cells

Boonrat Chantong, Denise V Kratschmar, Lyubomir G Nashev, Zoltan Balazs and Alex Odermatt\*

### Abstract

**Background:** Microglia, the resident macrophage-like cells in the brain, regulate innate immune responses in the CNS to protect neurons. However, excessive activation of microglia contributes to neurodegenerative diseases. Corticosteroids are potent modulators of inflammation and mediate their effects by binding to mineralocorticoid receptors (MR) and glucocorticoid receptors (GR). Here, the coordinated activities of GR and MR on the modulation of the nuclear factor-kB (NF-kB) pathway in murine BV-2 microglial cells were studied.

**Methods:** BV-2 cells were treated with different corticosteroids in the presence or absence of MR and GR antagonists. The impact of the glucocorticoid-activating enzyme 11 $\beta$ -hydroxysteroid dehydrogenase type 1 (11 $\beta$ -HSD1) was determined by incubating cells with 11-dehydrocorticosterone, with or without selective inhibitors. Expression of interleukin-6 (IL-6), tumor necrosis factor receptor 2 (TNFR2), and 11 $\beta$ -HSD1 mRNA was analyzed by RT-PCR and IL-6 protein expression by ELISA. NF-kB activation and translocation upon treatment with various corticosteroids were visualized by western blotting, immunofluorescence microscopy, and translocation assays.

**Results:** GR and MR differentially regulate NF-kB activation and neuroinflammatory parameters in BV-2 cells. By converting inactive 11-dehydrocorticosterone to active corticosterone, 11 $\beta$ -HSD1 essentially modulates the coordinated action of GR and MR. Biphasic effects were observed for 11-dehydrocorticosterone and corticosterone, with an MR-dependent potentiation of IL-6 and tumor necrosis factor- $\alpha$  (TNF- $\alpha$ ) expression and NF-kB activation at low/moderate concentrations and a GR-dependent suppression at high concentrations. The respective effects were confirmed using the MR ligand aldosterone and the antagonist spironolactone as well as the GR ligand dexamethasone and the antagonist RU-486. NF-kB activation could be blocked by spironolactone and the inhibitor of NF-kB translocation Cay-10512. Moreover, an increased expression of TNFR2 was observed upon treatment with 11-dehydrocorticosterone and aldosterone, which was reversed by 11 $\beta$ -HSD1 inhibitors and/or spironolactone and Cay-10512.

**Conclusions:** A tightly coordinated GR and MR activity regulates the NF-kB pathway and the control of inflammatory mediators in microglia cells. The balance of GR and MR activity is locally modulated by the action of 11 $\beta$ -HSD1, which is upregulated by pro-inflammatory mediators and may represent an important feedback mechanism involved in resolution of inflammation.

**Keywords:** Mineralocorticoid receptor, Glucocorticoid receptor, 11 $\beta$ -hydroxysteroid dehydrogenase, Inflammation, Interleukin-6, NF-kB

\* Correspondence: alex.odermatt@unibas.ch  
 Division of Molecular and Systems Toxicology, Department of Pharmaceutical Sciences, University of Basel, Klingelbergstrasse 50, CH-4056, Basel, Switzerland



## Background

Glucocorticoids are essential for the coordinated regulation of metabolic and immune responses. They are well known due to their potent anti-inflammatory and immune suppressive effects, and therefore widely used in clinics to treat inflammatory and autoimmune diseases. Increasing evidence indicates that endogenously occurring glucocorticoids can, in some situations, stimulate inflammation by enhancing the production of pro-inflammatory mediators and promoting oxidative stress [1-3]. The underlying mechanisms and the role of corticosteroid receptors are, however, not fully understood.

Glucocorticoids exert their effects mainly by activating glucocorticoid receptors (GR) and mineralocorticoid receptors (MR). A comparison of corticosterone binding to MR and GR in rat hippocampal preparations revealed a 10-fold higher affinity for MR ( $K_d = 0.5$  nM) compared with GR ( $K_d = 5.0$  nM) [4,5]. Importantly, hippocampal MR was occupied about 80% while GR was occupied 10% only if samples were taken at the nadir of the hypothalamus-pituitary adrenal (HPA) axis diurnal rhythm in the morning. GR binding increased at higher corticosterone levels, suggesting that GR is activated during stress [6,7] and potentially also at diurnal peak levels. Differential binding by MR and GR in various brain cells needs to be considered in order to understand effects of glucocorticoids in the CNS [8-10].

In classical mineralocorticoid target tissues involved in electrolyte and volume regulation, such as renal cortical collecting ducts, distal colon, and salivary and sweat glands, MR is co-expressed with 11 $\beta$ -hydroxysteroid dehydrogenase 2 (11 $\beta$ -HSD2), which converts active (corticosterone, cortisol) into inactive glucocorticoids (11-dehydrocorticosterone, cortisone) [11-13]. The close proximity of 11 $\beta$ -HSD2 and MR has been proposed to prevent MR activation by glucocorticoids, thereby rendering specificity of the receptor to aldosterone [14]. Deficient 11 $\beta$ -HSD2 activity has been shown to result in sodium and water retention, causing edema formation and hypertension [15-17]. To avoid these adverse effects caused by excessive activation of renal and intestinal MR, synthetic glucocorticoids selectively activating GR have been designed and are widely used in therapy of inflammatory and autoimmune diseases [18,19].

Besides, MR has important functions in vascular cells, adipocytes, osteocytes, neutrophils, dendritic cells, and macrophage [11]. In the brain, MR plays an important role in hippocampal neurons and in immune cells [20-22]. Glucocorticoids are essentially involved in the modulation of the coordinated action of monocytes, macrophages, astrocytes, and microglia cells during inflammation in the brain [23]. Interestingly, in macrophage and microglia cells, MR and GR are co-expressed in the presence of 11 $\beta$ -HSD1, which converts inactive

11-dehydrocorticosterone and cortisone into active corticosterone and cortisol [11]. Since circulating glucocorticoid concentrations are 100 to 1,000 times higher than those of aldosterone, MR activity is most likely controlled by glucocorticoids but not aldosterone in these cells under physiological conditions [24].

So far, only few cell lines have been reported that express MR, GR, and 11 $\beta$ -HSD1 at sufficient levels, allowing to investigate the functional interactions between the two corticosteroid receptors and to assess the role of 11 $\beta$ -HSD1 in regulating their activities. In the present study, we show that the murine microglial cell line BV-2, which is considered to be a suitable model of microglia to study inflammatory parameters [25], expresses MR, GR, and 11 $\beta$ -HSD1. We compared the effects of the endogenous glucocorticoids 11-dehydrocorticosterone (which requires activation by 11 $\beta$ -HSD1) and corticosterone, the mineralocorticoid aldosterone and the synthetic glucocorticoid dexamethasone on NF- $\kappa$ B activation and IL-6 expression in the presence or absence of MR and GR antagonists. Moreover, the impact of pro-inflammatory cytokines and corticosteroids on the expression of TNFR2 and 11 $\beta$ -HSD1 was investigated.

## Methods

### Materials

Fetal bovine serum (FBS) was purchased from Atlanta Biologicals (Lawrenceville, GA, USA) and other cell culture media and supplements from Invitrogen (Carlsbad, CA, USA). *Escherichia coli* 0111:B4 lipopolysaccharide (LPS), TNF $\alpha$ , and IL-6 were purchased from Sigma-Aldrich (St. Louis, MO, USA), Cay-10512 was from Cayman Chemicals (Hamburg, Germany), [1,2- $^3$ H]-cortisone from American Radiolabeled Chemicals (St. Louis, MO, USA), IL-6 ELISA kit from BD Biosciences (Allschwil, Switzerland), and the HCS kit for evaluation of NF- $\kappa$ B activation (K010011) was obtained from Cellomics ThermoScientific (Pittsburgh, PA, USA). Antibodies against HDAC-1, TNFR2, NF- $\kappa$ B subunit p65, and phosphorylated p65 were obtained from Cell Signaling Technology (Danvers, MA, USA). Antibody against  $\beta$ -actin and goat anti-rabbit IgG-HRP were obtained from Santa Cruz Biotechnology (Santa Cruz, CA, USA).

### Cell culture

The immortalized mouse microglial cell line BV-2, developed by Blasi *et al.* [26,27], was kindly provided by Professor Wolfgang Sattler, University of Graz, Graz, Austria. Cells were cultivated in RPMI-1640 medium supplemented with 10% FBS, 2 mM glutamine, 100  $\mu$ g/mL streptomycin, 100 U/mL penicillin, 0.1 mM non-essential amino acids, and 10 mM HEPES, pH 7.4. Prior to treatment, cells were seeded in 96-well ( $1 \times 10^3$  cells), 24-well

( $2 \times 10^4$  cells), 12-well ( $5 \times 10^5$  cells), or 6-well ( $1 \times 10^6$  cells) plates in Dulbecco's modified Eagle's medium (DMEM) supplemented as indicated above and incubated for 24 h at 37°C. All experiments were performed under the permission A070126 by the Swiss Federal Department of Environment BAFU.

#### Quantification of mRNA expression

Total RNA from treated cells was isolated using Trizol reagent according to the protocol from the manufacturer (Invitrogen). The concentration and purity of the total RNA was assessed by a NanoDrop<sup>®</sup> spectrophotometer. A 260/280 nm absorbance ratio of 1.8 or higher was accepted for purity of total RNA. Total RNA was used for cDNA synthesis with oligo-dT primers and the Superscript-III first-strand synthesis system (Invitrogen). Total RNA (0.5 µg) and oligo-dT primers (0.5 µg) were incubated for 5 min at 56°C, followed by addition of 4.90 µL of 5 × first strand buffer, 1.5 µL of 0.1 M dithiothreitol (DTT), 0.5 µL of RNase H inhibitor (50 U), 1 µL of 10 mM dNTPs, and 0.1 µL of Superscript<sup>®</sup> Reverse Transcriptase III (total reaction volume 24.5 µL). The reaction was performed for 1 h at 42°C, followed by adding 80 µL of DEPC-treated water and storage at -20°C until further use. Relative quantification of mRNA expression levels was performed by real-time RT-PCR using the KAPA SYBR<sup>®</sup> FAST qPCR Kit (Kapa Biosystems, Boston, MA, USA) and gene-specific oligonucleotide primers. Quantitative real-time RT-PCR was performed in a final volume of 20 µL and using a Rotor-Gene 6000 thermal cycler (Corbett Research, Sydney, Australia). The following amplification procedure was applied: initial denaturation for 15 min at 95°C, followed by 40 cycles of denaturation for 15 s at 94°C, annealing for 30 s at 56°C, and extension for 30 s at 72°C. Three replicates were analyzed per sample. Relative gene expression compared with the internal control GAPDH was determined using the  $2^{-\Delta\Delta CT}$  method [28]. The oligonucleotide primers for real-time RT-PCR are listed in Additional file 1: Table S1.

#### Determination of IL-6 protein expression

Cells grown in 96-well plates were treated for 24 h with the compounds indicated, and cell-free supernatants were collected. IL-6 protein was measured using an ELISA kit from BD Biosciences. Briefly, a 96-well plate was coated with capture antibody overnight at 4°C, followed by washing five times with PBS-T (PBS containing 0.05% Tween-20). The wells were blocked with assay diluents for 1 h and washed five times. Standards and collected culture supernatants were added to the appropriate wells and samples were incubated for 2 h. After rinsing five times with PBS-T, each well was incubated with detection antibody for 1 h. After washing, avidin-

HRP was added for 30 min. After rinsing seven times, each well was incubated with substrate solution for 30 min in the dark. Reaction was stopped by adding 1 M H<sub>3</sub>PO<sub>4</sub>, and the plate was analyzed by measuring absorbance at 450 nm and subtracting the values at 570 nm using a UV-max kinetic microplate reader (Molecular Device, Devon, UK). IL-6 protein concentrations were calculated according to the standard curve of purified mouse IL-6.

#### Determination of NF-κB localization by fluorescence microscopy

BV-2 cells were grown on poly-L-lysine coated glass slides in 6-well plates. Following treatment, the medium was removed and cells were fixed and stained using Cellomics<sup>®</sup> NF-κB p65 activation HCS kit (Cellomics ThermoScientific, Pittsburgh, PA, USA) according to the manufacturer's instructions. Briefly, cells were fixed with 4% paraformaldehyde in PBS for 15 min at 25°C, washed three times with PBS, and permeabilized with PBS containing 0.5% Triton X-100 for 10 min. After three washes with PBS and blocking with 1% fatty acid-free bovine serum albumin for 1 h the samples were incubated with rabbit polyclonal antibody against the p65 subunit of NF-κB (1:500) for 2 h at 37°C. After washing, slides were incubated in the dark with blocking buffer containing goat anti-rabbit IgG conjugated to Alexa Fluor 488 and Hoechst 33342 dye for 1 h. Slides were washed with PBS and mounted with Mowiol<sup>®</sup> 4-88 antifade reagent (Hoechst, Frankfurt, Germany) on glass slides. Cells were analyzed using a confocal laser scanning microscope Olympus Fluoview FV1000. Images were captured using a magnification of 400×. The excitation and emission wavelengths were 488 nm and 510 nm, respectively.

Alternatively, cells were grown in 96-well plates, fixed and stained using Cellomics NF-κB p65 activation HCS reagent kit. The cells were soaked in PBS at 4°C until imaging procedure. The assay plate was analyzed on a Cellomics ArrayScan HCS reader. The Cytoplasm to Nucleus Translocation BioApplication software was used to calculate the ratio of cytoplasmic and nuclear NF-κB intensity [29]. The average intensity of 500 objects (cells) per well was quantified (magnification 200×). Nuclear stain (Hoechst 33342) was in channel 1 and NF-κB was visualized in channel 2. In channel 2 an algorithm was utilized to identify the nucleus and surrounding cytoplasm in each cell; this analysis method reports the average intensity within each nuclear mask as well as the total of the nuclear and cytoplasmic intensity. The results were reported as percentage of nuclear intensity from total intensity. All treatments were performed in triplicate.

#### Preparation of whole cell lysates and cytoplasmic and nuclear fractions

For preparation of whole cell lysates, cells grown in 6-well plates were washed twice with ice-cold PBS and lysed in cold RIPA buffer (Sigma-Aldrich) supplemented with protease inhibitor cocktail (Roche Diagnostics, Rotkreuz, Switzerland). The extract was centrifuged at  $10,000 \times g$  for 15 min at  $4^{\circ}\text{C}$  to remove cell debris.

For preparation of cytoplasmic and nuclear fractions cells were washed twice with PBS, harvested in 500  $\mu\text{L}$  PBS, followed by centrifugation at  $450 \times g$  for 5 min. Cell pellets were washed once with PBS, transferred to 1.5-mL tubes and pelleted again at  $1,000 \times g$  for 5 min. The cells were lysed by gentle resuspension in 200  $\mu\text{L}$  lysis buffer containing 0.01 M DTT and protease inhibitors, followed by incubation on ice for 15 min. IGEPAL CA-630 solution (Sigma-Aldrich) was added at 0.6% v/v final concentration and samples were vigorously mixed for 10 s, followed by centrifuging at  $10,000 \times g$  for 30 s. Supernatants (cytoplasmic fractions) were transferred to new tubes. The nuclear pellets were washed once with 100  $\mu\text{L}$  PBS, pelleted at  $450 \times g$  for 5 min, and resuspended in 100  $\mu\text{L}$  of extraction buffer containing 0.01 M DTT and protease inhibitors. Nuclear suspension was agitated for 30 min and centrifuged at  $12,000 \times g$  for 5 min. Nuclear fractions were frozen at  $-80^{\circ}\text{C}$  and thawed on ice to increase extraction of nuclear proteins from the insoluble material. Nuclear samples were then sonicated on ice three times for 5 s each to obtain the final nuclear fractions.

#### Detection of protein expression

Protein concentrations were determined using the Pierce<sup>®</sup> BCA protein assay kit (Thermo Scientific) according to the manufacturer's instructions and bovine serum albumin as standard. Cytoplasmic, nuclear, or whole cell extracts (30  $\mu\text{g}$  per sample) were resolved on 8% sodium dodecyl sulfate-polyacrylamide gel electrophoresis (SDS-PAGE). Proteins were then transferred to 0.2  $\mu\text{m}$  polyvinylidene difluoride (PVDF) membranes (Bio-Rad Laboratories, Hercules, CA, USA). Membranes were incubated in Tris-buffered saline, pH 7.4, containing 0.1% Tween-20 (TBS-T), and supplemented with 5% non-fat milk overnight at  $4^{\circ}\text{C}$  for blocking. The blots were then incubated with primary antibodies against the p65 subunit of NF- $\kappa\text{B}$  (1:500), the phosphorylated form of p65 (1:500), TNFR2 (1:1,000), HDAC1 (1:1,000) or  $\beta$ -actin (1:1,000) for 2 h at room temperature. After washing with TBS-T, blots were incubated with goat anti-rabbit IgG-horseradish peroxidase or anti-mouse IgG-horseradish peroxidase (1:5,000) for 1 h at room temperature. Blots were washed with TBS-T and immunolabeling was visualized using enhanced chemiluminescence HRP substrate (Millipore, Billerica, MA, USA)

according to the manufacturer's instructions using a Fujifilm LAS-4000 detection system (Bucher Biotec, Basel, Switzerland).  $\beta$ -actin was used as loading control for cytoplasmic and whole cell protein extracts. HDAC1 was used as loading control for nuclear fractions.

#### 11 $\beta$ -HSD1 activity measurements in intact BV-2 cells

BV-2 cells were grown in 24-well plates and treated with 20 ng/mL LPS in the presence or absence of 200 nM cortisone for 24 h. Medium was removed and replaced by assay medium containing 50 nM cortisone with 10 nCi [ $^3\text{H}$ ] cortisone as tracer. Following incubation for 12 h at  $37^{\circ}\text{C}$ , medium was collected and steroids were extracted with ethyl acetate. The extracts were dried under vacuum, reconstituted with methanol containing a mixture of 2 mM unlabeled cortisone and cortisol, and steroids were separated in a chloroform/methanol solvent system (9:1, v/v). The conversion of cortisone to cortisol was determined by scintillation counting.

#### Statistical analysis

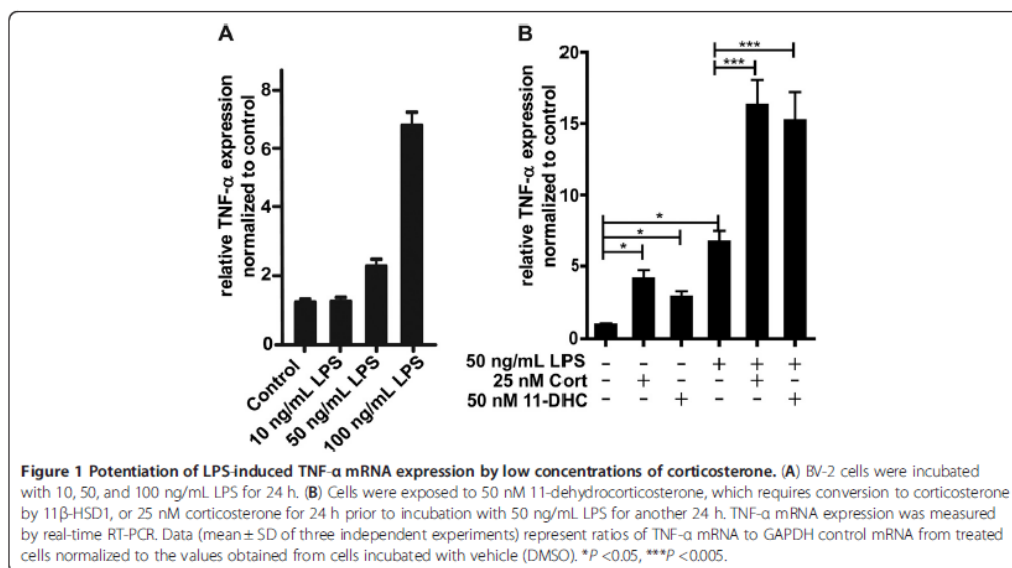
The data were analyzed using one-way ANOVA (V5.00; GraphPad Prism Software Inc., San Diego, CA, USA). When ANOVA showed significant differences between groups, Tukey's post hoc test was used to determine whether specific pairs of groups showed statistically significant differences.  $P < 0.05$  was considered statistically significant.

## Results

#### Potential of LPS-induced pro-inflammatory cytokine expression by low concentrations of endogenous glucocorticoids

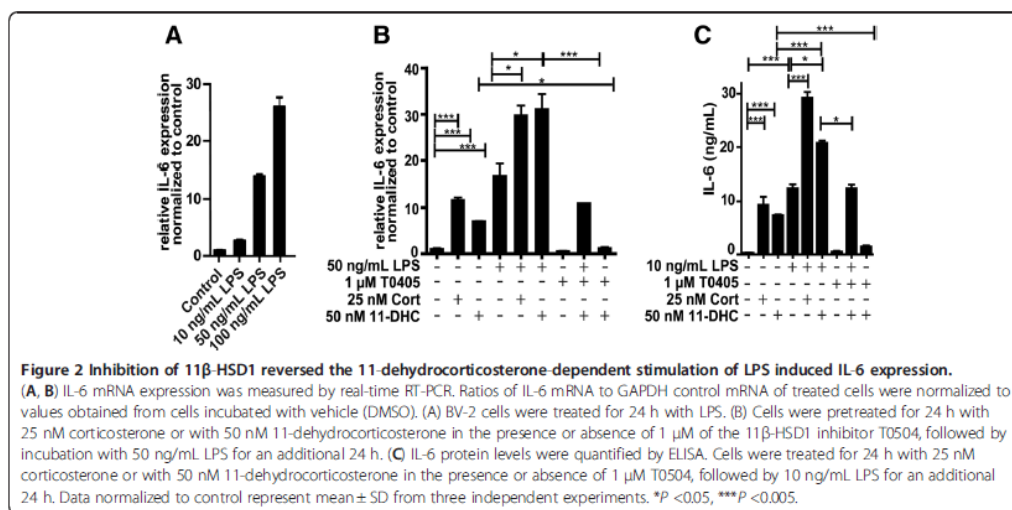
To test whether the murine microglia cell line BV-2 might represent a suitable cell system to study the role of corticosteroid receptors and local glucocorticoid activation on pro-inflammatory cytokine production, we first determined the mRNA expression of GR, MR, and 11 $\beta$ -HSD1 using real-time RT-PCR. Substantial levels of mRNA expression for all three genes were detected. Approximately 10-fold higher GR mRNA than MR mRNA expression was obtained, in line with evidence for an order of magnitude higher expression of GR compared with MR in the kidney [30]. Thus, the expression pattern suggests that BV-2 cells can be used to investigate mechanisms of corticosteroid-mediated modulation of NF- $\kappa\text{B}$  activation and pro-inflammatory cytokine expression.

BV-2 cells are sensitive to LPS, and incubation with LPS resulted in a concentration-dependent increase in the expression of TNF- $\alpha$  mRNA (Figure 1A). It is important to note that the absolute response depends on the batch of LPS and on batch and state of BV-2 cells.



The three independent experiments shown in Figure 1A were performed with different batches of LPS and BV-2 cells than the three independent experiments shown in Figure 1B. Another factor influencing the absolute response values is the composition of the culture medium. Performing the experiments shown in Figure 1B in medium with charcoal-treated FBS resulted in almost two-fold higher TNF- $\alpha$  mRNA expression levels, whereby the relative expression changes were

comparable (data not shown). As shown in Figure 1B preincubation of cells for 24 h with 25 nM corticosterone, corresponding to low physiological glucocorticoid concentrations, resulted in a pronounced stimulation of TNF- $\alpha$  expression upon treatment with LPS. Comparable effects, although somewhat less efficient, were observed when using 11-dehydrocorticosterone as substrate. This suggests a pro-inflammatory effect of low endogenous glucocorticoid concentrations and a role of the



glucocorticoid-activating enzyme 11 $\beta$ -HSD1 in stimulating inflammation.

We measured IL-6 expression as an accepted read-out to assess the sensitivity of exposure to LPS and subsequent activation of NF- $\kappa$ B [31]. LPS induced IL-6 expression in a concentration-dependent manner (Figure 2A).

Preincubation with 25 nM corticosterone potentiated IL-6 expression (Figure 2B). A similar stimulation of IL-6 expression was observed upon preincubation with 50 nM 11-dehydrocorticosterone, an effect which was reversed by the two structurally distinct selective 11 $\beta$ -HSD1 inhibitors BNW-16 [32] (data not shown) and T0504

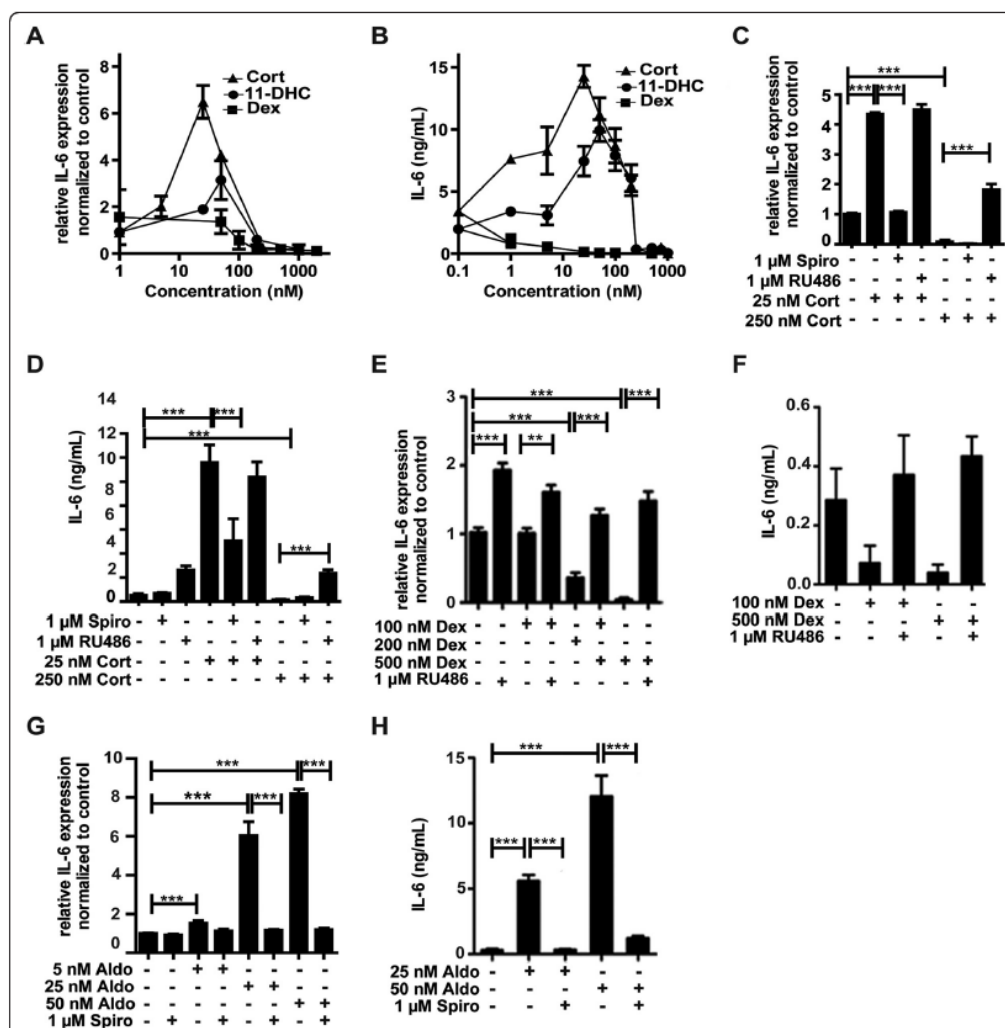


**Figure 3 Differential modulation of IL-6 expression by MR and GR.** BV-2 cells were treated with various concentrations of 11-dehydrocorticosterone (A, B), corticosterone (A-D), dexamethasone (E, F), or aldosterone (G, H) in the presence or absence of 1  $\mu$ M of MR antagonist spironolactone (C, D, G, H) or 1  $\mu$ M of GR antagonist RU-486 (C-F) for 24 h, as indicated. (A, C, G, E) Quantification of IL-6 mRNA expression by real-time RT-PCR. Data represent ratios of IL-6 mRNA to GAPDH control mRNA from treated cells normalized to the values obtained from cells incubated with vehicle (DMSO). (B, D, F, H) Quantification of IL-6 protein expression by ELISA. Data represent mean  $\pm$  SD from three independent experiments. \*\* $P$  < 0.01, \*\*\* $P$  < 0.005.

(Figure 2B, also known as Merck-544 [33,34]). The impact of LPS and glucocorticoids on IL-6 protein expression was assessed by ELISA. Increased IL-6 protein was observed upon treatment of cells with LPS, whereby the effect on protein expression was more pronounced than the effect on mRNA levels, suggesting enhanced translation and/or protein stability in addition to enhanced gene expression. Importantly, both preincubation with corticosterone and 11-dehydrocorticosterone further increased IL-6 expression, whereby the effect of the latter was blocked by 11 $\beta$ -HSD1 inhibitors (Figure 2C). In the absence of LPS, incubation of BV-2 cells with 25 nM corticosterone and 50 nM 11-dehydrocorticosterone both enhanced IL-6 expression. As expected, the effect of 11-dehydrocorticosterone was abolished by 11 $\beta$ -HSD1 inhibition.

#### MR and GR differentially modulate the IL-6 expression

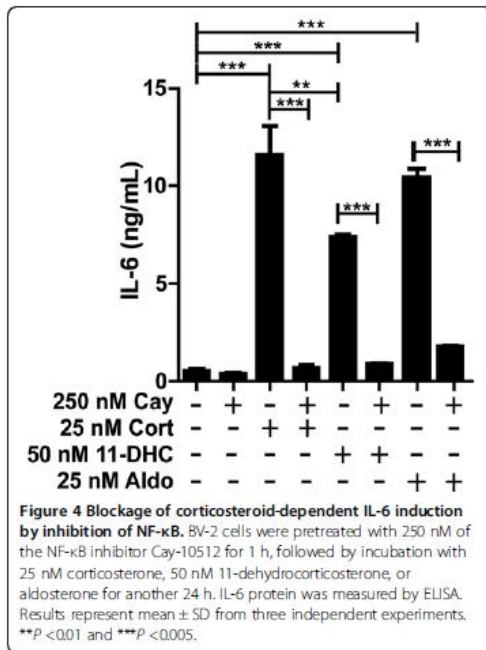
Since glucocorticoids are known as potent anti-inflammatory drugs, we next determined the concentration dependence of IL-6 expression and compared the effects of 11-dehydrocorticosterone, corticosterone, and dexamethasone. The potent GR agonist dexamethasone suppressed IL-6 mRNA and protein expression in a concentration-dependent manner (Figure 3A, B). Unlike the GR-selective ligand dexamethasone, 11-dehydrocorticosterone (upon conversion to corticosterone by 11 $\beta$ -HSD1) showed a bi-phasic response with peak stimulatory effects at about 50 nM and potent suppression at concentrations higher than 250 nM. Neither spironolactone nor RU-486 at a concentration of 1  $\mu$ M inhibited 11 $\beta$ -HSD1 enzyme activity (measured as conversion of radiolabeled cortisone to cortisol in cell lysates). At 20  $\mu$ M, spironolactone showed weak inhibition with 78  $\pm$  14% remaining activity, and in the presence of RU-486 remaining activity was 69  $\pm$  9%, thus excluding that the observed effects of the antagonists on IL-6 expression were due to 11 $\beta$ -HSD1 inhibition. A similar bi-phasic response, with maximal stimulation at 25 nM, was obtained using corticosterone. The stimulatory effect, but not the suppressive effect, could be prevented by co-treatment with the MR antagonist spironolactone (Figure 3C). The bi-phasic response to corticosterone of IL-6 expression and suppression by spironolactone was confirmed on the protein level using ELISA (Figure 3D). High corticosterone concentrations, that is 250 nM, decreased IL-6 protein levels. The GR antagonist RU-486 did not affect the corticosterone-induced stimulation of IL-6 mRNA and protein expression. Importantly, at 250 nM corticosterone, which suppressed IL-6 expression, co-incubation with RU-486 caused an increase in IL-6 mRNA and protein expression (Figure 3C, D). This suggests that at higher glucocorticoid concentrations GR prevents MR-mediated activation of IL-6 production and that GR blockade

results in pronounced MR-mediated stimulation of production of pro-inflammatory cytokines. Dexamethasone did not affect IL-6 mRNA expression at 100 nM but resulted in a decrease at higher concentrations (Figure 3E). Interestingly, IL-6 protein production was significantly decreased at 100 nM dexamethasone (Figure 3F), suggesting an inhibition of IL-6 translation or decreased protein stability. The reason for the high concentration of dexamethasone needed to suppress IL-6 expression remains unclear; however, since intact cells were used, an efflux pump may be involved. As expected, spironolactone did not affect the dexamethasone-mediated effects (data not shown), whereas they were reversed by RU-486 (Figure 3E, F). Opposite effects were obtained upon incubation of BV-2 cells with the MR ligand aldosterone, which induced IL-6 mRNA and protein expression, whereby these effects were fully reversed by co-treatment with spironolactone (Figure 3G, H).

#### Effect of corticosteroids on IL-6 expression is mediated through NF- $\kappa$ B

Next, we tested whether the stimulation of IL-6 production by low/moderate concentrations of 11-dehydrocorticosterone, corticosterone, and aldosterone is dependent on NF- $\kappa$ B activation. Treatment of cells with the NF- $\kappa$ B translocation inhibitor Cay-10512 diminished the corticosteroid-mediated IL-6 production (Figure 4), suggesting that MR-dependent activation of NF- $\kappa$ B is involved in the stimulation of IL-6 expression. To visualize NF- $\kappa$ B activation, immune-fluorescence staining using antibody against the p65 subunit of NF- $\kappa$ B was performed. As shown in Figure 5, incubation of cells with 25 nM corticosterone or 25 nM aldosterone enhanced the presence of p65 in the nuclei, whereby the corticosteroid-induced NF- $\kappa$ B translocation could be prevented by co-treatment with either spironolactone or Cay-10512.

The MR-dependent NF- $\kappa$ B activation was further analyzed by determination of the distribution of p65 using Cellomics ArrayScan high-content imaging (Figure 6). Incubation with aldosterone enhanced the presence of p65 in the nucleus, an effect that was blocked by spironolactone. In contrast, incubation with dexamethasone diminished the presence of p65 in the nucleus, and co-incubation with the GR antagonist RU-486 prevented this effect. The subcellular distribution of p65 was further assessed by western blot analysis of cytoplasmic and nuclear fractions of BV-2 cells. Incubation of cells in the presence of corticosterone or aldosterone led to elevated amounts of the phosphorylated form of p65 in the nucleus, an effect that was prevented by co-treatment with spironolactone (Figure 7A) or Cay-10512 (Figure 7B).



#### Differential modulation of TNFR2 expression by MR and GR

The sensitivity of microglia cells to pro-inflammatory cytokines such as TNF- $\alpha$  is dependent, among other factors, on the expression levels of membrane surface receptors like TNFR2 that control intracellular signaling pathways. As observed for IL-6 expression, low/moderate concentrations of corticosterone, that is 25 nM and 50 nM, induced TNFR2 mRNA expression but high concentrations of 250 nM or higher decreased its expression (Figure 8A). The induction by low/moderate corticosterone was reversed by co-treatment with the MR antagonist spironolactone, whereas GR antagonist RU-486 abolished the suppressive effect of high corticosterone. The selective GR ligand dexamethasone had an opposite effect with a concentration-dependent suppression of TNFR2 mRNA expression that was reversed by co-incubation with RU-486 (Figure 8B). As observed for low corticosterone, TNFR2 mRNA expression was induced upon treatment with aldosterone (Figure 8C). The induction of TNFR2 expression by corticosterone (50 nM) and aldosterone (25 nM) was confirmed on the protein level by western blotting (Figure 8D). Moreover, we found that the inhibitor of NF- $\kappa$ B translocation Cay-10512 was able to completely abolish the induction of TNFR2 mRNA expression by IL-6, low/moderate glucocorticoids or aldosterone (Figure 8C). Western blotting revealed the potentiation of TNFR2 protein expression by 50 nM

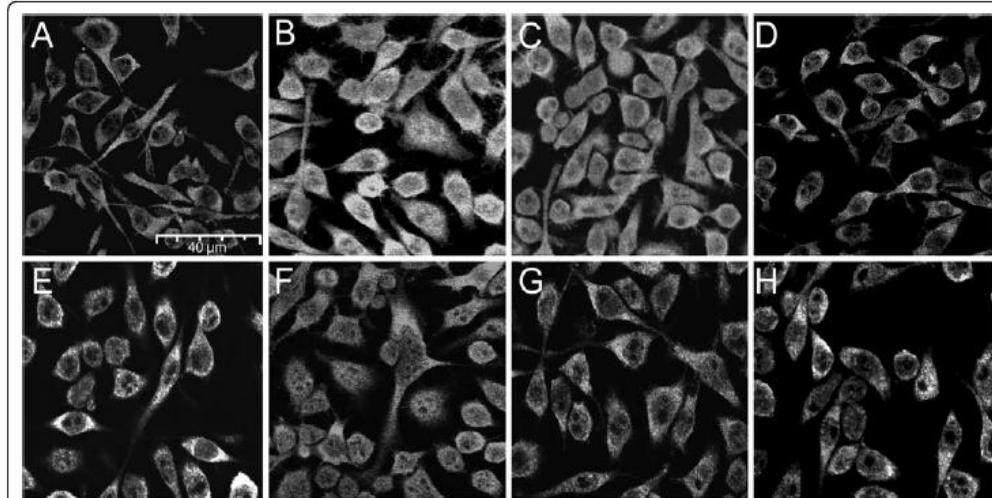
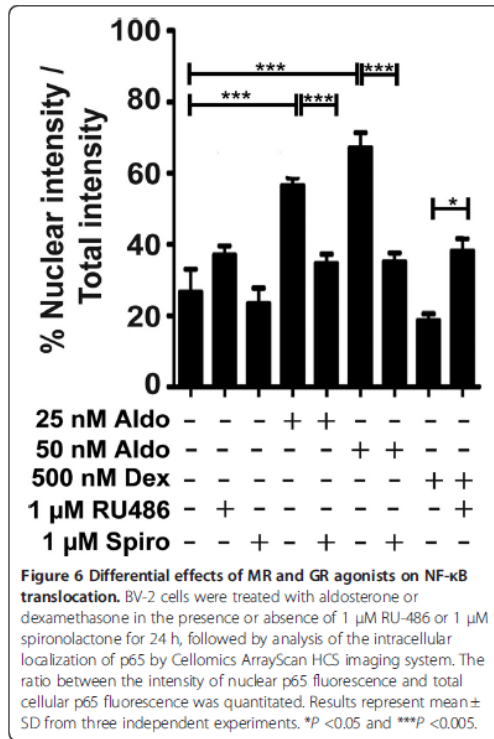


**Figure 5 Corticosterone- and aldosterone-mediated NF- $\kappa$ B translocation is dependent on MR.** BV-2 cells were treated for 24 h with vehicle (A), 50 ng/mL TNF- $\alpha$  (B), 25 nM corticosterone (C), 25 nM corticosterone and 1  $\mu$ M spironolactone (D), 25 nM corticosterone and 250 nM Cay-10512 (E), 50 nM aldosterone (F), 50 nM aldosterone and 1  $\mu$ M spironolactone (G), or 50 nM aldosterone and 250 nM Cay-10512 (H). The localization of the p65 subunit of NF- $\kappa$ B was visualized by immunofluorescence microscopy using a primary antibody against p65 and a secondary ALEXA fluor 488 labeled antibody (magnification 400 $\times$ ).

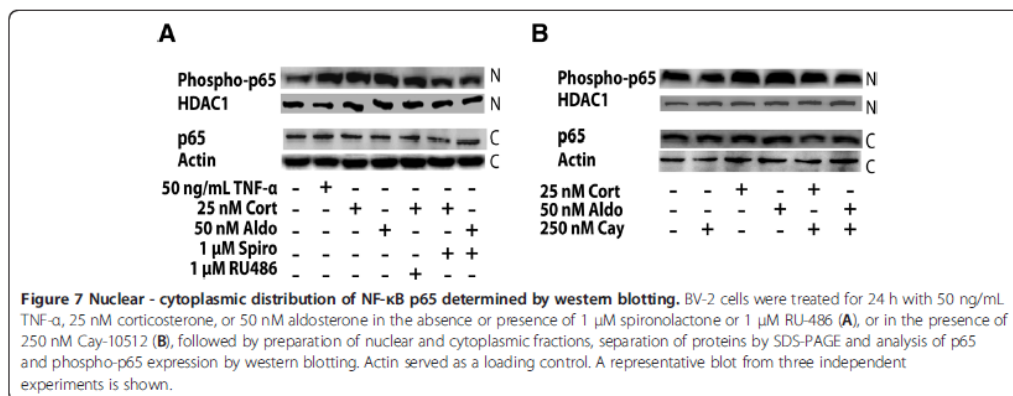


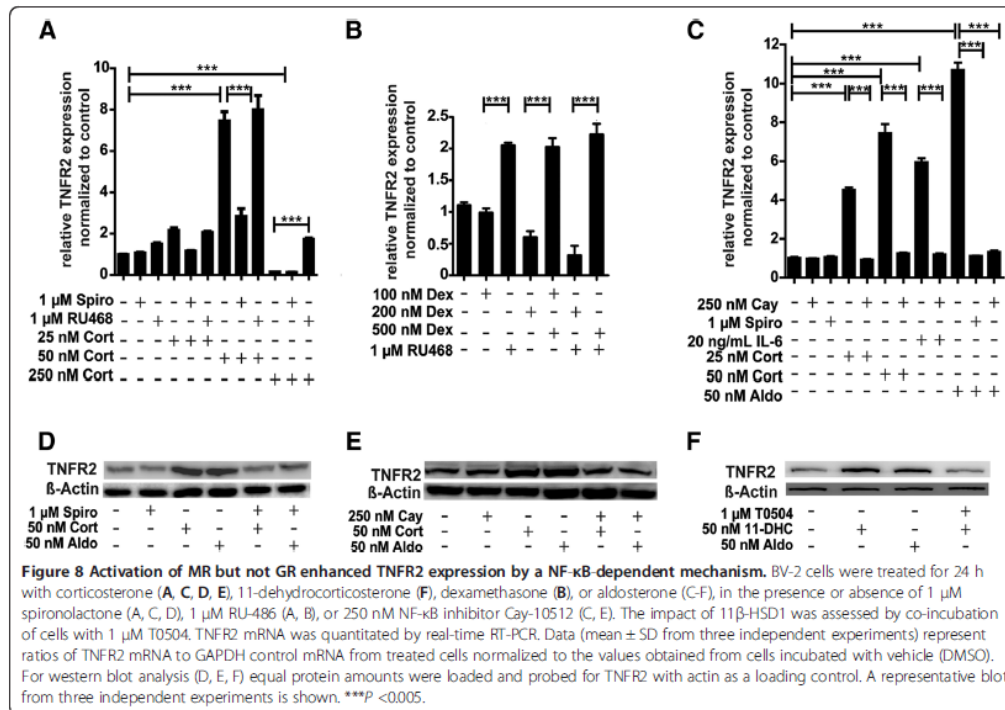
corticosterone and 50 nM aldosterone, and further demonstrated the requirement of NF-κB activation for this induction (Figure 8E). 11-dehydrocorticosterone similarly induced TNFR2 expression, which was prevented by inhibition of 11β-HSD1 (Figure 8F).

**IL-6 and low glucocorticoids synergistically increased 11β-HSD1 mRNA expression and reductase activity**

Glucocorticoids showed a bi-phasic effect on the production of pro-inflammatory cytokines, depending on activation of MR only, at low concentrations, or both MR and GR at higher concentrations. Thus, an elevation of the intracellular concentration of active glucocorticoids by 11β-HSD1 may play an important role in the resolution of inflammation by causing a shift from MR- to GR-mediated regulation of pro-inflammatory cytokine expression. As shown in Figure 9, incubation of BV-2 cells with 20 ng/mL of IL-6 resulted in increased 11β-HSD1 mRNA expression, which was strongly enhanced by co-incubation with 50 nM 11-dehydrocorticosterone. Pharmacological inhibition of 11β-HSD1 prevented the effects of 11-dehydrocorticosterone. To test whether incubation with IL-6 would enhance 11β-HSD1 enzyme activity, we measured the conversion of radiolabeled cortisone to cortisol. Due to technical reasons cortisone instead of 11-dehydrocorticosterone was used to study the effect on enzyme activity. Both IL-6 and cortisone resulted in increased 11β-HSD1 reductase activity, which was strongly enhanced by co-incubation with IL-6 and cortisone (data not shown), indicating that the changes observed on the mRNA level are translated to enzyme activity.

Interestingly, while low corticosterone in the absence of IL-6 showed weak stimulatory effects on 11β-HSD1 expression, higher concentrations resulted in a more pronounced induction of expression (Figure 10). Spironolactone and RU-486 both were able to block the induction of 11β-HSD1 expression. Both, treatment of cells with aldosterone and dexamethasone enhanced 11β-HSD1 mRNA expression. Together with the fact that low and high glucocorticoid concentrations led to increased 11β-HSD1 expression, the results suggest a feed-forward regulation including both MR and GR.





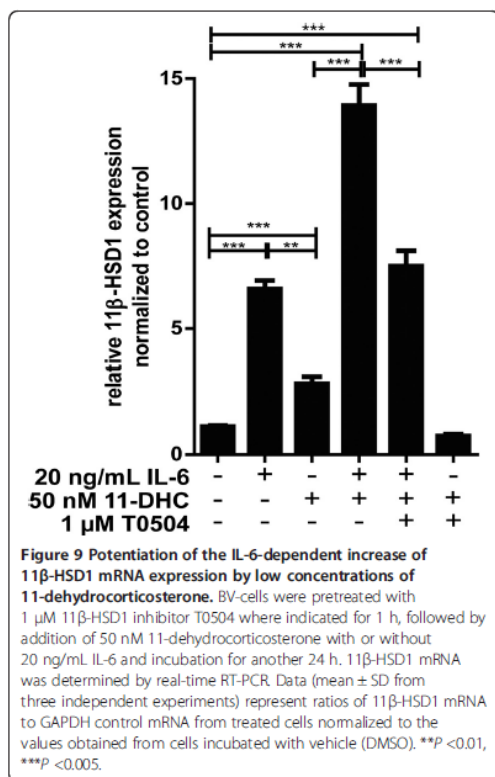
## Discussion

A recent comparison of the murine BV-2 cell line with primary mouse microglia cells revealed highly overlapping gene expression profiles upon stimulation with LPS, although the response in BV-2 was generally less pronounced [25]. Approximately 90% of the genes induced by LPS in BV-2 cells were also induced in primary microglia, and 50% of the genes were also affected in hippocampal microglia following *in-vivo* stimulation of mice by intracerebroventricular LPS injection. These observations indicate that the BV-2 cell line is a suitable model of murine microglia to study neuroinflammatory parameters.

In the present study, we employed BV-2 cells as a macrophage/microglia cell model to characterize the impact of endogenous and synthetic corticosteroids on NF- $\kappa$ B activation and on IL-6 and TNFR2 expression. We found that BV-2 cells functionally express MR, GR, and 11 $\beta$ -HSD1, and our results emphasize the importance of a well-balanced activity of MR, which stimulates pro-inflammatory mediators, and GR that counteracts these effects. The selective MR ligand aldosterone exclusively resulted in NF- $\kappa$ B activation and upregulation of IL-6 and TNFR2 expression, whereas the selective GR ligand

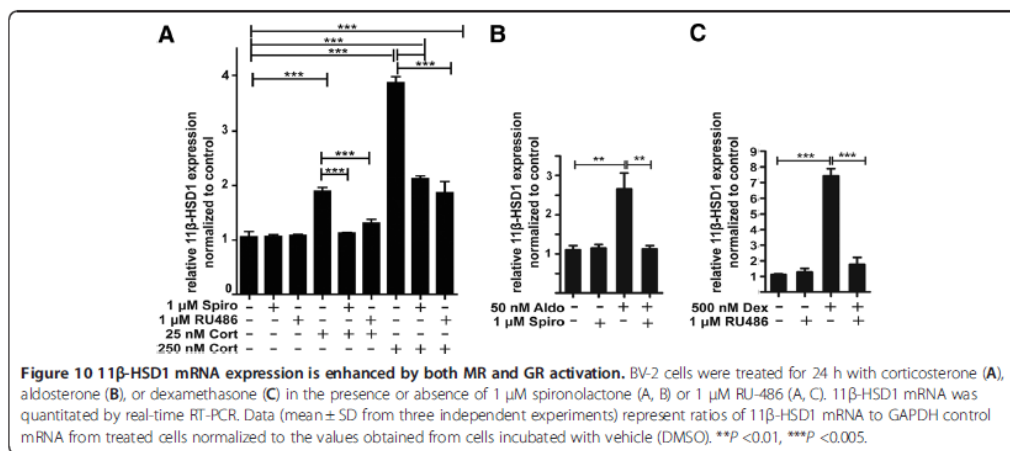
dexamethasone had opposite effects. The concentration of aldosterone to activate MR in BV-2 cells was approximately one order of magnitude higher than anticipated based on its  $K_d$  of about 0.5 nM. The effect on mRNA levels was more pronounced than that on protein expression, indicating increased translation and/or protein stability. Similar observations were made using dexamethasone, for which  $K_d$  values for GR of 3–4 nM have been reported [5,35]. While 100 nM dexamethasone readily suppressed IL-6 protein it had no effect on mRNA expression. As a possible explanation an efflux pump expressed in BV-2 cells may lower the actual intracellular concentration of aldosterone and dexamethasone.

Corticosterone and 11-dehydrocorticosterone (upon conversion to corticosterone by 11 $\beta$ -HSD1) stimulated the expression of IL-6 and TNFR2 and activated NF- $\kappa$ B at low/moderate concentrations by acting through MR, whereas higher concentrations exerted suppressive effects by acting through GR. Over 95% of the circulating corticosterone is bound to transcortin and albumin. Under normal conditions peak corticosterone concentrations in mice and rats in the unstressed state range between 250 nM and 500 nM, thus assuming that the free fraction in plasma reaches concentrations up to 25 nM.



The intracellular concentrations may differ significantly from this value depending on uptake and 11β-HSD-dependent metabolism. In the presented experiments, we used 25 nM as a low and 250 nM as a high corticosterone concentration in culture medium containing 10% FBS. Despite the reduced amount of serum proteins present in the culture medium, the capacity should be sufficient to bind most of the 25 nM corticosterone added, probably resulting in a free steroid concentration below 2 nM. Nevertheless, the MR with a  $K_d$  of 0.5 nM for corticosterone is expected to be occupied, whereas the GR with a  $K_d$  of 5 to 10 nM is probably not activated, thus reflecting the situation under normal physiological conditions. In contrast, at 250 nM the binding capacity of the FBS present in the culture medium is probably saturated, resulting in high unbound corticosterone levels, reflecting levels reached during stress conditions and leading to occupation of GR.

Upon further increasing corticosterone from concentrations needed for maximal induction of IL-6 expression, a rapid decline was observed (Figure 3A, B). This may be explained by the higher expression levels of GR compared with MR, suggesting that occupation of few GR molecules may be sufficient to suppress MR activity. It is not clear at present whether GR suppresses MR function by competing for coactivators/corepressors, by competing for binding sites on the promoter of a given target gene, or by formation of heterodimers. Interestingly, RU-486 enhanced IL-6 and TNFR2 expression in the absence of added steroids (Figure 3E, Figure 8B). In preliminary experiments using transfected cells, we observed ligand-independent MR activity that was lowered upon co-expressing GR. RU-486 might act as an inverse agonist and induce a conformational change upon binding to GR, which may prevent heterodimer



formation or, alternatively, GR may compete with MR for a corepressor protein, thereby increasing MR activity.

Nevertheless, the results suggest a tightly controlled and coordinated action of MR and GR in the regulation of NF- $\kappa$ B activity and the production of and sensitivity to pro-inflammatory cytokines in microglia cells. Pro-inflammatory cytokines such as TNF- $\alpha$ , IL-1 $\beta$ , and IL-6, and subsequent activation of NF- $\kappa$ B, lead to elevated expression and activity of 11 $\beta$ -HSD1, which results in enhanced local levels of active glucocorticoids (this study, and [18]). The fact that both GR and MR promote 11 $\beta$ -HSD1 expression may represent an important feed-forward regulation of glucocorticoid activation in order to increase the intracellular concentration of active glucocorticoids and to shift the balance from an initially predominantly MR-mediated stimulation to a GR-mediated suppression of inflammation. The enhanced local glucocorticoid activation may be necessary for the resolution of inflammation. The suppression of pro-inflammatory cytokines and NF- $\kappa$ B activity upon activation of GR should then allow normalization of 11 $\beta$ -HSD1 expression and activity.

Evidence for a stimulation of inflammatory parameters by low to moderate glucocorticoid concentrations was also obtained from recent experiments with murine 3 T3-L1 adipocytes [1]. Decreased adiponectin mRNA and increased IL-6 mRNA were observed upon incubation of 3 T3-L1 adipocytes with 100 nM corticosterone or cortisol. These effects were partially reversed by treatment with the MR antagonist eplerenone but not by GR antagonist RU486, suggesting that MR activation was responsible for the observed effects. Furthermore, 100 nM of the glucocorticoids increased NADPH oxidase subunit p22 mRNA levels and decreased catalase mRNA levels, which were reversed by co-treatment with eplerenone. However, the authors did not test the effects of various concentrations, nor was the role of 11 $\beta$ -HSD1 addressed.

Other investigators observed elevated 11 $\beta$ -HSD1 mRNA and activity in 3 T3-L1 adipocytes that were treated with LPS, TNF- $\alpha$ , or IL-1 $\beta$  [2]. Pharmacological inhibition of 11 $\beta$ -HSD1 diminished the TNF- $\alpha$ -induced activation of NF- $\kappa$ B and MAPK signaling. Their study, however, did not assess the role of MR and the impact of higher glucocorticoid concentrations. At high glucocorticoid levels, pharmacological inhibition of 11 $\beta$ -HSD1 might abolish GR activation, thereby promoting MR-mediated pro-inflammatory effects. Since actual glucocorticoid concentrations in intact microglia cannot be measured, it will be important to assess the effects of 11 $\beta$ -HSD1 inhibitors on neuroinflammation *in vivo* in future studies. Nevertheless, these observations are in line with our findings in microglia cells that low/moderate

glucocorticoid concentrations mainly act through MR, thereby promoting inflammatory parameters.

During acute inflammation, TNF- $\alpha$  acts through membrane-bound TNF-receptors on macrophage and microglial cells, leading to activation of transcription factors such as NF- $\kappa$ B and AP1, which can induce a second wave of pro-inflammatory cytokines, including TNF- $\alpha$ , IL-1 $\beta$  and IL-6. TNFR2 is highly expressed on microglia cells and plays an important role in the regulation of innate immune response following brain injury on infection [36]. An elevated expression of TNFR2 upon MR activation, as observed in the present study, is expected to result in a higher sensitivity and more pronounced response to external pro-inflammatory stimuli.

Disruption of MR- and GR-mediated regulation of gene transcription and interaction with other transcription factors can occur at several levels. Reduced GR activity and/or enhanced MR activity, thus exacerbating inflammation, may be caused by the presence of xenobiotics differentially modulating receptor activity, post-translational receptor modifications, altered function of receptor-associated proteins, or altered protein stability

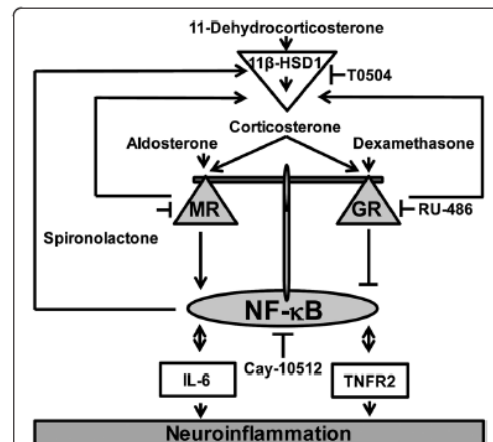


**Figure 11 Model for the role of MR and GR in regulating neuroinflammation in BV-2 cells.** This study suggests that MR promotes a neuroinflammatory response mediated through NF- $\kappa$ B activation, which can be blocked by activation GR. The control of local glucocorticoid availability by 11 $\beta$ -HSD1 is important in regulating the fine-tuning of the balance between MR and GR activity. Corticosterone binds with high affinity to MR, followed by binding to GR with lower affinity. 11 $\beta$ -HSD1 inhibitors (such as T0504) block the differential effects of 11-dehydrocorticosterone on MR and GR. IL-6 stimulated 11 $\beta$ -HSD1 expression, suggesting that IL-6 is involved in a regulatory feed-forward mechanism to adjust the local levels of active glucocorticoids and therefore the balance between MR and GR. IL-6 and TNFR2 activation both lead to the activation of NF- $\kappa$ B, and their own expression is upregulated upon NF- $\kappa$ B activation.

[30]. The pro-inflammatory cytokines TNF- $\alpha$ , IL-1 $\beta$ , and IL-6 were shown to activate the HPA axis [37], thereby enhancing circulating glucocorticoids and exerting suppressive effects through GR activation. However, high levels of TNF- $\alpha$  have been associated with glucocorticoid resistance [38]. Upon excessive HPA activation, a down-regulation of GR activity, probably caused by altered phosphorylation of the receptor and reduced protein stability [38,39], with concomitant glucocorticoid resistance has been observed, which may cause a shift from GR- to MR-mediated glucocorticoid effects. GR blockade by administration of RU486 or elimination of glucocorticoids by adrenalectomy sensitized C57BL/6 mice to low-dose TNF- $\alpha$  [38]. Moreover, hepatic GR-deficient mice showed significantly higher levels of IL-6 in response to TNF- $\alpha$  treatment.

Glucocorticoid-resistance represents a major problem in chronic inflammation, including rheumatoid arthritis, ulcerative colitis, Crohn's disease, atherosclerosis, cystic fibrosis, and chronic obstructive pulmonary disease [40]. An impaired suppression by GR may lead to chronically enhanced MR activity. It remains to be investigated whether MR antagonists may prove beneficial in these diseases.

Increasing evidence indicates that neuroinflammation contributes to neuronal degeneration and the progression of Parkinson's disease [41,42]. Activated microglial cells and increased expression of pro-inflammatory mediators have been found in the substantia nigra of patients. Interestingly, elevated circulating cortisol levels were measured in Parkinson's disease patients together with decreased GR expression in the substantia nigra [43]. Selective ablation of GR in macrophage/microglia exacerbated the loss of dopaminergic neurons induced by 1-methyl-4-phenyl-1,2,3,6-tetrahydropyridine (MPTP), enhanced the production of pro-inflammatory parameters, and diminished the expression of anti-inflammatory mediators. Based on the findings of the present study, we hypothesize that the potentiation of neuroinflammation in GR-deficient states is due to an impaired balance of pro- and anti-inflammatory mediators as a result of a dysbalance of MR and GR activity. The role of MR in Parkinson's disease and whether MR antagonists may prove useful in the treatment of this disease remain to be investigated.

## Conclusions

BV-2 cells represent a suitable microglia cell model for studying effects of endogenous and synthetic corticosteroids on inflammatory parameters (Figure 11). These cells co-express MR and GR, which differentially modulate NF- $\kappa$ B activity, the production of pro-inflammatory cytokines and membrane-surface receptors involved in the sensitivity to TNF- $\alpha$ . The availability of active endogenous glucocorticoids in these cells is tightly

controlled by 11 $\beta$ -HSD1, whose expression and activity is induced by pro-inflammatory cytokines and subsequent NF- $\kappa$ B activation. By enhancing intracellular concentrations of active glucocorticoids, 11 $\beta$ -HSD1 impacts on the balanced regulation of MR- and GR-mediated responses and may play a crucial role in resolution of inflammation. Impaired function of each of the three proteins is expected to cause disturbed inflammation.

## Additional file

**Additional file 1: Table S1.** Real-time PCR primers.

## Abbreviations

11 $\beta$ -HSD1: 11 $\beta$ -hydroxysteroid dehydrogenase 1; BCA: Bicinchoninic acid; DEPC: Diethyl pyrocarbonate; DMEM: Dulbecco's Modified Eagle Medium; DMSO: Dimethyl sulfoxide; DTT: Dithiothreitol; ELISA: Enzyme-linked immunosorbent assay; FBS: Fetal bovine serum; GAPDH: Glyceraldehyde 3-phosphate dehydrogenase; GR: Glucocorticoid receptor; HCS: High-content screening; HDAC-1: Histone deacetylase 1; HEPES: 4-(2-hydroxyethyl)-1-piperazineethanesulfonic acid; HRP: Horseradish peroxidase; IL-6: Interleukin-6; LPS: Lipopolysaccharide; MR: Mineralocorticoid receptor; NF- $\kappa$ B: Nuclear factor kappa-light-chain-enhancer of activated B cells; PBS: Phosphate buffered saline; PVDf: Polyvinylidene difluoride; SDS-PAGE: Sodium dodecyl sulfate polyacrylamide gel electrophoresis; TNF- $\alpha$ : Tumor necrosis factor-alpha; TNFR2: Tumor necrosis factor receptor 2.

## Competing interests

The authors declare that they have no competing interests.

## Authors' contribution

BC and AO designed the study. BC performed the experiments and analyzed the data. DK, LN, and ZB helped planning experiments and analyzing the data. BC, DK, and AO wrote the manuscript. All authors read and approved the final manuscript.

## Acknowledgements

This work was supported by the Swiss National Science Foundation (31003A-140961 and 316030-133859). AO has a Chair for Molecular and Systems Toxicology by the Novartis Research Foundation.

Received: 12 June 2012 Accepted: 14 November 2012

Published: 28 November 2012

## References

- Hirata A, Maeda N, Nakatsuji H, Hiuge-Shimizu A, Okada T, Funahashi T, Shimomura I: **Contribution of glucocorticoid-mineralocorticoid receptor pathway on the obesity-related adipocyte dysfunction.** *Biochem Biophys Res Commun* 2012, **419**:182-187.
- Ishii-Yonemoto T, Masuzaki H, Yasue S, Okada S, Kozuka C, Tanaka T, Noguchi M, Tomita T, Fujikura J, Yamamoto Y, Ebihara K, Hosoda K, Nakao K: **Glucocorticoid reamplification within cells intensifies NF- $\kappa$ B and MAPK signaling and reinforces inflammation in activated preadipocytes.** *Am J Physiol Endocrinol Metab* 2010, **298**:E930-E940.
- Marzolla V, Armani A, Zennaro MC, Cinti F, Mammi C, Fabbri A, Rosano GM, Caprio M: **The role of the mineralocorticoid receptor in adipocyte biology and fat metabolism.** *Mol Cell Endocrinol* 2012, **350**:281-288.
- De Kloet ER, Vreugdenhil E, Oitzl MS, Joels M: **Brain corticosteroid receptor balance in health and disease.** *Endocr Rev* 1998, **19**:269-301.
- De Kloet ER, Veldhuis HD, Wagenaars JL, Bergink EW: **Relative binding affinity of steroids for the corticosterone receptor system in rat hippocampus.** *J Steroid Biochem Mol Biol* 1984, **21**:173-178.
- Reul JM, de Kloet ER: **Two receptor systems for corticosterone in rat brain: microdistribution and differential occupation.** *Endocrinology* 1985, **117**:2505-2511.

7. Reul JM, van den Bosch FR, de Kloet ER: **Relative occupation of type-I and type-II corticosteroid receptors in rat brain following stress and dexamethasone treatment: functional implications.** *J Endocrinol* 1987, **115**:459-467.
8. Sapolsky RM, Romero LM, Munck AU: **How do glucocorticoids influence stress responses? Integrating permissive, suppressive, stimulatory, and preparative actions.** *Endocr Rev* 2000, **21**:55-89.
9. Funder JW: **Mineralocorticoid receptors in the central nervous system.** *J Steroid Biochem Mol Biol* 1996, **56**:179-183.
10. Cintra A, Bhatnagar M, Chadi G, Tinner B, Lindberg J, Gustafsson JA, Agnati LF, Fuxe K: **Glial and neuronal glucocorticoid receptor immunoreactive cell populations in developing, adult, and aging brain.** *Ann N Y Acad Sci USA* 1994, **746**:42-61.
11. Odermatt A, Kratschmar DV: **Tissue-specific modulation of mineralocorticoid receptor function by 11beta-hydroxysteroid dehydrogenases: an overview.** *Mol Cell Endocrinol* 2012, **350**:168-186.
12. Edwards CR, Stewart PM, Burt D, Brett L, Mdnityre MA, Sutanto WS, de Kloet ER, Monder C: **Localisation of 11 beta-hydroxysteroid dehydrogenase-tissue specific protector of the mineralocorticoid receptor.** *Lancet* 1988, **2**:986-989.
13. Funder JW, Pearce PT, Smith R, Smith AL: **Mineralocorticoid action: target tissue specificity is enzyme, not receptor, mediated.** *Science* 1988, **242**:583-585.
14. Odermatt A, Arnold P, Frey FJ: **The intracellular localization of the mineralocorticoid receptor is regulated by 11beta-hydroxysteroid dehydrogenase type 2.** *J Biol Chem* 2001, **276**:28484-28492.
15. Ferrati P: **The role of 11beta-hydroxysteroid dehydrogenase type 2 in human hypertension.** *Biochim Biophys Acta* 2010, **1802**:1178-1187.
16. Frey FJ, Odermatt A, Frey BM: **Glucocorticoid-mediated mineralocorticoid receptor activation and hypertension.** *Curr Opin Nephrol Hypertens* 2004, **13**:451-458.
17. Mune T, Rogerson FM, Nikkila H, Agarwal AK, White PC: **Human hypertension caused by mutations in the kidney isozyme of 11 beta-hydroxysteroid dehydrogenase.** *Nat Genet* 1995, **10**:394-399.
18. Tischner D, Reichardt HM: **Glucocorticoids in the control of neuroinflammation.** *Mol Cell Endocrinol* 2007, **275**:62-70.
19. Barnes PJ: **Glucocorticosteroids: current and future directions.** *Br J Pharmacol* 2011, **163**:29-43.
20. de Kloet ER, Van Acker SA, Sibug RM, Oitzl MS, Meijer OC, Rahmouni K, de Jong W: **Brain mineralocorticoid receptors and centrally regulated functions.** *Kidney Int* 2000, **57**:1329-1336.
21. Hugin-Flores ME, Steimer T, Aubert ML, Schulz P: **Mineralo- and glucocorticoid receptor mRNAs are differently regulated by corticosterone in the rat hippocampus and anterior pituitary.** *Neuroendocrinology* 2004, **79**:174-184.
22. Groeneweg FL, Karst H, de Kloet ER, Joels M: **Mineralocorticoid and glucocorticoid receptors at the neuronal membrane, regulators of nongenomic corticosteroid signalling.** *Mol Cell Endocrinol* 2012, **350**:299-309.
23. Gottfried-Blackmore A, Sierra A, McEwen BS, Ge R, Bullock K: **Microglia express functional 11 beta-hydroxysteroid dehydrogenase type 1.** *Glia* 2010, **58**:1257-1266.
24. Funder JW: **Aldosterone and mineralocorticoid receptors: a personal reflection.** *Mol Cell Endocrinol* 2012, **350**:146-150.
25. Henn A, Lund S, Hedtjam M, Schratzenholz A, Porzgen P, Leist M: **The suitability of BV2 cells as alternative model system for primary microglial cultures or for animal experiments examining brain inflammation.** *ALTEX* 2009, **26**:83-94.
26. Bocchini V, Mazzolla R, Barluzzi R, Blasi E, Sick P, Kettenmann H: **An immortalized cell line expresses properties of activated microglial cells.** *J Neurosci Res* 1992, **31**:616-621.
27. Blasi E, Barluzzi R, Bocchini V, Mazzolla R, Bistoni F: **Immortalization of murine microglial cells by a v-raf/v-myc carrying retrovirus.** *J Neuroimmunol* 1990, **27**:229-237.
28. Livak KJ, Schmittgen TD: **Analysis of relative gene expression data using real-time quantitative PCR and the 2(-delta delta C(T)) method.** *Methods* 2001, **25**:402-408.
29. Ding GJ, Fischer PA, Boltz RC, Schmidt JA, Colananne JJ, Gough A, Rubin RA, Miller DK: **Characterization and quantitation of NF-kappaB nuclear translocation induced by interleukin-1 and tumor necrosis factor-alpha. Development and use of a high capacity fluorescence cytometric system.** *J Biol Chem* 1998, **273**:28897-28905.
30. Odermatt A, Atanasov AG: **Mineralocorticoid receptors: emerging complexity and functional diversity.** *Steroids* 2009, **74**:163-171.
31. Fiers W, Beyaert R, Brouckaert P, Everaerd B, Haegeman C, Suffers P, Tavemier J, Vanhaesebroeck B: **TNF: its potential as an antitumour agent.** *Dev Biol Stand* 1988, **69**:143-151.
32. Schuster D, Maurer EM, Laggner C, Nashev LG, Wildkens T, Langer T, Odermatt A: **The discovery of new 11beta-hydroxysteroid dehydrogenase type 1 inhibitors by common feature pharmacophore modeling and virtual screening.** *J Med Chem* 2006, **49**:3454-3466.
33. Hemanowski-Vosatka A, Balkovec JM, Cheng K, Chen HY, Hernandez M, Koo GC, Le Grand CB, Li Z, Metzger JM, Mundt SS, Noonan H, Nunes CN, Olson SH, Pikounis B, Ren N, Robertson N, Schaeffer JM, Shah K, Springer MS, Strack AM, Strowski M, Wu K, Wu T, Xiao J, Zhang BB, Wright SD, Thieringer R: **11beta-HSD1 inhibition ameliorates metabolic syndrome and prevents progression of atherosclerosis in mice.** *J Exp Med* 2005, **202**:517-527.
34. Arampatzis S, Kadereit B, Schuster D, Balazs Z, Schweizer RA, Frey FJ, Langer T, Odermatt A: **Comparative enzymology of 11beta-hydroxysteroid dehydrogenase type 1 from six species.** *J Mol Endocrinol* 2005, **35**:89-101.
35. Rebuffat AG, Tam S, Nawrocki AR, Baker ME, Frey BM, Frey FJ, Odermatt A: **The 11-ketosteroid 11-ketodexamethasone is a glucocorticoid receptor agonist.** *Mol Cell Endocrinol* 2004, **214**:27-37.
36. Veroni C, Gabriele L, Canini L, Castiello L, Cocchia E, Remoli ME, Columba-Cabezas S, Arico E, Aloisi F, Agresti C: **Activation of TNF receptor 2 in microglia promotes induction of anti-inflammatory pathways.** *Mol Cell Neurosci* 2010, **45**:234-244.
37. Chrousos GP: **The hypothalamic-pituitary-adrenal axis and immune-mediated inflammation.** *New Engl J Med* 1995, **332**:1351-1362.
38. Van Bogaert T, Vandevyver S, Dejager L, Van Hauwemeiren F, Pinheiro I, Petta I, Engblom D, Kleyman A, Schutz G, Tuckermann J, Libert C: **Tumor necrosis factor inhibits glucocorticoid receptor function in mice: a strong signal toward lethal shock.** *J Biol Chem* 2011, **286**:26555-26567.
39. Van Bogaert T, De Bosscher K, Libert C: **Crosstalk between TNF and glucocorticoid receptor signaling pathways.** *Cytokine Growth F R* 2010, **21**:275-286.
40. Barnes PJ, Adcock IM: **Glucocorticoid resistance in inflammatory diseases.** *Lancet* 2009, **373**:1905-1917.
41. Hirsch EC, Hunot S: **Neuroinflammation in Parkinson's disease: a target for neuroprotection?** *Lancet Neurol* 2009, **8**:382-397.
42. Hirsch EC, Vyas S, Hunot S: **Neuroinflammation in Parkinson's disease.** *Parkinsonism Relat Disord* 2012, **15**:210-221.
43. Ros-Bernal F, Hunot S, Herrero MT, Pamadeau S, Corvol JC, Lu L, Alvarez-Fischer D, Carrillo-de Sauvage MA, Saurini F, Coussieu C, Kinugawa K, Prigent A, Hoglinger G, Harmon M, Tronche F, Hirsch EC, Vyas S: **Microglial glucocorticoid receptors play a pivotal role in regulating dopaminergic neurodegeneration in parkinsonism.** *Proc Natl Acad Sci USA* 2011, **108**:6632-6637.

doi:10.1186/1742-2094-9-260

**Cite this article as:** Chantong et al.: Mineralocorticoid and glucocorticoid receptors differentially regulate NF-kappaB activity and pro-inflammatory cytokine production in murine BV-2 microglial cells. *Journal of Neuroinflammation* 2012 **9**:260.

**Submit your next manuscript to BioMed Central and take full advantage of:**

- Convenient online submission
- Thorough peer review
- No space constraints or color figure charges
- Immediate publication on acceptance
- Inclusion in PubMed, CAS, Scopus and Google Scholar
- Research which is freely available for redistribution

Submit your manuscript at  
[www.biomedcentral.com/submit](http://www.biomedcentral.com/submit)



## CHAPTER 3

**Virtual screening as a strategy for the identification of xenobiotics disrupting corticosteroid action**

# Virtual Screening as a Strategy for the Identification of Xenobiotics Disrupting Corticosteroid Action

Lyubomir G. Nashev<sup>1‡</sup>, Anna Vuorinen<sup>2‡</sup>, Lukas Praxmarer<sup>2</sup>, Boonrat Chantong<sup>1</sup>, Diego Cereghetti<sup>1</sup>, Rahel Winiger<sup>1</sup>, Daniela Schuster<sup>2\*</sup>, Alex Odermatt<sup>1\*</sup>

**1** Swiss Center for Applied Human Toxicology and Division of Molecular and Systems Toxicology, Department of Pharmaceutical Sciences, University of Basel, Basel, Switzerland, **2** Institute of Pharmacy/Pharmaceutical Chemistry and Center for Molecular Biosciences Innsbruck – CMBI, University of Innsbruck, Innsbruck, Austria

## Abstract

**Background:** Impaired corticosteroid action caused by genetic and environmental influence, including exposure to hazardous xenobiotics, contributes to the development and progression of metabolic diseases, cardiovascular complications and immune disorders. Novel strategies are thus needed for identifying xenobiotics that interfere with corticosteroid homeostasis. 11 $\beta$ -hydroxysteroid dehydrogenase 2 (11 $\beta$ -HSD2) and mineralocorticoid receptors (MR) are major regulators of corticosteroid action. 11 $\beta$ -HSD2 converts the active glucocorticoid cortisol to the inactive cortisone and protects MR from activation by glucocorticoids. 11 $\beta$ -HSD2 has also an essential role in the placenta to protect the fetus from high maternal cortisol concentrations.

**Methods and Principal Findings:** We employed a previously constructed 3D-structural library of chemicals with proven and suspected endocrine disrupting effects for virtual screening using a chemical feature-based 11 $\beta$ -HSD pharmacophore. We tested several *in silico* predicted chemicals in a 11 $\beta$ -HSD2 bioassay. The identified antibiotic lasalocid and the silane-coupling agent AB110873 were found to concentration-dependently inhibit 11 $\beta$ -HSD2. Moreover, the silane AB110873 was shown to activate MR and stimulate mitochondrial ROS generation and the production of the proinflammatory cytokine interleukin-6 (IL-6). Finally, we constructed a MR pharmacophore, which successfully identified the silane AB110873.

**Conclusions:** Screening of virtual chemical structure libraries can facilitate the identification of xenobiotics inhibiting 11 $\beta$ -HSD2 and/or activating MR. Lasalocid and AB110873 belong to new classes of 11 $\beta$ -HSD2 inhibitors. The silane AB110873 represents to the best of our knowledge the first industrial chemical shown to activate MR. Furthermore, the MR pharmacophore can now be used for future screening purposes.

**Citation:** Nashev LG, Vuorinen A, Praxmarer L, Chantong B, Cereghetti D, et al. (2012) Virtual Screening as a Strategy for the Identification of Xenobiotics Disrupting Corticosteroid Action. PLoS ONE 7(10): e46958. doi:10.1371/journal.pone.0046958

**Editor:** Kang Sun, Fudan University, China

**Received:** May 17, 2012; **Accepted:** September 6, 2012; **Published:** October 4, 2012

**Copyright:** © 2012 Nashev et al. This is an open-access article distributed under the terms of the Creative Commons Attribution License, which permits unrestricted use, distribution, and reproduction in any medium, provided the original author and source are credited.

**Funding:** This work was supported by the Swiss National Science Foundation (No. 31003A-124912, <http://www.snf.ch>) and the Swiss Center for Applied Human Toxicology ([www.scaht.org](http://www.scaht.org)). A.O. has a Chair for Molecular and Systems Toxicology by the Novartis Research Foundation. D.S. and A.V. are grateful for their Young Talents Grants from the University of Innsbruck (Nachwuchsförderung). The funders had no role in study design, data collection and analysis, decision to publish, or preparation of the manuscript.

**Competing Interests:** The authors have declared that no competing interests exist.

\* E-mail: [daniela.schuster@uibk.ac.at](mailto:daniela.schuster@uibk.ac.at) (DS); [alex.odermatt@unibas.ch](mailto:alex.odermatt@unibas.ch) (AO)

‡ These authors contributed equally to this work.

## Introduction

Several chemicals used in agriculture and industrial production, in body care products, as food preservatives or pharmaceuticals, have been found to interfere with endocrine regulation [1,2]. Numerous endocrine disrupting chemicals (EDCs) affecting sex steroid receptor activity have been described [3,4,5]. There is less known, however, on EDCs acting on corticosteroid homeostasis by disrupting the function of glucocorticoid receptors (GR), mineralocorticoid receptors (MR) or glucocorticoid metabolizing enzymes [6,7].

Excessive MR activation, particularly when combined with high-salt diet, has been associated with renal inflammation, fibrosis, mesangial cell proliferation and podocyte injury [8]. Elevated MR activation due to enhanced local corticosteroid synthesis and impaired glucocorticoid inactivation by 11 $\beta$ -HSD2 have been associated with cardiovascular diseases [9,10]. Importantly, clinical studies demonstrated a reduced morbidity and mortality in patients

with acute myocardial infarction upon treatment with selective MR antagonists [10,11]. MR is also expressed in different types of neuronal cells, and impaired MR activity has been associated with disturbed cognitive functions and behavior [12,13].

On a cellular level, MR and GR activities are tightly regulated by 11 $\beta$ -HSD1 and 11 $\beta$ -HSD2 (Fig. 1), catalyzing the interconversion of inactive 11-ketoglucocorticoids (cortisone, 11-dehydrocorticosterone) and active 11 $\beta$ -hydroxyglucocorticoids (cortisol, corticosterone) [14]. Glucocorticoids and mineralocorticoids can bind with comparable affinities to MR. It is postulated that 11 $\beta$ -HSD2-dependent inactivation of 11 $\beta$ -hydroxyglucocorticoids protects MR from undesired activation by cortisol [15,16]. Patients with loss-of-function mutations in the gene encoding 11 $\beta$ -HSD2 suffer from apparent mineralocorticoid excess, with hypokalemia, hypernatremia and severe hypertension [17,18]. Inhibition of 11 $\beta$ -HSD2 by the licorice constituent glycyrrhetic acid can lead to

undesired cortisol-dependent MR activation [19]. Furthermore, studies with human placentas and animal studies have shown that inhibition of placental 11 $\beta$ -HSD2 by carbenoxolone leads to enhanced fetal glucocorticoid exposure, ultimately causing impaired metabolic and cardiovascular functions in the adulthood of the offspring [20,21]. Recently, Deuchar et al. reported an increased progression of atherosclerosis in apolipoprotein E<sup>-/-</sup>/11 $\beta$ -HSD2<sup>-/-</sup> double knock-out mice [22], whereby the MR antagonist eplerenone significantly decreased plaque formation and macrophage infiltration.

Regarding the increasing evidence for adverse health effects of 11 $\beta$ -HSD2 inhibition and excessive MR activation, the development of novel strategies for identifying xenobiotics that interfere with the function of these proteins is needed.

Pharmacophore-based virtual screening is a powerful strategy for predicting bioactivities of small organic molecules [23]. A pharmacophore model consists of a three-dimensional arrangement of the most important chemical functionalities for an interaction with a specific pharmacological target macromolecule [24]. It describes the locations of hydrogen bonds, hydrophobic areas, aromatic features, ionizable groups, and metal binding fragments for optimal interaction with the ligand binding site. Such a model can be applied to a large chemical database as a filter to reduce this library to only those compounds fulfilling the same interaction pattern. Virtual screening leads to an enrichment of active compounds. An initial focus on virtual hits increases the probability to find active compounds, while decreasing the number of compounds to be tested, thus saving time and costs.

This method is well established in drug discovery and has been successfully applied in lead discovery projects for various proteins [25,26,27,28]. Recently, a pharmacophore-based virtual screening approach was applied for the identification of inhibitors of 17 $\beta$ -hydroxysteroid dehydrogenase (17 $\beta$ -HSD) 3 and 5 [29]. However, pharmacophore modeling and virtual screening can be also used for toxicological studies: by virtual screening e.g. environmental chemical databases, toxicological effects of already known chemicals can be investigated. Moreover, the toxicological potential of widely used chemicals can be studied. Recently, a pharmacophore model for 17 $\beta$ -hydroxysteroid dehydrogenase 3 (17 $\beta$ -HSD3) has been successfully employed to identify potential testosterone synthesis-disrupting compounds [30]. The virtual screening pointed towards benzophenone-type UV-filter chemicals. Systematic testing of several representatives of this class led to the identification of benzophenone-1 as a potent 17 $\beta$ -HSD3 inhibitor.

Here, we performed a virtual screening of a previously constructed endocrine disruptors database (EDB) [30] using a 11 $\beta$ -HSD pharmacophore model [31] and tested selected hits in a 11 $\beta$ -HSD2 bioassay. The identified silane-coupling agent AB110873 inhibited 11 $\beta$ -HSD2 and was further shown to activate MR. We further investigated the silane AB110873 and generated a MR pharmacophore that successfully identified AB110873.

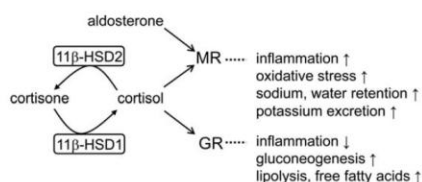


**Figure 1. Schematic overview of corticosteroid receptor regulation by 11 $\beta$ -HSD enzymes.**  
doi:10.1371/journal.pone.0046958.g001

## Results

### Virtual Screening of the EDB using the 11 $\beta$ -HSD Pharmacophore Model and Selection of Hits for Biological Testing

In order to identify xenobiotics potentially inhibiting 11 $\beta$ -HSD2 we used the previously constructed endocrine disruptors database (EDB) [30] for virtual screening using an 11 $\beta$ -HSD pharmacophore model (Fig. 2) [31]. Out of the 76'677 database entries, only 29 fitted into the model (Table S1). The majority of the compounds represent steroids or triterpenoids, followed by antibiotics and dyes. Some of the hits are reported to be used in industry, like dyes and the silicon-containing coupling agent bis[3-(triethoxysilyl)propyl] tetrasulfide AB110873. Others are natural products with known bioactivities, especially cardiac glycosides, but also already known 11 $\beta$ -HSD inhibitors. For the biological testing, we had to focus on commercially available hits. From the class of cardiac glycosides, digitoxigenin monodigitoxoside was selected as representative testing hit. Because only the aglycon form was commercially available and the glycoside part of the molecule took no part in fitting to the model, digitoxigenin was actually purchased. As hit representing antibiotics lasalocid, which is used in chicken farms, was selected. Cephaeline was tested because it is a bioactive constituent of Ipecacuanha sirup, which is used as an emetic. Another natural product, hecogenin acetate, was tested because its use in cosmetics and therefore, humans are directly exposed to this agent. Also in this case, the acetate form was not available for testing, and hecogenin was biologically evaluated. Finally, AB110873 was tested as a widely used industrial chemical. Additionally, it was the only hit containing silicon; therefore it was especially interesting to evaluate this chemical composition in the context of 11 $\beta$ -HSD inhibition.

### Inhibition of 11 $\beta$ -HSD1 and 11 $\beta$ -HSD2 by the Selected Compounds

The selected virtual hits were tested for their potential to inhibit human 11 $\beta$ -HSD1 and 11 $\beta$ -HSD2 using lysates of stably transfected HEK-293 cells (Table 1). Glycyrrhetic acid was used as a positive control and potently inhibited both enzymes as expected. The identification of carbenoxolone, 18 $\alpha$ -glycyrrhetic acid, and uranic acid acetate, compounds shown previously to inhibit 11 $\beta$ -HSD1 and 11 $\beta$ -HSD2 [31,32,33], confirmed the validity of the pharmacophore used in the present study. In addition, fenofibrate, which was recently reported to inhibit mouse 11 $\beta$ -HSD1 activity in C2C12 cells [34], was identified by the virtual screening process and found to inhibit human 11 $\beta$ -HSD1 with an IC<sub>50</sub> of 3.8 $\pm$ 0.3  $\mu$ M. 11 $\beta$ -HSD2 was not inhibited by 20  $\mu$ M fenofibrate. Other compounds that were not previously reported to inhibit 11 $\beta$ -HSD1 include the cardiac glycoside digitoxigenin and hecogenin.

Among the compounds inhibiting 11 $\beta$ -HSD2, the silane coupling agent AB110873 (Fig. 3) was most potent, followed by the antibiotic chemical lasalocid with IC<sub>50</sub> values of 6.1 $\pm$ 1.3  $\mu$ M for AB110873 and 14 $\pm$ 3  $\mu$ M for lasalocid. Based on this first hit of a silane-coupling agent as 11 $\beta$ -HSD inhibitor, a related, commercially available silane was investigated. In contrast to AB110873, the silane 3-mercaptopropyl triethoxysilane, which contains only one silane group, showed very weak inhibition (80 $\pm$ 7% remaining activity at 20  $\mu$ M). In addition, we tested whether the silane AB110873 might irreversibly inhibit 11 $\beta$ -HSD2 and preincubated the enzyme with this compound. However, unlike inhibition of 11 $\beta$ -HSD2 by dithiocarbamates [35], preincubation with AB110873 did not aggravate its inhibitory effect, suggesting a reversible mode of inhibition.

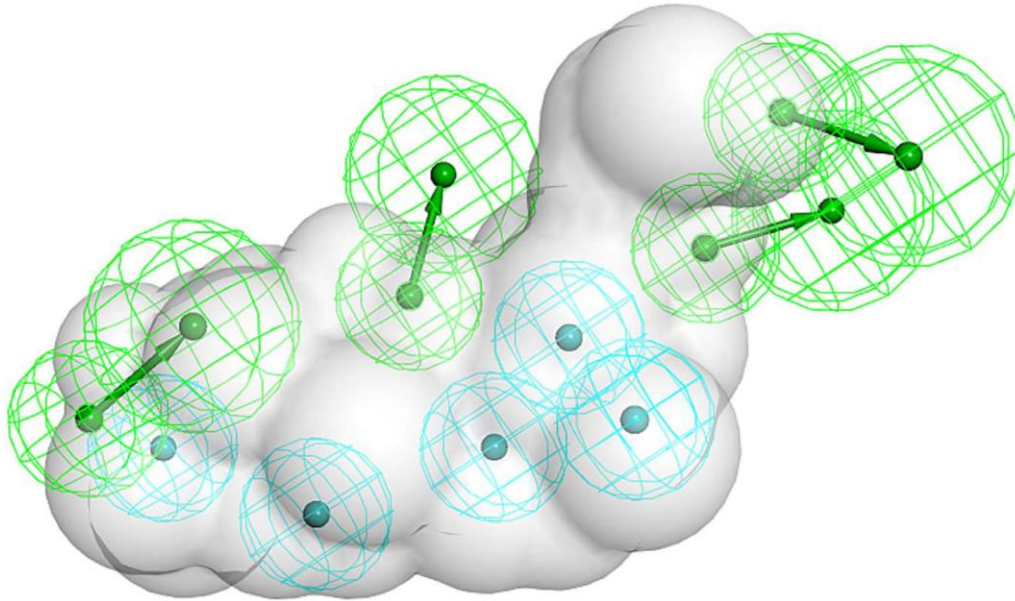


**Figure 2. 11 $\beta$ -HSD inhibitors pharmacophore model.** The hydrogen bond acceptor features are represented in green, and the hydrophobic features in blue. The shape of carbenoxolone, as a steric constraint to prevent too large molecules from fitting, is shown as a grey volume. doi:10.1371/journal.pone.0046958.g002

#### Assessment of Potential Cytotoxic Effects of the Silane AB110873

Next, we examined whether the silane AB110873 affects general cytotoxicity parameters. HEK-293 cells were incubated for 24 h at 37°C in the presence of vehicle or various concentrations of rotenone (Fig. 4A) or the silane AB110873 (Fig. 4B), followed by simultaneous incubation of the cells with Hoechst 33342 for staining of nuclei, DHE for detection of cytoplasmic ROS generation, and SYTOX Green to assess cell membrane

permeability. Cells were analyzed using a Cellomics Array Scan high-content screening system as described in the methods section. Rotenone, a potent inhibitor of the mitochondrial electron transport chain that induces intracellular ROS production, showed a concentration-dependent decrease in the average cell number per field with a concomitant increase in plasma membrane permeability and the production of cytoplasmic ROS (Fig. 4A). The silane AB110873 at concentrations up to 30  $\mu$ M had no significant effect (Fig. 4B). Similarly, the silane AB110873 did not affect these general cytotoxicity parameters in monkey

**Table 1.** Inhibition of 11 $\beta$ -HSD1 and 11 $\beta$ -HSD2 by compounds predicted by virtual screening.

Compound (20 $\mu$ M)	11 $\beta$ -HSD1 activity (% of control)	11 $\beta$ -HSD2 activity (% of control)
Vehicle (0.1% dimethylsulfoxide)	100	100
T0504	N.D.	5 $\pm$ 3
Fenofibrate	5 $\pm$ 1	140 $\pm$ 40
Glycyrrhethinic acid	5 $\pm$ 3	N.D.
Digitoxigenin	36 $\pm$ 2	104 $\pm$ 4
Lasalocid	84 $\pm$ 3	42 $\pm$ 10
Hecogenin	49 $\pm$ 9	82 $\pm$ 2
(-)- Cephaeline dihydrochloride	100 $\pm$ 2	74 $\pm$ 2
Bis[3-(triethoxysilyl)propyl] tetrasulfide (AB110873)	79 $\pm$ 3	15 $\pm$ 3

11 $\beta$ -HSD1-dependent conversion of cortisone (200 nM cortisone, 500  $\mu$ M NADPH) to cortisol was determined by incubating lysates of HEK-293 cells stably expressing the human enzyme in the presence of vehicle or 20  $\mu$ M of the respective compound for 10 min at 37°C. Similarly, 11 $\beta$ -HSD2-dependent conversion of cortisol (50 nM cortisol, 500  $\mu$ M NAD<sup>+</sup>) to cortisone was measured. Data represent mean  $\pm$  SD from at least three independent experiments. T0504 and fenofibrate were used as synthetic positive controls, glycyrrhethinic acid as natural product positive control. N.D., not detectable (complete inhibition). doi:10.1371/journal.pone.0046958.t001

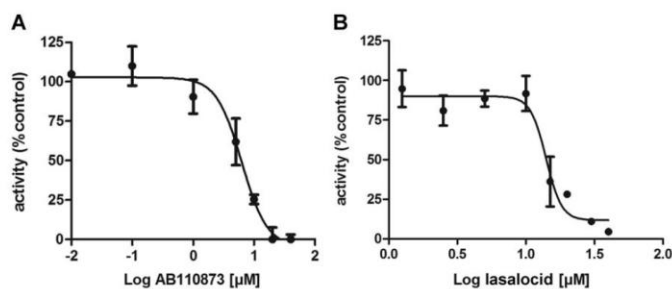


**Figure 3. Inhibition of human 11 $\beta$ -HSD2 by AB110873 and lasalocid.** Concentration-dependent inhibition of 11 $\beta$ -HSD2 by the silane-coupling agent AB110873 (A) and the anti-biotic lasalocid (B) measured in cell lysates of stably transfected HEK-293 cells. Data represent mean  $\pm$  SD from three independent experiments. doi:10.1371/journal.pone.0046958.g003

kidney COS-1 cells (data not shown) and in BV2 microglial cells (Fig. 4C), which express endogenous MR.

#### Activation of MR by the Silane AB110873

To investigate whether the silane AB110873 directly modulates MR activity, we performed transactivation assays using HEK-293 cells transfected with human MR and a galactosidase reporter gene under the control of the MR sensitive MMTV-promoter. The silane AB110873 stimulated reporter gene activity in a concentration-dependent manner (Fig. 5A) with an EC<sub>50</sub> of 15.4  $\pm$  0.5  $\mu$ M. Maximal reporter gene stimulation obtained with AB110873 was comparable to maximal activation observed with aldosterone (Fig. 5B). Importantly, the MR antagonist spironolactone was able to completely abolish receptor activation by AB110873 (Fig. 5B). In contrast, the silane AB110873 did not activate the human GR and was unable to block GR activation mediated by cortisol (Fig. 5C). The 3-mercaptopropyl triethoxysilane did not activate MR at concentrations up to 30  $\mu$ M (data not shown).

#### The Silane AB110873 Increases Mitochondrial Superoxide Generation and Induces IL-6 Expression through MR Activation in BV-2 Microglial Cells

MR activation in macrophage-derived cells has been associated with an elevation in mitochondrial ROS production. Therefore, we investigated whether aldosterone and the silane AB110873 might activate MR in mouse microglial BV2 cells that express endogenous levels of the receptor. Incubation of BV2 cells for 24 h with aldosterone, followed by MitoSox staining, revealed increased mitochondrial superoxide formation, an effect which was abolished by coinubation with the MR antagonist spironolactone (Fig. 6A). This confirms the functional expression of MR in microglial BV2 cells. Similarly, the silane AB110873 enhanced mitochondrial superoxide generation by a concentration-dependent manner in BV2 cells, and spironolactone was able to almost fully prevent mitochondrial ROS production (Fig. 6B).

Previous reports associated MR activation with an increased expression of the pro-inflammatory cytokine IL-6 [36,37]. In microglial BV-2 cells aldosterone at 50 nM led to increased IL-6 protein levels, which was suppressed by spironolactone (Fig. 6C). The silane AB110873 stimulated IL-6 protein expression by

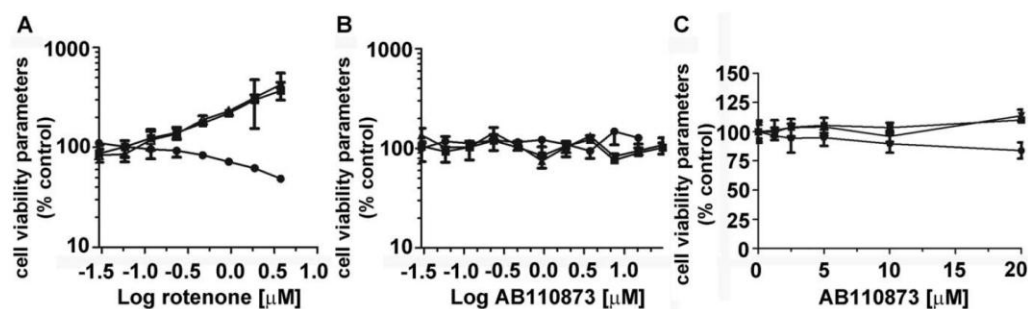


**Figure 4. Assessment of the cytotoxic potential of the silane AB110873 and of rotenone.** HEK-293 cells or BV2 cells were incubated with rotenone or AB110873 for 24 h, followed by incubation for 30 min with staining solution containing Hoechst 33342, SYTOX Green and dihydroethidium. After fixation and washing, fluorescence was analyzed using Cellomics ArrayScan high-content screening system as described in the Methods section. A, Effect of rotenone on cytotoxicity parameters measured in HEK-293 cells. Filled circles, average cell number per field; filled squares, cytoplasmic ROS production assessed by staining with dihydroethidium; filled triangles, membrane permeability assessed by SYTOX Green staining. Effect of the silane AB110873 on cytotoxicity parameters measured in HEK-293 cells (B) and in BV2 cells (C). Data show one of three independent experiments performed in eight replicates (mean  $\pm$  SD, n=8). doi:10.1371/journal.pone.0046958.g004

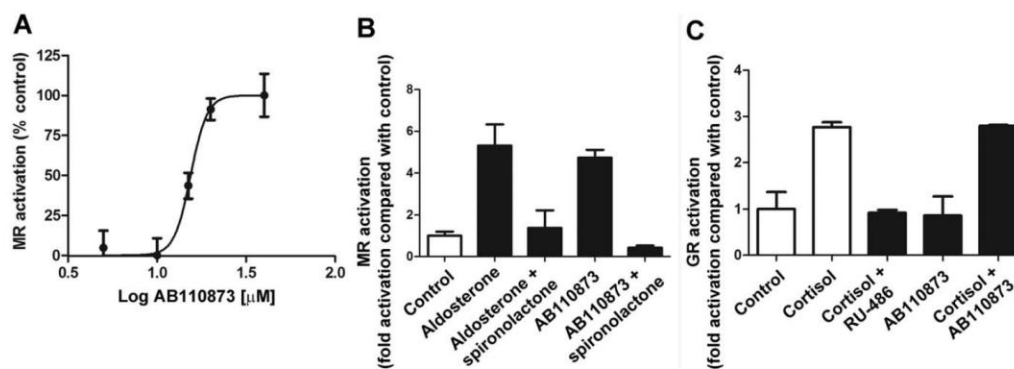


**Figure 5. Effect of the silane AB110873 on the activation of mineralocorticoid (MR) and glucocorticoid receptors (GR).** The impact of silane AB110873 on MR and GR transactivation was measured in HEK-293 cells transfected with MMTV-LacZ reporter, MR (A,B) or GR (C) and luciferase transfection control. Cells were incubated with the receptor ligands for 24 h, followed by analysis of reporter activity as given in the Methods section. A, Concentration-dependent activation of the human MR by the silane AB110873. Maximal activation at 30  $\mu$ M was set as 100%. B, effect of the antagonist spironolactone (1  $\mu$ M) on MR activation by aldosterone (5 nM) or by the silane AB110873 (20  $\mu$ M); C, activation of human GR by cortisol (100 nM) and effect of AB110873 (20  $\mu$ M) and antagonist RU-486 (1  $\mu$ M) (MR and GR activity of the vehicle control was set as 1, data represent fold activation). Data were obtained from four independent experiments, each performed in triplicates (mean  $\pm$  SD). doi:10.1371/journal.pone.0046958.g005

a concentration-dependent manner. At 30  $\mu$ M AB110873 IL-6 levels were comparable with those of aldosterone treated cells. Importantly, spironolactone almost completely reversed the effect of AB110873. The 3-mercaptopropyl triethoxysilane did not affect mitochondrial superoxide generation and IL-6 protein expression (data not shown).

#### Generation of an MR Ligands Pharmacophore Model

A structure-based pharmacophore model for MR ligands was generated based on the physicochemical interactions between the endogenous MR agonist aldosterone and the MR receptor. For this purpose, interaction information was derived from an X-ray crystal structure of the two binding partners (PDB entry 2aa2). All observed interactions were translated into an interaction model consisting of seven features: four hydrogen bond acceptors with Asn770, Cys942, Gln776, and Thr945, from which the latter is defined as a bidirectional hydrogen bond specified as an additional hydrogen bond donor feature with this residue, and two hydrophobic features placed on the methyl group of aldosterone and to the ring D of steroidal core. The model was used to virtually screen a set of active and inactive MR ligands from several publicly accessible databases (see experimental section). Unfortunately, this model was too restrictive and not able to correctly identify a large fraction of active ligands throughout all datasets. In order to better represent the chemical features essential for MR binding, four of the features were removed. The final MR ligands model consisted of four features: two hydrogen bond acceptors (with Gln776 and Thr945) and two hydrophobic features (Fig. 7A). Exclusion volumes - forbidden areas for the ligand due to steric clashes with the protein - were added to represent the shape of the binding site. This new model showed an improved recognition rate of MR ligands and was therefore used for further experiments. To explore how the silane AB110873 would bind to the MR, it was fitted first into the MR pharmacophore model. The silane fits to the MR model with a high fit score of 46.13, the maximum possible fit score being 49.00. Unfortunately, when aligning the silane AB110873 with the

pharmacophore into the MR ligand binding pocket, some severe steric clashes were observed. Additionally, AB110873 stucked out from the binding pocket (Fig. 7B). This suggested that silane AB110873 may adopt a different binding orientation within the MR binding site compared to aldosterone.

#### Docking Studies on AB110873 Fitting into the 11 $\beta$ -HSD2 and MR Binding Sites

The silane AB110873 is anchored mostly via hydrophobic interactions to the ligand binding site of 11 $\beta$ -HSD2 (Fig. 8A,B). Two hydrogen bonds are formed between the sulfur bridge and the catalytic residues Tyr232 and Ser219. Because of the chemical nature of sulfur, these hydrogen bonds are not especially strong, and there are no other stronger interactions to fix the silane AB110873 in the vicinity of the catalytic residues. Therefore, the inhibitory activity could be explained by two ways: first, the hydrogen bonds disrupt the catalytic function and/or, second, the bulky silane AB110873 prevents any other ligand binding via steric effects.

The docking studies of silane AB110873 in MR suggested an interesting binding mode that extends the one of aldosterone. Silane AB110873 binds to the ligand binding pocket with similar hydrophobic interactions compared to aldosterone, but it additionally occupies a hydrophobic side pocket formed by Val750, Val780, Leu809, and Ala813 (Fig. 8C). Remarkably, the channel between these two pockets is constricted and the hydrophobic side pocket is buried in the receptor.

The automatically calculated ligand-protein interactions by LigandScout revealed that silane AB110873 binds to the MR by hydrophobic interactions (Fig. 8D). The only hydrogen bond is formed between Arg817 and a sulfur atom. The silane AB110873 has some common hydrophobic interactions with Phe941, Leu938, Met845, Met807, and Ala773 as the original agonist aldosterone. However, it does not form the typical hydrogen bonding network of steroidal agonists described by Bledsoe et al. (Fig. 9) [38]. In addition, the hydrophobic side pocket that the silane AB110873 is occupying is located between helices 3 and 5 as

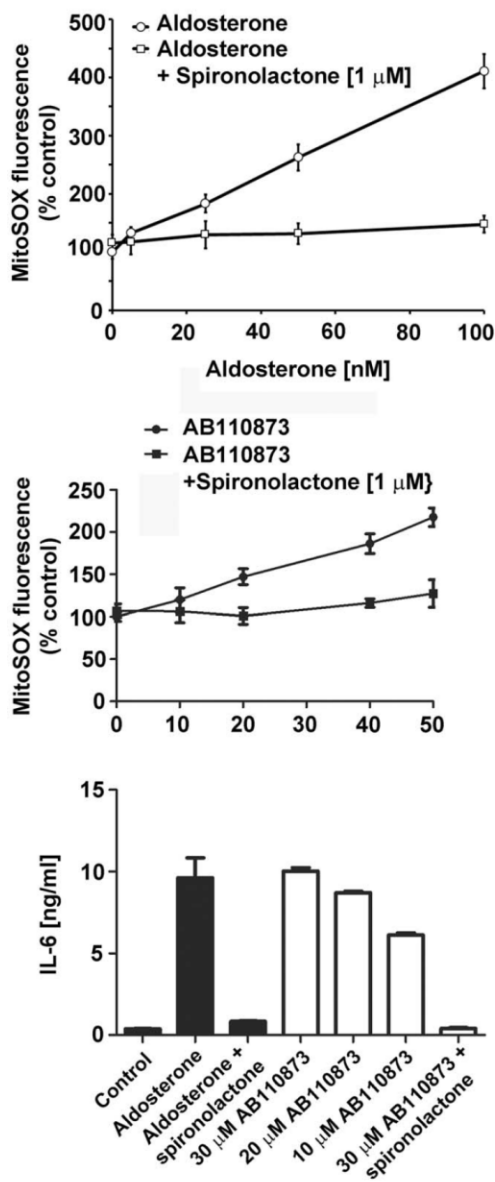


**Figure 6. Increased mitochondrial superoxide generation and induction of IL-6 production upon MR activation in BV2 cells.** BV2 microglial cells were incubated for 24 h with increasing concentrations of aldosterone (A) or silane AB110873 (B) in the presence or absence of 1 μM spironolactone, followed by determination of mitochondrial superoxide using MitoSox staining as described in the Methods section. Fluorescence was analyzed using a Cellomics ArrayScan high-content screening system. C, BV2 cells were incubated for 24 h with aldosterone (5 nM) or various concentrations of silane AB110873 in the presence or absence of spironolactone, followed by

quantification of IL-6 protein levels in the medium of the cultured cells by ELISA. Data (mean  $\pm$  SD) were obtained from three independent experiments each performed in six replicates. doi:10.1371/journal.pone.0046958.g006

well as a  $\beta$ -sheet (Fig. 9). Therefore, the silane AB110873 is not interfering with the MR-coactivator peptide.

## Discussion

In the present study, we describe a novel approach using *in silico* and *in vitro* tools for the rapid screening of large numbers of compounds in order to identify and characterize xenobiotics that inhibit 11 $\beta$ -HSD2 or act directly on MR. In this proof-of-concept study, the previously constructed endocrine disruptor database (EDB), containing approximately 80,000 compounds [30], was screened against an 11 $\beta$ -HSD pharmacophore. Of five compounds predicted to bind to 11 $\beta$ -HSDs and that were chosen for biological testing, four showed more than 50% inhibition of one of the two 11 $\beta$ -HSD enzymes. Thus, the *in silico* screening had a very high hit rate, compared with high-content screening, and led to the identification of non-steroidal and non-triterpenoid compounds that have not been reported before. The *in silico* tools used in this study have thereby shown high predictive power and can be subsequently used in future screening projects, e.g. using virtual natural compound libraries to identify compounds with glycyrrhetic acid-like effects or virtual drug libraries to detect unwanted side-effects.

Due to its low general cytotoxicity, also when compared with other hits of the *in silico* screening, and its rather unexpected structure compared with known 11 $\beta$ -HSD2 inhibitors, the silane coupling agent AB110873 was further investigated. Silane derivatives are used at concentrations higher than 1% in resin-composite cement [39]. They are also used in fluoride varnishes for caries prevention [40], and silane-based hydrogels are used in clinical practice for delivery of nitric oxide donors [41]. The specific silane coupling agent AB110873, also known as KH-69 or Si-69, is one of the most widely used rubber additives, developed thirty years ago (<http://www.rubber-silanes.com/product/rubber-silanes/en/about/pages/default.aspx>). AB110873 leads to improved strength and optimized dynamic properties of rubbers, including increased abrasion resistance. It is used in many applications where white fillers containing silanol groups are involved and optimum technical properties are required. AB110873 is widely used in the production of tires, shoe soles, mechanical rubber goods, and as adhesion promoter for rubber adhesives, sealants and coatings. Further, AB110873 and other bis-type silanes are used to protect metals from corrosion [42]. Despite of the wide use of AB110873, there are currently no studies available on concentrations measured in humans. Regarding the expected low release of silane derivatives from their products, occupational exposure during the production process probably represents the most critical issue.

Nevertheless, our results show that the silane AB110873 at subcytotoxic concentrations can enhance MR activity by two distinct mechanisms: first, by inhibition of 11 $\beta$ -HSD2, thereby leading to locally increased levels of active glucocorticoids that activate MR, and second, by direct activation of the receptor. Inhibition of 11 $\beta$ -HSD2 is relevant in classical mineralocorticoid-responsive cells involved in water and electrolyte regulation that coexpress MR and 11 $\beta$ -HSD2 such as renal cortical collecting ducts, distal colon and salivary and sweat glands [14]. It is further relevant in the placenta as a barrier to protect the fetus from maternal glucocorticoids.

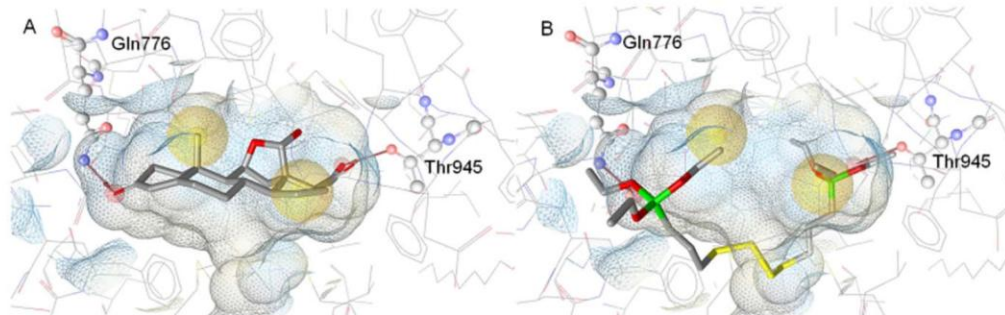


**Figure 7. Binding of aldosterone and the silane AB110873 to the MR.** A, MR pharmacophore model with the cocrystallized ligand aldosterone. B, the silane AB110873 fitted to the MR ligand binding site with the pharmacophore model. Hydrogen bond acceptors are shown as red arrows, hydrophobic areas as yellow spheres. Exclusion volumes are not shown for clarity. Receptor binding pocket is colored by aggregated lipophilicity (grey)/hydrophilicity (blue).  
doi:10.1371/journal.pone.0046958.g007

A direct activation of MR is further relevant in cells not expressing  $11\beta$ -HSD2. MR and GR are coexpressed in the presence of the glucocorticoid activating enzyme  $11\beta$ -HSD1 in cells like macrophage and microglia, adipocytes and osteoblasts [14], where an impaired MR activation has been associated with elevated inflammation and oxidative stress [43,44]. Thus, a chronic exposure to MR activating chemicals can be expected to result in exaggerated inflammatory response and impaired ability to cope

with oxidative stress. Our results show that the silane AB110873 selectively binds to MR but not GR, and molecular modeling revealed a binding mode distinct to that of aldosterone. The finding that AB110873 occupies an additional hydrophobic side pocket of MR may offer an opportunity for drug development, since MR antagonists are of considerable pharmaceutical interest.

In conclusion, virtual screening of the EDB using a  $11\beta$ -HSD pharmacophore led to the identification of non-steroidal and non-

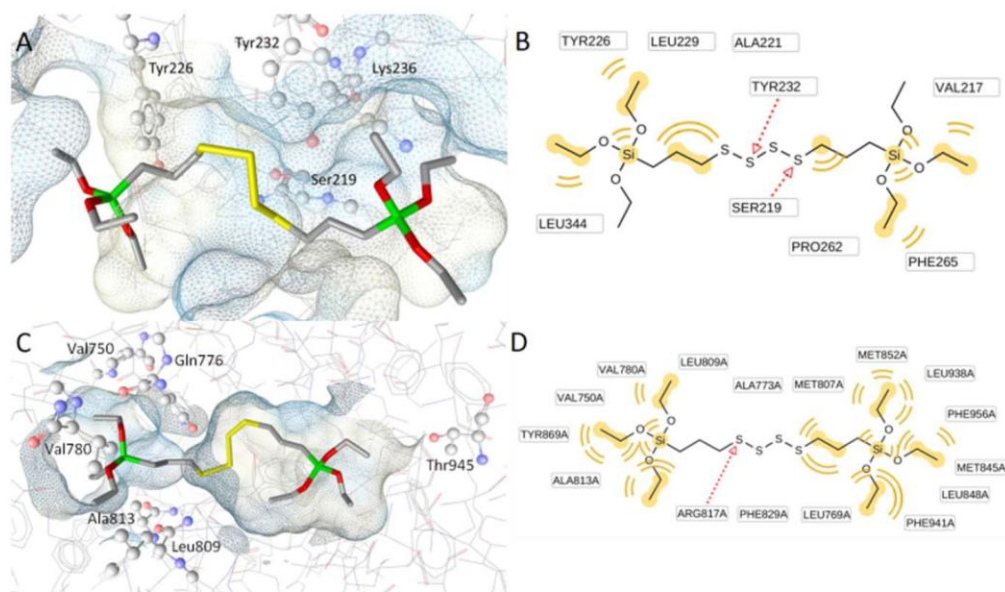


**Figure 8. AB110873 binds to both  $11\beta$ -HSD2 and MR.** Proposed binding modes of AB110873 in  $11\beta$ -HSD2 (A,B) and in the MR (C,D). In the 3D-figures, selected amino acid residues are highlighted with ball and stick, and the receptor binding pockets are colored by aggregated lipophilicity (grey)/hydrophilicity (blue). The 2D figures represent the binding interactions, color-coded as following: red arrow – hydrogen bond acceptor, yellow – hydrophobic interaction.  
doi:10.1371/journal.pone.0046958.g008

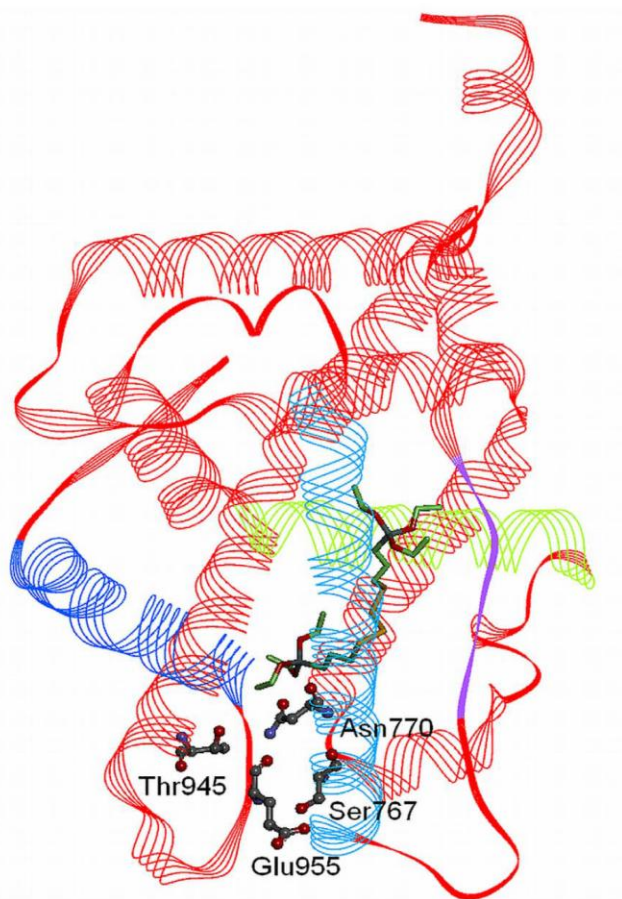


**Figure 9. MR with silane AB110873.** The amino acids that form the hydrogen bond network with steroidal agonists are highlighted in ball and stick style. AF-2 (helix 12) is colored in dark blue, helix 5 in green, helix 3 in light blue, and the  $\beta$ -sheet in lilac. The buried hydrophobic pocket additionally occupied by AB110873 is formed by amino acids from helices 3 (Val780) and 5 (Leu809, Ala813), and from the  $\beta$ -sheet (Val750). doi:10.1371/journal.pone.0046958.g009

triterpenoid xenobiotics, including the antibiotic lasalocid and the silane AB110873. The latter was further shown to activate recombinant and endogenous MR. Molecular modeling revealed the binding mode of AB110873 in the ligand binding pocket, explaining the fact that AB110873-mediated MR activation was blocked by spironolactone. Finally, a newly generated MR pharmacophore successfully recognized AB110873, indicating its value for future screening experiment.

## Materials and Methods

### Materials

[1,2,6,7- $^3\text{H}$ ]-cortisol was purchased from PerkinElmer (Waltham, MA), [1,2,6,7- $^3\text{H}$ ]-cortisone from American Radiolabeled Chemicals (St. Louis, MO), 5H-1,2,4-triazolo(4,3-a)azepine,6,7,8,9-tetrahydro-3-tricyclo(3:3:1-13:7)dec-1-yl (T0504) from Enamine (Kiev, Ukraine) and aldosterone from Steraloids (Wilton, NH). Digitoxigenin, lasalocid, and (-)-cephaeline dihydrochloride were kindly provided by the National Cancer Institute (NCI, Bethesda, US). All other chemicals were from Fluka AG (Buchs, Switzerland)

of the highest grade available. Cell culture media were purchased from Sigma Aldrich (Buchs, Switzerland).

#### Inhibitor-based 11 $\beta$ -HSD2 Pharmacophore Model and Virtual Screening of a 3D-structure Database of Potential Endocrine Disrupting Chemicals (EDCs)

For this study, a previously reported and experimentally validated 11 $\beta$ -HSD inhibitor pharmacophore model was used [31]. The model was based on two triterpenoid 11 $\beta$ -HSD inhibitors with preference to inhibit 11 $\beta$ -HSD2 more potently than 11 $\beta$ -HSD1. The model consisted of five hydrophobic features, placed on the triterpene core of the training compounds, and four hydrogen bond acceptors (Fig. 2).

The EDB was screened with the 11 $\beta$ -HSD2 inhibitors model using Catalyst 4.11 ([www.accelrys.com](http://www.accelrys.com)). For the virtual screening, the best flexible search algorithm was used. This screening protocol minimizes the pre-computed compound conformations from the screening database into the model in order to find the best fittings also for flexible compounds.

#### Cell Culture

HEK-293 (CRL-1573) and COS-1 (CRL-1650) cells were purchased from American Type Culture Collection (Manassas, VA, USA) and cultured in Dulbecco's modified Eagle medium (DMEM) supplemented with 10% fetal bovine serum (FBS), 4.5 g/L glucose, 50 U/mL penicillin/streptomycin, 2 mM glutamine, and 1 mM HEPES, pH 7.4. They were used at passage number between 5 and 30. Immortalized mouse microglia BV2 cells, developed by Bocchini et al. [45], were a kind gift from Dr. Ernst Malle (University of Graz, Graz, Austria) and were cultivated in RPMI-1640 medium, supplemented with 10% fetal bovine serum, 1 g/L glucose, 100 U/mL penicillin, 100  $\mu$ g/mL streptomycin, 2 mM glutamine and 0.1 mM non-essential amino acids. BV2 cells were used at passage number between 7 and 15.

#### 11 $\beta$ -HSD1 and 11 $\beta$ -HSD2 Activity Assay

Enzyme activities were measured as described earlier using lysates of HEK-293 cells stably expressing human 11 $\beta$ -HSD1 or 11 $\beta$ -HSD2 [46]. 11 $\beta$ -HSD1 oxoreductase activity was determined by incubation of lysates with 200 nM of radiolabeled cortisone, 500  $\mu$ M NADPH and vehicle or inhibitor. 11 $\beta$ -HSD2 activity was measured in the presence of 50 nM radiolabeled cortisol, 500  $\mu$ M NAD<sup>+</sup> and vehicle (dimethylsulfoxide (DMSO)) or inhibitor. Samples were incubated for 10 min at 37°C. Control samples in the presence of vehicle converted 20% of the radiolabeled substrate. Data represent percentage of activity of the enzyme in the presence of test compound relative to its activity (set as 100%) in the presence of vehicle control.

#### MR and GR Transactivation Assay

HEK-293 cells (150,000 cells/well) were seeded in poly-L-lysine coated 24-well plates and incubated for 24 h. Cells were transfected using calcium phosphate precipitation with pMMTV-lacZ  $\beta$ -galactosidase reporter (0.20  $\mu$ g/well), pCMV-LUC luciferase transfection control (0.04  $\mu$ g/well) and plasmid for human recombinant MR or GR (0.35  $\mu$ g/well). The medium was changed 6 h post-transfection, followed by incubation for another 18 h. Cells were washed twice with charcoal-treated DMEM containing 10% FBS and incubated with either 10 nM aldosterone or 100 nM cortisol and various concentrations of compounds for 24 h to allow sufficient reporter gene expression. The solvent concentration was below 0.1%. Cells were washed once with PBS and lysed with 50  $\mu$ L lysis buffer of the Tropix kit (Applied

Biosystems, Foster City, CA) supplemented with 0.5 mM dithiothreitol. Lysed samples were frozen at  $-80^{\circ}\text{C}$  prior to analysis of  $\beta$ -galactosidase activity using the Tropix kit and luciferase activity using a luciferase-solution [46]. Relative light units (RLU) of 4,100 and 195,000 for luciferase and  $\beta$ -galactosidase activity were obtained for vehicle controls. The RLU of luciferase control was not significantly altered by treatment with compounds. Data were normalized to the ratio of  $\beta$ -galactosidase to luciferase activity of the vehicle control.

#### Determination of Cellular Toxicity Parameters and Cytoplasmic ROS Production

HEK-293 and COS-1 cells (9'000 cells/well) were seeded in poly-L-lysine coated 96-well plates and allow to attach for 24 h prior to incubation with compounds for another 24 h. Upon addition of 50  $\mu$ L staining solution (DMEM containing 2.5  $\mu$ M SytoxGreen, 500 nM Hoechst 33342 and 2.5  $\mu$ g/mL dihydroethidium (DHE)) cells were incubated for 30 min at 37°C. The solution was aspirated and cells were fixed with 3.5% paraformaldehyde in PBS for 15 min. Cells were washed three times with PBS and plates stored at 4°C until analysis using a Cellomics ArrayScan high-content screening system (Cellomics Thermo-Scientific, Pittsburgh, PA). Data acquisition and image analysis was performed by automated fluorescence imaging. Fluorescence intensity measurements (population averages) were captured on 20 fields, each field containing approximately 1000 cells. Values were normalized to vehicle control and data represent percentage of fluorescence intensity compared with control. Images were acquired for each fluorescence channel (Hoechst 33342, Sytox-Green, DHE) using suitable filters, a 20 $\times$  objective and the application software according to the manufacturer. Cells were identified using Hoechst 33342, and a nuclear mask was generated from images of stained nuclei. Automatic focusing was performed in the nuclear channel to ensure focusing regardless of staining intensities in the other channels. Images and data regarding intensity and texture of the fluorescence within each cell as well as average fluorescence of the cell population within the well were quantified from a shell surrounding the nuclear mask.

The MTT assay was performed with 23'000 cells/well seeded in poly-L-lysine coated 96-well plates. After overnight incubation, the medium was replaced and cells were incubated with compounds for 24 h, followed by adding 5 mg/mL MTT and examination for appearance of purple formazan crystals using light microscopy after another 2 h. The medium was carefully aspirated and 200  $\mu$ L DMSO were added to each well to dissolve the formazan crystals. After 30 min, the plate was measured at 565 nm with a reference filter at 650 nm.

#### Measurement of Mitochondrial Superoxide Production in BV2 Cells

To determine whether compounds affected steady-state levels of mitochondrial superoxide production in BV2 microglial cells that express endogenous MR, the cationic superoxide-sensitive dye MitoSOX Red was used. Cells were washed once with PBS and labeled with MitoSOX Red (5  $\mu$ M) at 37°C for 20 min. Cells were washed with PBS and fixed with 3.5% paraformaldehyde for 15 min, followed by washing and incubation with nuclei staining solution (1  $\mu$ g/ml Hoechst 33342 dissolved in medium) for 30 min. The plate was washed twice with PBS, cells were imaged and the amount of fluorescence was quantified using an ArrayScan high-content screening system. Fluorescence intensity measurements (population averages) at 590 nm were captured on 20 fields with each field containing approximately 1000 cells. The amount

of mitochondrial superoxide production is given as percentage of fluorescence intensity compared with control.

#### Detection of Interleukin-6 (IL-6) Expression by Enzyme-linked Immunosorbent Assay (ELISA)

IL-6 protein in culture media from BV2 microglial cells was measured using the IL-6 ELISA Ready-SET-Go kit (BD Biosciences, CA) according to the manufacturer. Cells were seeded in 96-well plates at a density of  $5 \times 10^4$  cell/mL. Cell-free supernatants were collected after incubation for 24 h with AB110873 and aldosterone in the presence or absence of spironolactone. The 96-well plate was incubated overnight at 4°C with coating buffer containing capture antibody. Samples were washed 5 times with PBS-T (PBS containing 0.05% Tween-20), blocked for 1 h, washed again, and standards and collected culture media were added to the appropriate wells and incubated for 2 h. After washing 5 times with PBS-T, each well was incubated with detection antibody for 1 h, washed and incubated with avidin-horseradish peroxidase for 30 min. After washing 7 times, samples were incubated with substrate solution for 30 min in the dark. Reactions were stopped with 1 M  $H_3PO_4$ , and the plate was analyzed at 450 nm by subtraction of the values obtained at 570 nm using a UV-max kinetic microplate reader (Molecular Device, Birkshire, UK). The concentrations of IL-6 were calculated according to the standard curve of purified mouse IL-6.

#### Generation of a MR Ligands Pharmacophore Model

The structure-based MR ligands pharmacophore model was generated using LigandScout 2.02 ([47]; www.inteligand.com). The model was based on the interactions of the MR binding site and its cocrystallized endogenous ligand aldosterone (Protein Data Bank (PDB) code 2aa2, [38]). The pharmacophore model was validated by virtual screening of MR data sets from the directory of useful decoys (DUD) [48], the ChEMBL database version 02 (www.ebi.ac.uk/chembl/), and a previously reported drug-like virtual library [49]. To analyze whether the silane AB110873 fits to the MR pharmacophore model, a database of 500 conformations of this molecule was calculated with Omega-best settings using the idbgen-tool of LigandScout, followed by screening the MR model against this database using LigandScout 3.03a [47].

#### References

- Diamanti-Kandarakis E, Bourguignon JP, Giudice LC, Hauser R, Prins GS, et al. (2009) Endocrine-disrupting chemicals: an Endocrine Society scientific statement. *Endocr Rev* 30: 293–342.
- Neel BA, Sargis RM (2011) The paradox of progress: environmental disruption of metabolism and the diabetes epidemic. *Diabetes* 60: 1838–1848.
- Allera A, Lo S, King I, Steglich F, Klingmüller D (2004) Impact of androgenic/antiandrogenic compounds (AAC) on human sex steroid metabolizing key enzymes. *Toxicology* 205: 75–85.
- Luccio-Camelo DC, Prins GS (2011) Disruption of androgen receptor signaling in males by environmental chemicals. *J Steroid Biochem Mol Biol* 127: 74–82.
- Schug TT, Janesick A, Blumberg B, Heindel JJ (2011) Endocrine disrupting chemicals and disease susceptibility. *J Steroid Biochem Mol Biol* 127: 204–215.
- Odermatt A, Gumy C (2008) Glucocorticoid and mineralocorticoid action: why should we consider influences by environmental chemicals? *Biochem Pharmacol* 76: 1184–1193.
- Ma X, Lian QQ, Dong Q, Ge RS (2011) Environmental inhibitors of 11 $\beta$ -hydroxysteroid dehydrogenase type 2. *Toxicology* 285: 83–89.
- Briet M, Schiffrin EL (2010) Aldosterone: effects on the kidney and cardiovascular system. *Nat Rev Nephrol* 6: 261–273.
- Hadlock PW, Iqbal J, Walker BR (2009) Therapeutic manipulation of glucocorticoid metabolism in cardiovascular disease. *Br J Pharmacol* 156: 689–712.
- Lastra G, Dhuper S, Johnson MS, Sowers JR (2010) Salt, aldosterone, and insulin resistance: impact on the cardiovascular system. *Nat Rev Cardiol* 7: 577–584.

#### Docking Studies

To propose the molecular binding modes of the most active compound to the 11 $\beta$ -HSD2 and MR binding sites, docking studies using GOLD software [50,51] were performed. To generate the binding modes, GOLD uses a genetic algorithm, which creates ten low-energy binding solutions for each ligand within the binding site. No further energy minimization for the predicted binding modes was performed. In the absence of an X-ray crystal structure of 11 $\beta$ -HSD2, a previously published homology model of 11 $\beta$ -HSD2 [46] was used. The binding site was defined as a 15 Å sphere with the Tyr232 oxygen as center. GoldScore was used as a scoring function and ten docking poses were reported for the ligand. The program was set to define the atom types of the protein and the ligand automatically. For the MR, the PDB entry 2aa2 [38] was selected. The binding site was again defined as a 15 Å sphere, which center was the oxygen atom of Asn770. The same settings were applied as in the 11 $\beta$ -HSD2 docking run. Using these settings, the program successfully reproduced the binding mode of the cocrystallized ligand aldosterone. After both docking experiments, LigandScout [47] was used for analyzing the predicted protein-ligand interactions.

#### Supporting Information

**Table S1** Virtual hits derived from the EDB by virtual screening of the 11 $\beta$ -HSD pharmacophore. (DOC)

#### Acknowledgments

We thank Dr. Wolfgang Sattler, University of Graz, Austria, for providing the BV-2 cell line and IntelLigand GmbH (Vienna, Austria) for LigandScout software.

#### Author Contributions

Conceived and designed the experiments: LGN AV DS AO. Performed the experiments: LGN AV LP BC DC RW. Analyzed the data: LGN AV DS AO. Contributed reagents/materials/analysis tools: DS AO. Wrote the paper: LGN AV DS AO.

20. Lindsay RS, Lindsay RM, Edwards CR, Seckl JR (1996) Inhibition of 11 $\beta$ -hydroxysteroid dehydrogenase in pregnant rats and the programming of blood pressure in the offspring. *Hypertension* 27: 1200–1204.
21. Benediktsson R, Calder AA, Edwards CR, Seckl JR (1997) Placental 11 $\beta$ -hydroxysteroid dehydrogenase: a key regulator of fetal glucocorticoid exposure. *Clin Endocrinol* 46: 161–166.
22. Deuchar GA, McLean D, Hadjok PW, Brownstein DG, Webb DJ, et al. (2011) 11 $\beta$ -hydroxysteroid dehydrogenase type 2 deficiency accelerates atherosclerosis and causes proinflammatory changes in the endothelium in apoE $^{-/-}$  mice. *Endocrinology* 152: 236–246.
23. Schuster D (2010) 3D pharmacophores as tools for activity profiling. *Drug Discov Today Technol* 7: 205–211.
24. Wermuth CG, Gandlin CR, Lindberg P, Mitscher LA (1998) *Pure Appl Chem* 70: 1129–1143.
25. Duwensee K, Schwaiger S, Tancevski I, Eller K, van Eck M, et al. (2011) Leoginin, the major lignan from Edelweiss, activates cholesteryl ester transfer protein. *Atherosclerosis* 219: 109–115.
26. Markt P, Feldmann C, Röllinger JM, Raduner S, Schuster D, et al. (2009) Discovery of Novel GPR109A Receptor Ligands by a Pharmacophore-Based Virtual Screening Workflow. *J Med Chem* 52: 369–378.
27. Schuster D, Markt P, Griente U, Mihaly-Bison J, Binder M, et al. (2011) Pharmacophore-based discovery of FXR agonists. Part I: Model development and experimental validation. *Bioorg Med Chem* 19: 7168–7180.
28. Hein M, Zilian D, Sotrieff CA (2010) *Drug Discov Today Technol* 7: 229–236.
29. Schuster D, Kowalk D, Kirchmaier J, Laggner C, Markt P, et al. (2011) Identification of chemically diverse, novel inhibitors of 17 $\beta$ -hydroxysteroid dehydrogenase type 3 and 5 by pharmacophore-based virtual screening. *J Steroid Biochem Mol Biol* 125: 148–161.
30. Nashev LG, Schuster D, Laggner C, Sodha S, Langer T, et al. (2010) The UV-filter benzophenone-1 inhibits 17 $\beta$ -hydroxysteroid dehydrogenase type 3: Virtual screening as a strategy to identify potential endocrine disrupting chemicals. *Biochem Pharmacol* 79: 1189–1199.
31. Schuster D, Maurer EM, Laggner C, Nashev LG, Wickens T, et al. (2006) The discovery of new 11 $\beta$ -hydroxysteroid dehydrogenase type 1 inhibitors by common feature pharmacophore modeling and virtual screening. *J Med Chem* 49: 3454–3466.
32. Diederich S, Grossmann C, Hanke B, Quinkler M, Herrmann M, et al. (2000) In the search for specific inhibitors of human 11 $\beta$ -hydroxysteroid-dehydrogenases (11 $\beta$ -HSDs): chondroxycholic acid selectively inhibits 11 $\beta$ -HSD-I. *Eur J Endocrinol* 142: 200–207.
33. Classen-Houben D, Schuster D, Da Cunha T, Odermatt A, Wolber G, et al. (2009) Selective inhibition of 11 $\beta$ -hydroxysteroid dehydrogenase 1 by 18 $\alpha$ -glycyrrhetic acid but not 18 $\beta$ -glycyrrhetic acid. *J Steroid Biochem Mol Biol* 113: 248–252.
34. Kim CH, Ramu R, Ahn JH, Bae MA, Cho YS (2010) Fenofibrate but not fenofibric acid inhibits 11 $\beta$ -hydroxysteroid dehydrogenase 1 in C2C12 myotubes. *Mol Cell Biochem* 344: 91–98.
35. Aranasov AG, Tam S, Rocken JM, Baker ME, Odermatt A (2003) Inhibition of 11 $\beta$ -hydroxysteroid dehydrogenase type 2 by dithiocarbamates. *Biochem Biophys Res Commun* 308: 257–262.
36. Luther JM, Gainer JV, Murphy LJ, Yu C, Vaughan DE, et al. (2006) Angiotensin II induces interleukin-6 in humans through a mineralocorticoid receptor-dependent mechanism. *Hypertension* 48: 1050–1057.
37. Frierl RA, Meng H, Duan SZ, Berger S, Schutz G, et al. (2011) Myeloid-specific deletion of the mineralocorticoid receptor reduces infarct volume and alters inflammation during cerebral ischemia. *Stroke* 42: 179–185.
38. Bledsoe RK, Madaus KP, Holt JA, Apolito CJ, Lambert MH, et al. (2005) A ligand-mediated hydrogen bond network required for the activation of the mineralocorticoid receptor. *J Biol Chem* 280: 31283–31293.
39. Matilainen J, Ozcan M, Lassila L, Kalk W, Vallittu P (2008) Effect of the cross-linking silane concentration in a novel silane system on bonding resin-composite cement. *Acta Odontol Scand* 66: 250–255.
40. Seppä L (2004) Fluoride varnishes in caries prevention. *Med Princ Pract* 13: 307–311.
41. Friedman A, Friedman J (2009) New biomaterials for the sustained release of nitric oxide: past, present and future. *Exp Opin Drug Deliv* 6: 1113–1122.
42. Pan G, Schaefer DW, Ilavsky J (2006) Morphology and water barrier properties of organosilane films: the effect of curing temperature. *J Colloid Interface Sci* 302: 287–293.
43. McCurley A, Jaffe IZ (2012) Mineralocorticoid receptors in vascular function and disease. *Mol Cell Endocrinol* 350: 256–265.
44. Young MJ, Rickard AJ (2012) Mechanisms of mineralocorticoid salt-induced hypertension and cardiac fibrosis. *Mol Cell Endocrinol* 350: 248–255.
45. Bocchini V, Mazzolla R, Barluzzi R, Blasi E, Sica P, et al. (1992) An immortalized cell line expresses properties of activated microglial cells. *J Neurosci Res* 31: 616–621.
46. Kratschmar DV, Vuorinen A, Da Cunha T, Wolber G, Classen-Houben D, et al. (2011) Characterization of activity and binding mode of glycyrrhetic acid derivatives inhibiting 11 $\beta$ -hydroxysteroid dehydrogenase type 2. *J Steroid Biochem Mol Biol* 125: 129–142.
47. Wolber G, Langer T (2005) LigandScout: 3-D pharmacophores derived from protein-bound ligands and their use as virtual screening filters. *J Chem Inf Model* 45: 160–169.
48. Huang N, Shoichet BK, Irwin JJ (2006) Benchmarking sets for molecular docking. *J Med Chem* 49: 6789–6801.
49. Schuster D, Laggner C, Steindl TM, Paluszczak A, Hartmann RW, et al. (2006) Pharmacophore modeling and in silico screening for new P450 19 (aromatase) inhibitors. *J Chem Inf Model* 46: 1301–1311.
50. Verdonk ML, Cole JC, Hartshorn MJ, Murray CW, Taylor RD (2003) Improved protein-ligand docking using GOLD. *Proteins* 52: 609–623.
51. Jones G, Willett P, Glen RC, Leach AR, Taylor R (1997) Development and validation of a genetic algorithm for flexible docking. *J Mol Biol* 267: 727–748.

## CHAPTER 4

**Dibutyltin promotes oxidative stress and increases inflammatory mediators in BV-2 microglia cells**

## **Dibutyltin promotes oxidative stress and increases inflammatory mediators in BV-2 microglia cells**

Boonrat Chantong, Denise V. Kratschmar, Adam Lister and Alex Odermatt

Swiss Center for Applied Human Toxicology and Division of Molecular and Systems Toxicology, Department of Pharmaceutical Sciences, University of Basel, Klingelbergstrasse 50, 4056 Basel, Switzerland

E-mail addresses: [boonrat.chantong@unibas.ch](mailto:boonrat.chantong@unibas.ch); [denise.kratschmar@unibas.ch](mailto:denise.kratschmar@unibas.ch); [adam.lister@unibas.ch](mailto:adam.lister@unibas.ch); [alex.odermatt@unibas.ch](mailto:alex.odermatt@unibas.ch).

### **Correspondence to:**

Dr. Alex Odermatt, Division of Molecular and Systems Toxicology, Department of Pharmaceutical Sciences, University of Basel, Klingelbergstrasse 50, CH-4056 Basel, Switzerland

Phone: +41 61 267 1530, Fax: +41 61 267 1515, E-mail: [alex.odermatt@unibas.ch](mailto:alex.odermatt@unibas.ch)

### **Abbreviations**

AMPK, AMP-activated protein kinase; DBT, dibutyltin; DHE, dihydroethidium; DMEM, Doubecco's modified Eagles medium; DTT, dithiothreitol; ERK, extracellular signal-regulated protein kinase; FBS, fetal bovine serum; HBSS, Hank's balanced salt solution; HEPES, 4-(2-hydroxyethyl)-1-piperazine ethanesulfonic acid; IL-6, interleukin-6; iNOS, inducible nitric oxide synthase; JNK, c-Jun NH(2)-terminal kinase; MAPK, mitogen-activated protein kinase; NEAA, non-essential amino acids; NOX-2, NF- $\kappa$ B, nuclear factor- $\kappa$ B; NADPH-dependent oxidase 2; PI3K/Akt, phosphatidylinositol 3 kinase/proteinkinase B; PKC, protein kinase C; PLC, phospholipase C; PVDF, polyvinylidene difluoride; ROS, reactive oxygen species; TBS, tris-buffered saline; TBT, tributyltin.

**Abstract**

The organotin dibutyltin (DBT) is used as biocide and as stabilizer in the manufacture of silicones, polyvinyl chloride plastics, polyurethanes and polyester systems. Although the immuno- and neurotoxicity of DBT has been recognized, the underlying mechanisms remained unclear and the impact of DBT on microglia cells has not yet been established. We now used cultured mouse BV-2 cells as a model of activated microglia to investigate the impact of DBT on oxidative stress and pro-inflammatory cytokines. DBT, at subcytotoxic concentrations, increased intracellular reactive oxygen species (ROS), mitochondrial mass, mitochondrial ROS, and the mRNA expression of inducible nitric oxide synthase (iNOS) and NADPH-dependent oxidase-2 (NOX-2). ATP levels were decreased by DBT, followed by activation of AMP-activated protein kinase (AMPK). Moreover, DBT potentiated the expression of tumor necrosis factor- $\alpha$  (TNF- $\alpha$ ) and interleukin-6 (IL-6). Inhibition of NOX-2 diminished both ROS production and induction of IL-6 expression. The DBT-mediated increase in NF- $\kappa$ B activity and subsequent up regulation of IL-6 was abolished by co-treatment with a NF- $\kappa$ B inhibitor. Treatment of cells with pharmacological inhibitors indicated a role for mitogen-activated protein kinases (MAPKs), PI3K/Akt, protein kinase C (PKC) and phospholipase C (PLC) in the DBT-induced toxicity. Finally, the calcium chelator BAPTA-AM diminished oxidative stress and induction of IL-6 expression, indicating the involvement of increased intracellular calcium in the enhanced microglia activity upon exposure to DBT. Together, the results suggest that a potentiation of oxidative stress and pro-inflammatory cytokine expression in microglia cells contribute to the toxicity of DBT in the CNS.

Key words: Organotin, dibutyltin, microglia, inflammation, oxidative stress, neurotoxicity

## 1. Introduction

Dibutyltin (DBT) is a toxic organotin found in the environment and in dietary sources (Choi et al., 2012; Rastkari et al., 2012). It has been used as biocide and stabilizer in a wide range of agricultural and industrial products (Fent, 1996). In some countries, DBT has been detected in drinking water upon leaching from polyvinyl chloride plastics pipes (Mundy and Freudenrich, 2006; Sadiki and Williams, 1999; Sadiki et al., 1996). In addition to its direct use, DBT is formed as a major degradation product from tributyltin (TBT) in humans and higher animals (Gipperth, 2009; Ohhira et al., 2003; Ueno et al., 2003). Thus, at least some of the toxic effects of TBT, which has been widely used as a fungicide, wood preservative and antifouling agent, are caused by DBT. Unlike TBT, which has been banned recently by the International Maritime Organization for the use as antifouling agent, DBT is still in use. DBT has been found in human blood at concentrations as high as 300 nM (Kannan et al., 1999; Whalen et al., 1999). Furthermore, it was detected in liver tissue of humans and wild terrestrial animals at concentrations up to 100 nM (Appel, 2004; Nielsen and Strand, 2002; Takahashi et al., 1999).

In contrast to TBT, the toxicity of DBT is less well investigated. Nevertheless, several *in vitro* and *in vivo* studies reported severe immunotoxic and neurotoxic effects of DBT (Jenkins et al., 2004; Seinen et al., 1977; Whalen et al., 1999). High doses of DBT have been shown to cause acute pancreatitis in rats (Hense et al., 2003). DBT, like TBT, causes thymus atrophy in rodents by decreasing T-lymphocyte proliferation and inducing apoptosis and necrosis at higher concentrations (Gennari et al., 2000; Tomiyama et al., 2009). Furthermore, DBT altered the expression of several transcriptional regulators and the release of pro-inflammatory cytokines in human natural killer cells by a mechanism involving mitogen-activated protein kinases (MAPKs) (Hurt et al., 2013; Odman-Ghazi et al., 2010; Person and Whalen, 2010). The immunotoxic and pro-inflammatory effects of DBT were further supported by observations in cultured macrophage, where DBT suppressed glucocorticoid receptor activity and enhanced NF- $\kappa$ B activity as well as the production of inflammatory cytokines such as TNF- $\alpha$  and IL-6 (Gumy et al., 2008).

Developmental neurotoxic effects of DBT have been demonstrated in cynomolgus monkeys and in rodents (Ema et al., 2009; Jenkins et al., 2004; Moser et al., 2009). Interestingly, DBT was consistently detected in the brain in a two-generation reproductive toxicity study of rats treated with TBT (Omura et al., 2004), suggesting that DBT is responsible for at least part of the

observed neurotoxic effects following TBT exposure. In rats, DBT caused neurotoxicity with increasing apoptotic cell death in the neocortex and hippocampus of offspring (Jenkins et al., 2004). DBT in aggregating brain cell cultures affected myelin content and the cholinergic neurons (Eskes et al., 1999). Markers for astrocytes and oligodendrocytes were diminished. Furthermore, DBT induced apoptosis of cerebellar granule cells through activation of MAPKs (Mundy and Freudenrich, 2006), and a concentration-dependent decrease in cell viability, mitochondrial potential and cell proliferation in neuroblastoma cells was recently reported (Ferreira et al., 2013).

Despite increasing evidence for severe immuno- and neurotoxic effects of DBT, few studies focused on neuronal cell models, whereby microglia cells have been mostly neglected. Microglia are macrophage-like resident cells in the CNS. Excessive inflammation involving microglia activation underlies many neurodegenerative diseases such as Parkinson's disease, Alzheimer's disease and multiple sclerosis (Collins et al., 2012; Kozirowski et al., 2012; Morales et al., 2010; Rubio-Perez and Morillas-Ruiz, 2012; Sorenson et al., 2013). Upon activation, microglia release inflammatory cytokines and increase the production of inducible nitric oxide synthase (iNOS) and reactive oxygen species (ROS), two inflammatory markers that have been associated with demyelination and axonal damage in cerebellar cultures (di Penta et al., 2013). Initial microglia activation was suggested to promote glial neuroimmune responses, resulting in persistent increases in classical innate immune gene expression (Qin et al., 2007). The inflammatory response in the injured brain elicits cytokines such as interleukin-1 $\beta$  (IL-1 $\beta$ ), tumor necrosis factor- $\alpha$  (TNF- $\alpha$ ) and interleukin-6 (IL-6) (Clark et al., 2013; Woodcock and Morganti-Kossmann, 2013). Oxidative imbalance and subsequent oxidative stress also play an important role in the progression of neurodegenerative diseases (Butterfield et al., 2006; Glass et al., 2010). The CNS appears to be especially vulnerable to oxidative stress due to its high rate of oxygen consumption, low levels of molecular antioxidants and the susceptibility of neurons or oligodendrocytes due to their specific metabolic properties.

Among the transcription factors regulating inflammation and oxidative stress, NF- $\kappa$ B is one of the most relevant in microglia cells. Activation of NF- $\kappa$ B is triggered by phosphorylation, inducing its translocation into the nucleus where it modulates gene expression (Jang et al., 2005; Lee et al., 2006). NF- $\kappa$ B is activated by ROS and various kinases (Crews et al., 2011).

Phosphatidylinositol 3-kinase (PI3K)/protein kinase B (Akt) are also known to regulate the expression of inflammatory mediators in microglia (Hu et al., 2012; Lee et al., 2006; Xing et al., 2008). MAPKs, including p38 MAPK, c-Jun NH(2)-terminal kinase (JNK), and extracellular signal-regulated protein kinase (ERK1/2), have been suggested to be critical regulators of oxidative stress and proinflammatory signaling cascades (Wang et al., 2011). Several reports have shown that NF- $\kappa$ B, PI3K/Akt, and MAPKs are regulated by intracellular calcium levels and consequently influence cytokine expression and release in inflammation-responsive cells (Fukuno et al., 2011; Lee et al., 2004; Li et al., 2009; Yamashiro et al., 2010; Yang et al., 2000; Zhou et al., 2010; Zhou et al., 2006). In addition, it has been shown that activation of MAPKs or NF- $\kappa$ B can be mediated via activation of phospholipase C (PLC) and stimulation of protein kinase C (PKC) in various cell types (Katz et al., 2006; Lee et al., 2013; Zhou et al., 2006).

Although the neurotoxic potential of DBT has been reported, its impact on microglia cells remained unclear. BV-2 cells represent a valuable alternative model system for primary mouse microglia (Henn et al., 2009). Their response to LPS was found to be similar to that in primary microglia, although the effects were generally less pronounced. BV-2 cells also showed normal NO production and functional response to interferon- $\gamma$  (Henn et al., 2009). In the present work, we investigated the response of BV-2 mouse microglia cells to DBT and assessed the impact of DBT on inflammatory mediators and oxidative stress as well as the role of several relevant signaling pathways.

## **2. Materials and methods**

### **2.1. Chemicals and reagents**

Dulbecco's modified Eagle's medium (DMEM), RPMI-1640 medium, penicillin, streptomycin, 0.05% (w/v) trypsin/EDTA, non-essential amino acids (NEAA), 4-(2-hydroxyethyl)-1-piperazineethanesulfonic acid (HEPES), Hank's balanced salt solution (HBSS), Hoechst-33342, dihydroethidium (DHE), Sytox-Green, LysoTracker-Red, Mitotracker Red CMXRos and MitoSOX Red were obtained from Invitrogen (Carlsbad, CA, USA) and the XTT cell viability kit from Cell Signaling Technology Inc. (Danvers, MA, USA). Fetal bovine serum (FBS) was purchased from Atlanta Biologicals (Lawrenceville, GA, USA), CellTiter-Glo Assay kit from Promega (Madison, WI, USA), ELISA kit for IL-6 from BD Biosciences, (BD Biosciences, CA,

USA) and Cellomics HCS kit for evaluation of NF- $\kappa$ B activation (K010011) from Cellomics Inc (Cellomics Inc, Pittsburgh, PA, USA). Inhibitors of ERK1/2 (PD-98059), p38 MAPK (SB-202190), JNK (SP-600125), PLC (U-73122), PKC (GF-109203x), PI3K (LY-294002 and wortmanin), Akt and NOX-2 (apocynin), DBT-chloride, thapsigargin, AMPK activator AICAR, BAPTA-AM, sodium dodecyl sulfate, polyacrylamide/bis-acrylamide, Tween-20,  $\beta$ -mercaptoethanol and dimethylsulfoxide were purchased from Sigma-Aldrich (St. Louis, MO, USA). Compound C was obtained from Calbiochem (San Diego, CA, USA). Cay-10512 was purchased from Cayman chemical (Hamburg, Germany). Antibodies against AMPK, NF- $\kappa$ B (p65) and their phosphorylated forms were obtained from Cell Signaling Technology Inc. and antibody against  $\beta$ -actin and goat anti-rabbit IgG-horseradish peroxidase from Santa Cruz Biotechnology (Santa Cruz, CA, USA).

## **2.2. Cultivation of BV-2 cells and basal activation state**

BV-2 cells (immortalized mouse microglia), kindly provided by Dr Wolfgang Sattler, University of Graz, Austria, were grown at 37°C and 5% CO<sub>2</sub> in RPMI 1640 medium containing 10% (v/v) FBS, 100 U/ml penicillin, 100  $\mu$ g/ml streptomycin, 2 mM glutamine, 0.1 mM NEAA and 10 mM HEPES, pH 7.4. Cells were harvested at 80% confluence. Prior to the experiments, cells were transferred to 96-well ( $1 \times 10^3$  cells/well), 24-well ( $2 \times 10^4$  cells/well), 12-well ( $0.5 \times 10^6$  cells/well) or 6-well ( $1.0 \times 10^6$  cells/well) plates containing DMEM supplemented with 10% FBS, 1 g/L glucose, 2 mM glutamine, 100  $\mu$ g/mL streptomycin, 100 U/mL penicillin, 0.1 mM NEAA and 10 mM HEPES, followed by incubation for 24 h.

Under the conditions applied, the cultivated BV-2 cells showed basal mRNA expression of IL-1 $\beta$ , IL-6, TNF- $\alpha$ , interferon- $\gamma$  and iNOS, genes characteristic of the classically activated M1 state, whereas mRNA expression of the M2 markers IL-4 and IL-10 were low (data not shown). Thus, the BV-2 cells used in this study represent a model of partially activated microglia.

## **2.3. Determination of cellular toxicity parameters**

BV-2 cells grown in 96-well plates were incubated with various concentrations of DBT for 24 h. Following addition of 50  $\mu$ l staining solution (DMEM containing 2.5  $\mu$ M Sytox-Green, 250 nM LysoTracker-Red and 500 nM Hoechst-33342, cells were incubated for 30 min at 37°C. Cells

were rinsed twice with pre-warmed PBS (37°C), followed by fixation with 4% paraformaldehyde in PBS for 15 min. Cells were washed three times with PBS. Plates were analyzed using a Cellomics ArrayScan high-content screening system (Cellomics ThermoScientific, Pittsburgh, PA, USA) (Nashev et al., 2012). Data acquisition and image analysis was conducted using automated fluorescence imaging. Fluorescence intensity measurements (population averages) were captured on 20 fields, each containing approximately 1000 cells. Images were acquired for each fluorescence channel (Hoechst-33342, LysoTracker-Red, Sytox-Green) using appropriate filters, a 20 × objective and the bioapplication software from the manufacturer. Additionally, cytotoxicity was assessed using the XTT cell viability kit (Cell Signaling Technology Inc.), reflecting mitochondrial enzyme activity of living cells.

#### **2.4. Measurement of mitochondrial content and ROS**

Cellular ROS, mitochondrial ROS and mitochondrial content were determined using the fluorescent dyes dihydroethidium (DHE), MitoSOX Red and MitoTracker Red CMXRos, respectively. Following treatment, cells were washed with PBS and labeled with DHE (10 µg/ml, 10 min), MitoSOX Red (5 µM, 20 min) or MitoTracker Red CMXRos (200 nM, 30 min). Cells were washed twice with PBS and fixed with 4% paraformaldehyde for 15 min. Cells were washed twice with PBS containing 0.1% Tween-20 and nuclei staining solution (1 µg/ml Hoechst-33342 dissolved in medium) was added, followed by incubation for 30 min. Cells were analyzed by high-content imaging as described above. Cells were identified using Hoechst-33342 and a nuclear mask was generated from images of Hoechst-stained nuclei. Cellular ROS, mitochondrial ROS and mitochondrial content were reported as percentage of fluorescence intensity compared with control.

#### **2.5. Quantification of mRNA expression by real-time RT-PCR**

Relative quantification of mRNA expression levels was performed by real-time RT-PCR. The cDNA (5 ng), gene-specific primers (200 nM) and KAPA SYBR FAST qPCR reagent (Kapasystems, Boston, MA) (5 µl), in a final volume of 10 µl, were subjected to quantitative real-time RT-PCR in a rotor-gene 3000A (Corbett Research, Australia). Thermal cycler parameters were as follows: denaturation for 15 min at 95°C, followed by amplification of cDNA

for 40 cycles with melting for 15 s at 94°C, annealing for 30 s at 56°C and extension for 30 s at 72°C. Three replicates were analyzed per sample. Relative gene expression normalized to the internal control gene GAPDH was obtained by the  $2^{-\Delta\Delta Ct}$  method (Livak and Schmittgen, 2001). The primers for real-time PCR are listed under Supplementary data Table A.

## **2.6. Determination of ATP content**

ATP levels were measured using the CellTiter-Glo Luminescence Cell Viability Assay Kit (Promega) following the manufacturer's instructions. Briefly, 100  $\mu$ l of luminescent reagent was added to each well and samples were gently mixed for 30 min at room temperature on an orbital shaker, protected from light. Luminescence was then quantified using a SpectraMax-L luminometer (Molecular Device, Devon, UK). The luminescence from the treated cells was normalized to the luminescence from control cells, which was set as 100%.

## **2.7. Preparation of whole cell lysates, cytoplasmic and nuclear fractions**

For preparation of whole cell lysates, cells grown in 6-well plates were washed twice with ice-cold PBS, harvested and lysed in RIPA buffer (Sigma-Aldrich) supplemented with protease inhibitor cocktail (Roche Diagnostics, Rotkreuz, Switzerland). Extracts were centrifuged at 10,000 $\times$ g for 15 min at 4°C to remove cell debris. For preparation of cytoplasmic and nuclear fractions, cells seeded in 6-well plates were washed twice with ice-cold PBS and harvested. Cell pellets were collected by centrifugation at 450 $\times$ g for 5 min, washed once with PBS and pelleted again at 1,000 $\times$ g for 5 min. Cells were suspended in 200  $\mu$ l hypotonic lysis buffer (100 mM KCl, 15 mM MgCl<sub>2</sub>, 100 mM HEPES, pH 7.9) containing 0.01 M DTT and protease inhibitors and kept on ice for 15 min. IGEPAL CA-630 solution (Sigma-Aldrich) (0.6% v/v final concentration) was added to the cell suspension, followed by mixing for 10 s and centrifugation at 10,000 $\times$ g for 30 s. The supernatant, representing the cytoplasmic fraction, was transferred to a new tube. The pellets were washed once with 100  $\mu$ l PBS, pelleted at 450 $\times$ g for 5 min and resuspended in 100  $\mu$ l ice-cold nuclear extraction buffer (0.42 M NaCl, 1.5 mM MgCl<sub>2</sub>, 0.2 mM EDTA, 20 mM HEPES, pH 7.9, and 25% (v/v) glycerol) containing 0.01 M DTT and protease inhibitors. The nuclear suspension was mixed thoroughly for 30 min and centrifuged at 12,000 $\times$ g for 5 min. The supernatant, representing the nuclear fraction, was stored at -80°C until use.

## 2.8. Western blot analysis

Equivalent protein amounts (30  $\mu$ g) of cytoplasmic, nuclear or whole cell extracts were separated by SDS-PAGE, followed by transfer onto 0.2  $\mu$ m polyvinylidene difluoride (PVDF) membranes (Bio-Rad Laboratories, Hercules, CA, USA) for 1 h at 150 mA. Membranes were incubated for 1 h at room temperature in Tris-buffered saline (TBS), pH 7.4, containing 0.1% Tween-20 (TBS-T) and 5% non-fat milk. The membranes were incubated overnight at 4°C with primary antibodies against AMPK $\alpha$  (1:1000), phospho-AMPK $\alpha$  (Thr172) (1:1000), NF- $\kappa$ B p65 (1:500), phospho-NF- $\kappa$ B p65 (1:500), HDAC1 (1:1000) or  $\beta$ -actin (1:1000). After washing with TBS-T, blots were incubated with goat anti-rabbit IgG-horseradish peroxidase or anti-mouse IgG horseradish peroxidase for 2 h at room temperature. Blots were then washed with TBS-T and immunolabeling was visualized using enhanced chemiluminescence HRP substrate (Millipore, Billerica, MA, USA) according to the manufacturer's instructions using a Fujifilm LAS-4000 detection system (Bucher Biotec, Basel, Switzerland).  $\beta$ -actin was used as loading control for cytoplasmic and whole cell protein extracts. HDAC1 was used as loading control for nuclear fractions.

## 2.9. Determination of the intracellular localization of NF- $\kappa$ B

Experiments were performed in 96-well plates. Following treatment, the medium was removed and cells were fixed and stained using a Cellomics NF- $\kappa$ B p65 Activation HCS Reagent Kit (Cellomics Inc) according to the manufacturer's instructions. Briefly, cells were fixed with 4% formaldehyde, washed, permeabilized and incubated with a rabbit polyclonal anti-NF- $\kappa$ B p65 IgG antibody 1 h, followed by a 15 min wash with detergent buffer and two washes with PBS. Cells were then incubated with staining solution consisting of goat anti-rabbit IgG conjugated to Alexa Fluor 488 and Hoechst-33342 for 1 h prior to a 10 min wash with detergent buffer and two washes with PBS. Cells were then soaked in PBS at 4°C until analysis by imaging.

The assay plate was analyzed using an ArrayScan HCS Reader (Cellomics Inc) as described earlier (Chantong et al., 2012). The Cytoplasm to Nucleus Translocation BioApplication software was used to calculate the ratio of cytoplasmic to nuclear NF- $\kappa$ B signal. The average intensity of 500 cells/well was quantified using a 20 $\times$  objective. The signal of the nuclear staining was measured in channel 1 and NF- $\kappa$ B was visualized in channel 2. In channel 2, an algorithm was

utilized to identify the nucleus and surrounding cytoplasm in each cell; this analysis method reports the average intensity within each nuclear mask as well as the total nuclear and cytoplasmic intensity. The results were reported as the percentage of nuclear intensity against the total intensity.

### **2.10. Measurement of IL-6 expression**

The concentration of IL-6 released into the culture medium was quantified by the specific mouse IL-6 ELISA kit according to the manufacturer's protocol (BD Biosciences, CA, USA). Briefly, 96-well plates were coated with capture antibody overnight at 4°C. After 5 washes with PBS-T (PBS containing 0.05% Tween-20), the wells were blocked with assay diluents for 1 h. After repeated washing, standards and collected culture media supernatants of treated cells were added to the coated wells, followed by incubation for 2 h, washing 5 times with PBS-T and incubation with detection antibody for 1 h. After washing with PBS-T, Avidin–HRP was added for 30 min, plates washed 7 times with PBS-T and incubated with substrate solution for 30 min in the dark. Reactions were stopped with 1 M H<sub>3</sub>PO<sub>4</sub> and plates measured at 450 nm with subtraction of the values at 570 nm using a UV-max kinetic microplate reader (Molecular Device). The concentration of IL-6 was calculated from a calibration curve using purified mouse IL-6.

### **2.11. Statistical analysis**

Data represent mean ± SD and were analyzed using one-way ANOVA (V5.00; GraphPad Prism Software Inc., San Diego, CA, USA). When ANOVA showed significant differences between groups, Tukey's post-hoc test was used to determine the specific pairs of groups showing statistically significant differences. A *p*-value < 0.05 was considered statistically significant.

## **3. Results**

### **3.1 Enhanced ROS production upon exposure of BV-2 microglia to DBT**

The murine BV-2 microglia cell line was chosen to investigate the effect of DBT on oxidative stress and inflammatory mediators. In a first step, BV-2 cells were incubated with various concentrations of DBT for 24 h and analyzed for cell viability and morphology. Minor morphological changes were observed at 200 nM DBT, whereas at 100 nM and less no changes could be observed. At concentrations higher than 400 nM, cells started to detach. Determination

of cell number, nuclear size, membrane permeability and lysosomal mass by high-content imaging revealed no significant changes at DBT concentrations of up to 300 nM (values between 102-94% of control, n=8). At 400 nM DBT, overt cytotoxicity was observed. Cell number, membrane permeability and lysosomal mass dropped to  $82\pm 12\%$ ,  $80\pm 8\%$  and  $76\pm 6\%$ , respectively. Assessment of mitochondrial activity using an XTT cell viability kit revealed no differences at concentrations up to 100 nM DBT, whereas at 200 nM and 300 nM values dropped to  $81\pm 15\%$  and  $68\pm 11\%$ , respectively, indicating impaired mitochondrial function. Based on these results, the subcytotoxic concentration of 50 nM DBT was used for most subsequent experiments.

Next, the effect of DBT on oxidative stress parameters including intracellular ROS, mitochondrial mass, mitochondrial ROS and iNOS mRNA expression was measured. Incubation of cells with DBT for 24 h resulted in a concentration-dependent increase in cellular ROS, measured by DHE (Fig. 1A). Staining of DBT treated BV-2 cells with MitoTracker Red CMXRos, which measures mitochondrial mass and yields a fluorescence signal proportional to the density of mitochondria, revealed a concentration-dependent increase in mitochondrial content (Fig. 1B). To evaluate mitochondrial superoxide production in DBT-treated cells, the fluorescent MitoSOX Red dye was applied. A concentration-dependent increase in mitochondrial ROS was observed after 24 h of incubation with DBT (Fig. 1C). Cells treated with 50 nM DBT had increased mitochondrial superoxide production ( $340 \pm 40\%$ ) compared with control cells. In addition, the relative expression of iNOS mRNA was measured by quantitative real-time RT-PCR. A significant increase in iNOS mRNA was detected after incubation of cells with DBT (Fig. 1D).

### **3.2. Energy depletion and AMPK activation upon exposure to DBT**

Mitochondrial ROS generation upon exposure to DBT suggests mitochondrial dysfunction. Since ATP depletion may promote oxidative stress (Schutt et al., 2012), we investigated whether DBT enhances the impairment of oxidative phosphorylation, via depletion of ATP levels. DBT induced a time- and concentration-dependent decrease in ATP levels (Fig. 2A). No significant change in ATP levels was observed after 30 min of exposure to DBT at 10, 50 and 100 nM. At 2 h, a decrease of  $16 \pm 3\%$  and  $25 \pm 3\%$  was detected at 50 and 100 nM DBT, respectively. A

significant ATP depletion ( $28 \pm 3\%$ ) was observed at 200 nM DBT after 15 min. The fact that intracellular ROS, mitochondrial mass and mitochondrial ROS was not enhanced after 2 h of exposure to DBT (data not shown), suggests that mitochondrial ATP depletion preceded the induction of oxidative stress, and that a lack of ATP and mitochondrial dysfunction are responsible for DBT-mediated oxidative stress.

AMPK is a kinase inducible by ATP depletion (Hardie, 2007). Therefore, we examined the impact of DBT on the levels of phosphorylated (Thr-172) AMPK protein in BV-2 cells by immunoblot analysis. Treatment of BV-2 cells with DBT did not affect total AMPK expression. Basal signals for AMPK phosphorylation were very low. Nevertheless, the signals obtained from DBT treated cells suggested a time-dependent increase in phosphorylated AMPK, which became evident after 1 h of exposure to DBT and was most pronounced after 2 h of treatment (Fig. 2B).

### **3.3. Elevated expression of pro-inflammatory cytokines upon exposure to DBT**

In order to determine whether DBT promotes inflammatory responses in microglia cells, we first analyzed the expression and secretion of the inflammatory cytokines TNF- $\alpha$  and IL-6. Treatment with DBT (5-500 nM) for 24 h enhanced IL-6 and TNF- $\alpha$  mRNA expression as well as IL-6 protein secretion in a concentration-dependent manner (Fig. 3A and B). The elevation of IL-6 mRNA and protein expression occurred in a time-dependent manner (Fig. 3C and D). After treatment for 24 h with 200 nM DBT, IL-6 mRNA and protein increased by about 7- and 730-fold, respectively, compared with vehicle treated controls (Fig. 3A and B). LPS served as positive control. These results indicate that DBT promoted BV-2 microglia activation.

### **3.4. Role of NOX-2-derived ROS in DBT-dependent IL-6 expression**

NADPH oxidase-2 (NOX-2) plays a major role in mediating the inflammatory response in microglia cells (Wang et al., 2012). Endogenously generated ROS from NOX-2 was suggested to act in a manner similar to secondary messengers to dynamically influence cytokine expression (Jendrysik et al., 2011). Therefore, NOX-2 mRNA expression levels were measured. Treatment with 50 nM DBT for 24 h increased NOX-2 mRNA expression 4-fold compared with the control group (Fig. 4A), suggesting that DBT may interfere with the signaling pathway mediated by NOX-2. To test whether DBT-dependent ROS generation is mediated by NOX-2, we pretreated

BV-2 cells for 1 h with apocynin (inhibitor of NADPH oxidases, specifically of phagocytic NOX-2, (Stefanska et al., 2008)) prior to incubation with 50 nM DBT for a further 24 h. As shown in Fig. 4B, pretreatment with apocynin abrogated DBT-induced ROS production. These results suggest that exposure to DBT results in NOX-2 activation, thereby increasing ROS production. Next, we investigated whether NOX-2 plays a role in the DBT-mediated IL-6 expression. Quantitative RT-PCR revealed that apocynin partially prevented the DBT-mediated increase in IL-6 mRNA expression (Fig. 4C). Similarly, apocynin lowered the secretion of IL-6 protein in DBT treated cells (Fig. 4D), suggesting that NOX-2 is responsible at least in part for the increased expression of pro-inflammatory cytokines by BV-2 cells upon exposure to DBT.

### **3.5. Involvement of NF- $\kappa$ B in the DBT-mediated IL-6 expression**

NF- $\kappa$ B is known to play a role in microglia activation and it has been reported that NF- $\kappa$ B activation is necessary for IL-6 induction in microglia (Memet, 2006). Therefore, we examined whether NF- $\kappa$ B activation is involved in the signal transduction pathway responsible for DBT-dependent IL-6 expression. Under normal conditions, the p65 subunit of NF- $\kappa$ B is mainly located in the cytoplasm and upon activation undergoes phosphorylation and nuclear translocation. Western blot analysis of nuclear and cytoplasmic fractions suggested an enhanced level of phospho-p65 in the nuclear fraction following DBT treatment (Fig. 5A). NF- $\kappa$ B blocker Cay-10512 prevented phosphorylation of the p65 subunit. The level of unphosphorylated p65 protein in the cytoplasmic fraction was not affected by DBT treatment. NF- $\kappa$ B activation was further evaluated by analyzing its cytoplasmic-nuclear translocation using the Cellomics ArrayScan HCS imaging system. Treatment of cells with DBT resulted in a marked translocation of the p65 subunit of NF- $\kappa$ B from the cytosol to the nucleus (Fig. 5B). As shown in Fig. 5C and D, the NF- $\kappa$ B inhibitor Cay-10512 effectively inhibited the DBT-induced IL-6 mRNA and protein expression.

### **3.6. Involvement of MAPKs in the DBT-dependent IL-6 production**

The MAPK signaling pathway has been implicated to play key regulatory roles in the expression of inflammatory mediators. Several studies showed that DBT influences the activity of MAPKs in human natural killer cells (Lane et al., 2009; Odman-Ghazi et al., 2010; Person and Whalen, 2010). Hence, in an attempt to assess whether the pro-inflammatory mediators enhanced by DBT

are mediated through the MAPK signaling pathway in microglia cells, we pretreated BV-2 cells for 1 h with specific inhibitors for ERK1/2 (PD98059), p38 MAPK (SB202190) or JNK (SP600125) prior to the addition of 50 nM DBT for a further 24 h. The concentrations of the pharmacological inhibitors used did not have any cytotoxic effect on the BV-2 cells (data not shown). Pretreatment with 50  $\mu$ M PD98059 significantly reduced the DBT-mediated expression of IL-6 mRNA (4.5-fold) and protein (5.5-fold) compared with cells treated with DBT alone (Fig. 6). Inhibitors of p38 MAPK (20  $\mu$ M) and JNK (20  $\mu$ M) also decreased IL-6 mRNA and protein levels induced by DBT; however, they were less efficient.

### **3.7. Modulation of the DBT-dependent IL-6 expression by the PI3K/Akt pathway**

We next investigated a possible role of the PI3K/Akt pathway in DBT-stimulated IL-6 expression. Cells were pre-treated for 1 h with the PI3K inhibitors LY294002 (20  $\mu$ M) and wortmannin (100 nM) as well as with Akt inhibitor (10  $\mu$ M) prior to incubation with 50 nM DBT for a further 24 h. None of the inhibitors affected cell viability. As shown in Fig. 7, DBT-stimulated IL-6 mRNA and protein expression was inhibited by treatment with LY294002, wortmannin and an Akt inhibitor. The data suggest that activation of the PI3K/Akt pathway is involved in the DBT-mediated elevation of IL-6 expression in BV-2 microglia cells.

### **3.8. Involvement of PKC and PLC in the DBT-mediated IL-6 production**

Since PLC and PKC can modulate the PI3K/Akt pathway, we assessed whether the DBT-stimulated IL-6 expression was dependent on these two enzymes. BV-2 cells were pretreated with 10  $\mu$ M of the PLC inhibitor U73122 for 1 h prior to incubation with DBT for a further 24 h. As shown in Fig. 8, pretreatment with U73122 inhibited DBT-dependent IL-6 expression, suggesting that the effect of DBT was mediated through the  $Ca^{2+}$ -dependent PKC-PLC pathway. Recent reports suggested that activation of the NOX/ROS signaling pathway might be mediated through PKC (Fontayne et al., 2002; Hsieh et al., 2010). Therefore, a role of PKC on DBT-induced IL-6 expression was investigated. Cells were pretreated with 5  $\mu$ M of the non-specific PKC inhibitor GF109203X for 1 h prior to further incubation with DBT for 24 h. As shown in Fig. 8, pretreatment with GF109203X markedly inhibited the DBT-dependent IL-6 expression.

### 3.9. Suppression of DBT-mediated IL-6 expression by Ca<sup>2+</sup> chelators

It was reported that DBT is able to elevate cytosolic calcium levels in human natural killer (NK) cells (Lane et al., 2009) and in HL-60 promyelocytic leukemia cells (Ade et al., 1996). Consequently, we investigated whether the DBT-dependent activation of BV-2 microglia cells may be mediated by calcium and prevented by treatment with a calcium chelator. BAPTA-AM effectively antagonized the DBT-induced increase in IL-6 mRNA expression, indicating that DBT exposure stimulated IL-6 mRNA through a calcium-dependent manner in microglia cells (Fig. 9A). Importantly, BAPTA-AM also prevented the DBT-dependent ROS production (measured by DHE and MitoSOX Red) and mitochondrial dysfunction (measured by MitoTracker Red CMXRos) (Fig. 9B-D). Furthermore, the calcium chelator abolished the DBT-stimulated expression of iNOS (Fig. 9E). These results indicate that the DBT effects in BV-2 microglia cells are dependent on an increase of intracellular calcium.

## 4. Discussion

Although the toxic responses of DBT in various cell types have been documented and neurotoxic effects of DBT are well known (Ema et al., 2009; Ferreira et al., 2013; Hurt et al., 2013; Odman-Ghazi et al., 2010; Person and Whalen, 2010; Tomiyama et al., 2009; Yanik et al., 2011), its effects on microglia have not yet been studied. Microglia are implicated in the regulation of neural homeostasis and the response to injury and repair (Harry, 2013). Upon injury-mediated activation, the release of various cytokines, chemokines as well as NO and ROS from microglia is induced (Gao and Hong, 2008). Impaired control of microglial functions and over activation leads to a dysregulation in the inflammatory network and oxidative imbalance, key components in the pathogenesis of neurodegenerative diseases. The capacity of microglia to shift from a pro-inflammatory to an anti-inflammatory state to regulate injury and repair is limited with increasing age (Harry, 2013). Thus, aging and any insult leading to impaired microglia function likely results in an increased susceptibility to neural damage and neurodegeneration.

The main objective of the present study was to characterize the DBT-dependent modulation of the activity of BV-2 mouse microglia cells, to assess the impact on oxidative stress and inflammatory responses, and to start to understand the underlying mechanisms. To our knowledge, this is the first study to show toxic effects of DBT in microglia cells and to describe

the mechanism underlying the modulation of oxidative and inflammatory responses upon exposure to DBT.

It has been reported that DBT has cytotoxic effects in neuroblastoma SH-SY5Y cells (Isomura et al., 2013) and in rat thymocytes, where it increases intracellular calcium, followed by ROS production and cytochrome c release from mitochondria, and subsequent activation of caspases, ultimately resulting in DNA fragmentation (Gennari et al., 2000). However, the action of DBT in microglia cells has not been investigated. In the present study, we show that exposure to DBT causes oxidative stress in BV-2 microglia cells. Specifically, DBT potentiated ROS generation in the cytoplasm and in mitochondria and enhanced mitochondrial mass, which ultimately leads to mitochondrial dysfunction. Mitochondrial mass reflects the maintenance of mitochondrial membrane potential (Chen et al., 2005; Macho et al., 1996) and there is evidence that mitochondrial mass increases during apoptotic cell death (Kluza et al., 2004; Mahyar-Roemer et al., 2001), probably as an adaptive response to energy demand after a toxic insult. Nitric oxide (NO), which is produced by iNOS, is a signaling molecule involved in ROS generation. Chuang *et al.* observed a correlative increase in NO production following induction of iNOS expression (Chuang et al., 2013) in BV-2 microglia cells. In the present study, DBT significantly up-regulated iNOS mRNA expression suggesting elevated NO production. Furthermore, we found enhanced NOX-2 mRNA expression following DBT treatment. Importantly, the NOX-2 inhibitor apocynin diminished DBT-mediated ROS production and IL-6 expression. A pivotal role of over activated NOX-2 in inflammation-mediated neurodegeneration is generally accepted. Thus, our data confirmed the role of NOX-2 mediated ROS generation during the inflammatory process in macrophage-like cells, in agreement with a recent report (Gandhirajan et al., 2013).

ATP depletion leads to increased cellular oxidative stress and ROS production in the mitochondria (Kolamunne et al., 2011). In the present study, DBT decreased ATP production within 2 h, suggesting that DBT affected mitochondrial function and ATP synthesis. This result is consistent with observations from human natural killer cells where DBT markedly decreased ATP levels (Dudimah et al., 2007). However, in contrast to our observations in microglia cells, the ATP depletion was observed after 48 h of exposure with DBT in neuroblastoma cells. AMPK is a key regulator of energy homeostasis and is characterized as a ROS-inducible kinase (Hwang et al., 2005; Ronnett et al., 2009). Moreover, inhibition of mitochondrial activity stimulates AMPK (Hardie, 2007). We show that the exposure of BV-2 cells to DBT resulted in an

enhancement of AMPK phosphorylation, following ATP-depletion. The extent of AMPK phosphorylation at Thr-172 strongly reflects its activity (Hardie, 2004). AMPK has been identified as a major regulator of mitochondrial biogenesis in response to energy depletion (Reznick and Shulman, 2006). This activation is crucial for a multitude of compensatory responses aiming to preserve cellular energy and avoid apoptosis. Activated AMPK may restore mitochondrial functions, thus promoting cell survival. However, prolonged AMPK activation using the activator AICAR has been shown to be toxic for cells (Meisse et al., 2002). Taken together, these results demonstrate that DBT interfered with AMPK phosphorylation, which may be due to increased ROS production, since AMPK is an oxidative stress-inducible kinase, even in the absence of ATP depletion (Sanchez et al., 2008). DBT not only induced energy imbalance but also ROS and mitochondrial dysfunction, which are expected to stimulate AMPK activity by indirect mechanisms.

Activated microglia cells produce several inflammatory cytokines such as TNF- $\alpha$ , IL-1 $\beta$  and IL-6, which are critical in regulating the physiological immune responses in the CNS (Sadasivan et al., 2012; Smith et al., 2012). However, chronic activation of microglia cells excessively prolongs the inflammatory response and causes neuronal damage, which triggers the development of neurodegenerative diseases. It has been shown that DBT increased the secretion of TNF- $\alpha$  in human natural killer cells (Hurt et al., 2013). DBT also induced chronic pancreatitis with increased cytokine mRNA levels and lymphocyte infiltration (Hense et al., 2003; Sparmann et al., 2001; Zhou et al., 2013). In the present study, we show that the expression of TNF- $\alpha$  and IL-6 were up-regulated by treatment with subcytotoxic concentrations of DBT in BV-2 microglia cells. The evidence suggests that chronic DBT exposure promotes inflammatory cytokine release in multiple inflammatory cell types including microglia and that the neurotoxicity of DBT may be due to persistent exposure to inflammatory cytokines.

The activation of NF- $\kappa$ B is involved in the transcription and production of several pro-inflammatory cytokines in microglia cells, including TNF- $\alpha$ , IL-1 $\beta$ , IL-6, IL-12 and IFN- $\gamma$  (Murakami and Hirano, 2012; Napetschnig and Wu, 2013). Moreover, it has been reported that NF- $\kappa$ B activation is necessary for IL-6 induction in microglia. When activated by oxidative stress and signals sourced from pathogens, NF- $\kappa$ B translocates to the nucleus, leading to the augmented transcription of pro-inflammatory genes. NF- $\kappa$ B is frequently found to be activated at the site of

inflammation (Zordoky and El-Kadi, 2009). It has been reported that chronic pancreatitis induced by DBT in rats increased NF- $\kappa$ B p65 expression (Zhou et al., 2013). In the present study, Cay10512, a NF- $\kappa$ B inhibitor, diminished DBT-mediated IL-6 expression and secretion. Likewise, DBT increased the translocation of the p65 NF- $\kappa$ B from the cytoplasm into the nucleus. These observations, therefore, demonstrated that the increased IL-6 production was mediated by NF- $\kappa$ B activation.

NF- $\kappa$ B signaling is tightly linked with PI3K/Akt and MAPK signaling (Qi et al., 2012). The PI3K/Akt pathway is involved in the expression of inflammatory mediators such as IL-6 in microglia cells (Lu et al., 2009; Tang et al., 2007), although the exact mechanism remains unclear. In addition, PI3K/Akt is involved in NF- $\kappa$ B activation associated with ROS production in LPS-treated BV2 cells (Kim and Moudgil, 2008). We examined the effect of DBT treatment on the indicated signaling pathways using two different PI3K inhibitors. LY294002 is a potent and reversible inhibitor of PI3K activity by inhibiting the ATP binding site of the enzyme and casein kinase II. Wortmannin is a covalent and irreversible inhibitor of the classes I, II and III PI3K members (Vanhaesebroeck et al., 2001). Both PI3K inhibitors were able to block the action of DBT on IL-6 mRNA expression. In addition, an Akt inhibitor also blocked the effects of DBT, suggesting a role for PI3K/Akt in the DBT-induced IL-6 mRNA expression in BV-2 cells.

NF- $\kappa$ B activation is also regulated by MAPKs (Jang et al., 2005; Nikodemova et al., 2006). MAPKs play a critical role in the regulation of cell survival, apoptosis and differentiation as well as in the control of cellular response to cytokines and stress. MAPKs, including ERK1/2, p38 MAPK and JNK, have been implicated in the transcriptional regulation of inflammatory genes in microglia cells (Jung et al., 2010; Oh et al., 2009; Skaper, 2007). MAPKs are activated by ROS. Several studies showed that DBT activated MAPKs in human natural killer cells (Lane et al., 2009; Odman-Ghazi et al., 2010; Person and Whalen, 2010). In the present study, pretreatment of BV-2 cells with an inhibitor of ERK1/2 strongly inhibited the mRNA expression and secretion of IL-6, suggesting a role of p42/44 in the activation of BV-2 cells by DBT. Pretreatment of cells with p38 MAPK and JNK inhibitors also decreased IL-6 production, although not as efficient as the ERK1/2 inhibitor. This indicates that p38 MAPK and JNK may also be involved in DBT-dependent BV-2 cell activation.

Moreover, we provide evidence for an involvement of PKC and PLC in the DBT-mediated effects. Pretreatment of microglia cells with inhibitors of PKC and PLC partially blocked the

DBT-stimulated IL-6 expression, indicating a role of the PI-PLC pathway, which increases diacylglycerol levels and results in the activation of PKC.

It has been reported that DBT induced an increase in cytosolic calcium levels in human natural killer cells (Lane et al., 2009). Inflammatory cytokine production is associated with elevated calcium levels in activated microglia cells (Brawek and Garaschuk, 2013; Dolga et al., 2012). In the present study, we observed that the  $\text{Ca}^{2+}$  chelator BAPTA-AM was able to block the stimulation of IL-6 expression and the production of oxidative stress caused by exposure of BV-2 microglia cells to DBT. These results suggest that the DBT-stimulated inflammation and oxidative stress are dependent on an increase of intracellular calcium in microglia cells.

## 5. Conclusions

To our knowledge, this is the first report where the effects of DBT at concentrations found in humans (i.e. up to 300 nM) have been investigated on oxidative stress parameters and the inflammatory response in microglia cells. DBT potentiated ROS production as well as iNOS and NOX-2 mRNA expression in BV-2 cells that were in a partially activated state under basal culture conditions. Mitochondrial dysfunction was observed upon exposure to DBT, with an increased mitochondrial mass, mitochondrial ROS production and ATP-depletion. The observed AMPK activation is suggested to be a result of increased energy demand after exposure to DBT. DBT enhanced inflammatory responses such as the expression of IL-6 and TNF- $\alpha$ , activation of NF- $\kappa$ B, phosphorylation of PI3K/Akt and MAPKs. Furthermore, a role of PKC and PLC in the DBT-mediated toxicity was shown. Importantly, the DBT-mediated production of oxidative stress and expression of pro-inflammatory cytokines could be prevented using a calcium chelator. Together, the data suggest that DBT potentiates oxidative stress and cytokine expression in activated microglia cells, which might result in an increased susceptibility to neural damage and neurodegeneration.

## 6. Acknowledgments

This work was supported by the Swiss Center for Applied Human Toxicology. AO has a Chair for Molecular and Systems Toxicology by the Novartis Research Foundation. AL has received

funding from the European Community's Seventh Framework Programme (FP7/2007-2013) under grant agreement n°246539. BC was supported by a grant from the Royal Thai Government.

### Supplementary data

Table A

### References

- Ade, T., Zaucke, F., Krug, H.F., 1996. The structure of organometals determines cytotoxicity and alteration of calcium homeostasis in HL-60 cells. *Anal Bioanal Chem* 354, 609-614.
- Appel, K.E., 2004. Organotin compounds: toxicokinetic aspects. *Drug Metab Rev* 36, 763-786.
- Brawek, B., Garaschuk, O., 2013. Microglial calcium signaling in the adult, aged and diseased brain. *Cell Calcium* 53, 159-169.
- Butterfield, D.A., Perluigi, M., Sultana, R., 2006. Oxidative stress in Alzheimer's disease brain: new insights from redox proteomics. *Eur J Pharmacol* 545, 39-50.
- Chantong, B., Kratschmar, D.V., Nashev, L.G., Balazs, Z., Odermatt, A., 2012. Mineralocorticoid and glucocorticoid receptors differentially regulate NF-kappaB activity and pro-inflammatory cytokine production in murine BV-2 microglial cells. *J Neuroinflammation* 9, 260.
- Chen, X., Medeiros, D.M., Jennings, D., 2005. Mitochondrial membrane potential is reduced in copper-deficient C2C12 cells in the absence of apoptosis. *Biol Trace Elem Res* 106, 51-64.
- Choi, M., Moon, H.B., Choi, H.G., 2012. Intake and potential health risk of butyltin compounds from seafood consumption in Korea. *Arch Environ Contam Toxicol* 62, 333-340.
- Chuang, D.Y., Chan, M.H., Zong, Y., Sheng, W., He, Y., Jiang, J.H., Simonyi, A., Gu, Z., Fritsche, K.L., Cui, J., Lee, J.C., Folk, W.R., Lubahn, D.B., Sun, A.Y., Sun, G.Y., 2013. Magnolia polyphenols attenuate oxidative and inflammatory responses in neurons and microglial cells. *J Neuroinflammation* 10, 15.
- Clark, K.H., Wiley, C.A., Bradberry, C.W., 2013. Psychostimulant abuse and neuroinflammation: emerging evidence of their interconnection. *Neurotox Res* 23, 174-188.
- Collins, L.M., Toulouse, A., Connor, T.J., Nolan, Y.M., 2012. Contributions of central and systemic inflammation to the pathophysiology of Parkinson's disease. *Neuropharmacology* 62, 2154-2168.

- Crews, F.T., Zou, J., Qin, L., 2011. Induction of innate immune genes in brain create the neurobiology of addiction. *Brain Behav Immun* 25 Suppl 1, S4-S12.
- di Penta, A., Moreno, B., Reix, S., Fernandez-Diez, B., Villanueva, M., Errea, O., Escala, N., Vandenbroeck, K., Comella, J.X., Villoslada, P., 2013. Oxidative stress and proinflammatory cytokines contribute to demyelination and axonal damage in a cerebellar culture model of neuroinflammation. *PLoS One* 8, e54722.
- Dolga, A.M., Letsche, T., Gold, M., Doti, N., Bacher, M., Chiamvimonvat, N., Dodel, R., Culmsee, C., 2012. Activation of KCNN3/SK3/K(Ca)<sub>2.3</sub> channels attenuates enhanced calcium influx and inflammatory cytokine production in activated microglia. *Glia* 60, 2050-2064.
- Dudimah, F.D., Gibson, C., Whalen, M.M., 2007. Effect of dibutyltin on ATP levels in human natural killer cells. *Environ Toxicol* 22, 117-123.
- Ema, M., Arima, A., Fukunishi, K., Matsumoto, M., Hirata-Koizumi, M., Hirose, A., Ihara, T., 2009. Developmental toxicity of dibutyltin dichloride given on three consecutive days during organogenesis in cynomolgus monkeys. *Drug Chem Toxicol* 32, 150-157.
- Eskes, C., Honegger, P., Jones-Lepp, T., Varner, K., Matthieu, J.M., Monnet-Tschudi, F., 1999. Neurotoxicity of dibutyltin in aggregating brain cell cultures. *Toxicol In Vitro* 13, 555-560.
- Fent, K., 1996. Ecotoxicology of organotin compounds. *Crit Rev Toxicol* 26, 1-117.
- Ferreira, M., Blanco, L., Garrido, A., Vieites, J.M., Cabado, A.G., 2013. In vitro approaches to evaluate toxicity induced by organotin compounds tributyltin (TBT), dibutyltin (DBT), and monobutyltin (MBT) in neuroblastoma cells. *J Agric Food Chem* 61, 4195-4203.
- Fontayne, A., Dang, P.M., Gougerot-Pocidallo, M.A., El-Benna, J., 2002. Phosphorylation of p47phox sites by PKC alpha, beta II, delta, and zeta: effect on binding to p22phox and on NADPH oxidase activation. *Biochemistry* 41, 7743-7750.
- Fukuno, N., Matsui, H., Kanda, Y., Suzuki, O., Matsumoto, K., Sasaki, K., Kobayashi, T., Tamura, S., 2011. TGF-beta-activated kinase 1 mediates mechanical stress-induced IL-6 expression in osteoblasts. *Biochem Biophys Res Commun* 408, 202-207.
- Gandhirajan, R.K., Meng, S., Chandramoorthy, H.C., Mallilankaraman, K., Mancarella, S., Gao, H., Razmpour, R., Yang, X.F., Houser, S.R., Chen, J., Koch, W.J., Wang, H., Soboloff, J., Gill, D.L., Madesh, M., 2013. Blockade of NOX2 and STIM1 signaling limits lipopolysaccharide-induced vascular inflammation. *J Clin Invest* 123, 887-902.

- Gao, H.M., Hong, J.S., 2008. Why neurodegenerative diseases are progressive: uncontrolled inflammation drives disease progression. *Trends Immunol* 29, 357-365.
- Gennari, A., Viviani, B., Galli, C.L., Marinovich, M., Pieters, R., Corsini, E., 2000. Organotins induce apoptosis by disturbance of  $[Ca^{2+}]_i$  and mitochondrial activity, causing oxidative stress and activation of caspases in rat thymocytes. *Toxicol Appl Pharmacol* 169, 185-190.
- Gipperth, L., 2009. The legal design of the international and European Union ban on tributyltin antifouling paint: Direct and indirect effects. *J Environ Manage* 90, S86-S95.
- Glass, C.K., Saijo, K., Winner, B., Marchetto, M.C., Gage, F.H., 2010. Mechanisms underlying inflammation in neurodegeneration. *Cell* 140, 918-934.
- Gumy, C., Chandsawangbhuwana, C., Dzyakanchuk, A.A., Kratschmar, D.V., Baker, M.E., Odermatt, A., 2008. Dibutyltin disrupts glucocorticoid receptor function and impairs glucocorticoid-induced suppression of cytokine production. *PLoS One* 3, e3545.
- Hardie, D.G., 2004. The AMP-activated protein kinase pathway--new players upstream and downstream. *J Cell Sci* 117, 5479-5487.
- Hardie, D.G., 2007. AMP-activated protein kinase as a drug target. *Annu Rev Pharmacol Toxicol* 47, 185-210.
- Harry, G.J., 2013. Microglia during development and aging. *Pharmacol Ther* 139, 313-326.
- Henn, A., Lund, S., Hedtjarn, M., Schratzenholz, A., Porzgen, P., Leist, M., 2009. The suitability of BV2 cells as alternative model system for primary microglia cultures or for animal experiments examining brain inflammation. *Altx* 26, 83-94.
- Hense, S., Spammann, G., Weber, H., Liebe, S., Emmrich, J., 2003. Immunologic characterization of acute pancreatitis in rats induced by dibutyltin dichloride (DBTC). *Pancreas* 27, e6-12.
- Hsieh, H.L., Wang, H.H., Wu, C.Y., Yang, C.M., 2010. Reactive Oxygen Species-Dependent c-Fos/Activator Protein 1 Induction Upregulates Heme Oxygenase-1 Expression by Bradykinin in Brain Astrocytes. *Antioxid Redox Signal* 13, 1829-1844.
- Hu, X., Zhou, H., Zhang, D., Yang, S., Qian, L., Wu, H.M., Chen, P.S., Wilson, B., Gao, H.M., Lu, R.B., Hong, J.S., 2012. Clozapine protects dopaminergic neurons from inflammation-induced damage by inhibiting microglial overactivation. *J Neuroimmune Pharmacol* 7, 187-201.
- Hurt, K., Hurd-Brown, T., Whalen, M., 2013. Tributyltin and dibutyltin alter secretion of tumor necrosis factor alpha from human natural killer cells and a mixture of T cells and natural killer cells. *J Appl Toxicol* 33, 503-510.

- Hwang, J.T., Ha, J., Park, O.J., 2005. Combination of 5-fluorouracil and genistein induces apoptosis synergistically in chemo-resistant cancer cells through the modulation of AMPK and COX-2 signaling pathways. *Biochem Biophys Res Commun* 332, 433-440.
- Isomura, M., Kotake, Y., Masuda, K., Miyara, M., Okuda, K., Samizo, S., Sanoh, S., Hosoi, T., Ozawa, K., Ohta, S., 2013. Tributyltin-induced endoplasmic reticulum stress and its Ca(2+)-mediated mechanism. *Toxicol Appl Pharmacol* 272, 137-146.
- Jang, B.C., Paik, J.H., Kim, S.P., Shin, D.H., Song, D.K., Park, J.G., Suh, M.H., Park, J.W., Suh, S.I., 2005. Catalase induced expression of inflammatory mediators via activation of NF-kappaB, PI3K/AKT, p70S6K, and JNKs in BV2 microglia. *Cell Signal* 17, 625-633.
- Jendrysik, M.A., Vasilevsky, S., Yi, L., Wood, A., Zhu, N., Zhao, Y., Koontz, S.M., Jackson, S.H., 2011. NADPH oxidase-2 derived ROS dictates murine DC cytokine-mediated cell fate decisions during CD4 T helper-cell commitment. *PLoS One* 6, e28198.
- Jenkins, S.M., Ehman, K., Barone, S., Jr., 2004. Structure-activity comparison of organotin species: dibutyltin is a developmental neurotoxicant in vitro and in vivo. *Brain Res Dev Brain Res* 151, 1-12.
- Jung, W.K., Lee, D.Y., Park, C., Choi, Y.H., Choi, I., Park, S.G., Seo, S.K., Lee, S.W., Yea, S.S., Ahn, S.C., Lee, C.M., Park, W.S., Ko, J.H., Choi, I.W., 2010. Cilostazol is anti-inflammatory in BV2 microglial cells by inactivating nuclear factor-kappaB and inhibiting mitogen-activated protein kinases. *Br J Pharmacol* 159, 1274-1285.
- Kannan, K., Senthilkumar, K., Giesy, J.P., 1999. Occurrence of butyltin compounds in human blood. *Environ Sci Technol* 33, 1776-1779.
- Katz, S., Boland, R., Santillan, G., 2006. Modulation of ERK 1/2 and p38 MAPK signaling pathways by ATP in osteoblasts: involvement of mechanical stress-activated calcium influx, PKC and Src activation. *Int J Biochem Cell Biol* 38, 2082-2091.
- Kim, E.Y., Moudgil, K.D., 2008. Regulation of autoimmune inflammation by pro-inflammatory cytokines. *Immunol Lett* 120, 1-5.
- Kluza, J., Marchetti, P., Gallego, M.A., Lancel, S., Fournier, C., Loyens, A., Beauvillain, J.C., Bailly, C., 2004. Mitochondrial proliferation during apoptosis induced by anticancer agents: effects of doxorubicin and mitoxantrone on cancer and cardiac cells. *Oncogene* 23, 7018-7030.

- Kolamunne, R.T., Clare, M., Griffiths, H.R., 2011. Mitochondrial superoxide anion radicals mediate induction of apoptosis in cardiac myoblasts exposed to chronic hypoxia. *Arch Biochem Biophys* 505, 256-265.
- Koziorowski, D., Tomasiuk, R., Szlufik, S., Friedman, A., 2012. Inflammatory cytokines and NT-proCNP in Parkinson's disease patients. *Cytokine* 60, 762-766.
- Lane, R., Ghazi, S.O., Whalen, M.M., 2009. Increases in cytosolic calcium ion levels in human natural killer cells in response to butyltin exposure. *Arch Environ Contam Toxicol* 57, 816-825.
- Lee, C.W., Chien, C.S., Yang, C.M., 2004. Lipoteichoic acid-stimulated p42/p44 MAPK activation via Toll-like receptor 2 in tracheal smooth muscle cells. *Am J Physiol Lung Cell Mol Physiol* 286, L921-930.
- Lee, I.T., Lin, C.C., Lin, W.N., Wu, W.L., Hsiao, L.D., Yang, C.M., 2013. Lung inflammation caused by adenosine-5'-triphosphate is mediated via Ca/PKC-dependent COX-2/PGE induction. *Int J Biochem Cell Biol* 45, 1657-1668.
- Lee, J.Y., Jhun, B.S., Oh, Y.T., Lee, J.H., Choe, W., Baik, H.H., Ha, J., Yoon, K.S., Kim, S.S., Kang, I., 2006. Activation of adenosine A3 receptor suppresses lipopolysaccharide-induced TNF- $\alpha$  production through inhibition of PI 3-kinase/Akt and NF- $\kappa$ B activation in murine BV2 microglial cells. *Neurosci Lett* 396, 1-6.
- Li, X.Q., Cao, W., Li, T., Zeng, A.G., Hao, L.L., Zhang, X.N., Mei, Q.B., 2009. Amlodipine inhibits TNF- $\alpha$  production and attenuates cardiac dysfunction induced by lipopolysaccharide involving PI3K/Akt pathway. *Int Immunopharmacol* 9, 1032-1041.
- Livak, K.J., Schmittgen, T.D., 2001. Analysis of relative gene expression data using real-time quantitative PCR and the 2(-Delta Delta C(T)) Method. *Methods* 25, 402-408.
- Lu, D.Y., Tang, C.H., Yeh, W.L., Wong, K.L., Lin, C.P., Chen, Y.H., Lai, C.H., Chen, Y.F., Leung, Y.M., Fu, W.M., 2009. SDF-1 $\alpha$  up-regulates interleukin-6 through CXCR4, PI3K/Akt, ERK, and NF- $\kappa$ B-dependent pathway in microglia. *Eur J Pharmacol* 613, 146-154.
- Macho, A., Decaudin, D., Castedo, M., Hirsch, T., Susin, S.A., Zamzami, N., Kroemer, G., 1996. Chloromethyl-X-Rosamine is an aldehyde-fixable potential-sensitive fluorochrome for the detection of early apoptosis. *Cytometry* 25, 333-340.

- Mahyar-Roemer, M., Katsen, A., Mestres, P., Roemer, K., 2001. Resveratrol induces colon tumor cell apoptosis independently of p53 and precede by epithelial differentiation, mitochondrial proliferation and membrane potential collapse. *Int J Cancer* 94, 615-622.
- Meisse, D., Van de Casteele, M., Beauloye, C., Hainault, I., Kefas, B.A., Rider, M.H., Fougelle, F., Hue, L., 2002. Sustained activation of AMP-activated protein kinase induces c-Jun N-terminal kinase activation and apoptosis in liver cells. *FEBS Lett* 526, 38-42.
- Memet, S., 2006. NF-kappaB functions in the nervous system: from development to disease. *Biochem Pharmacol* 72, 1180-1195.
- Morales, I., Farias, G., Maccioni, R.B., 2010. Neuroimmunomodulation in the pathogenesis of Alzheimer's disease. *Neuroimmunomodulation* 17, 202-204.
- Moser, V.C., McGee, J.K., Ehman, K.D., 2009. Concentration and persistence of tin in rat brain and blood following dibutyltin exposure during development. *J Toxicol Environ Health A* 72, 47-52.
- Mundy, W.R., Freudenrich, T.M., 2006. Apoptosis of cerebellar granule cells induced by organotin compounds found in drinking water: involvement of MAP kinases. *Neurotoxicology* 27, 71-81.
- Murakami, M., Hirano, T., 2012. The pathological and physiological roles of IL-6 amplifier activation. *Int J Biol Sci* 8, 1267-1280.
- Napetschnig, J., Wu, H., 2013. Molecular basis of NF-kappaB signaling. *Annu Rev Biophys* 42, 443-468.
- Nashev, L.G., Vuorinen, A., Praxmarer, L., Chantong, B., Cereghetti, D., Winiger, R., Schuster, D., Odermatt, A., 2012. Virtual screening as a strategy for the identification of xenobiotics disrupting corticosteroid action. *PLoS One* 7, e46958.
- Nielsen, J.B., Strand, J., 2002. Butyltin compounds in human liver. *Environ Res* 88, 129-133.
- Nikodemova, M., Duncan, I.D., Watters, J.J., 2006. Minocycline exerts inhibitory effects on multiple mitogen-activated protein kinases and IkappaBalpha degradation in a stimulus-specific manner in microglia. *J Neurochem* 96, 314-323.
- Odman-Ghazi, S.O., Abraha, A., Isom, E.T., Whalen, M.M., 2010. Dibutyltin activates MAP kinases in human natural killer cells, in vitro. *Cell Biol Toxicol* 26, 469-479.
- Oh, Y.T., Lee, J.Y., Lee, J., Kim, H., Yoon, K.S., Choe, W., Kang, I., 2009. Oleic acid reduces lipopolysaccharide-induced expression of iNOS and COX-2 in BV2 murine microglial cells:

- possible involvement of reactive oxygen species, p38 MAPK, and IKK/NF-kappaB signaling pathways. *Neurosci Lett* 464, 93-97.
- Ohhira, S., Watanabe, M., Matsui, H., 2003. Metabolism of tributyltin and triphenyltin by rat, hamster and human hepatic microsomes. *Arch Toxicol* 77, 138-144.
- Omura, M., Shimasaki, Y., Oshima, Y., Nakayama, K., Kubo, K., Aou, S., Ogata, R., Hirata, M., Inoue, N., 2004. Distribution of tributyltin, dibutyltin and monobutyltin in the liver, brain and fat of rats: two-generation toxicity study of tributyltin chloride. *Environ Sci* 11, 123-132.
- Person, R.J., Whalen, M.M., 2010. Effects of butyltin exposures on MAP kinase-dependent transcription regulators in human natural killer cells. *Toxicol Mech Methods* 20, 227-233.
- Qi, S., Xin, Y., Guo, Y., Diao, Y., Kou, X., Luo, L., Yin, Z., 2012. Ampelopsin reduces endotoxic inflammation via repressing ROS-mediated activation of PI3K/Akt/NF-kappaB signaling pathways. *Int Immunopharmacol* 12, 278-287.
- Qin, L., Wu, X., Block, M.L., Liu, Y., Breese, G.R., Hong, J.S., Knapp, D.J., Crews, F.T., 2007. Systemic LPS causes chronic neuroinflammation and progressive neurodegeneration. *Glia* 55, 453-462.
- Rastkari, N., Mesdaghinia, A., Yunesian, M., Ahmadkhaniha, R., 2012. Butyltin compounds in fish commonly sold in north of Iran. *Bull Environ Contam Toxicol* 88, 74-77.
- Reznick, R.M., Shulman, G.I., 2006. The role of AMP-activated protein kinase in mitochondrial biogenesis. *J Physiol* 574, 33-39.
- Ronnett, G.V., Ramamurthy, S., Kleman, A.M., Landree, L.E., Aja, S., 2009. AMPK in the brain: its roles in energy balance and neuroprotection. *J Neurochem* 109 Suppl 1, 17-23.
- Rubio-Perez, J.M., Morillas-Ruiz, J.M., 2012. A review: inflammatory process in Alzheimer's disease, role of cytokines. *ScientificWorldJournal* 2012, 756357.
- Sadasivan, S., Pond, B.B., Pani, A.K., Qu, C., Jiao, Y., Smeyne, R.J., 2012. Methylphenidate exposure induces dopamine neuron loss and activation of microglia in the basal ganglia of mice. *PLoS One* 7, e33693.
- Sadiki, A.I., Williams, D.T., 1999. A study on organotin levels in Canadian drinking water distributed through PVC pipes. *Chemosphere* 38, 1541-1548.
- Sadiki, A.I., Williams, D.T., Carrier, R., Thomas, B., 1996. Pilot study on the contamination of drinking water by organotin compounds from PVC materials. *Chemosphere* 32, 2389-2398.

- Sanchez, Y., Amran, D., Fernandez, C., de Blas, E., Aller, P., 2008. Genistein selectively potentiates arsenic trioxide-induced apoptosis in human leukemia cells via reactive oxygen species generation and activation of reactive oxygen species-inducible protein kinases (p38-MAPK, AMPK). *Int J Cancer* 123, 1205-1214.
- Schutt, F., Aretz, S., Auffarth, G.U., Kopitz, J., 2012. Moderately reduced ATP levels promote oxidative stress and debilitate autophagic and phagocytic capacities in human RPE cells. *Invest Ophthalmol Vis Sci* 53, 5354-5361.
- Seinen, W., Vos, J.G., van Krieken, R., Penninks, A., Brands, R., Hooykaas, H., 1977. Toxicity of organotin compounds. III. Suppression of thymus-dependent immunity in rats by di-n-butyltin dichloride and di-n-octyltin dichloride. *Toxicol Appl Pharmacol* 42, 213-224.
- Skaper, S.D., 2007. The brain as a target for inflammatory processes and neuroprotective strategies. *Ann N Y Acad Sci* 1122, 23-34.
- Smith, J.A., Das, A., Ray, S.K., Banik, N.L., 2012. Role of pro-inflammatory cytokines released from microglia in neurodegenerative diseases. *Brain Res Bull* 87, 10-20.
- Sorenson, M., Janusek, L., Mathews, H., 2013. Psychological stress and cytokine production in multiple sclerosis: correlation with disease symptomatology. *Biol Res Nurs* 15, 226-233.
- Sparmann, G., Behrend, S., Merkord, J., Kleine, H.D., Graser, E., Ritter, T., Liebe, S., Emmrich, J., 2001. Cytokine mRNA levels and lymphocyte infiltration in pancreatic tissue during experimental chronic pancreatitis induced by dibutyltin dichloride. *Dig Dis Sci* 46, 1647-1656.
- Takahashi, S., Mukai, H., Tanabe, S., Sakayama, K., Miyazaki, T., Masuno, H., 1999. Butyltin residues in livers of humans and wild terrestrial mammals and in plastic products. *Environ Pollut* 106, 213-218.
- Tang, C.H., Lu, D.Y., Yang, R.S., Tsai, H.Y., Kao, M.C., Fu, W.M., Chen, Y.F., 2007. Leptin-induced IL-6 production is mediated by leptin receptor, insulin receptor substrate-1, phosphatidylinositol 3-kinase, Akt, NF-kappaB, and p300 pathway in microglia. *J Immunol* 179, 1292-1302.
- Tomiyama, K., Yamaguchi, A., Kuriyama, T., Arakawa, Y., 2009. Analysis of mechanisms of cell death of T-lymphocytes induced by organotin agents. *J Immunotoxicol* 6, 184-193.
- Ueno, S., Kashimoto, T., Susa, N., Ishii, M., Chiba, T., Mutoh, K., Hoshi, F., Suzuki, T., Sugiyama, M., 2003. Comparison of hepatotoxicity and metabolism of butyltin compounds in the liver of mice, rats and guinea pigs. *Arch Toxicol* 77, 173-181.

- Vanhaesebroeck, B., Leever, S.J., Ahmadi, K., Timms, J., Katso, R., Driscoll, P.C., Woscholski, R., Parker, P.J., Waterfield, M.D., 2001. Synthesis and function of 3-phosphorylated inositol lipids. *Annu Rev Biochem* 70, 535-602.
- Wang, Q., Zhou, H., Gao, H., Chen, S.H., Chu, C.H., Wilson, B., Hong, J.S., 2012. Naloxone inhibits immune cell function by suppressing superoxide production through a direct interaction with gp91phox subunit of NADPH oxidase. *J Neuroinflammation* 9, 32.
- Wang, Y.P., Wu, Y., Li, L.Y., Zheng, J., Liu, R.G., Zhou, J.P., Yuan, S.Y., Shang, Y., Yao, S.L., 2011. Aspirin-triggered lipoxin A4 attenuates LPS-induced pro-inflammatory responses by inhibiting activation of NF-kappaB and MAPKs in BV-2 microglial cells. *J Neuroinflammation* 8, 95.
- Whalen, M.M., Loganathan, B.G., Kannan, K., 1999. Immunotoxicity of environmentally relevant concentrations of butyltins on human natural killer cells in vitro. *Environ Res* 81, 108-116.
- Woodcock, T., Morganti-Kossmann, M.C., 2013. The role of markers of inflammation in traumatic brain injury. *Front Neurol* 4, 18.
- Xing, B., Xin, T., Hunter, R.L., Bing, G., 2008. Pioglitazone inhibition of lipopolysaccharide-induced nitric oxide synthase is associated with altered activity of p38 MAP kinase and PI3K/Akt. *J Neuroinflammation* 5, 4.
- Yamashiro, K., Sasano, T., Tojo, K., Namekata, I., Kurokawa, J., Sawada, N., Suganami, T., Kamei, Y., Tanaka, H., Tajima, N., Utsunomiya, K., Ogawa, Y., Furukawa, T., 2010. Role of transient receptor potential vanilloid 2 in LPS-induced cytokine production in macrophages. *Biochem Biophys Res Commun* 398, 284-289.
- Yang, C.M., Luo, S.F., Wang, C.C., Chiu, C.T., Chien, C.S., Lin, C.C., Hsiao, L.D., 2000. Tumour necrosis factor-alpha- and interleukin-1beta-stimulated cell proliferation through activation of mitogen-activated protein kinase in canine tracheal smooth muscle cells. *Br J Pharmacol* 130, 891-899.
- Yanik, S.C., Baker, A.H., Mann, K.K., Schlezinger, J.J., 2011. Organotins are potent activators of PPARgamma and adipocyte differentiation in bone marrow multipotent mesenchymal stromal cells. *Toxicol Sci* 122, 476-488.

Zhou, C.H., Lin, L., Zhu, X.Y., Wen, T., Hu, D.M., Dong, Y., Li, L.Y., Wang, S.F., 2013. Protective effects of edaravone on experimental chronic pancreatitis induced by dibutyltin dichloride in rats. *Pancreatology* 13, 125-132.

Zhou, S., Yuan, X., Liu, Q., Zhang, X., Pan, X., Zang, L., Xu, L., 2010. BAPTA-AM, an intracellular calcium chelator, inhibits RANKL-induced bone marrow macrophages differentiation through MEK/ERK, p38 MAPK and Akt, but not JNK pathways. *Cytokine* 52, 210-214.

Zhou, X., Yang, W., Li, J., 2006. Ca<sup>2+</sup>- and protein kinase C-dependent signaling pathway for nuclear factor-kappaB activation, inducible nitric-oxide synthase expression, and tumor necrosis factor-alpha production in lipopolysaccharide-stimulated rat peritoneal macrophages. *J Biol Chem* 281, 31337-31347.

Zordoky, B.N., El-Kadi, A.O., 2009. Role of NF-kappaB in the regulation of cytochrome P450 enzymes. *Curr Drug Metab* 10, 164-178.

## Figure legends

**Fig. 1.** DBT induces oxidative stress in BV-2 microglia cells. Cells were treated with DBT (50 to 200 nM) for 24 h. (A) Determination of intracellular ROS using DHE. (B) Measurement of mitochondrial content using MitoTracker Red CMXRos. (C) Determination of mitochondrial ROS using MitoSOX Red. (D) Quantification of iNOS mRNA expression by real-time RT-PCR. Values were normalized to the GAPDH control. The values obtained from untreated cells (control) were set as 100%. Results represent mean  $\pm$  SD of four experiments. Significance was assessed by one-way ANOVA followed by Tukey's tests,  $*p < 0.05$ ,  $***p < 0.005$ .

**Fig. 2.** Effect of DBT on ATP levels and AMPK phosphorylation. (A) BV-2 cells were treated with various concentrations of DBT for different period of time, followed by determination of cellular ATP levels. Data (mean  $\pm$  SD) were obtained from three independent experiments. Significance was assessed by one-way ANOVA followed by Tukey's tests,  $*p < 0.05$ ,  $***p < 0.005$ . (B) Immunoblot analyses performed with lysates of BV-2 cells treated with DBT for a different period of time. Representative blots from three independent experiments are shown.

**Fig. 3.** DBT induces inflammatory cytokine expression in BV-2 microglia cells. (A) Cells were treated with DBT (5-500 nM) or vehicle (0.1% DMSO, control) for 24 h, followed by quantification of IL-6 and TNF- $\alpha$  mRNA by RT-PCR and normalization to GAPDH mRNA. (B) IL-6 protein levels in the culture medium of BV-2 cells treated for 24 h with DBT were quantified by ELISA. (C) Cells were exposed for 0.25, 0.5, 1, 6, 12, 18, and 24 h with 50 nM DBT, 10 ng/ml LPS or 0.1% DMSO (vehicle control). IL-6 mRNA was measured by RT-PCR and normalized to GAPDH mRNA. (D) IL-6 protein was detected by ELISA at the time indicated. Results (mean  $\pm$  SD) were obtained from three independent experiments.

**Fig. 4.** NOX-2 is involved in DBT-induced IL-6 expression. (A) Cells were treated with 50 nM DBT or 0.1% DMSO (vehicle control) for 24 h. NOX-2 mRNA was quantified by RT-PCR and normalized to GAPDH mRNA. Cells were exposed to 250  $\mu$ M apocynin for 1 h, followed by the addition of 50 nM DBT and incubation for a further 24 h. (B) Intracellular ROS levels were determined using DHE. (C) IL-6 mRNA expression was quantified by RT-PCR and normalized to GAPDH mRNA. (D) IL-6 protein was quantified by ELISA. Results (mean  $\pm$  SD) were obtained from at least three experiments. Significance was tested by one-way ANOVA followed by Tukey's tests,  $*p < 0.05$ ,  $**p < 0.01$ ;  $***p < 0.005$ .

**Fig. 5.** NF- $\kappa$ B is involved in the DBT-mediated induction of IL-6. Cells were pretreated for 1 h with vehicle or 250 nM Cay10512, followed by incubation for a further 24 h with 50 nM DBT or 0.1% DMSO. (A) Western blot analysis using antibodies against the p65 subunit of NF- $\kappa$ B and its phosphorylated form in nuclear and cytoplasmic fractions. TNF- $\alpha$  served as positive control. HDAC1 and  $\beta$ -actin served as loading controls for cytoplasmic and nuclear fractions. Representative blots from three independent experiments are shown. (B) Analysis of the intracellular localization of the p65 subunit of NF- $\kappa$ B using the Cellomics ArrayScan HCS imaging system. The ratio between the intensity of nuclear p65 fluorescence and total cellular p65 fluorescence was quantified. (C) IL-6 mRNA was measured by RT-PCR and normalized to GAPDH mRNA. (D) IL-6 protein was quantified by ELISA. Results represent mean  $\pm$  SD of at least three independent experiments and significance was determined by one-way ANOVA followed by Tukey's tests, \* $p$  < 0.05, \*\* $p$  < 0.01; \*\*\* $p$  < 0.005.

**Fig. 6.** The DBT-induced IL-6 expression is modulated by the MAPK pathway. BV-2 cells were pretreated with inhibitors for Erk1/2 (50  $\mu$ M PD98059), p38 MAPK (20  $\mu$ M SB202190) or JNK (20  $\mu$ M SP600125) for 1 h prior to treatment with 50 nM DBT for a further 24 h. (A) IL-6 mRNA was quantified by RT-PCR and normalized to GAPDH mRNA. (B) IL-6 protein in the culture medium of treated cells was measured by ELISA. Results represent mean  $\pm$  SD of at least three independent experiments. Significance was determined by one-way ANOVA followed by Tukey's tests, \* $p$  < 0.05, \*\* $p$  < 0.01; \*\*\* $p$  < 0.005.

**Fig 7.** Inhibition of the PI3K/Akt pathway reduces DBT-induced IL-6 expression. Cells were pre-incubated with or without wortmannin (100 nM), LY294002 (20  $\mu$ M) or Akt inhibitor (10  $\mu$ M) for 1 h prior to treatment with 50 nM DBT or 0.1% DMSO for a further 24 h. (A) IL-6 mRNA was measured by RT-PCR and normalized to GAPDH mRNA. (B) IL-6 protein was quantified by ELISA. Results are expressed as mean  $\pm$  SD of at least three independent experiments and significance was tested by one-way ANOVA followed by Tukey's tests, \* $p$  < 0.05, \*\* $p$  < 0.01; \*\*\* $p$  < 0.005.

**Fig. 8.** PLC and PKC are involved in the DBT-induced expression of IL-6. Cells were pre-incubated with or without 10  $\mu$ M PLC inhibitor U73122 or 5  $\mu$ M PKC inhibitor GF109203X for 1 h prior to further treatment for 24 h with 50 nM DBT or 0.1% DMSO. (A) IL-6 mRNA levels were determined by RT-PCR and normalized to GAPDH mRNA. (B) IL-6 protein was quantified

by ELISA. Results (mean  $\pm$  SD) were obtained from at least three independent experiments and significance was determined by one-way ANOVA followed by Tukey's tests,  $*p < 0.05$ ,  $**p < 0.01$ ;  $***p < 0.005$ .

**Fig 9.** The DBT-induced elevation of IL-6 expression and oxidative stress are dependent on calcium. BV-2 cells were pre-incubated for 1 h with vehicle or 1  $\mu$ M BAPTA-AM prior to further incubation for 24 h with 50 nM DBT or 0.1% DMSO. (A) IL-6 mRNA was quantified by RT-PCR and normalized to GAPDH mRNA. (B) Determination of intracellular ROS using DHE. (C) Measurement of mitochondrial mass using MitoTracker Red CMXRos. (D) Determination of mitochondrial ROS using MitoSOX Red. (E) Quantification of iNOS mRNA normalized to GAPDH mRNA by RT-PCR. Values obtained from untreated cells (control) were set as 100%. Results are expressed as mean  $\pm$  SD from three independent experiments. Significance was determined by one-way ANOVA followed by Tukey's tests,  $*p < 0.05$ ,  $**p < 0.01$ ;  $***p < 0.005$ .

Figure 1

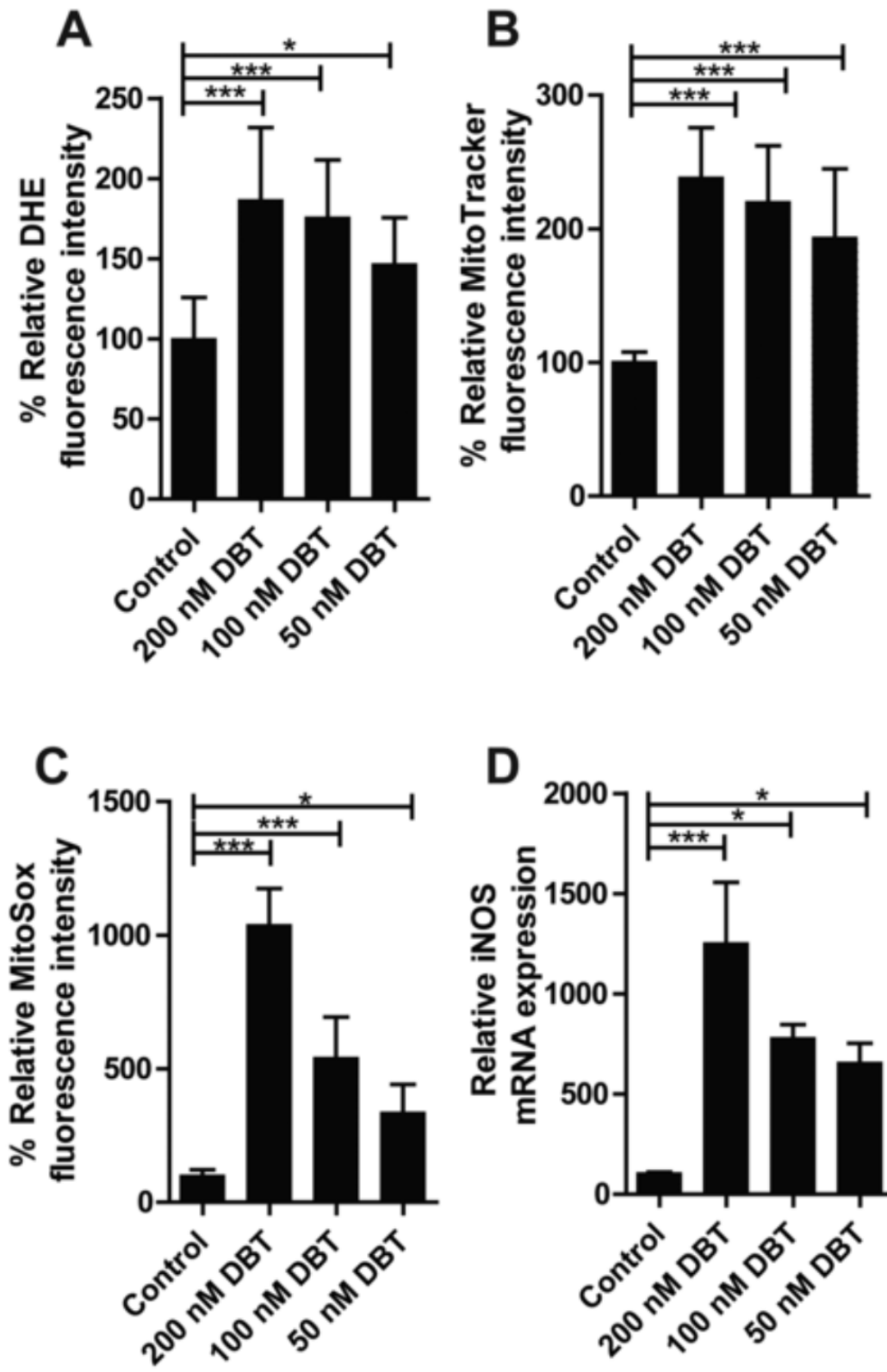
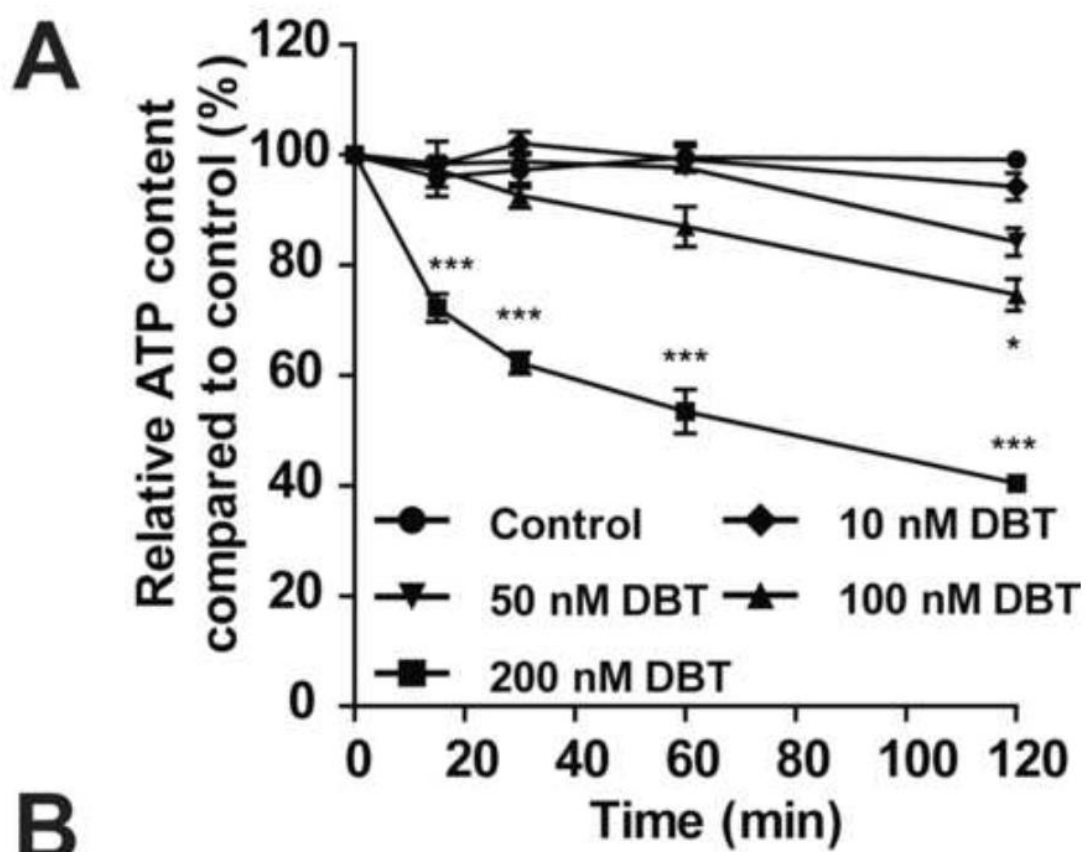


Figure 2



**B**

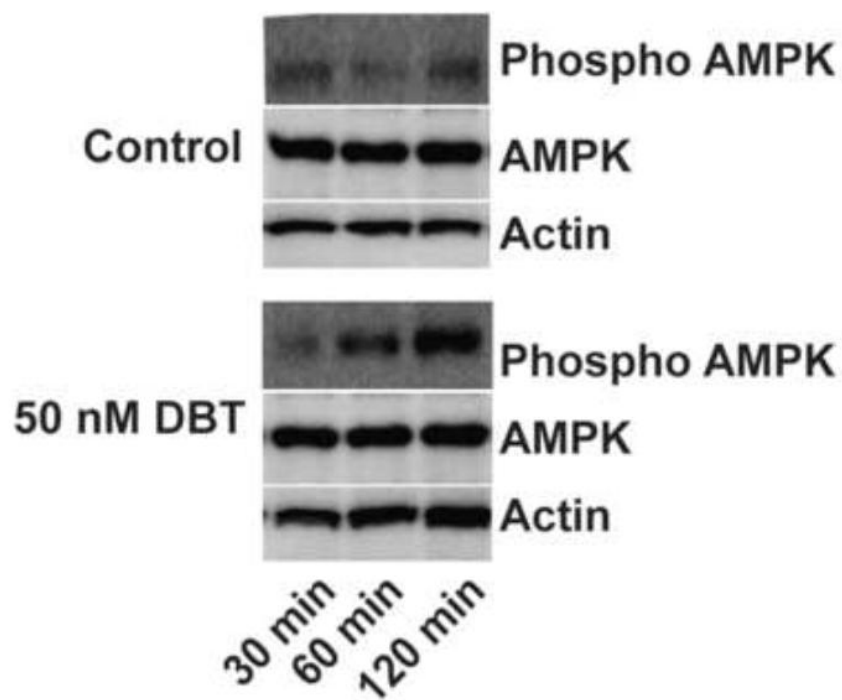


Figure 3

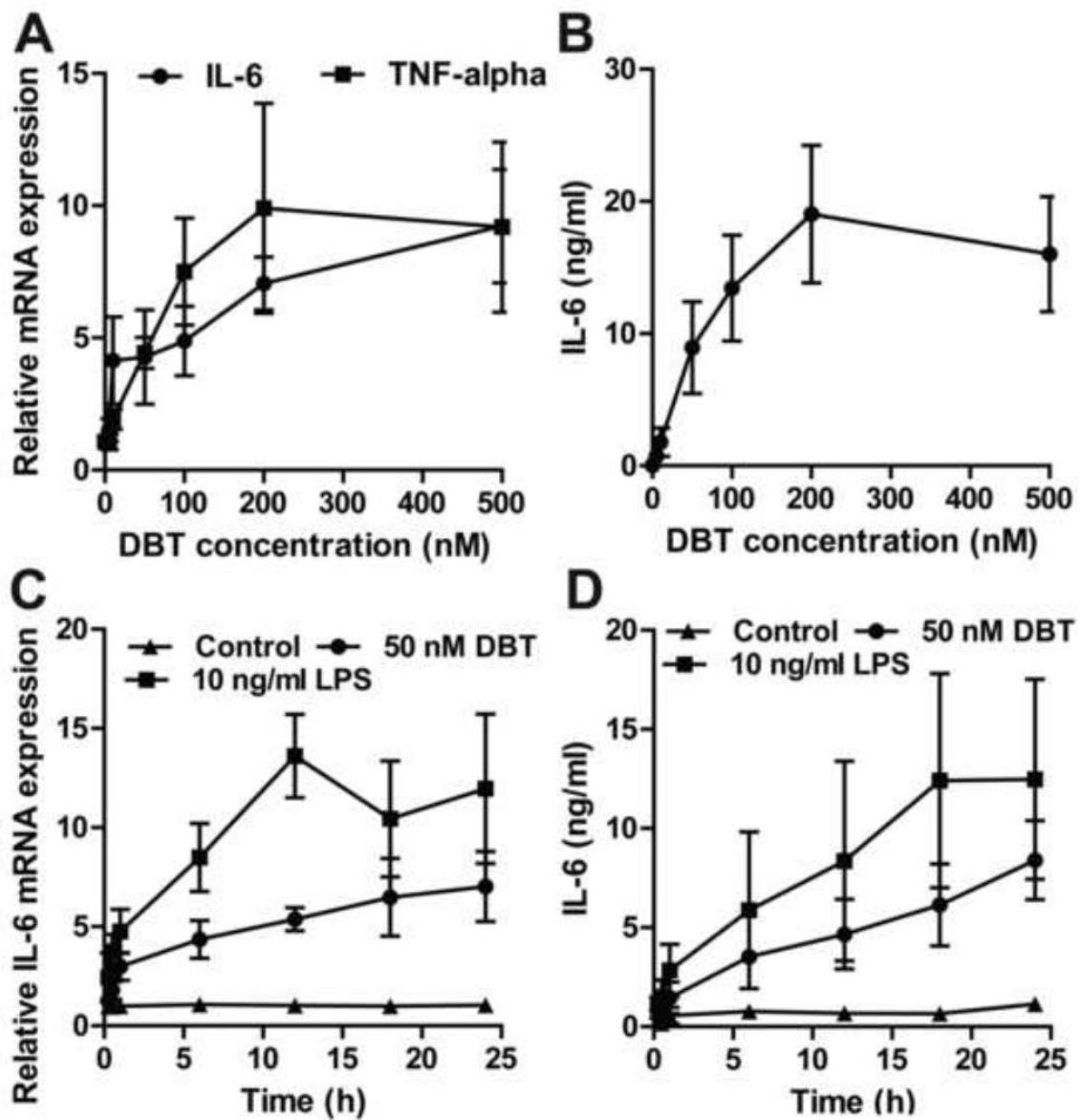


Figure 4

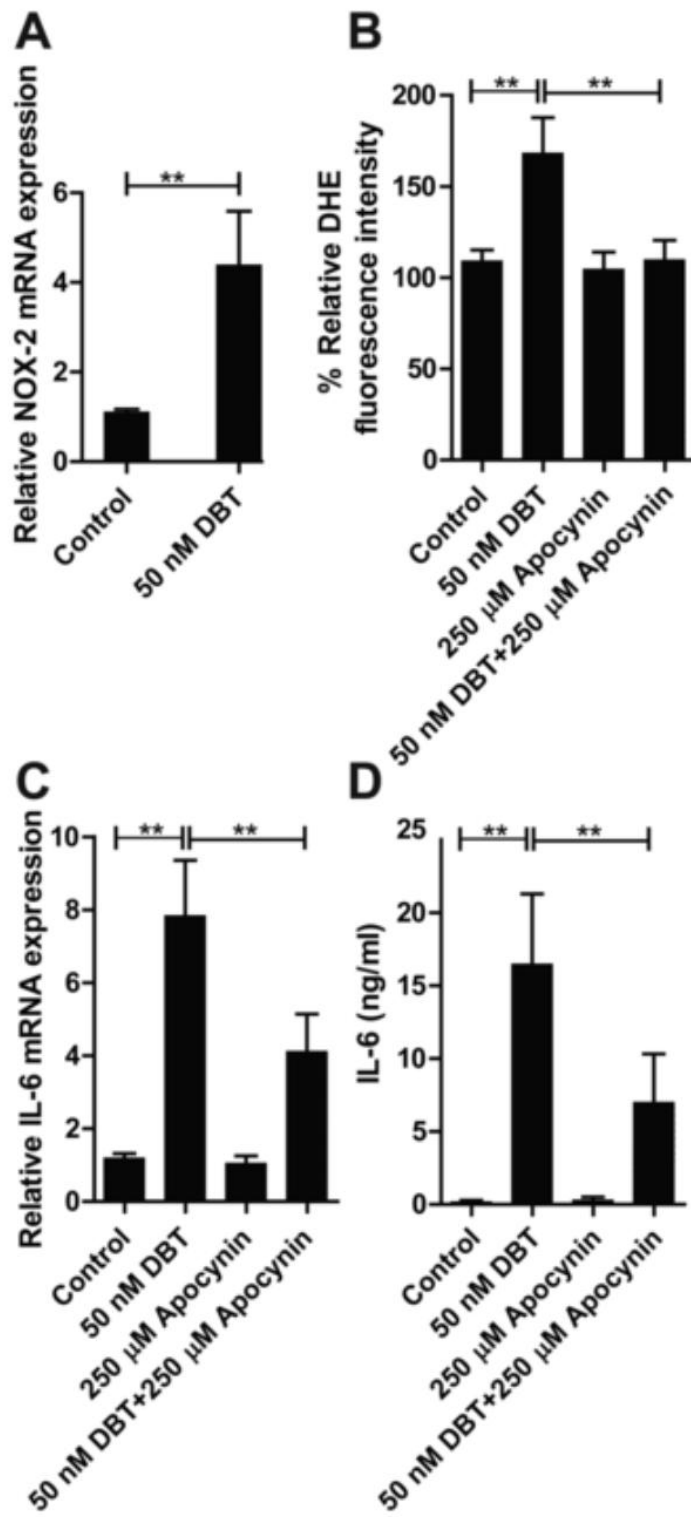


Figure 5

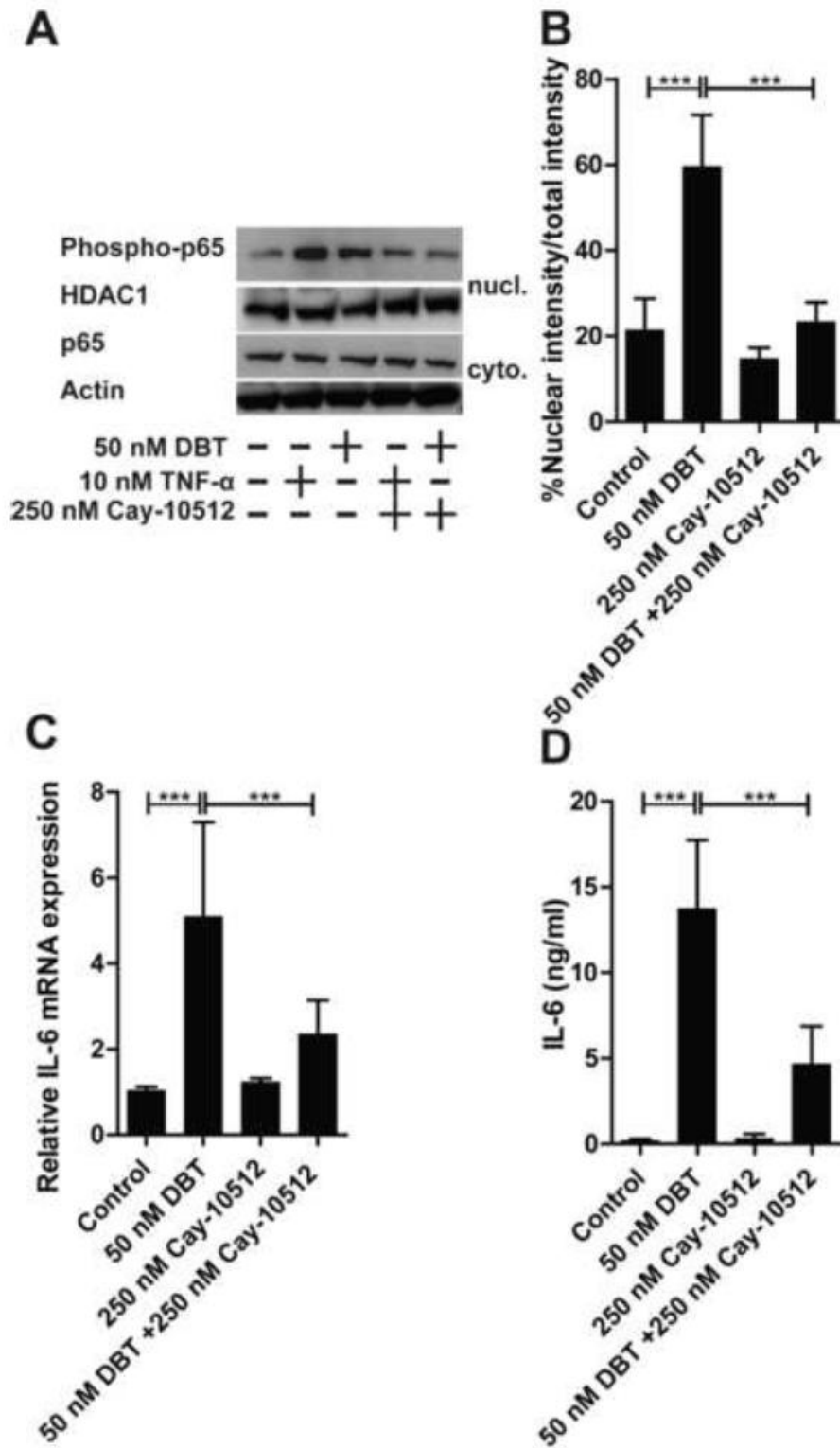


Figure 6

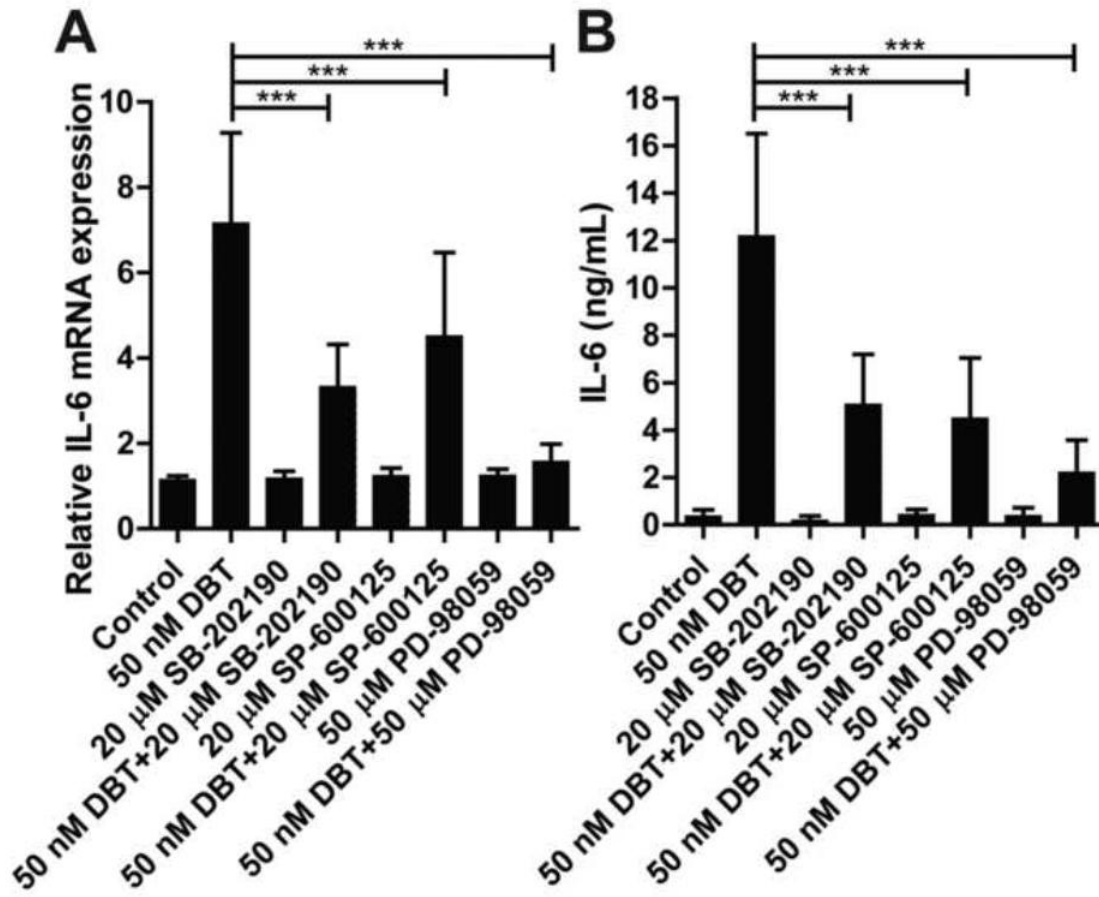


Figure 7

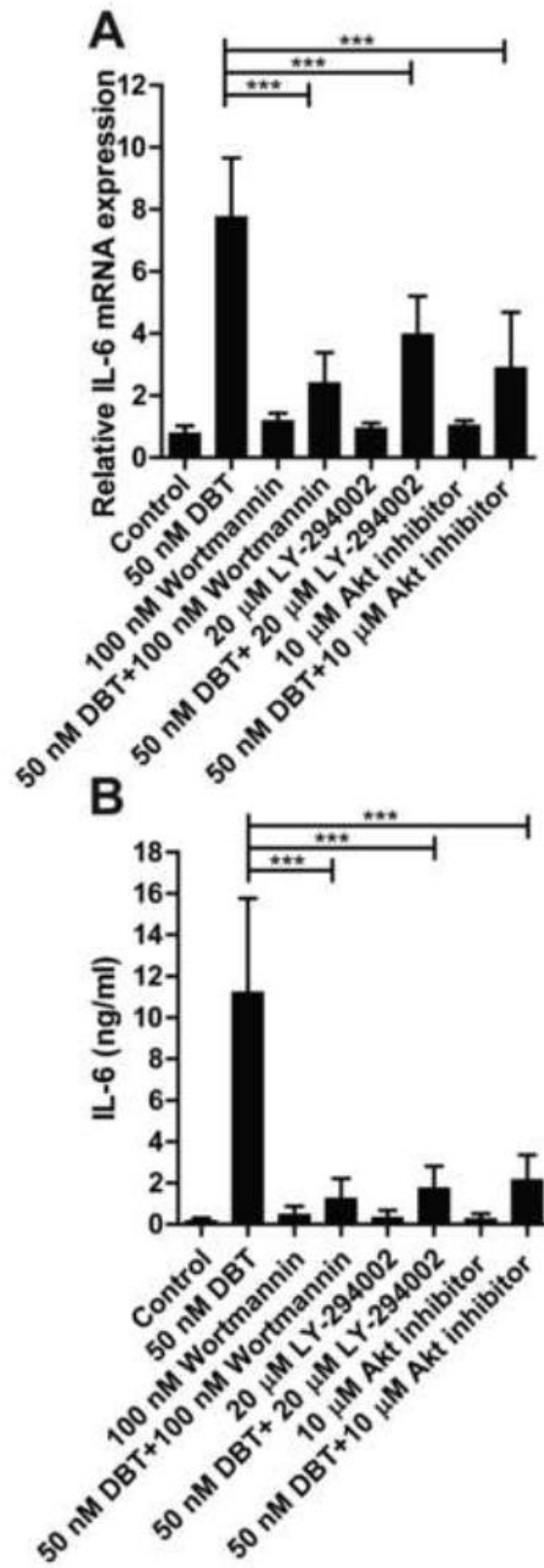


Figure 8

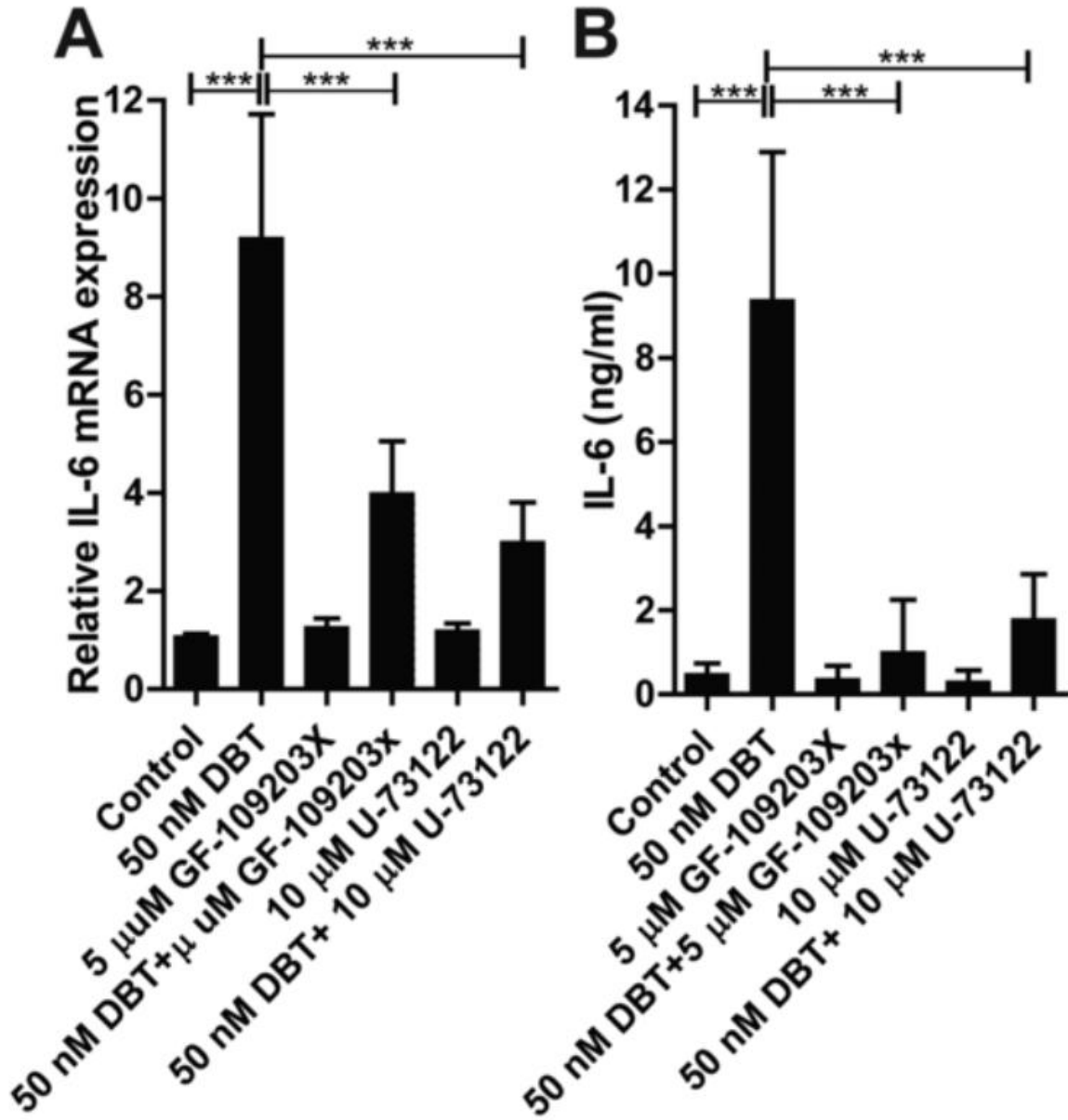
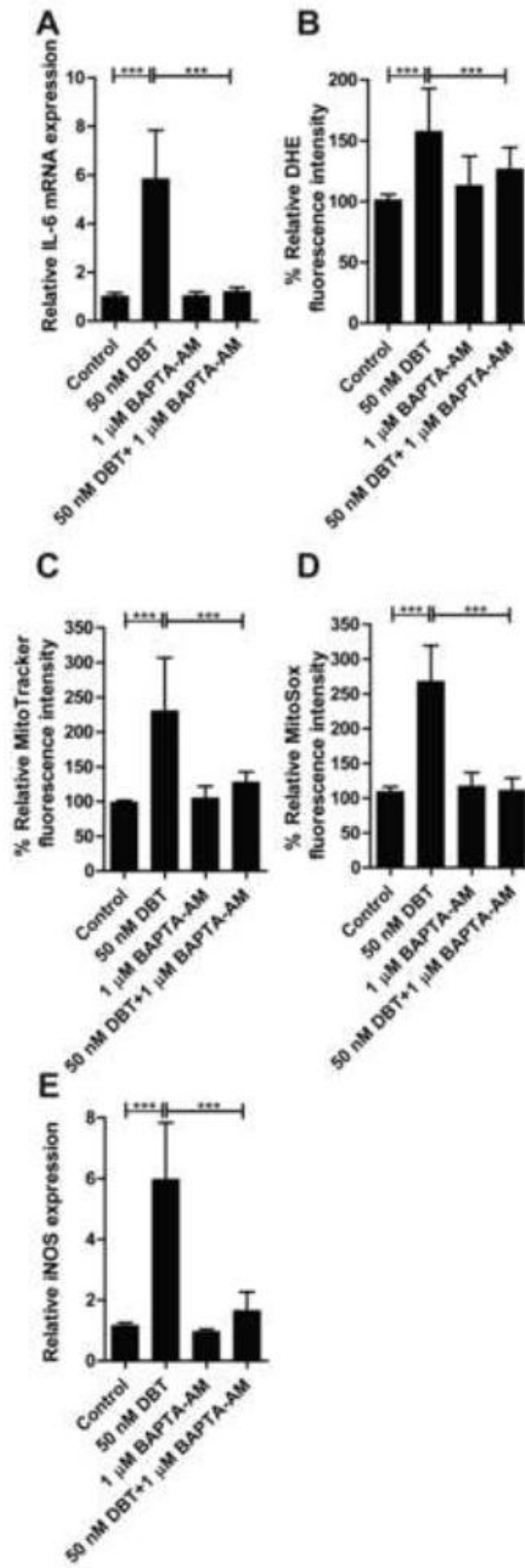


Figure 9



**Table A**

Real-time PCR primers

<b>Genes</b>	<b>Primers</b>	<b>Sequences</b>
GAPDH (mouse)	forward	CTCGTGGAGTCTACTGGTGT
	reverse	GTCATCATACTTGGCAGGTT
IL-6 (mouse)	forward	GGAGGCTTAATTACACATGTT
	reverse	TGATTTCAAGATGAATTGGAT
TNF- $\alpha$ (mouse)	forward	TTCTGTCTACTGAACTTCGG
	reverse	GTATGAGATAGCAAATCGGC
iNOS (mouse)	forward	ATGAGGTACTIONCAGCGTGCTCCAC
	reverse	CCACAATAGTACAATACTACTTGG

## CHAPTER 5

**Metabotropic glutamate receptor 5 modulates ER stress through pertussis toxin-sensitive G proteins**

# **Metabotropic glutamate receptor 5 modulates ER stress through Pertussis toxin-sensitive heterotrimeric G proteins**

Boonrat Chantong, Denise V. Kratschmar, Adam Lister, and Alex Odermatt

Division of Molecular and Systems Toxicology, Department of Pharmaceutical Sciences, University of  
Basel, Klingelbergstrasse 50, 4056 Basel, Switzerland

E-mail addresses: [boonrat.chantong@unibas.ch](mailto:boonrat.chantong@unibas.ch); [denise.kratschmar@unibas.ch](mailto:denise.kratschmar@unibas.ch); [adam.lister@unibas.ch](mailto:adam.lister@unibas.ch);  
[alex.odermatt@unibas.ch](mailto:alex.odermatt@unibas.ch).

## **Correspondence to:**

Dr. Alex Odermatt, Division of Molecular and Systems Toxicology, Department of Pharmaceutical  
Sciences, University of Basel, Klingelbergstrasse 50, CH-4056 Basel, Switzerland  
Phone: +41 61 267 1530, Fax: +41 61 267 1515, E-mail: [alex.odermatt@unibas.ch](mailto:alex.odermatt@unibas.ch)

## Abstract

**Background:** Metabotropic glutamate receptor 5 (mGluR5) activation by (RS)-2-chloro-5-hydroxyphenylglycine (CHPG) decreases microglial activation and the release of associated pro-inflammatory factors *in vitro* and *in vivo*. AMP-dependent protein kinase (AMPK) and calcium mediated signaling are associated with oxidative stress and inflammation in microglia cells. Here we examined whether mGluR5 antagonism by 2-methyl-6-(phenylethynyl)-pyridine (MPEP) enhances oxidative stress and inflammation through AMPK and  $\text{Ca}^{2+}$  mediated signaling pathways in mouse BV-2 microglia cells.

**Methods:** Dihydroethidium (DHE), MitoTracker<sup>®</sup>Red CMXRos, and MitoSOX Red was used to assay intracellular ROS production, mitochondrial mass, and mitochondrial ROS production, respectively. mRNA expression of interleukin-6 (IL-6), inducible nitric oxide synthase (iNOS) glucose-regulated protein 78 (GRP78), glucose-regulated protein 94 (GRP94), and transcriptional factor C/EBP homologous protein (CHOP) was assessed by real-time PCR. Protein expression of IL-6, cellular ATP-content, and phospholipase C activity were measured by ELISA, luminescent, and fluorescent assay, respectively. Changes in free intracellular  $\text{Ca}^{2+}$  ( $[\text{Ca}^{2+}]_i$ ) was determined by Fuo-4 fluorescent in calcium free medium. The AMPK activity was determined by Western analysis of AMPK $\alpha$  phosphorytion.

**Results:** MPEP significantly increased oxidative stress parameters in a concentration dependent manner following MPEP exposure including, intracellular ROS levels, mitochondrial ROS levels, mitochondrial mass, and iNOS. Concentration and time-dependent activation of the inflammatory response with increasing IL-6 mRNA expression and secretion was observed. MPEP (100  $\mu\text{M}$ ) reduced ATP production and changed the phosphorylation state of AMPK. MPEP increased levels of  $[\text{Ca}^{2+}]_i$  in a concentration dependent manner. Thapsigargin (1  $\mu\text{M}$ ) was unable to further enhance the elevation of free intracellular  $\text{Ca}^{2+}$  ( $[\text{Ca}^{2+}]_i$ ) induced by MPEP. In addition, MPEP had no effect on the thapsigargin

induced elevation of  $[Ca^{2+}]_i$  rise. These results suggest that the  $[Ca^{2+}]_i$  pool originated from the ER. Pretreatment of the cells with xestospongine C, an inhibitor of the  $IP_3$  receptor, blocked the action of MPEP on  $[Ca^{2+}]_i$ . ER stress markers including, CHOP, GRP78, and GRP96 were induced by MPEP and were blocked by 4-phenyl butyric acid (1 mM) and BAPTA-AM (1  $\mu$ M). Pretreatment of the cells with AICAR (1 mM) partially abolished ER stress induced by MPEP. Pretreatment of the cells with compound C (1  $\mu$ M) potentiated ER stress induced by MPEP. U73122 (5  $\mu$ M), a PLC inhibitor, and pertussis toxin (PTX; 100 ng/ml), a Gi protein inhibitor blocked MPEP induced  $[Ca^{2+}]_i$ . MPEP (100  $\mu$ M) also significantly increased PLC activity. In addition, pretreatment the cells with AICAR, BAPTA-AM, U73122, and PTX prevented oxidative stress as well as inflammatory response induced by MPEP.

**Conclusions:** This study highlights the potential pathophysiological role of mGluR5 antagonism in mediating oxidative stress, ER stress and inflammation through both  $Ca^{2+}$  dependent and independent pathways in microglial cells. The  $Ca^{2+}$  dependent pathways involve Gi protein-coupled receptors, PLC and the  $IP_3$  receptor. AMPK may also play a role in the regulation of mGluR5 by interfering the energy balance.

### **Keywords**

MPEP, mGluR5, intracellular free calcium  $[Ca^{2+}]_i$ , ER stress, oxidative stress, inflammation, microglia

## Background

Neuroinflammation involves, i) an activation and recruitment of immune cells, such as, microglia, macrophages, and lymphocytes, and ii) an expression of factors designed to respond to the injury and aid in repair. Microglia are resident immune cells in the central nervous system and play an integral role in the neuroinflammatory response. Microglia activation is widely implicated as hallmarks in several neurodegenerative diseases [1]. Metabotropic glutamate receptors (mGluRs) are expressed in many different cell types throughout the brain and spinal cord [2]. Recently, mGluRs have been considered to be a promising target for neuroprotective agents in both acute and chronic neurodegenerative disorders [3, 4]. mGluRs are G-protein-coupled receptors of which there are eight subtypes divided into three groups (I–III) based on their sequence homology, signal transduction pathways and pharmacological profiles [3, 5]. Metabotropic glutamate receptor subtype 5 (mGluR5) is a group I member, which are typically postsynaptic and mediate their signaling through G $\alpha$ q-proteins. This results in the stimulation of the phospholipase C, leading to phosphoinositide hydrolysis and intracellular Ca<sup>2+</sup> mobilization and also activation of ERK1/2 downstream signaling pathways [3]. mGluR5 is expressed in microglia [2, 6] and the mGluR5 specific agonist (R,S)-2-chloro-5-hydroxyphenylglycine (CHPG) inhibits microglia activation, oxidative stress, and the release of inflammatory mediators both in vitro and in vivo [7-12]. Moreover, mGluR5 activation reduced fibrinogen-induced microglia activation which resulted in neuronal protection [13]. mGluR5 activation reduced  $\beta$ -amyloid-induced cell death in primary neuronal cultures [14]. It has been reported that mGluR5 is significantly expressed in activated microglia which surround the site of injury following traumatic brain injury in rats. This observation may support the idea that pharmacological manipulation of the mGluR5 may be beneficial in neuroinflammatory diseases [15, 16]. The use of mGluR5 agonists as a therapy for chronically injured spinal cord has been proposed [4]. Therefore, the dysregulation of mGluR5 may result in initiation or progression of neurodegenerative disorders.

Oxidative stress is a common feature of neurodegenerative diseases which increased levels of reactive oxygen species (ROS) [17, 18]. Under physiological conditions, cellular redox balance is maintained by the equilibrium between the formation and elimination of free radicals such as ROS and nitric oxide (NO). Excessive generation of ROS/NO or inadequate antioxidant defenses can result in damage to cellular structures. ROS plays a key role in microglial response in neurodegeneration [19-22]. Microglial intracellular ROS generation facilitates pro-inflammatory pathways by activating the mitogen-activated protein kinases (MAPKs) and NF- $\kappa$ B signaling [23-26]. mGluR5 modulates cellular oxidative status by affecting ROS and nitric oxide (NO) production through inhibition of NOX-2 activity [7, 10-12]. The central nervous system (CNS) strongly depends on efficient mitochondrial function, because the brain has a high energy demand. Defects in mitochondrial dynamics, generation of ROS, and environmental factors especially oxidative stress may have an influence on energy metabolism and contribute to the pathogenesis of several neurodegenerative diseases [27, 28]. The mitochondria generates ATP through oxidative phosphorylation. Under condition of low ATP levels the cellular energy sensor, AMP-dependent protein kinase (AMPK) positively regulates signaling pathways which replenish ATP [29-31]. Alternatively, AMPK is directly targeted and activated by pro-oxidant species or intracellular calcium levels [32, 33]. Although AMPK is considered to be a pro-survival kinase, it has been reported that prolong activation can induce cell damage including endoplasmic reticulum (ER) stress [33-36]. AMPK can also interact with the MAPK signaling cascade to mediate apoptosis, a process elicited by both energetic imbalance and pro-oxidant conditions, such as treatment with H<sub>2</sub>O<sub>2</sub> or UV [37]. AMPK can also modulate inflammation in muscle cells [38].

Changes in Ca<sup>2+</sup> level have been implicated to regulate several activities of microglia including cytokine release, migration, ROS generation, and proliferation [39-42]. Calcium also serves as the key link coupling cellular energy balance and mitochondrial ATP production. Mitochondrial calcium uptake is associated with an increase in mitochondrial bioenergetics and inflammatory response. However, a

consequence of mitochondrial calcium uptake is the production of ROS which plays a major role in the neurodegenerative diseases. In response to different stimuli, intracellular free  $\text{Ca}^{2+}$  level ( $[\text{Ca}^{2+}]_i$ ) are increased either by the release of  $\text{Ca}^{2+}$  from ER or by entry across the plasma membrane [43, 44]. The ER also serves as a  $\text{Ca}^{2+}$  reservoir regulated by two major  $\text{Ca}^{2+}$  release channels, the 1,4,5-trisphosphate receptor ( $\text{IP}_3\text{R}$ ) [45, 46] and the ryanodine receptor ( $\text{RyR}$ ) [46], as well as by  $\text{Ca}^{2+}$  ATPases which control  $\text{Ca}^{2+}$  transport into the ER [46]. The prolonged depletion of  $\text{Ca}^{2+}$  in the ER and  $\text{Ca}^{2+}$  overload in cytoplasm are mainly causes of ER stress [47, 48]. ER stress is generally caused by an overload of unfolded proteins in the ER, which activates the unfolded protein response (UPR) which consists of the transcriptional up-regulation of ER-chaperones, attenuation of protein translation; and ER-associated degradation of misfolded proteins [48, 49]. Inositol-requiring enzyme-1 (IRE1), activating transcription factor 6 (ATF6), and PKR-like ER kinase (PERK) act as transducers in the UPR signaling pathway. The ER-resident molecular chaperones including glucose-regulated protein 78 (GRP78) and glucose-regulated protein 94 (GRP94) as well as the transcriptional factor C/EBP homologous protein (CHOP) are induced by the UPR and they increase ER protein-folding capacity and maintain storage of ER  $\text{Ca}^{2+}$  [49, 50]. In addition, perturbation of ER integrity and increased ROS production are induced by an accumulation of misfolded proteins in the ER, leading to the activation of the UPR [51]. Prolonged ER stress results in cell death by the apoptotic pathway mediated by caspase-12, an ER localized cysteine protease [49]. In addition to calcium homeostasis, impairment of mitochondrial function and AMPK signaling have been considered to modulate the ER stress response [37, 52-56]. Specifically, mitochondrial dysfunction activated AMPK, leading to ER stress through NO production, resulting in apoptosis of pancreatic  $\beta$ -cells [54]. Activation of AMPK resulted in ER stress in several cell types [37, 53, 56]. Conversely, AMPK activation by AICAR attenuated ER stress and protected SH-SY5Y neuroblastoma cells against homocysteine-induced neurotoxicity [52].

The elevation in intracellular calcium is mediated by Phospholipase C (PLC)-mediated IP<sub>3</sub> formation which is a well-established downstream signaling effector of G protein-coupled receptor (GPCR) activation. Stimulation of GPCRs activates the Gq protein, promoting its dissociation into Gq $\alpha$  and Gq $\beta\gamma$ . Gq $\beta\gamma$  and the exchange of guanosine diphosphate bound to Gq $\alpha$  for GTP. The resulting GTP-Gq $\alpha$  complex activates the  $\beta$  isoforms of PLC [57]. mGluR5 activation in microglia has been suggested to involve in the Gq $\alpha$ -protein signal transduction pathway through PLC, PKC and Ca<sup>2+</sup> [8]. However, pertussis toxin (PTX)-sensitive Gi proteins and IP<sub>3</sub> signaling resulting in [Ca<sup>2+</sup>]<sub>i</sub> increase has been reported [58-61]. Taken together, these evidences suggest that not only Gq-coupled receptors but also Gi-coupled receptors can contribute to release of [Ca<sup>2+</sup>]<sub>i</sub> from the ER. In addition, many examples indicate that the synthesis of IP<sub>3</sub> and [Ca<sup>2+</sup>]<sub>i</sub> signaling by one type of G-protein-coupled receptor can be influenced by the stimulation of a different type of GPCR [62-64].

To our knowledge, the direct effect of mGluR5 inhibition on [Ca<sup>2+</sup>]<sub>i</sub> has not been tested in microglia. We showed in this present study that of mGluR5 inhibition resulted in [Ca<sup>2+</sup>]<sub>i</sub> elevation mainly through IP<sub>3</sub> receptor activation. The key contributions of increased calcium in microglia cells including oxidative stress, mitochondrial function, the releasing of pro-inflammatory cytokines, and ER stress were induced by blockage of mGluR5. Furthermore signaling pathways of Gi-coupled receptor, AMPK, and PLC-IP<sub>3</sub> pathway involved in mGluR5 inhibition.

## **Methods**

### **Materials**

Dulbecco's modified Eagle's medium (DMEM), RPMI 1640 medium, penicillin, streptomycin, 0.05% (w/v) trypsin/EDTA, non-essential amino acids (NEAA), 4-(2-hydroxyethyl)-1-piperazineethanesulfonic acid (HEPES), Hank's balanced salt solution (HBSS), EnzChek Direct Phospholipase C Assay kit, Hoechst 33342 dihydroethidium (DHE), Mitotracker Red CMXRos,

MitoSOX Red, Furo-4, and probenecid were obtained from Invitrogen (Carlsbad, CA, USA). Fetal bovine serum was from Atlanta Biologicals (Lawrenceville, GA, US). Cell Titer Glo<sup>®</sup> Assay kit was purchased from Promega (Madison, WI, USA). Dibutyltin dichloride (DBT), thapsigargin, AICAR, (RS)-2-chloro-5-hydroxyphenylglycine (CHPG), 6-methyl-2-(phenylethynyl)-pyridine (MPEP), BAPTA-AM, pertussis toxin (PTX), dantolene sodium, and sodium phenylbutyrate (PBA) were purchased from Sigma-Aldrich (St. Louis, MO, USA). Compound C and Xestrospongic acid were obtained from Calbiochem (San Diego, CA, USA). Specific antibodies against AMPK, and phosphorylated form and GRP78 were obtained from Cell Signaling Technology (Danvers, MA, USA). Specific antibodies for  $\beta$ -actin and goat anti-rabbit IgG-horseradish peroxidase were obtained from Santa Cruz Biotechnology (Santa, CA, USA).

### **Cell culture and experimental procedure**

BV-2 murine microglial cells immortalized by infection with v-raf/c-myc recombinant retrovirus [65] were kindly provided by Professor Wolfgang Sattler, University of Graz, Graz, Austria. The BV-2 cells were propagated in 75 cm<sup>2</sup> flasks in RPMI 1640 medium plus 10% fetal bovine serum, 2 mM glutamine, 100  $\mu$ g/mL streptomycin, and 100 U/mL penicillin, HEPES and 0.1 mM NEAA at 37°C, 5% CO<sub>2</sub>. The medium was changed every second day. Cells were sub-cultured at a level of approx. 70-80% confluence. Prior to initiating the experiments, cells were re-suspended in culture medium, and cells were seeded again to reach confluency of 70% in DMEM supplemented with 10% fetal bovine serum 1000 mg/L glucose, 2 mM glutamine, 100  $\mu$ g/mL streptomycin, and 100 U/mL penicillin, HEPES, and 0.1 mM NEAA. Prior to initiating the experiments, cells were cultured in 96-well ( $1 \times 10^3$  cells/well), 24-well ( $2 \times 10^4$  cells/well), 12-well ( $0.5 \times 10^6$  cells/well) or 6-well ( $1.0 \times 10^6$  cells/well) plates with fresh DMEM supplemented with 10% fetal bovine serum 1000 mg/L glucose, 2 mM glutamine, 100  $\mu$ g/mL streptomycin, and 100 U/mL penicillin, HEPES, and 0.1 mM NEAA. For experimental purposes, cells in exponential growth phase (approximately 60–70% confluency) were used. The

following cell numbers for seeding were used:  $1 \times 10^3$  cells/well in 96-well plates for determination of total ROS, mitochondrial ROS, mitochondrial mass, IL-6 protein level, total ATP content, and intracellular calcium level;  $5 \times 10^5$  cells/well in 12-well plates for gene expression analysis;  $1.0 \times 10^6$  cells/well in 6-well plates for Western blot analysis.

## **RNA isolation, reverse-transcriptase (RT) reaction and real-time PCR**

### **Isolation of total RNA**

Total RNA was isolated from cultured cells using RNA was isolated using Tri-reagent from Sigma Aldrich (St. Louis, MO, USA) according to the manufacturer's instructions with a few modifications, and stored at  $-80^{\circ}\text{C}$ . Briefly, cells from each well of 12-well plate were collected in the presence of 1 ml Tri-reagent to disrupt the cells and release the RNA and then 0.2 ml chloroform was added. After vigorous shaking and incubation at room temperature for 30 min, the samples were centrifuged at  $12,000\times g$  for 30 min at  $4^{\circ}\text{C}$ . The clear upper phase containing the RNA was aspirated. An equal volume of cold isopropanol was added and the solution was allowed to stand at room temperature for overnight before being centrifuged as mentioned above. The pellet was collected and washed with 1 ml cold 75% ethanol followed by centrifugation at  $7500\times g$  for 10 min. After the final wash, the ethanol was removed and the pellet was air-dried and re-dissolved in DEPC-treated water. Efficiency and quality of RNA extraction was measured using 260/280 ratios of optical density from each sample with a NanoDrop<sup>®</sup> Spectrophotometer (NanoDrop Technologies). The 260/280 ratios above 1.8 was accepted as pure quality total RNA.

### **cDNA synthesis**

Complementary DNA was synthesized from 0.5  $\mu\text{g}$  total RNA using Superscript III reverse transcriptase (Invitrogen, Carlsbad, CA). The cDNA reaction containing with 0.5  $\mu\text{g}$  of total RNA and 0.5  $\mu\text{g}$  of oligo (dT) primers was incubated at  $56^{\circ}\text{C}$  for 5 min and then the reaction mix (containing

with 5x first strand buffer, dithiothreitol (DTT), RNase out inhibitor (50 units), dNTPs , and Superscript<sup>®</sup> Reverse Transcriptase (RT)-III). The reaction was performed at 42 °C. After 1 h., DEPC-treated water was added. The concentration and the purity of the single stand DNA were assessed with a NanoDrop<sup>®</sup> Spectrophotometer (NanoDrop Technologies). Synthesized first strand cDNA samples were stored at -20 °C until used.

### **RT-PCR assay and data analysis**

Quantitative real-time RT-PCRs were performed using the rotor-gene-3000A (Corbett Research, Australia) in a total reaction volume of 10 µl. The reverse-transcriptase (RT) mixture was mixed with the KAPA SYBR<sup>®</sup> FAST qPCR Kit (Kapasystems, Boston, MA) and gene-specific primers. Primers for GAPDH, iNOS, IL-6, CHOP, GRP78, and GRP96 were purchased from Sigma-Aldrich (St. Louis, MO, USA). Thermal cycler parameters were as follows: hold for 15 min at 95°C, followed by amplification of cDNA for 40 cycles with melting for 15 s at 94°C and annealing for 30 s at 56°C, and extension for 30 s at 72°C. For each sample, three replicates were analyzed. Expression was normalized to GAPDH. Fold changes were quantified as  $2^{-(\Delta C_t \text{ sample} - \Delta C_t \text{ control})}$ , as described previously [66] The primers for real-time PCR were listed in **Table 1S**.

### **Preparation of whole cell lysates**

Cells grown in 6-well plates ( $1.0 \times 10^6$  cells/well) were treated with selected compounds for indicated times. For making whole cell lysates, the cells were washed twice with ice-cold phosphate-buffered saline and harvested in cold RIPA buffer (Sigma-Aldrich, St. Louis, MO) supplemented with 2% protease inhibitor cocktail (Roche Diagnostics, Mannheim, Germany). The extract was centrifuged at  $10,000 \times g$  for 15 minutes at 4°C in order to remove cell debris.

### **Western blot analysis**

Equal amounts of whole cell protein (30 µg) for each sample were separated by electrophoresis in 10% sodium dodecyl sulfate-polyacrylamide gel electrophoresis (SDS-PAGE) and transferred onto polyvinylidene difluoride (PVDF) membranes (Bio-Rad Laboratories, Hercules, CA, US) at 120 mA for 1 h. The membranes were blocked for 1 h at 25 °C in Tris-buffered saline, pH 7.4 (TBS) with 0.1% Tween 20 (TBS-T) containing 5% non-fat milk. Next, the blots were incubated overnight at 4°C with primary antibodies against AMPK $\alpha$ (D63G4) (1:1000), phospho-AMPK $\alpha$ (Thr172) (1:1000), GRP78 (1:500), and  $\beta$ -actin (1:2000). All primary antibodies used in this study were purchased from Cell Signaling Technology (Danvers, MA). The membranes were washed with TBS-T and then incubated with goat anti-rabbit IgG-horseradish (1:5000; Santa Cruz Biotechnology, Santa Cruz, CA) for 2 h at 25 °C. After washing the membranes with TBS-T, immunolabeling was detected using an enhanced chemiluminescence HRP substrate (Millipore, Billerica, MA, US) according to the manufacturer's instructions using a Fujifilm LAS-4000 detection system (Bucher Biotec, Basel, Switzerland).  $\beta$ -actin was used for loading control of whole cell protein extracts.

### **Measurement of intracellular ROS, and mitochondrial content, mitochondrial ROS by ArrayScan<sup>®</sup> high-content screening system**

Total ROS, mitochondrial mass, and mitochondrial ROS were determined by using the specific fluorescent dyes including dihydroethidium (DHE), MitoTracker<sup>®</sup>Red CMXRos, and MitoSOX Red, respectively (Invitrogen, Carlsbad, CA, USA). After the treatments, DHE (10 µg/ml), MitoTracker<sup>®</sup>Red CMXRos (200 nM), or MitoSOX Red (5 µM) were added to live cells and incubated for 10, 30, and 20 min, respectively. Cells were washed with PBS and fixed with 4% formaldehyde for 15 min. Fixed cells were permeabilized with 0.1% Triton X-100 in PBS. Nucleus was stained with Hoechst 33342. Stained cells were visualized and images were captured and the amount of fluorescent was quantified using ArrayScan<sup>®</sup> high-content screening system (Cellomics Inc, Pittsburgh, PA). Cell health profiling bioapplication module was used to quantify the fluorescence intensities of each dye and captured with

appropriate filter on 20 fields with each field containing approximately 1000 cells. Cells were identified using Hoechst dye and a nuclear mask was generated from images of Hoechst-stained nuclei. The intracellular ROS, mitochondrial content, and mitochondrial ROS were reported as the percentage of fluorescent intensity compared with control group.

### **Phospholipase C activity assay**

Phosphatidylcholine-specific PLC activity was determined in whole-cell lysates by using the EnzChek Direct Phospholipase C Assay (Invitrogen Corporation, Carlsbad, CA, USA). The assay measures PLC activity by addition of a proprietary substrate, which is cleaved by phosphatidylcholine-specific PLC. The cleavage releases the dye-labeled diacylglycerol, which produces a positive fluorescence signal that can be measured. Briefly, 100  $\mu$ l cell lysates of treated cells were incubated with 100  $\mu$ l substrate working solution (glycerol-phosphoethanolamine with a dye-labeled *sn*-2acyl chain) for 30 min then fluorescence (490 nm excitation and 520 nm emission) was measured by a SpectraMax Gemini EM (Molecular Device, Devon, UK). To account for different protein concentrations of the samples enzyme activity was normalized to protein concentration of the respective cell lysate resulting in mU per  $\mu$ g of protein.

### **ATP-content**

Total ATP content was measured by a luminescence-based assay with CellTiter-Glo<sup>®</sup> Luminescent Cell Viability Assay kit following the manufacturer's instruction (Promega, Madison, WI). Briefly, the assay buffer and substrate were equilibrated to room temperature, and the buffer was transferred to and gently mixed with the substrate to obtain a homogeneous solution. After treatment protocol, 100  $\mu$ l of the assay reagent was added into each well and the content was gently mixed with light protection on an orbital shaker to induce cell lysis. After 30 min, the luminescence was quantified on a Microplate Reader (SpectraMax GeminiEM, Molecular Devices, Devon, UK). The luminescent signals for the

treated cells were normalized to the luminescent signal of cells treated with control group, which was arbitrarily set to 100%.

### **Protein determination**

Protein concentrations were determined by using a Pierce<sup>®</sup> BCA protein assay kit (Thermo Scientific, US) according to the manufacturer's instructions. Bovine serum albumin was used as a protein standard. Absorbance was measured at 595 nm by using a UV-max kinetic microplate reader (Molecular Device, Devon, UK)

### **Detection of IL-6 by enzyme-linked immunosorbent assay**

Supernatant protein concentrations of IL-6 were quantified by commercially available ELISA kit (BD Biosciences, CA, USA). After treatment with selected compounds for indicated times, the supernatants were collected. 96-well plate was coated with coating buffer containing primary antibody for mouse IL-6 overnight at 4 °C. After washing with PBS-T (PBS containing 0.05% Tween-20), the wells were blocked with assay diluents. The plates were incubated for 1 h at room temperature. After 1 h, plates were washed and 100 µl of samples or standards were added to the wells. After 2 h, plates were washed and 100 µL IL-6 detection antibody diluted 1:250 in assay diluent was added per well. Plates were incubated for a further 1 h before being washed. The enzyme streptavidin alkaline phosphatase was diluted 1:250 in assay diluent and 100 µL was added per well. Plates were then incubated for 30 min. After washing, substrate solution was added and incubated for 30 min in the dark. The reaction was stopped with 50 µL of 1 M H<sub>3</sub>PO<sub>4</sub> (stop solution), and the absorbance of the wells was read at 450 nm with a correction of 570 nm using UV max kinetic microplate reader (Molecular Device, Devon, UK). IL-6 concentrations were calculated from the linear equation derived from the standard curve of known concentrations of purified mouse IL-6.

### **Determination of intracellular Ca<sup>2+</sup> concentration**

Intracellular Ca<sup>2+</sup> signaling was measured with the calcium-sensitive dye Furo-4. Cells were stained with 1 µg/ml Hoechst 33342 in medium for 30 min. Then cells were washed with Hanks' balanced salt solution (HBSS) containing 20 mM HEPES and equilibrated with loading solution containing with 5 µM Furo-4, 2.5 mM probencid and 20 mM HEPES in HBSS for 30 min at 37 °C and followed by 30 min at room temperature. After loading, cells were washed twice with HBSS in order to remove excess fluorescent dye. Cells were then treated for different durations with various compounds in HBSS in a humidified incubator which provided an atmosphere of 5 % CO<sub>2</sub> and 95 % air at a constant temperature of 37 °C. The fluorescence intensity of fluo-4 was measured by using ArrayScan<sup>®</sup> high-content screening system (Cellomics Inc, Pittsburgh, PA). Measurements of fluorescent intensity with appropriate filter were captured with appropriate filter on 10 fields with each field containing approximately 500 cells. Relative changes in calcium concentration using fluo-4 were analyzed as a function of time, were expressed as  $\Delta F/F$  (in %), with F being the baseline fluorescence and  $\Delta F$  the variation of fluorescence.

### **Statistical analysis**

The data are expressed as the mean  $\pm$  SD and were analyzed using one-way ANOVA (V5.00; GraphPad Prism Software Inc., San Diego, CA). When ANOVA showed significant differences between groups, Tukey's post hoc test was used to determine the specific pairs of groups showing statistically significant differences. A *p* value of less than 0.05 was considered statistically significant.

## Results

### Blockage of mGluR5 induced oxidative stress and inflammatory responses in BV-2 cells

There is a close resemblance between BV2 microglial cells and primary microglia in terms of their inflammatory signaling pathways. Therefore, BV-2 microglial cells can be used as an appropriate model for the activation of microglia *in vitro* [67]. Upon activation, BV2 microglial cells are known to increase their production of neuroinflammatory molecules including iNOS, cytokines, and ROS. For the present study, we used, 2-methyl-6-(phenylethynyl)-pyridine (MPEP) which is a specific antagonist for mGluR5 to mimic the situation of mGluR5 blockage. The intracellular redox status was evaluated with DHE, MitoTracker<sup>®</sup>Red CMXRos, and MitoSOX Red which are markers of ROS, mitochondrial mass, and ROS in mitochondria, respectively (Fig. 1A-Fig. 1C). In addition, the expression of iNOS mRNA was also investigated (Fig. 1D). The inflammatory responses of BV-2 cells were measured by both mRNA and protein levels of IL-6 (Fig. 1D and Fig. 1E). After a 24-h incubation time, the mGluR5 antagonist, MPEP (100  $\mu$ M) induced a significant increase in oxidative stress parameters with  $132.2\pm 4.56$ ,  $133.6\pm 5.77$ , and  $313.7\pm 14.59\%$  of intracellular ROS, mitochondrial mass, and intramitochondrial ROS, compared with control group, respectively. The level of iNOS mRNA was increased  $3.04\pm 0.23$  fold compared with control. MPEP also enhanced the inflammatory responses of BV-2 cells by increasing IL-6 mRNA and protein expression by  $6.23\pm 0.85$  and  $29.20\pm 3.25$  fold respectively compared with control. In parallel, the biological effects of mGluR5 agonist CHPG (100  $\mu$ M) on BV-2 cells were investigated. As expected, no significant changes were observed after 24 h of CHPG exposure. Moreover, the actions of mGluR5 were completely blocked when cells were pretreated with CHPG before adding MPEP (data not shown). This suggests that the effects of MPEP are mediated through mGluR5.

### **Blockage of mGluR5 induced cellular energy depletion and disturbed AMPK phosphorylation**

Because mitochondrial dysfunction can result in alterations in oxidative stress and inflammatory responses, it may also affect ATP synthesis. We measured the intracellular ATP content in BV-2 cells following MPEP (100  $\mu$ M) exposure as shown in Fig. 2A. Total ATP content was significantly decreased  $16.46\pm 1.04\%$  following incubation of cells with MPEP for 1 h compared to control. Interestingly, ATP production also decreased in time-dependent manner. This result demonstrates that a single dose of MPEP significantly affects ATP levels in BV-2 cells.

The role of AMPK was examined because AMPK activation has influence on ATP production and the sensitivity of cells to such toxicants. DBT altered energy balance in BV-2 cells and consequently, the effects of AMPK inhibitor Compound C as well as AMPK activator (AICAR) on MPEP diminished ATP production were examined. Fig. 2B shows that treatment of cells with 1  $\mu$ M Compound C alone resulted in a decreased in cellular ATP levels  $71.51\pm 4.68\%$  compared to control. As expected, pretreating the cells with Compound C potentiated the toxicity of MPEP to reduced ATP levels to  $14.83\pm 1.34\%$ . On contrary, 1 mM AICAR alone slightly increased ATP production  $133.0\pm 7.28\%$  compared to control. Pretreating the cells with AICAR completely reversed ATP depletion induced by MPEP exposure. These results suggest that AMPK may be involved in MPEP-induced ATP depletion.

To examine whether MPEP and AICAR stimulated AMPK activation in BV-2 cells, the phosphorylation of AMPK $\alpha$  subunit was measured after the indicated chemicals treatment for 0.5, 1, and 2 h. Fig. 2C shows that the level of pAMPK increased in the presence of AICAR (1mM) or MPEP (100  $\mu$ M) for 1 h. However, no further increase in pAMPK levels was observed when the cells were treated with either AICAR or MPEP for 2h. These results suggest that AMPK is maximally activated in BV-2 cells after 1 h stimulation.

To investigate if DBT-stimulated phosphorylation of AMPK can be further modulated by an inhibitor or an activator of AMPK, cells were pre-treated with either compound C (1  $\mu$ M) or AICAR (1mM) for 1 h,

and then co-exposed to MPEP (100  $\mu$ M) for 1h. The phosphorylation state of AMPK-induced by MPEP was reversed by compound C but enhanced by AICAR (Fig. 2D).

### **mGluR5 increased intracellular calcium released from the endoplasmic reticulum**

Disturbances in  $[Ca^{2+}]_i$  regulate a wide variety of targets such as kinases, phosphatases, and transcriptional factors. The effects of MPEP on  $[Ca^{2+}]_i$  were determined using a fluorescent indicator Fura-4. Cells were exposed to MPEP and kinetic  $[Ca^{2+}]_i$  changes were analysed every minute. In  $Ca^{2+}$ -free medium, MPEP (100  $\mu$ M) significantly increased  $[Ca^{2+}]_i$  in BV-2 cells (Fig. 3A). Next, we explored the specific intracellular  $Ca^{2+}$  store involved in MPEP-induced cytoplasmic  $[Ca^{2+}]_i$  rise. It has been shown that the endoplasmic reticulum (ER) is the major  $Ca^{2+}$  store in microglia cells. Fig. 3A shows that in  $Ca^{2+}$ -free medium, the addition of MPEP (100  $\mu$ M) induced a substantial reduction of the amplitude of the  $[Ca^{2+}]_i$  response to thapsigargin, an ER  $Ca^{2+}$  pump inhibitor. Fig. 3B shows that thapsigargin induced a  $[Ca^{2+}]_i$  rise, and subsequently added MPEP (100  $\mu$ M) blocked the  $[Ca^{2+}]_i$  rise.

To determine the specific receptors involved in the  $Ca^{2+}$  efflux from the ER following exposure to MPEP, we used two different inhibitors before MPEP treatment. We used dantrolene to inhibit ryanodine receptors (RyRs) in the ER [68] and xestospongine C as inhibitor of inositol triphosphate receptors (IP<sub>3</sub>Rs) in the ER. Inhibition of IP<sub>3</sub>R  $Ca^{2+}$ -channels by xestospongine C in the ER partially prevented the increase in  $[Ca^{2+}]_i$  provoked by MPEP (Fig. 3D). However, pretreatment cells with dantrolene abolished an elevation of  $[Ca^{2+}]_i$  after MPEP exposure (Fig. 3C).

### **Blockage of mGluR5 results in increasing of ER stress**

Disturbances in  $Ca^{2+}$  homeostasis can trigger ER stress and MPEP induced  $[Ca^{2+}]_i$  elevation. Consequently, we tested whether blockage of mGluR5 with MPEP induces ER stress. The expression of GRP78 protein was examined after cells were treated with MPEP for 0.5, 1, and 2 h by Western

blotting. MPEP treatment induced a time-dependent increase in GRP78 protein expression in BV-2 cells (Fig. 4A). Consistent with our hypothesis, the protein levels of GRP78 were elevated 1 h after MPEP exposure, with the maximal expression at 2 h.

Furthermore, we also assessed the mRNA expression level of CHOP, GRP78, and GRP94 after MPEP exposure for 24 h. As shown in Fig. 4B, real-time PCR analysis showed that the expression of CHOP, as well as GRP78, and GRP94 mRNA increased significantly  $3.54 \pm 0.25$ ,  $3.00 \pm 0.064$ , and  $3.83 \pm 0.30$  fold respectively in response to MPEP treatment compared with control. To confirm the action of MPEP on ER stress, cells were pretreated for 1 h with 4-phenyl butyric acid (4-PBA), a chemical chaperone, and incubated with MPEP for 24 h. 4-PBA significantly reversed MPEP-induced mRNA expression of the major ER chaperone (Fig. 4B).

DBT triggered the accumulation of cytosolic  $\text{Ca}^{2+}$  by enhancing  $\text{Ca}^{2+}$  release from ER (Fig. 3A and 3B) that in turn could trigger an ER stress response. This meant that blocking  $\text{Ca}^{2+}$  release by the calcium chelator BAPTA-AM could potentially inhibit ER stress-induced by MPEP. We therefore analyzed the effects of BAPTA-AM on MPEP-induced CHOP, GRP78, and GRP94 mRNA expression. Pretreatment of cells with BAPTA-AM (1  $\mu\text{M}$ ) followed by MPEP treatment, blocked induction in expression of these three ER stress markers. This confirms that ER  $\text{Ca}^{2+}$  release is a critical element of the ER stress response.

The results suggest that MPEP acts, at least in part, on AMPK pathways to regulate mitochondrial biogenesis and function in BV-2 cells (Fig. 2B-2D).

To evaluate whether effect of MPEP on ER stress was mediated through AMPK, we examined the effect of AICAR and compound C on the protein level of GRP78 in BV-2 cells. We pretreated cells with either AICAR (1 mM) or compound C (1  $\mu\text{M}$ ) for 1 h., followed by MPEP (100  $\mu\text{M}$ ) for 2 h. AICAR or compound C treatment alone did not significantly interfere on GRP78 protein level (data not shown). As shown in Fig. 4C, compound C increased the potency of MPEP to enhance GRP78 level. In

contrast, activation of AMPK activity with AICAR reduced MPEP-induced GRP78 protein expression (Fig. 4B). To determine whether the alteration in of CHOP, GRP78, and GRP94 mRNA levels observed with MPEP treatment was the result of AMPK, we pretreated cells with either AICAR (1 mM) or compound C (1  $\mu$ M) for 1 h. then followed by co-incubation with MPEP (100  $\mu$ M) for 24 h and measured the levels of CHOP, GRP78, and GRP94 mRNA. As shown in Fig. 4D, AICAR partially abolished the increase in CHOP, GRP78, and GRP94 mRNA levels seen with MPEP treatment, again indicating that AMPK-regulated to energy balance may play a role in regulation of CHOP, GRP78, and GRP94 mRNA transcription. These findings strongly suggest that AMPK may mediate the action of MPEP on ER stress in BV-2 cells.

### **Phospholipase C is the target of mGluR5 modulation**

It is widely accepted that activation of PLC produces  $IP_3$ , which opens  $IP_3$ Rs to induce  $Ca^{2+}$  release from the ER in a variety of cells. As such, we speculated that PLC may play a role in MPEP-induced  $Ca^{2+}$  elevation. As compared with the vehicle, as shown in Fig. 5A, MPEP increased the intracellular calcium concentration in a concentration dependent manner. We also pretreated cells with an inhibitor of PLC, U73122, at an effective concentration (5  $\mu$ M) and the response of MPEP (100  $\mu$ M) was significantly inhibited. MPEP induced increases in CHOP, GRP78, and GRP 96 mRNA expression were also reduced by pretreatment with U73122 (Fig. 5B). These results demonstrated that PLC may play a role in MPEP-induced  $Ca^{2+}$  elevation and ER stress. To address this issue, we investigate whether MPEP could activate PLC in BV-2 cells. The results are shown in Fig. 5C, in which total PLC activity was significantly increased in cells following MPEP exposure for 2 h compared with control. The MPEP induced increase in the activity of total PLC was completely blocked by pretreatment with U73122 for 1 h. In addition, U73122 also significantly decreased on the basal activity of PLC in BV-2 cells (Fig. 4C).

To evaluate if PLC was involved in the  $\text{Ca}^{2+}$ -dependent processes we used U73122 as an inhibitor of PLC and BAPTA-AM and studied their effect on the GRP78 protein levels-mediated by MPEP (Fig. 5D). U73122 blocked the MPEP-induced response completely, indicating that PLC is involved in GRP78 expression. Pretreating the cells with BAPTA-AM also abolished the action of MPEP t confirming that calcium is directly involved in MPEP-induced ER stress.

### **PTX-sensitive G proteins/PLC/ $\text{Ca}^{2+}$ pathways mediated by mGluR5**

Several studies have demonstrated that G protein-coupled receptors may exert their effects through activation of PLC, which hydrolyzes phospholipids in cell membrane to  $\text{IP}_3$  and DAG. To investigate the  $[\text{Ca}^{2+}]_i$  responses to MPEP, we pretreated cells with a specific inhibitor of Gi/o-type G proteins, pertussis toxin (PTX; 100 ng/ml) for 6 h. As shown in Fig. 6A, pretreatment of cells with PTX completely suppressed  $[\text{Ca}^{2+}]_i$  release induced by MPEP treatment suggesting the involvement of Gi/o proteins in  $[\text{Ca}^{2+}]_i$  responses to MPEP.

We showed that MPEP activated PLC activity and PTX blocked  $[\text{Ca}^{2+}]_i$  induced by MPEP. Therefore, we investigated whether PTX inhibit MPEP-activated PLC activity. As shown in Fig. 6B, the actions of the MPEP were markedly inhibited by PTX pretreatment. This result suggests that MPEP may utilize PTX-sensitive G-protein in the PLC activation.

To confirm the downstream effects of MPEP after PLC activation and increase in  $[\text{Ca}^{2+}]_i$ , we investigated whether PTX suppresses GRP78 expression after MPEP exposure. As shown in Fig. 6C, pretreatment cells with PTX completely inhibited the action of MPEP on GRP78 synthesis.

### **mGluR5 regulated oxidative stress and inflammatory responses through PTX-sensitive G proteins/PLC/AMPK/ $\text{Ca}^{2+}$ pathway**

The role of mGluR5 and intracellular signaling on the regulation of oxidative stress and inflammatory responses were confirmed by pretreating the cells with AICAR, compound C, BAPTA-AM, U73122, or

PTX (AMPK activator, AMPK inhibitor,  $\text{Ca}^{2+}$  chelator, PLC inhibitor, and  $\text{G}_{i/o}$ -type G protein inhibitor, respectively) followed by MPEP exposure. Consequently, the levels of intracellular ROS, mitochondrial mass, mitochondrial ROS, iNOS mRNA, IL-6 mRNA, and IL-6 protein were measured. Pretreatment of cells with compound C potentiated the actions of MPEP on oxidative stress and cytokine expression (Fig. 7A-7F). On contrary, AICAR, BAPTA-AM, U73122, and PTX could prevent the action of MPEP on total ROS production and ROS-generated in the mitochondria (Fig. 7A and 7C) as well as preventing the mitochondrial toxicity of MPEP as indicated by mitochondrial mass (Fig. 7B). Moreover, these chemicals markedly attenuated MPEP-induced iNOS IL-6 mRNA levels as well as IL-6 expression (Fig. 7C-7D). These data suggested that blockage of mGluR5 by MPEP may modulate PTX-sensitive G proteins, PLC, AMPK, and  $[\text{Ca}^{2+}]_i$  and contribute to oxidative stress and inflammatory responses in BV-2 cells.

## Discussion

Several reports have shown that the metabotropic glutamate receptor 5 (mGluR5) mediates neuroprotective effects in microglia cells by the modulation of oxidative stress and inflammatory cytokine release both *in vitro* and *in vivo*. It was demonstrated that the mGluR5 agonist, (R,S)-2-chloro-5-hydroxyphenylglycine (CHPG) reduced NF- $\kappa$ B activity and nitrite production in lipopolysaccharide-stimulated microglia and improved functional recovery after traumatic brain injury [10, 15, 16]. Activation of mGlu5 receptors abolished the toxic effect produced by 1-methyl-4-phenylpyridinium in SK-N-SH cells [69]. Delayed CHPG administration reduced chronic neuroinflammation and associated neurodegeneration after experimental traumatic brain injury in mice [7]. Stimulation of mGluR5 reduced ROS production, NO production, proliferation and TNF- $\alpha$  production in microglia cells after LPS exposure [8]. In addition, the expression and the distribution of mGluR5 was changed after brain damage [15, 70]. mGluR5 is down-regulated in activated microglia by proinflammatory cytokine stimulation[71].

However, the consequence of direct antagonism of the mGluR5 on the cellular functions of microglia has yet to be studied. Therefore, in the present study, we used 2-methyl-6-phenylethynyl-pyridine (MPEP), a non-competitive mGluR5 antagonist, to block mGluR5 in BV-2 cells and we measured the oxidative stress and inflammatory responses. MPEP increased the total ROS production as well as mitochondrial dysfunction representing with mitochondrial swelling and ROS. MPEP enhanced the inflammatory response by increasing IL-6 expression and release of microglia. CHPG completely reversed the actions of MPEP. This indicates that oxidative stress and cytokine up-regulation induced by MPEP through mGluR5 inactivation. These results are consistent with the previous studies which found that activation of mGluR5 in microglia cells protect neuronal cells and prevent brain damage [7-10, 69]. However, MPEP has been shown the neuroprotection in several investigations. In particular, prolonged treatment with MPEP prevented excitotoxic death of cultured spinal cord motor neurons [72]. 6-hydroxydopamine induced nigrostriatal lesions was abrogated following MPEP administration [73]. Mitochondrial dysfunction leading to ATP depletion has been suggested to be implicated in an increase in oxidative stress and inflammation [74-77]. Consequently, the downstream effect of mGluR5 blockage on cellular ATP content was investigated. Cellular ATP content was decreased after mGluR5 blockage by MPEP within 1 h. The involvement of AMPK was tested. Pretreatment of cells with compound C, an AMPK inhibitor, enhanced the action of MPEP but pretreatment cells with AICAR prevented ATP depletion. This was considered to be related to the production of inflammatory mediators [78, 79]. AICAR inhibited the proinflammatory response in glial cells [78]. However, AMPK is activated by phosphorylation after depletion of ATP levels [80]. Activation of AMPK has been reported to enhance apoptosis, ROS production, and cytokine release [81-83]. AMPK phosphorylation by MPEP increased after 1 h while significant ATP depletion was observed. These results indicate that a blockage of mGluR5 may influence AMPK activation through the inhibition of ATP production. Our observations show the first evidence of an association between inhibition of mGluR5 and the activation of AMPK signaling that involved energy balance in microglia cells.

Calcium disturbances have implications for the health and function of many types of cells for instance in oxidative stress, in oxidative injury and inflammation [44, 84-87]. In microglia cells, changes in the intracellular free  $\text{Ca}^{2+}$  concentration ( $[\text{Ca}^{2+}]_i$ ) represent one of the major pathways for signal transduction in microglia. LPS leads a chronic elevation of basal  $[\text{Ca}^{2+}]_i$  and BAPTA strongly prevented the LPS-induced release of NO and the cytokines  $\text{TNF}\alpha$ , IL-6, and IL-12 [88]. Some studies have indicated that intracellular calcium may act directly on the mitochondrial membrane, leading to enhanced ROS production [89, 90]. It is also indicated that intracellular calcium elevation could enhance ROS production in various culture cells, such as astrocytes [91, 92], neurons [93], and microglia cells [86, 94]. Overload of calcium also decreases mitochondrial function by triggering the opening of the mitochondria permeability transition pore and results in mitochondrial swelling, increase in the generation of ROS, mitochondrial membrane depolarization and decrease in the production of ATP [95-97]. Accordingly, we hypothesized that MPEP might promote oxidative stress as well as pro-inflammatory cytokine up-regulation through increasing intracellular calcium in microglia cells. As shown in Fig. 3A, exposure of BV-2 cells to MPEP caused a burst of fluorescence intensity that reaches a peak at 15 min and returned to baseline within 40 min. Previous studies showed that microglial  $\text{Ca}^{2+}$  signals occur predominantly under pathological conditions [42]. For example, an exposure to  $\text{A}\beta$  increased  $[\text{Ca}^{2+}]_i$  in cultured microglia. Basal  $[\text{Ca}^{2+}]_i$  levels in microglia isolated from the brain of AD patients is higher than that of microglia from non-demented individuals [98, 99]. Increase of intracellular  $[\text{Ca}^{2+}]_i$  can be elicited through two main mechanisms; firstly, mobilization of  $\text{Ca}^{2+}$  from intracellular stores and secondly, entry from the extracellular space through the opening of plasma membrane  $\text{Ca}^{2+}$  channels. In our experiments, we investigated the effect of MPEP on the  $[\text{Ca}^{2+}]_i$  under  $\text{Ca}^{2+}$ -free medium condition. This strategy showed that  $[\text{Ca}^{2+}]_i$  induced by MPEP originated from intracellular organelles and not extracellular influx. In addition, the endoplasmic reticulum (ER) is a intracellular storage compartment for calcium in microglia cells [44]. In our study, pre-exposure of BV-2 cells to thapsigargin completely blocked MPEP-induced  $[\text{Ca}^{2+}]_i$  elevation and conversely, MPEP

pretreatment also reduced thapsigargin-induced  $[Ca^{2+}]_i$  level. Therefore, these results confirm that MPEP increased  $[Ca^{2+}]_i$  because of ER perturbation. We then identified the specific receptors modulating MPEP induced calcium release from the ER, inositol 1,4,5-trisphosphate (IP<sub>3</sub>R) not the ryanodine (RyRs) receptors [100]. We found that xestospongine C, IP<sub>3</sub>R receptor antagonist, significantly blocked MPEP-induced  $[Ca^{2+}]_i$  rise. However, RyRs receptor antagonist, dantolene only partially diminished  $[Ca^{2+}]_i$  induced by MPEP indicating that mGluR5 may modulate through the IP<sub>3</sub>R receptor. Moreover, these results are agreement with previous observation showing that xestospongine C prevented the induction of TNF- $\alpha$  and IL-6 in microglia cells [101].

The depletion of luminal ER calcium stores is believed to trigger ER stress which activates the unfolded protein response (UPR) pathway to induce the expression of ER chaperone proteins, such as CHOP, GRP78, and GRP96 [49]. In our study found that MPEP treatment enhanced the expression of ER stress proteins (CHOP, GRP78, and GRP96) in BV-2 cells and was strongly attenuated by BAPTA-AM, suggesting that mGluR5 modulate ER stress through  $[Ca^{2+}]_i$  homeostasis. Not only intracellular calcium dysregulation but AMPK has been documented to be involved in ER stress in several cells [52, 53, 56, 102]. MPEP was able to disturb AMPK function and led to a decrease in ATP production and we found that compound C promoted ER stress induced by MPEP. Conversely, AICAR reversed the action. In addition, pretreatment of either compound C or AICAR had no effect on  $[Ca^{2+}]_i$  (data not shown) suggesting that the action of AMPK on MPEP-mediated ER stress is independent of  $[Ca^{2+}]_i$  but related to energy balance. AMPK activation has already been shown to be involved in cell energy metabolism through elevation in fatty acid oxidation and levels ATP increased following AICAR stimulation [103]. Accordingly, incubation with AICAR has been reported to protect endothelial cells from a loss of intracellular ATP induced by hyperglycemia [104]. The protective potential of AICAR on ER stress has been documented [52, 105-108]. However, an activation of AMPK was reported to potentiated ER stress [7, 36, 56].

PLC activation induces IP<sub>3</sub> production, resulting in the release of Ca<sup>2+</sup> from ER through the IP<sub>3</sub> receptor. We found that U73122, a PLC inhibitor, abrogated MPEP-induced Ca<sup>2+</sup> increases and ER stress. BAPTA-AM prevented MPEP-induced ER stress. Taken together, these results demonstrate that MPEP induces ER stress via the PLC-IP<sub>3</sub> pathway. MPEP increased PLC activity supporting our hypothesis. However, there is evidence that the mGluR5 agonist, CHPG reduced inflammation induced by LPS in microglia this was associated with phospholipase C activation and an increase in intracellular calcium [8]. It is possible that mGluR5 might cross regulate a toll-like receptor and resulting in a muted inflammatory response.

To examine the possible involvement of G proteins, cells were pretreated with PTX which completely inhibits the effect of MPEP on PLC activation, [Ca<sup>2+</sup>]<sub>i</sub> rise, ER stress, oxidative stress responses and pro-inflammatory cytokine release. Classically, the activation of PLC resulting in the synthesis of IP<sub>3</sub> and the release of Ca<sup>2+</sup> from ER, was linked to G<sub>q</sub>-coupled receptors [57]. In the present study, the MPEP-induced increase in [Ca<sup>2+</sup>]<sub>i</sub> was attenuated by PTX (an inhibitor of G<sub>i</sub> protein), U73122 (a PLC inhibitor), and xestospongin C (an IP<sub>3</sub> receptor antagonist). Crosstalk among mGluR5 receptors to modulate PLC through G<sub>i</sub>-protein subunits is possible, because several studies in a variety of cells and tissues demonstrated that the mobilization of [Ca<sup>2+</sup>]<sub>i</sub> is stimulated by G<sub>i</sub>-coupled receptors [57, 61, 109]. For instance, PTX treatment of natural killer cells reduced [Ca<sup>2+</sup>]<sub>i</sub> release and chemotactic induction [61]. Chronic activation of G<sub>i</sub>-proteins interfered with basal L-type Ca<sup>2+</sup> channel activity in heart failure [110]. PTX totally blocked the Ca<sup>2+</sup> responses induced by endomorphin-1 (an endogenous μ-opioid receptor agonist) in astrocytes [111].

Our study is the first that describes the direct effect of mGluR5 antagonism on oxidative stress, inflammation and ER stress mediated by Ca<sup>2+</sup> homeostasis through PTX-sensitive G protein/PLC/IP<sub>3</sub>/Ca<sup>2+</sup> pathway. In addition, the Ca<sup>2+</sup> independent AMPK also is involved in mGluR receptor regulation by interfering with energy metabolism.

## Conclusions

In summary, the present study demonstrates that antagonism of mGluR5 in BV-2 cells results in increased oxidative stress including ROS production and mitochondrial dysfunction as well as enhancing inflammatory responses exhibited by an up-regulation of pro-inflammatory cytokines. mGluR5 may modulate the action via a  $\text{Ca}^{2+}$ -dependent pathway involving PTX-sensitive G protein. Accumulation of  $[\text{Ca}^{2+}]_i$  originating from ER is suggested to be via the  $\text{PI}_3$  receptor which is regulated by PLC and the PTX-sensitive G protein. Antagonism of mGluR5 decreased ATP production which was reversed by AMPK activation. Therefore, mGluR5 might also regulate energy balance through AMPK activation. Our study suggests that according mGluR5 antagonist through  $\text{Ca}^{2+}$ -dependent pathways and the AMPK pathway may act separately or in concert to regulate the redox status, inflammation, and energy balance of BV-2 cells.

## Abbreviations

$[\text{Ca}^{2+}]_i$ , free intracellular  $\text{Ca}^{2+}$ ; AMPK, AMP-dependent protein kinase; ATF6, activating transcription factor 6; CHOP, transcriptional factor C/EBP homologous protein; CHPG, (RS)-2-chloro-5-hydroxyphenylglycine; CNS, central nervous system; DEPC, diethylpyrocarbonate; DHE, dihydroethidium; DMEM, Dulbecco's modified Eagle's medium; ELISA, enzyme-linked immunosorbent assay; ER, endoplasmic reticulum; ERK1/2, extracellular signal-regulated protein kinase1/2; GAPDH, glyceraldehyde 3-phosphate dehydrogenase; GPCR, G protein-coupled receptor; GRP78, glucose-regulated protein 78; GRP94, glucose-regulated protein 94; HBSS, Hank's balanced salt solution; HEPES, 4-(2-hydroxyethyl)-1-piperazineethanesulfonic acid; HRP, Horseradish peroxidase; IL-6, interleukin-6; iNOS, inducible nitric oxide synthase; IP3, inositol trisphosphate;  $\text{IP}_3\text{R}$ , 1,4,5-trisphosphate receptor; IRE1, inositol-requiring enzyme-1; MAPKs, mitogen-activated protein kinases; mGluR5, metabotropic glutamate receptor 5; MPEP, 2-methyl-6-(phenylethynyl)-pyridine; NEAA, non-essential amino acids; NF- $\kappa$ B, Nuclear factor kappaB; NO, nitric oxide; NOX-2, NADPH

oxidase type 2; PBA, sodium phenylbutyrate; PDVF, polyvinylidene difluoride; PERK, PKR-like ER kinase; PKC, protein kinase C; PLC, phospholipase C; PTX, pertusis toxin; RIPA, radio immunoprecipitation assay; ROS, reactive oxygen species; RyR, ryanodine receptor; SDS-PAGE, sodium dodecyl sulfate-polyacrylamide gel electrophoresis; TBS, Tris-buffered saline; TBS-T, Tris-buffered saline with Tween; UPR, unfolded protein response

### **Acknowledgements**

This work was supported by the Swiss National Science Foundation.

### **Competing interests**

The authors declare that they have no competing interests.

### **Authors contribution**

BC and AO designed the study. BC performed the experiments and analyzed the data. DK and AL helped planning experiments and analyzing the data. BC, DK, AL and AO wrote the manuscript. All authors read and approved the final manuscript.

## References

1. Block ML, Zecca L, Hong JS: Microglia-mediated neurotoxicity: uncovering the molecular mechanisms. *Nature reviews Neuroscience* 2007, 8:57-69.
2. Ferraguti F, Shigemoto R: Metabotropic glutamate receptors. *Cell and tissue research* 2006, 326:483-504.
3. Byrnes KR, Loane DJ, Faden AI: Metabotropic glutamate receptors as targets for multipotential treatment of neurological disorders. *Neurotherapeutics : the journal of the American Society for Experimental NeuroTherapeutics* 2009, 6:94-107.
4. Pajooheh-Ganji A, Byrnes KR: Novel neuroinflammatory targets in the chronically injured spinal cord. *Neurotherapeutics : the journal of the American Society for Experimental NeuroTherapeutics* 2011, 8:195-205.
5. Conn PJ, Pin JP: Pharmacology and functions of metabotropic glutamate receptors. *Annual review of pharmacology and toxicology* 1997, 37:205-237.
6. Biber K, Laurie DJ, Berthele A, Sommer B, Tolle TR, Gebicke-Harter PJ, van Calker D, Boddeke HW: Expression and signaling of group I metabotropic glutamate receptors in astrocytes and microglia. *Journal of neurochemistry* 1999, 72:1671-1680.
7. Byrnes KR, Loane DJ, Stoica BA, Zhang J, Faden AI: Delayed mGluR5 activation limits neuroinflammation and neurodegeneration after traumatic brain injury. *Journal of neuroinflammation* 2012, 9:43.
8. Byrnes KR, Stoica B, Loane DJ, Riccio A, Davis MI, Faden AI: Metabotropic glutamate receptor 5 activation inhibits microglial associated inflammation and neurotoxicity. *Glia* 2009, 57:550-560.
9. Byrnes KR, Stoica B, Riccio A, Pajooheh-Ganji A, Loane DJ, Faden AI: Activation of metabotropic glutamate receptor 5 improves recovery after spinal cord injury in rodents. *Annals of neurology* 2009, 66:63-74.
10. Loane DJ, Stoica BA, Byrnes KR, Jeong W, Faden AI: Activation of mGluR5 and inhibition of NADPH oxidase improves functional recovery after traumatic brain injury. *Journal of neurotrauma* 2013, 30:403-412.

11. Loane DJ, Stoica BA, Pajoohesh-Ganji A, Byrnes KR, Faden AI: Activation of metabotropic glutamate receptor 5 modulates microglial reactivity and neurotoxicity by inhibiting NADPH oxidase. *The Journal of biological chemistry* 2009, 284:15629-15639.
12. Mead EL, Mosley A, Eaton S, Dobson L, Heales SJ, Pocock JM: Microglial neurotransmitter receptors trigger superoxide production in microglia; consequences for microglial-neuronal interactions. *Journal of neurochemistry* 2012, 121:287-301.
13. Piers TM, Heales SJ, Pocock JM: Positive allosteric modulation of metabotropic glutamate receptor 5 down-regulates fibrinogen-activated microglia providing neuronal protection. *Neuroscience letters* 2011, 505:140-145.
14. Movsesyan VA, Stoica BA, Faden AI: MGLuR5 activation reduces beta-amyloid-induced cell death in primary neuronal cultures and attenuates translocation of cytochrome c and apoptosis-inducing factor. *Journal of neurochemistry* 2004, 89:1528-1536.
15. Wang JW, Wang HD, Zhong WZ, Li N, Cong ZX: Expression and cell distribution of metabotropic glutamate receptor 5 in the rat cortex following traumatic brain injury. *Brain research* 2012, 1464:73-81.
16. Wang JW, Wang HD, Cong ZX, Zhang XS, Zhou XM, Zhang DD: Activation of metabotropic glutamate receptor 5 reduces the secondary brain injury after traumatic brain injury in rats. *Biochemical and biophysical research communications* 2013, 430:1016-1021.
17. Agostinho P, Cunha RA, Oliveira C: Neuroinflammation, oxidative stress and the pathogenesis of Alzheimer's disease. *Current pharmaceutical design* 2010, 16:2766-2778.
18. Kovacic P, Somanathan R: Redox processes in neurodegenerative disease involving reactive oxygen species. *Current neuropharmacology* 2012, 10:289-302.
19. Domercq M, Vazquez-Villoldo N, Matute C: Neurotransmitter signaling in the pathophysiology of microglia. *Frontiers in cellular neuroscience* 2013, 7:49.
20. Wong WT: Microglial aging in the healthy CNS: phenotypes, drivers, and rejuvenation. *Frontiers in cellular neuroscience* 2013, 7:22.
21. Kettenmann H, Hanisch UK, Noda M, Verkhratsky A: Physiology of microglia. *Physiological reviews* 2011, 91:461-553.

22. Beraud D, Hathaway HA, Trecki J, Chasovskikh S, Johnson DA, Johnson JA, Federoff HJ, Shimoji M, Mhyre TR, Maguire-Zeiss KA: Microglial activation and antioxidant responses induced by the Parkinson's disease protein alpha-synuclein. *Journal of neuroimmune pharmacology : the official journal of the Society on NeuroImmune Pharmacology* 2013, 8:94-117.
23. Hu S, Sheng WS, Schachtele SJ, Lokensgard JR: Reactive oxygen species drive herpes simplex virus (HSV)-1-induced proinflammatory cytokine production by murine microglia. *Journal of neuroinflammation* 2011, 8:123.
24. Kacimi R, Giffard RG, Yenari MA: Endotoxin-activated microglia injure brain derived endothelial cells via NF-kappaB, JAK-STAT and JNK stress kinase pathways. *Journal of inflammation* 2011, 8:7.
25. Ibrahim AS, El-Remessy AB, Matragoon S, Zhang W, Patel Y, Khan S, Al-Gayyar MM, El-Shishtawy MM, Liou GI: Retinal microglial activation and inflammation induced by amadori-glycated albumin in a rat model of diabetes. *Diabetes* 2011, 60:1122-1133.
26. Peterson LJ, Flood PM: Oxidative stress and microglial cells in Parkinson's disease. *Mediators of inflammation* 2012, 2012:401264.
27. Filosto M, Scarpelli M, Cotelli MS, Vielmi V, Todeschini A, Gregorelli V, Tonin P, Tomelleri G, Padovani A: The role of mitochondria in neurodegenerative diseases. *Journal of neurology* 2011, 258:1763-1774.
28. Federico A, Cardaioli E, Da Pozzo P, Formichi P, Gallus GN, Radi E: Mitochondria, oxidative stress and neurodegeneration. *Journal of the neurological sciences* 2012, 322:254-262.
29. Hardie DG: AMP-activated/SNF1 protein kinases: conserved guardians of cellular energy. *Nature reviews Molecular cell biology* 2007, 8:774-785.
30. Hardie DG: AMP-activated protein kinase: an energy sensor that regulates all aspects of cell function. *Genes & development* 2011, 25:1895-1908.
31. Hardie DG: Energy sensing by the AMP-activated protein kinase and its effects on muscle metabolism. *The Proceedings of the Nutrition Society* 2011, 70:92-99.

32. Zhang J, Xie Z, Dong Y, Wang S, Liu C, Zou MH: Identification of nitric oxide as an endogenous activator of the AMP-activated protein kinase in vascular endothelial cells. *The Journal of biological chemistry* 2008, 283:27452-27461.
33. Cardaci S, Filomeni G, Ciriolo MR: Redox implications of AMPK-mediated signal transduction beyond energetic clues. *Journal of cell science* 2012, 125:2115-2125.
34. Ronnett GV, Ramamurthy S, Kleman AM, Landree LE, Aja S: AMPK in the brain: its roles in energy balance and neuroprotection. *Journal of neurochemistry* 2009, 109 Suppl 1:17-23.
35. Garcia-Gil M, Pesi R, Perna S, Allegrini S, Giannecchini M, Camici M, Tozzi MG: 5'-aminoimidazole-4-carboxamide riboside induces apoptosis in human neuroblastoma cells. *Neuroscience* 2003, 117:811-820.
36. Kuznetsov JN, Leclerc GJ, Leclerc GM, Barredo JC: AMPK and Akt determine apoptotic cell death following perturbations of one-carbon metabolism by regulating ER stress in acute lymphoblastic leukemia. *Molecular cancer therapeutics* 2011, 10:437-447.
37. Yao J, Bi HE, Sheng Y, Cheng LB, Wendu RL, Wang CH, Cao GF, Jiang Q: Ultraviolet (UV) and Hydrogen Peroxide Activate Ceramide-ER Stress-AMPK Signaling Axis to Promote Retinal Pigment Epithelium (RPE) Cell Apoptosis. *International journal of molecular sciences* 2013, 14:10355-10368.
38. Green CJ, Macrae K, Fogarty S, Hardie DG, Sakamoto K, Hundal HS: Counter-modulation of fatty acid-induced pro-inflammatory nuclear factor kappaB signalling in rat skeletal muscle cells by AMP-activated protein kinase. *The Biochemical journal* 2011, 435:463-474.
39. Ikeda M, Tsuno S, Sugiyama T, Hashimoto A, Yamoto K, Takeuchi K, Kishi H, Mizuguchi H, Kohsaka SI, Yoshioka T: Ca spiking activity caused by the activation of store-operated Ca channels mediates TNF-alpha release from microglial cells under chronic purinergic stimulation. *Biochimica et biophysica acta* 2013.
40. Noda M, Ifuku M, Mori Y, Verkhratsky A: Calcium influx through reversed NCX controls migration of microglia. *Advances in experimental medicine and biology* 2013, 961:289-294.
41. Zou J, Vetreno RP, Crews FT: ATP-P2X7 receptor signaling controls basal and TNFalpha-stimulated glial cell proliferation. *Glia* 2012, 60:661-673.

42. Eichhoff G, Brawek B, Garaschuk O: Microglial calcium signal acts as a rapid sensor of single neuron damage in vivo. *Biochimica et biophysica acta* 2011, 1813:1014-1024.
43. Cuchillo-Ibanez I, Albillos A, Aldea M, Arroyo G, Fuentealba J, Garcia AG: Calcium entry, calcium redistribution, and exocytosis. *Annals of the New York Academy of Sciences* 2002, 971:108-116.
44. Brawek B, Garaschuk O: Microglial calcium signaling in the adult, aged and diseased brain. *Cell calcium* 2013, 53:159-169.
45. Foskett JK, White C, Cheung KH, Mak DO: Inositol trisphosphate receptor  $Ca^{2+}$  release channels. *Physiological reviews* 2007, 87:593-658.
46. Sammels E, Parys JB, Missiaen L, De Smedt H, Bultynck G: Intracellular  $Ca^{2+}$  storage in health and disease: a dynamic equilibrium. *Cell calcium* 2010, 47:297-314.
47. Hacki J, Egger L, Monney L, Conus S, Rosse T, Fellay I, Borner C: Apoptotic crosstalk between the endoplasmic reticulum and mitochondria controlled by Bcl-2. *Oncogene* 2000, 19:2286-2295.
48. Xu H, Xu W, Xi H, Ma W, He Z, Ma M: The ER luminal binding protein (BiP) alleviates Cd-induced programmed cell death through endoplasmic reticulum stress-cell death signaling pathway in tobacco cells. *Journal of plant physiology* 2013.
49. Sano R, Reed JC: ER stress-induced cell death mechanisms. *Biochimica et biophysica acta* 2013.
50. Hotamisligil GS: Endoplasmic reticulum stress and inflammation in obesity and type 2 diabetes. *Novartis Foundation symposium* 2007, 286:86-94; discussion 94-88, 162-163, 196-203.
51. Malhotra JD, Miao H, Zhang K, Wolfson A, Pennathur S, Pipe SW, Kaufman RJ: Antioxidants reduce endoplasmic reticulum stress and improve protein secretion. *Proceedings of the National Academy of Sciences of the United States of America* 2008, 105:18525-18530.
52. Park YJ, Ko JW, Jang Y, Kwon YH: Activation of AMP-Activated Protein Kinase Alleviates Homocysteine-Mediated Neurotoxicity in SH-SY5Y Cells. *Neurochemical research* 2013, 38:1561-1571.

53. Zhuo XZ, Wu Y, Ni YJ, Liu JH, Gong M, Wang XH, Wei F, Wang TZ, Yuan Z, Ma AQ, Song P: Isoproterenol instigates cardiomyocyte apoptosis and heart failure via AMPK inactivation-mediated endoplasmic reticulum stress. *Apoptosis : an international journal on programmed cell death* 2013, 18:800-810.
54. W. AJ, Kim WH, Yeo J, Jung MH: ER stress is implicated in mitochondrial dysfunction-induced apoptosis of pancreatic beta cells. *Molecules and cells* 2010, 30:545-549.
55. Maria DA, de Souza JG, Morais KL, Berra CM, Zampolli Hde C, Demasi M, Simons SM, de Freitas Saito R, Chammas R, Chudzinski-Tavassi AM: A novel proteasome inhibitor acting in mitochondrial dysfunction, ER stress and ROS production. *Investigational new drugs* 2013, 31:493-505.
56. Yang L, Sha H, Davisson RL, Qi L: Phenformin activates the unfolded protein response in an AMP-activated protein kinase (AMPK)-dependent manner. *The Journal of biological chemistry* 2013, 288:13631-13638.
57. Rhee SG: Regulation of phosphoinositide-specific phospholipase C. *Annual review of biochemistry* 2001, 70:281-312.
58. Ethier MF, Madison JM: Adenosine A1 receptors mediate mobilization of calcium in human bronchial smooth muscle cells. *American journal of respiratory cell and molecular biology* 2006, 35:496-502.
59. Mizuta K, Mizuta F, Xu D, Masaki E, Panettieri RA, Jr., Emala CW: Gi-coupled gamma-aminobutyric acid-B receptors cross-regulate phospholipase C and calcium in airway smooth muscle. *American journal of respiratory cell and molecular biology* 2011, 45:1232-1238.
60. Sundstrom L, Greasley PJ, Engberg S, Wallander M, Ryberg E: Succinate receptor GPR91, a Galpha coupled receptor that increases intracellular calcium concentrations through PLCbeta. *FEBS letters* 2013.
61. Rolin J, Al-Jaderi Z, Maghazachi AA: Oxidized lipids and lysophosphatidylcholine induce the chemotaxis and intracellular calcium influx in natural killer cells. *Immunobiology* 2013, 218:875-883.

62. Werry TD, Wilkinson GF, Willars GB: Mechanisms of cross-talk between G-protein-coupled receptors resulting in enhanced release of intracellular Ca<sup>2+</sup>. *The Biochemical journal* 2003, 374:281-296.
63. Roach TI, Rebres RA, Fraser ID, Decamp DL, Lin KM, Sternweis PC, Simon MI, Seaman WE: Signaling and cross-talk by C5a and UDP in macrophages selectively use PLCbeta3 to regulate intracellular free calcium. *The Journal of biological chemistry* 2008, 283:17351-17361.
64. Flaherty P, Radhakrishnan ML, Dinh T, Rebres RA, Roach TI, Jordan MI, Arkin AP: A dual receptor crosstalk model of G-protein-coupled signal transduction. *PLoS computational biology* 2008, 4:e1000185.
65. Blasi E, Barluzzi R, Bocchini V, Mazzolla R, Bistoni F: Immortalization of murine microglial cells by a v-raf/v-myc carrying retrovirus. *Journal of neuroimmunology* 1990, 27:229-237.
66. Livak KJ, Schmittgen TD: Analysis of relative gene expression data using real-time quantitative PCR and the 2(-Delta Delta C(T)) Method. *Methods* 2001, 25:402-408.
67. Woo MS, Park JS, Choi IY, Kim WK, Kim HS: Inhibition of MMP-3 or -9 suppresses lipopolysaccharide-induced expression of proinflammatory cytokines and iNOS in microglia. *Journal of neurochemistry* 2008, 106:770-780.
68. Muehlschlegel S, Sims JR: Dantrolene: mechanisms of neuroprotection and possible clinical applications in the neurointensive care unit. *Neurocritical care* 2009, 10:103-115.
69. Sarnico I, Boroni F, Benarese M, Sigala S, Lanzillotta A, Battistin L, Spano P, Pizzi M: Activation of NF-kappaB p65/c-Rel dimer is associated with neuroprotection elicited by mGlu5 receptor agonists against MPP(+) toxicity in SK-N-SH cells. *Journal of neural transmission* 2008, 115:669-676.
70. Drouin-Ouellet J, Brownell AL, Saint-Pierre M, Fasano C, Emond V, Trudeau LE, Levesque D, Cicchetti F: Neuroinflammation is associated with changes in glial mGluR5 expression and the development of neonatal excitotoxic lesions. *Glia* 2011, 59:188-199.
71. Berger JV, Dumont AO, Focant MC, Vergouts M, Sternotte A, Calas AG, Goursaud S, Hermans E: Opposite regulation of metabotropic glutamate receptor 3 and metabotropic glutamate

receptor 5 by inflammatory stimuli in cultured microglia and astrocytes. *Neuroscience* 2012, 205:29-38.

72. D'Antoni S, Berretta A, Seminara G, Longone P, Giuffrida-Stella AM, Battaglia G, Sortino MA, Nicoletti F, Catania MV: A prolonged pharmacological blockade of type-5 metabotropic glutamate receptors protects cultured spinal cord motor neurons against excitotoxic death. *Neurobiology of disease* 2011, 42:252-264.
73. Vernon AC, Zbarsky V, Datla KP, Croucher MJ, Dexter DT: Subtype selective antagonism of substantia nigra pars compacta Group I metabotropic glutamate receptors protects the nigrostriatal system against 6-hydroxydopamine toxicity in vivo. *Journal of neurochemistry* 2007, 103:1075-1091.
74. Ferger AI, Campanelli L, Reimer V, Muth KN, Merdian I, Ludolph AC, Witting A: Effects of mitochondrial dysfunction on the immunological properties of microglia. *Journal of neuroinflammation* 2010, 7:45.
75. Deng YY, Lu J, Ling EA, Kaur C: Role of microglia in the process of inflammation in the hypoxic developing brain. *Frontiers in bioscience* 2011, 3:884-900.
76. Moss DW, Bates TE: Activation of murine microglial cell lines by lipopolysaccharide and interferon-gamma causes NO-mediated decreases in mitochondrial and cellular function. *The European journal of neuroscience* 2001, 13:529-538.
77. Ryu JK, Nagai A, Kim J, Lee MC, McLarnon JG, Kim SU: Microglial activation and cell death induced by the mitochondrial toxin 3-nitropropionic acid: in vitro and in vivo studies. *Neurobiology of disease* 2003, 12:121-132.
78. Giri S, Nath N, Smith B, Viollet B, Singh AK, Singh I: 5-aminoimidazole-4-carboxamide-1-beta-4-ribofuranoside inhibits proinflammatory response in glial cells: a possible role of AMP-activated protein kinase. *The Journal of neuroscience : the official journal of the Society for Neuroscience* 2004, 24:479-487.
79. Lu DY, Tang CH, Chen YH, Wei IH: Berberine suppresses neuroinflammatory responses through AMP-activated protein kinase activation in BV-2 microglia. *Journal of cellular biochemistry* 2010, 110:697-705.

80. Nam HG, Kim W, Yoo DY, Choi JH, Won MH, Hwang IK, Jeong JH, Hwang HS, Moon SM: Chronological changes and effects of AMP-activated kinase in the hippocampal CA1 region after transient forebrain ischemia in gerbils. *Neurological research* 2013, 35:395-405.
81. Sauer H, Engel S, Milosevic N, Sharifpanah F, Wartenberg M: Activation of AMP-kinase by AICAR induces apoptosis of DU-145 prostate cancer cells through generation of reactive oxygen species and activation of c-Jun N-terminal kinase. *International journal of oncology* 2012, 40:501-508.
82. Labuzek K, Liber S, Gabryel B, Okopien B: AICAR (5-aminoimidazole-4-carboxamide-1-beta-4-ribofuranoside) increases the production of toxic molecules and affects the profile of cytokines release in LPS-stimulated rat primary microglial cultures. *Neurotoxicology* 2010, 31:134-146.
83. Kim WH, Lee JW, Suh YH, Lee HJ, Lee SH, Oh YK, Gao B, Jung MH: AICAR potentiates ROS production induced by chronic high glucose: roles of AMPK in pancreatic beta-cell apoptosis. *Cellular signalling* 2007, 19:791-805.
84. Peng TI, Yu PR, Chen JY, Wang HL, Wu HY, Wei YH, Jou MJ: Visualizing common deletion of mitochondrial DNA-augmented mitochondrial reactive oxygen species generation and apoptosis upon oxidative stress. *Biochimica et biophysica acta* 2006, 1762:241-255.
85. Zhang X, Feng J, Zhu P, Zhao Z: Ketamine Inhibits Calcium Elevation and Hydroxyl Radical and Nitric Oxide Production in Lipopolysaccharide-Stimulated NR8383 Alveolar Macrophages. *Inflammation* 2013.
86. Wang X, Chen S, Ma G, Ye M, Lu G: Involvement of proinflammatory factors, apoptosis, caspase-3 activation and Ca<sup>2+</sup> disturbance in microglia activation-mediated dopaminergic cell degeneration. *Mechanisms of ageing and development* 2005, 126:1241-1254.
87. Sheu JN, Liao WC, Wu UI, Shyu LY, Mai FD, Chen LY, Chen MJ, Youn SC, Chang HM: Resveratrol suppresses calcium-mediated microglial activation and rescues hippocampal neurons of adult rats following acute bacterial meningitis. *Comparative immunology, microbiology and infectious diseases* 2013, 36:137-148.
88. Hoffmann A, Kann O, Ohlemeyer C, Hanisch UK, Kettenmann H: Elevation of basal intracellular calcium as a central element in the activation of brain macrophages (microglia):

suppression of receptor-evoked calcium signaling and control of release function. *The Journal of neuroscience : the official journal of the Society for Neuroscience* 2003, 23:4410-4419.

89. Grijalba MT, Vercesi AE, Schreier S:  $\text{Ca}^{2+}$ -induced increased lipid packing and domain formation in submitochondrial particles. A possible early step in the mechanism of  $\text{Ca}^{2+}$ -stimulated generation of reactive oxygen species by the respiratory chain. *Biochemistry* 1999, 38:13279-13287.
90. Jou MJ, Peng TI, Wu HY, Wei YH: Enhanced generation of mitochondrial reactive oxygen species in cybrids containing 4977-bp mitochondrial DNA deletion. *Annals of the New York Academy of Sciences* 2005, 1042:221-228.
91. Jou MJ, Peng TI, Hsu LF, Jou SB, Reiter RJ, Yang CM, Chiao CC, Lin YF, Chen CC: Visualization of melatonin's multiple mitochondrial levels of protection against mitochondrial  $\text{Ca}^{2+}$ -mediated permeability transition and beyond in rat brain astrocytes. *Journal of pineal research* 2010, 48:20-38.
92. Yang CS, Tzou BC, Liu YP, Tsai MJ, Shyue SK, Tzeng SF: Inhibition of cadmium-induced oxidative injury in rat primary astrocytes by the addition of antioxidants and the reduction of intracellular calcium. *Journal of cellular biochemistry* 2008, 103:825-834.
93. Ilmarinen-Salo P, Moilanen E, Kinnula VL, Kankaanranta H: Nitric oxide-induced eosinophil apoptosis is dependent on mitochondrial permeability transition (mPT), JNK and oxidative stress: apoptosis is preceded but not mediated by early mPT-dependent JNK activation. *Respiratory research* 2012, 13:73.
94. Lee S, Kim YK, Shin TY, Kim SH: Neurotoxic effects of bisphenol AF on calcium-induced ROS and MAPKs. *Neurotoxicity research* 2013, 23:249-259.
95. Huang X, Zhai D, Huang Y: Study on the relationship between calcium-induced calcium release from mitochondria and PTP opening. *Molecular and cellular biochemistry* 2000, 213:29-35.
96. Ichas F, Jouaville LS, Mazat JP: Mitochondria are excitable organelles capable of generating and conveying electrical and calcium signals. *Cell* 1997, 89:1145-1153.

97. Brookes PS, Yoon Y, Robotham JL, Anders MW, Sheu SS: Calcium, ATP, and ROS: a mitochondrial love-hate triangle. *American journal of physiology Cell physiology* 2004, 287:C817-833.
98. Korotzer AR, Whittimore ER, Cotman CW: Differential regulation by beta-amyloid peptides of intracellular free Ca<sup>2+</sup> concentration in cultured rat microglia. *European journal of pharmacology* 1995, 288:125-130.
99. McLarnon JG, Choi HB, Lue LF, Walker DG, Kim SU: Perturbations in calcium-mediated signal transduction in microglia from Alzheimer's disease patients. *Journal of neuroscience research* 2005, 81:426-435.
100. Hajnoczky G, Csordas G, Madesh M, Pacher P: Control of apoptosis by IP(3) and ryanodine receptor driven calcium signals. *Cell calcium* 2000, 28:349-363.
101. Li X, Cudaback E, Keene CD, Breyer RM, Montine TJ: Suppressed microglial E prostanoid receptor 1 signaling selectively reduces tumor necrosis factor alpha and interleukin 6 secretion from toll-like receptor 3 activation. *Glia* 2011, 59:569-576.
102. Salvado L, Coll T, Gomez-Foix AM, Salmeron E, Barroso E, Palomer X, Vazquez-Carrera M: Oleate prevents saturated-fatty-acid-induced ER stress, inflammation and insulin resistance in skeletal muscle cells through an AMPK-dependent mechanism. *Diabetologia* 2013, 56:1372-1382.
103. Dagher Z, Ruderman N, Tornheim K, Ido Y: The effect of AMP-activated protein kinase and its activator AICAR on the metabolism of human umbilical vein endothelial cells. *Biochemical and biophysical research communications* 1999, 265:112-115.
104. Ido Y, Carling D, Ruderman N: Hyperglycemia-induced apoptosis in human umbilical vein endothelial cells: inhibition by the AMP-activated protein kinase activation. *Diabetes* 2002, 51:159-167.
105. Lee EK, Jeong JU, Chang JW, Yang WS, Kim SB, Park SK, Park JS, Lee SK: Activation of AMP-activated protein kinase inhibits albumin-induced endoplasmic reticulum stress and apoptosis through inhibition of reactive oxygen species. *Nephron Experimental nephrology* 2012, 121:e38-48.

106. Kim J, Park YJ, Jang Y, Kwon YH: AMPK activation inhibits apoptosis and tau hyperphosphorylation mediated by palmitate in SH-SY5Y cells. *Brain research* 2011, 1418:42-51.
107. Jia F, Wu C, Chen Z, Lu G: Atorvastatin inhibits homocysteine-induced endoplasmic reticulum stress through activation of AMP-activated protein kinase. *Cardiovascular therapeutics* 2012, 30:317-325.
108. Lu J, Wang Q, Huang L, Dong H, Lin L, Lin N, Zheng F, Tan J: Palmitate causes endoplasmic reticulum stress and apoptosis in human mesenchymal stem cells: prevention by AMPK activator. *Endocrinology* 2012, 153:5275-5284.
109. Jiang H, Kuang Y, Wu Y, Smrcka A, Simon MI, Wu D: Pertussis toxin-sensitive activation of phospholipase C by the C5a and fMet-Leu-Phe receptors. *The Journal of biological chemistry* 1996, 271:13430-13434.
110. Kashihara T, Nakada T, Shimojo H, Horiuchi-Hirose M, Gomi S, Shibazaki T, Sheng X, Hirose M, Hongo M, Yamada M: Chronic receptor-mediated activation of Gi/o proteins alters basal t-tubular and sarcolemmal L-type Ca(2)(+) channel activity through phosphatases in heart failure. *American journal of physiology Heart and circulatory physiology* 2012, 302:H1645-1654.
111. Block L, Forshammar J, Westerlund A, Bjorklund U, Lundborg C, Biber B, Hansson E: Naloxone in ultralow concentration restores endomorphin-1-evoked Ca(2)(+) signaling in lipopolysaccharide pretreated astrocytes. *Neuroscience* 2012, 205:1-9.

## Figures and Figure Legend

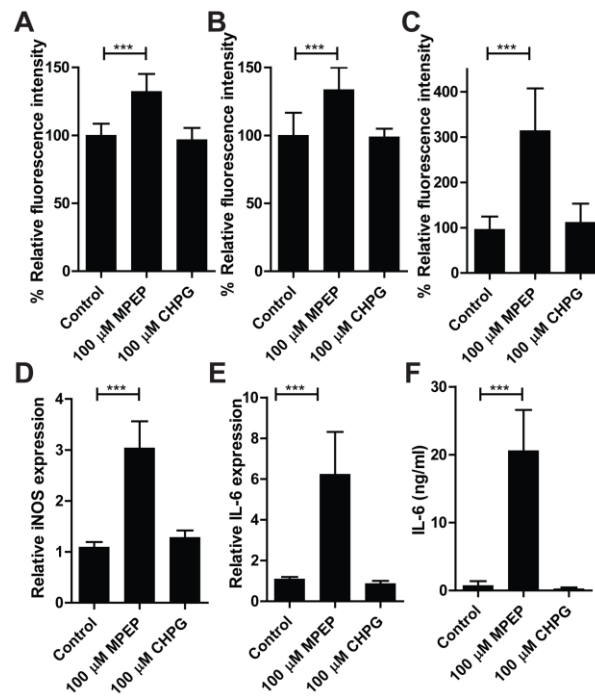


**Figure 1. Blockage of mGluR5 induced mitochondria dysfunction in BV-2 cells.** Cells were treated with either CHPG or MPEP for 24 h. *A*, Intracellular ROS levels were determined using DHE. *B*, Mitochondrial content was determined using MitoTracker<sup>®</sup> Red CMXRos. *C*, Mitochondrial ROS levels were determined using MitoSOX Red. *D*, iNOS mRNA expression and bar graphs representing iNOS/GAPDH ratios. *E*, IL-6 mRNA expression and bar graphs representing IL-6/GAPDH ratios. *F*, IL-6 protein. Results were expressed as the mean  $\pm$  SD of at least 3 experiments and significant was determined by one-way ANOVA followed by Turkey's tests, \* $p < 0.05$ , \*\* $p < 0.01$ ; \*\*\* $p < 0.005$

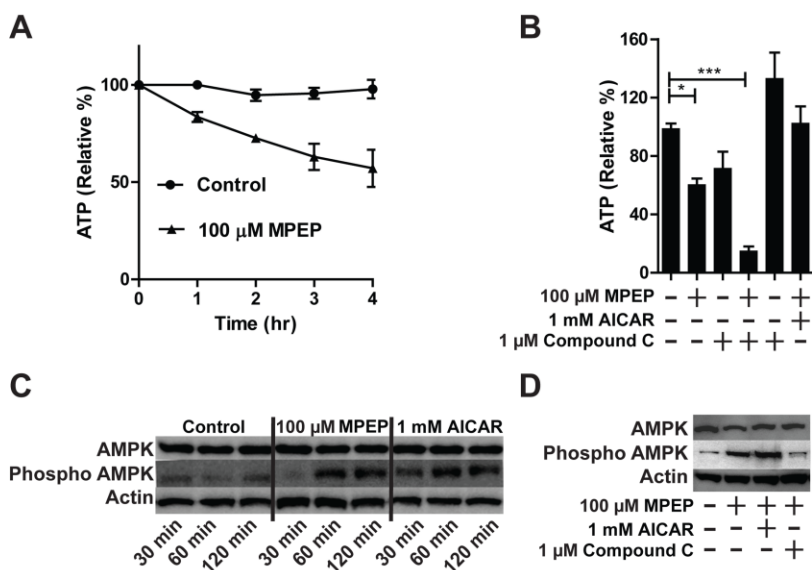


**Figure 2. Blockage of mGluR5 induced cellular energy depletion mediated by AMPK.** *A*, MPEP decreased ATP levels in a time dependent manner. Cells were treated with MPEP (100  $\mu$ M) for for 1, 2, 3, and 4 hr. *B*, AMPK inhibitor potentiated the action of MPEP on ATP production. Cells were treated for 2 hr. with 100  $\mu$ M MPEP alone or in combination, with or without 1  $\mu$ M compound C or 1 mM AICAR. The total cellular levels of ATP were analyzed as described in Materials and methods. Results were expressed as the mean  $\pm$  SD of at least 3 experiments and significant was determined by one-way ANOVA followed by Turkey's tests, \* $p < 0.05$ , \*\* $p < 0.01$ ; \*\*\* $p < 0.005$ . *C*, MPEP changed AMPK $\alpha$  phosphorylation in BV-2 cells. Immunoblot analyses were performed on lysates of BV-2 cells that had been treated with MPEP, and AICAR (positive control) for the indicated time period. (*D*) Immunoblot analyse as performed on lysates of BV-2 cells that had been pre-incubated with either AICAR (1 mM) or compound C (1  $\mu$ M) then cells were exposed with MPEP for 2 h.

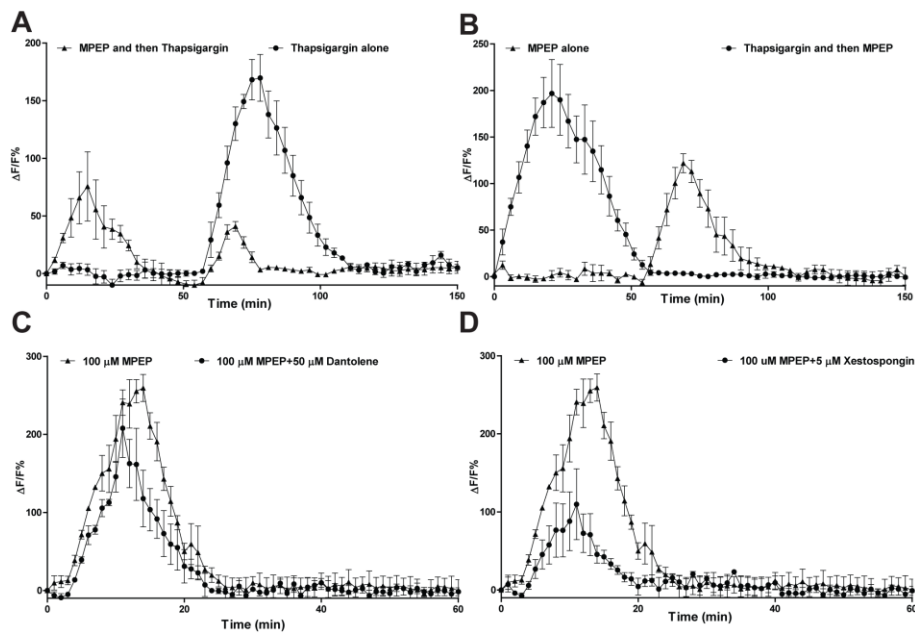


**Figure 3. MPEP induced  $\text{Ca}^{2+}$  release from ER.** Experiments were performed in  $\text{Ca}^{2+}$ -free medium. (A) Effect of thapsigargin ( $1\ \mu\text{M}$ ) on the kinetics of cytosolic  $\text{Ca}^{2+}$  increases induced by MPEP ( $100\ \mu\text{M}$ ) in Fura-4 loaded BV-2 cells. The  $\blacktriangle$  symbols indicate the trace of relative changes in of  $[\text{Ca}^{2+}]_i$  after exposure to MPEP ( $100\ \mu\text{M}$ ) for 60 min and followed by thapsigargin ( $1\ \mu\text{M}$ ) alone. The  $\bullet$  symbols indicate the trace of relative changes in of  $[\text{Ca}^{2+}]_i$  after exposure to thapsigargin ( $1\ \mu\text{M}$ ) at the time point of 60 min. (B) Effect of MPEP ( $100\ \mu\text{M}$ ) on the kinetics of cytosolic  $\text{Ca}^{2+}$  increases induced by thapsigargin ( $1\ \mu\text{M}$ ) in Fura-4 loaded BV-2 cells. The  $\blacktriangle$  symbols indicate the trace of relative changes in of  $[\text{Ca}^{2+}]_i$  after exposure to thapsigargin ( $1\ \mu\text{M}$ ) for 60 min and followed by MPEP ( $100\ \mu\text{M}$ ). The  $\bullet$  symbols indicate the trace of relative changes in of  $[\text{Ca}^{2+}]_i$  after exposure to MPEP ( $100\ \mu\text{M}$ ) alone at the time point of 60 min. (C) Effect of dantolene ( $50\ \mu\text{M}$ ) on the kinetics of cytosolic  $\text{Ca}^{2+}$  increases induced by MPEP ( $100\ \mu\text{M}$ ) in Fura-4 loaded BV-2 cells. Cells were pre-treated with  $50\ \mu\text{M}$  dantolene for 1 h. before loading with Fuo-4 and then cells were added with  $100\ \mu\text{M}$  MPEP. (D) Effect of xestospongine C ( $5\ \mu\text{M}$ ) on the kinetics of cytosolic  $\text{Ca}^{2+}$  increases induced by MPEP ( $100\ \mu\text{M}$ ) in Fura-4 loaded BV-2 cells. Cells were pre-treated with  $5\ \mu\text{M}$  xestospongine C for 1 h. before loading with Fuo-4 and then cells were added with  $100\ \mu\text{M}$  MPEP. Relative changes in calcium concentration using fluo-4 were analyzed, and were expressed as  $\Delta\text{F}/\text{F}$  (in %), with F being the baseline fluorescence and  $\Delta\text{F}$  the variation of fluorescence. Data are expressed as mean  $\pm$  SD.

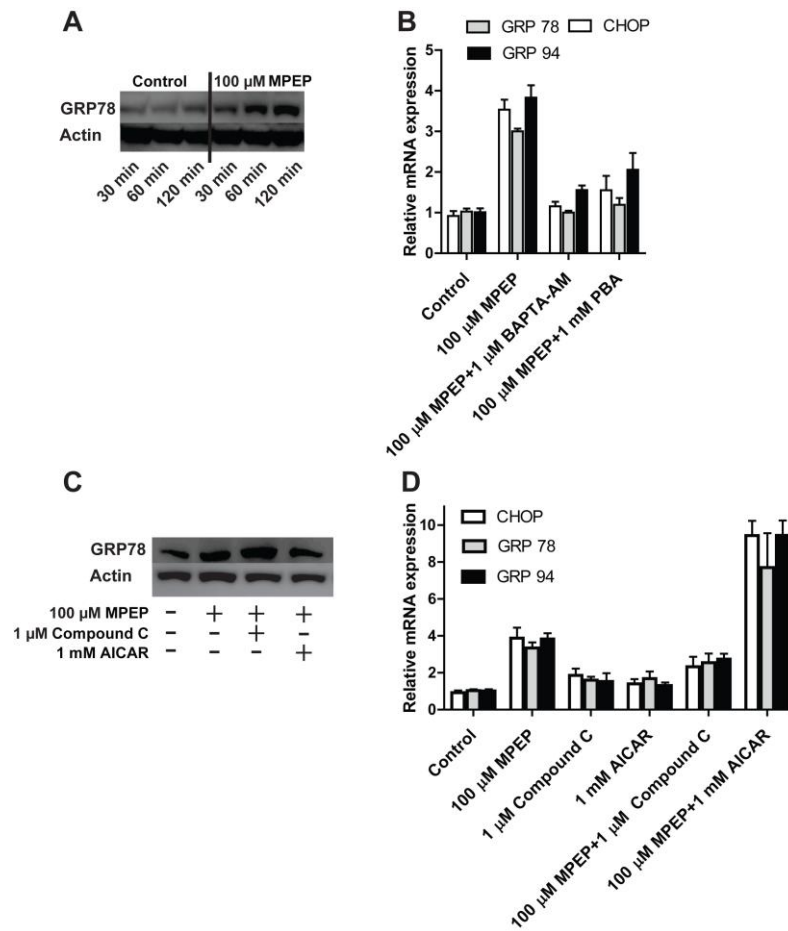


**Figure 4. Blockage of mGluR5 results in increasing of ER stress.** *A*, MPEP increased GRP78 protein levels. Immunoblot analyze as performed on lysates of BV-2 cells that had been treated with MPEP for the indicated time period. *B*, BAPTA-AM and PBA blocked MPEP-induced ER stress marker mRNA expression. Cells were pre-exposed with BAPTA-AMP (1 μM) or PBA (1 mM) for 1 h. Expression of CHOP, GRP78, and GRP94 was measured by RT-PCR after exposure to 100 μM MPEP for 24 hr. *C*, AMPK is involved in MPEP increased GRP78 protein levels. Cells were pre-exposed with AICAR (1 mM) or compound C (1 μM) for 1 h. GRP78 protein levels was analysed by immunoblot after exposure to 100 μM MPEP for 2 hr. *D*, Cells were pre-exposed with AICAR (1 mM) or compound C (1 μM) for 1 h. Expression of CHOP, GRP78, and GRP94 was measured by RT-PCR after exposure to 50 nM DBT for 24 hr. mRNA expression levels were normalized to GAPDH and plotted relative to the control value. Results were expressed as the mean ± SD of at least 3 experiments and significant was determined by one-way ANOVA followed by Turkey's tests, \* $p < 0.05$ , \*\* $p < 0.01$ ; \*\*\* $p < 0.005$

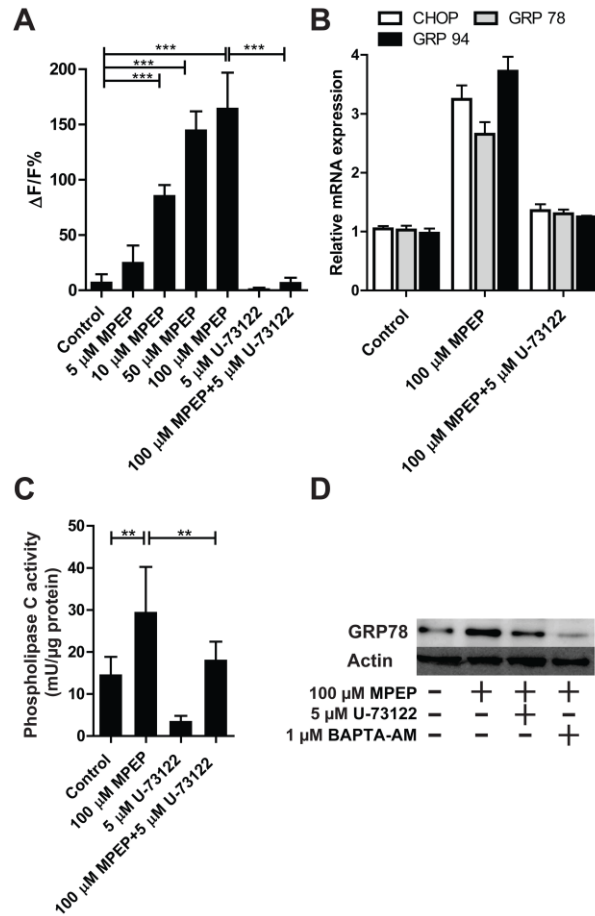


**Figure 5. Blockage of mGluR5 activated phospholipase C pathway.** *A*, MPEP induced intracellular calcium level mediated by Phospholipase C. Intracellular calcium was determined by detecting the fluorescence intensity with fluorochrome Fluo-4. BV-2 cells were pre-treated with 5 μM U731221 for 1 h. before loading with Fluo-4 and 100 μM MPEP was added to the cells in the absence of extracellular calcium. Relative changes in calcium concentration using fluo-4 were analyzed at the maximum level (15 min.), were expressed as  $\Delta F/F$  (in %), with  $F$  being the baseline fluorescence and  $\Delta F$  the variation of fluorescence. Data are expressed as mean  $\pm$  SD. *B*, Phospholipase C inhibitor (U731221) abolished MPEP and DBT-induced ER stress markers expression. *C*, mGluR5 increased phospholipase C. BV-2 cells were pre-treated with CHPG or MPEP for 2hr. Phospholipase activity presents as mU per μg protein. *D*, Calcium chelator and Phospholipase C inhibitor diminished MPEP-increased GRP78 protein expression.

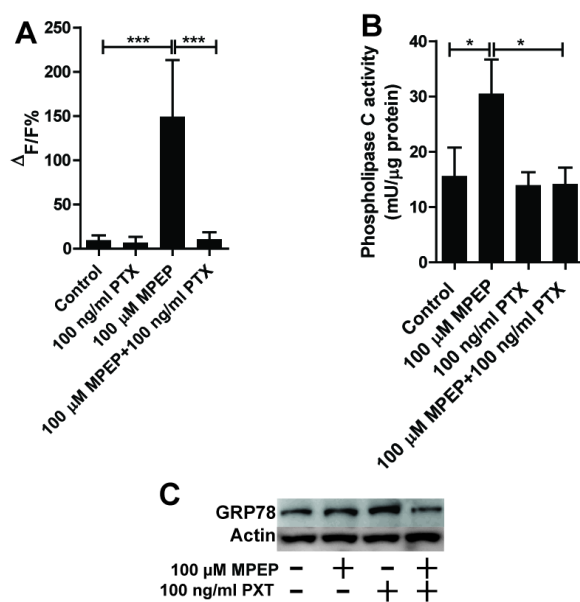


**Figure 6.** PTX-sensitive G proteins/PLC/ $\text{Ca}^{2+}$  pathways mediated by mGluR5. *A*, Pertussis toxin inhibited action of MPEP on calcium level. Intracellular calcium was determined by detecting the fluorescence intensity with fluorochrome Fluo-4. BV-2 cells were pre-treated with 100 ng/ml PTX for 6 hr before loading with Fluo-4 and then 100  $\mu$ M MPEP was added to the cells in the absence of extracellular calcium. Relative changes in calcium concentration using fluo-4 were analyzed at the maximum level (15 min.), were expressed as  $\Delta F/F$  (in %), with F being the baseline fluorescence and  $\Delta F$  the variation of fluorescence. *B*, Pertussis toxin inhibited action of MPEP on phospholipase C activity. BV-2 cells were pre-treated with 100ng/ml PTX for 6 h exposed to 100  $\mu$ M MPEP for 2 hr. Phospholipase activity C presents as mU per  $\mu$ g protein. Results were expressed as the mean  $\pm$  SD of at least 3 experiments and significant was determined by one-way ANOVA followed by Turkey's tests, \* $p < 0.05$ , \*\* $p < 0.01$ ; \*\*\* $p < 0.005$ . *C*, Pertussis toxin inhibited action of MPEP on GRP78 protein expression. Western blot analysis using antibodies against GRP78 protein expression in cells treated with indicated chemicals. Representative blots from 3 independent experiments.

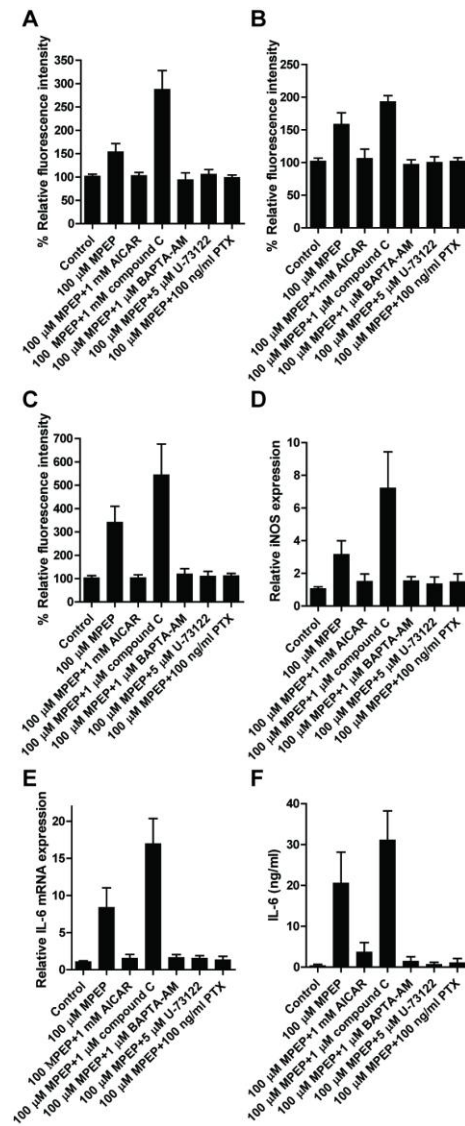


**Figure 7. Blockage of mGluR5 induced mitochondria dysfunction in BV-2 cells mediated by PTX-sensitive G proteins/PLC/AMPK/  $Ca^{2+}$  pathways.** Cells were pretreated with compound C (1  $\mu$ M) or BAPTA-AM (1  $\mu$ M) or U-73122 (1  $\mu$ M) for 1 hr or PTX (100 ng/ml) for 6 hr then exposed to MPEP (100  $\mu$ M) for 24 hr. *A*, Intracellular ROS levels were determined using DHE. *B*, Mitochondrial content was determined using MitoTracker<sup>®</sup>Red CMXRos. *C*, Mitochondrial ROS levels were determined using MitoSOX Red. *D*, iNOS mRNA expression and bar graphs representing iNOS/GAPDH ratios. *E*, IL-6 mRNA expression and bar graphs representing IL-6/GAPDH ratios. *F*, IL-6 protein. Results were expressed as the mean  $\pm$  SD of at least 3 experiments and significant was determined by one-way ANOVA followed by Turkey's tests, \* $p$  < 0.05, \*\* $p$  < 0.01; \*\*\* $p$  < 0.005

**Table 1S**

Real-time PCR primers

<b>Genes</b>	<b>Primers</b>	<b>Sequences</b>
GAPDH (mouse)	forward	CTCGTGGAGTCTACTGGTGT
	reverse	GTCATCATACTTGGCAGGTT
IL-6 (mouse)	forward	GGAGGCTTAATTACACATGTT
	reverse	TGATTTCAAGATGAATTGGAT
TNF- $\alpha$ (mouse)	forward	TTCTGTCTACTGAACTTCGG
	reverse	GTATGAGATAGCAAATCGGC
iNOS (mouse)	forward	ATGAGGTACTIONCAGCGTGCTCCAC
	reverse	CCACAATAGTACAATACTACTTGG

## CHAPTER 6

**Corticosterone potentiates trimethyltin induced inflammatory responses mediated by mineralocorticoid receptor in BV-2 cells**

## **Corticosterone potentiates trimethyltin induced inflammatory responses mediated by mineralocorticoid receptor in BV-2 cells**

Boonrat Chantong, Denise V. Kratschmar, Adam Lister and Alex Odermatt

Division of Molecular and Systems Toxicology, Department of Pharmaceutical Sciences,  
University of Basel, Klingelbergstrasse 50, 4056 Basel, Switzerland

E-mail addresses: [boonrat.chantong@unibas.ch](mailto:boonrat.chantong@unibas.ch); [denise.kratschmar@unibas.ch](mailto:denise.kratschmar@unibas.ch);  
[adam.lister@unibas.ch](mailto:adam.lister@unibas.ch); [alex.odermatt@unibas.ch](mailto:alex.odermatt@unibas.ch).

### **Correspondence to:**

Dr. Alex Odermatt, Division of Molecular and Systems Toxicology, Department of  
Pharmaceutical Sciences, University of Basel, Klingelbergstrasse 50, CH-4056 Basel,  
Switzerland

Phone: +41 61 267 1530, Fax: +41 61 267 1515, E-mail: [alex.odermatt@unibas.ch](mailto:alex.odermatt@unibas.ch)

## Abstract

Several reports suggest that the mechanism of trimethyltin (TMT) induced neurotoxicity involves the activation of microglia and endogenous glucocorticoid levels may play a role. The molecular mechanisms of TMT induced inflammation in microglia have not been investigated. Therefore the objectives of this research were to; (1) assess whether TMT induces proinflammatory mediator expression and if glucocorticoids can influence these changes. (2) investigate the possible mechanisms for such an induction. TMT induced the expression of interleukin-6 (IL-6) and inducible nitric oxide synthase (iNOS) in concentration dependent manner in BV-2 microglia cells. Pretreatment with a nuclear factor kappa B (NF- $\kappa$ B) inhibitor blocked the action of TMT. TMT induced translocation of NF- $\kappa$ B into nucleus. PD98059 and SB20190, inhibitors of ERK1/2 and p38 MAPK, respectively, inhibited the ability of TMT to induce IL-6 and iNOS expression. Interestingly, the proinflammatory action of TMT was substantially enhanced by corticosterone and 11-dehydrocorticosterone but suppressed by dexamethasone. Spironolactone, a MR antagonist not only blocked the action of TMT alone but also the potentiation effect of corticosterone on proinflammatory mediator expression. Similarly, the potentiation effect of corticosterone was inhibited by PD98059 and SB20190. An inhibitor of 11 $\beta$ -hydroxysteroid dehydrogenase type 1 (11 $\beta$ -HSD1), BNW-16, also blocked TMT-induced inflammation. 11 $\beta$ -HSD1 mRNA expression and activity were induced by TMT. Pharmacological manipulations indicated that NF- $\kappa$ B, ERK1/2, and p38 activation mediated by MR and GR are involved in the observed 11 $\beta$ -HSD1 mRNA induction. These results suggest that TMT and corticosterone may act through the same signaling pathways to activate inflammation. Within the context of inflammation, increased expression of proinflammatory mediators by TMT and endogenous glucocorticoids could be critical part of mechanism by which TMT exerts its neurotoxicity.

**Keywords:** Trimethyltin, neuroinflammation, 11 $\beta$ -hydroxysteroid dehydrogenase type 1 (11 $\beta$ -HSD1), and corticosterone

## INTRODUCTION

Trimethyltin chloride (TMT) is a classic neurotoxicant. TMT can accumulate in the body and pose a risk for workers chronically exposed to low doses. Animals exposed to TMT develop neurobehavioral changes (Tang et al., 2013). TMT-induced neurotoxicity by interfering with synaptic and neurodegeneration related networks, protein processing and degradation pathways (Little et al., 2012). One of the proposed mechanisms for TMT inducing neurotoxicity is the induction of the inflammatory response. Memory dysfunction induced by TMT in rat was observed, accompanied by an upregulation of reactive microglia marker and proinflammatory cytokine mRNA (Koda et al., 2009). TMT treatment induced the inflammatory response in adipocytes (Ravanan et al., 2011). In addition, TMT induced apoptosis in human neuroblastoma cells through activation of nuclear factor kappa B (NF- $\kappa$ B), c-Jun N-terminal kinase (JNK), extracellular signal-regulated kinases (ERKs), p38 mitogen-activated protein kinase (p38 MAPK) (Qing et al., 2013).

Increasing evidence indicates that the resident brain microglial immune cells contribute to neuroinflammation and result in the progression of neurodegenerative diseases through the release of pro-inflammatory mediators (Glass et al., 2010; Evans et al., 2013; Niranjana, 2013; Orre et al., 2013). Pro-inflammatory cytokines released from microglia such as interleukins-6 (IL-6), interleukins-1 $\beta$  (IL-1 $\beta$ ), and tumor necrosis factor (TNF- $\alpha$ ) play critical roles in microglia-mediated neurodegeneration (Smith et al., 2012; Ghosh et al., 2013; Qin et al., 2013). Nitric oxide (NO), produced by inducible nitric oxide synthase (iNOS) in microglia, is a well characterized pro-inflammatory factor that induce neuronal death (Brown and Neher, 2010; Li et al., 2012; Khasnavis et al., 2013). In addition, glucocorticoid-induced TNFR family related gene (GITR) is also suggested to play a role in the inflammatory response in microglia cells which contribute to inflammatory diseases (Cuzzocrea et al., 2007; Santucci et al., 2007; Motta et al., 2009; You et al., 2009).

The activation of NF- $\kappa$ B mediates the expression of pro-inflammatory factors including interleukins, TNF- $\alpha$  and iNOS (Cheng et al., 2009;Lukiw, 2012;Wongchana and Palaga, 2012). In quiescent cells, NF- $\kappa$ B which exists primarily as a p50/p65 heterodimer remains inactive in the cytoplasm due to the formation of complexes with the inhibitory protein nuclear factor of kappa light polypeptide gene enhancer in B-cells inhibitor, alpha (I $\kappa$ B $\alpha$ ). Upon stimulation, I $\kappa$ B $\alpha$  is degraded, which then allows NF- $\kappa$ B to translocate to the nucleus, bind to cognate DNA binding sites, and initiate the transcription of target proinflammatory genes (Barnes and Karin, 1997;Lukiw, 2012). MAPKs are serine and threonine protein kinases that function in multiple pathways and cell types. The MAPK family includes extracellular ERK1/2, JNK, and p38 (Waskiewicz and Cooper, 1995;Kolch, 2005), which have been implicated in the release of immune-related cytotoxic factors such as iNOS, COX-2, and proinflammatory cytokines (Choi et al., 2009;Lin et al., 2010;Wang et al., 2011b).

Interestingly, several studies show that stress and glucocorticoids can enhance neuroinflammation. For example, stress-induced priming of subsequent CNS pro-inflammatory cytokine production has been documented to worsen mortality in a rat stroke model (Caso et al., 2006). Stress enhances spinal neuroinflammatory responses leading to cell death (Grau et al., 2004). While glucocorticoids have long been used for anti-inflammatory therapy, there is increasing evidence that glucocorticoids, major hormones released during periods of stress, potentiate proinflammatory cytokine production following a subsequent immune challenge (Yeager et al., 2009;Frank et al., 2010). For example, prior exposure to corticosterone potentiates lipopolysaccharide (LPS) induced spinal neuroinflammation by elevating of IL-1 $\beta$  and IL-6 levels (Loram et al., 2011). In addition, elevation of corticosterone levels was found to be proinflammatory to exacerbate LPS regulation of NF- $\kappa$ B, MAPKs, and proinflammatory gene expression in the frontal cortex (Munhoz et al., 2010). In tissue, the action of glucocorticoids is regulated by activity of 11 $\beta$ -hydroxysteroid dehydrogenase type 1 (11 $\beta$ -HSD1) (Tomlinson et al., 2004;Cooper and Stewart, 2009). This enzyme converts inactive glucocorticoids such as cortisone and

dehydrocorticosterone to their active forms, cortisol and corticosterone, respectively.  $11\beta$ -HSD1 is highly expressed in many areas of the brain, including the hippocampus, cerebellum, and neocortex (Moisan et al., 1990). The expression of  $11\beta$ -HSD1 in microglia cells was observed and was proposed to modulate neuroinflammation and brain functions (Gottfried-Blackmore et al., 2010). Moreover,  $11\beta$ -HSD1 expression is modulated by NF- $\kappa$ B and MAPKs which involves in cytokine expression (Ishii-Yonemoto et al., 2010; Ahasan et al., 2012).

Corticosteroids such as corticosterone and cortisol mediate their effects by binding to either mineralocorticoid receptors (MR) or glucocorticoid receptors (GR) with different affinities. MR expressed on microglia may play a role in the modulation of microglia activity (Frieler et al., 2011). Evidence suggests that spironolactone, an MR antagonist, inhibits the production of several pro-inflammatory cytokines, including TNF- $\alpha$  and IL-1 $\beta$  and shows positive effects in patients with immunoinflammatory diseases (Hansen et al., 2004; Miura et al., 2006; Syngle et al., 2013). It has been reported that spironolactone could block MR regulated microglial activation mediated by corticosterone and aldosterone on microglial activation (Tanaka et al., 1997). However, corticosterone inhibits the proliferation of microglia cells through GR, not MR (Nakatani et al., 2012). In mice, microglial GR protected dopaminergic neurons after acute 1-methyl-4-phenyl-1,2,3,6-tetrahydropyridine (MPTP) intoxication. Microglial GR gene inactivation exacerbated both microglial and astroglial reactivity after acute MPTP treatment (Ros-Bernal et al., 2011). Both MR and GR differentially regulate the function of MAPKs and NF- $\kappa$ B (Kiyomoto et al., 2008; Nguyen Dinh Cat et al., 2011; Chantong et al., 2012; Queisser et al., 2013). To date, however, there are no findings on the roles of MR and GR in TMT-induced inflammation in the murine microglia cells.

Reports reveal the involvement of endogenous corticosterone in the pathological phenomena related to TMT toxicity. Specifically, plasma corticosterone concentrations transiently increased in the TMT-treated rats (Shirakawa et al., 2007) together with neuropathological changes, behavioral changes

(Tsutsumi et al., 2002), and elevated hippocampal necrosis (Imai et al., 1998). In mice, time- and concentration-dependent changes in plasma corticosterone were also observed following TMT injection (Ogita et al., 2012). Both endogenous and exogenous glucocorticoids prevented neuronal degeneration induced by TMT in the mouse brain (Shuto et al., 2009a). In addition, it has been proposed that the extent of TMT cytotoxicity is dependent on the balance between GR and MR activity. Spironolactone protects neurons in the dentate granule cell layer from TMT cytotoxicity. The GR antagonist mifepristone potentiated the TMT cytotoxicity in neurons (Ogita et al., 2012). However, it is still unclear whether corticosterone acts as a protective or as a deleterious factor in TMT-induced inflammation.

We are interested in the proinflammatory mechanisms mediated by TMT, particularly the NF- $\kappa$ B and MAPKs pathways and the expression of iNOS and/or IL-6 in microglial cells. The role and the regulation of glucocorticoids on the action of TMT were also investigated. Microglial BV-2 cells were used in the present study. This cell line exhibits many of the morphological, phenotypic, and functional properties of freshly isolated microglial cells (Blasi et al., 1990; Juknat et al., 2012) and has long been used as a research model of microglial cells (Lee et al., 2010; Juknat et al., 2012). These studies provided mechanistic evidence of TMT activity at low concentration in inflammatory-responsive glial cells. MR mediates the inflammatory response induced by TMT through NF- $\kappa$ B, ERK1/2, p38. The potentiation of TMT-stimulated inflammation by corticosterone depends on the local glucocorticoid balance which is regulated by 11 $\beta$ -HSD1. TMT was shown to directly induce 11 $\beta$ -HSD1 mRNA expression and activity.

## MATERIAL AND METHODS

### *Chemicals*

Dulbecco's modified Eagle's medium (DMEM), RPMI 1640 medium, penicillin, streptomycin, 0.05% (w/v) trypsin/EDTA, non-essential amino acids (NEAA), 4-(2-hydroxyethyl)-1-piperazineethanesulfonic acid (HEPES), Hank's balanced salt solution (HBSS), Hoechst 33342, were obtained from Invitrogen (Carlsbad, CA, USA). Fetal bovine serum was from Atlanta Biologicals (Lawrenceville, GA, US). ELISA kit for IL-6 was purchased from BD Biosciences, (BD Biosciences, CA, US). Cellomics HCS reagent kits evaluation size NF  $\kappa$ B activation (K010011) was obtained by Cellomics, Inc (Cellomics, Inc, Pittsburgh, PA, USA). Cay-10512 was from Cayman Chemicals (Hamburg, Germany). [1,2-<sup>3</sup>H]-cortisone from American Radiolabeled Chemicals (St. Louis, MO, USA). Extracellular signal-regulated kinase (ERK)1/2, p38 and JNK inhibitors (PD98059, SB202190 and SP600125, respectively), trimethyltin chloride (TMT), sodium dodecyl sulphate, polyacrylamide/bis-acrylamide, Tween-20,  $\beta$ -mercaptoethanol, and dimethylsulfoxide were purchased from Sigma-Aldrich (St. Louis, MO, USA). Specific antibodies against AMPK, ERK1/2, p38 MAPK, JNK, NF- $\kappa$ B (p65) and their phosphorylated forms were obtained from Cell Signaling Technology (Danvers, MA, USA). Specific antibodies for  $\beta$ -actin and goat anti-rabbit IgG- horseradish peroxidase were obtained from Santa Cruz Biotechnology (Santa, CA, USA).

### *Cell culture*

The mouse BV-2 microglial cell line (obtained from Professor Wolfgang Sattler, University of Graz, Graz, Austria) was immortalized by infecting primary microglial cell cultures with a v- raf/v-myc oncogene (Blasi et al., 1990). BV-2 cells were maintained at 37 °C under a 5 % CO<sub>2</sub> humidified atmosphere in RPMI 1640 supplemented with 10 % fetal bovine serum (FBS), 2 mM glutamine, 100  $\mu$ g/ml streptomycin, 100 U/ml penicillin, HEPES, and 0.1 mM NEAA. The cells were cultured at a

density of  $5 \times 10^5$  cells/25 cm<sup>2</sup> flask, and were passaged every 2–3 days using 0.25 % trypsin. This study used only cells between passages 5–15. Prior to initiating the experiments, cells were cultured in fresh Dulbecco's modified Eagle medium (DMEM) supplemented with 10% fetal bovine serum 1000 mg/L glucose, 2 mM glutamine, 100 µg/mL streptomycin, and 100 U/mL penicillin, HEPES, and 0.1 mM NEAA. The following cell seeding numbers were used:  $1 \times 10^3$  cells/well in a 96-well plate for determination of IL-6 protein level and NF-κB localization;  $5 \times 10^5$  cells/well in a 12-well plate for gene expression analysis by RT-PCR;  $1.0 \times 10^6$  cells/well in a 6-well plate for Western blot analysis.

### ***Total mRNA isolation and quantitative real-time PCR***

The mRNA expression of IL-6, iNOS, and GITR mRNA as well as GAPDH was determined by quantitative real-time PCR (RT-PCR). Briefly, total RNA from BV-2 cells was extracted with Tri-reagent from Sigma Aldrich (St. Louis, MO, USA) according to the manufacturer's protocol. The resulting RNA was dissolved in nuclease-free water (Invitrogen, Carlsbad, CA). The total RNA concentrations were measured using the NanoDrop ND-1000 (ThermoScientific, Wilmington, DE). 0.5 µg of total RNA was reverse transcribed to first strand complementary DNA (cDNA). The cDNA was synthesized using the Superscript III reverse transcriptase (Invitrogen, Carlsbad, CA). cDNA was amplified by rotor-gene-3000A (Corbett Research, Australia) using the KAPA SYBR<sup>®</sup> FAST qPCR Kit (Kapasystems, Boston, MA). Each 10 µl reaction mixture consisted of 5 µl SYBR mater mix, 0.4 µl of each primer (5 µM), 2 µl of cDNA, and 2.2 µl RNase-free dH<sub>2</sub>O. Expression was normalized to glyceraldehyde 3-phosphate dehydrogenase (GAPDH). Fold changes are reported relative to vehicle control. Fold changes were quantified as  $2^{-(\Delta C_t \text{ sample} - \Delta C_t \text{ control})}$ , as described previously (Livak and Schmittgen, 2001). The primers for real-time PCR were listed in **Table 1S**.

### *Assay for IL-6*

The presence of immunoreactive IL-6 in cell culture supernatants was determined using mouse-specific ELISA for interleukin-6 (IL-6) from BD Biosciences (CA, USA) following the protocols provided by the manufacturer. The results were expressed in ng/ml.

### *Determination of NF- $\kappa$ B localization by ArrayScan HCS Reader*

After treatment, the medium was discarded and cells were fixed and stained using Cellomics<sup>®</sup> NF- $\kappa$ B activation kit from Thermo Scientific according to the manufacturer's instructions. Briefly, cells were fixed with 4% formaldehyde (pH 7.2) at room temperature for 30 min, washed with PBS and then permeabilized with PBS containing 0.5% Triton X-100 for 10 min. After three washes with PBS and blocking with 1% fatty acid-free bovine serum albumin for 1 h the cells were incubated with rabbit polyclonal antibody against the p65 subunit of NF- $\kappa$ B (1:500) for 1 h at 37°C. Cells were then incubated with detergent buffer for 15 min and washed twice with PBS. Cells were then incubated with staining solution consisting of goat anti-rabbit IgG conjugated to Alexa Fluor 488 and Hoechst-33342 for 1 h prior to a 10 min wash with detergent buffer and two washes with PBS. Cells were then soaked in PBS at 4°C and covered with aluminum foil until analysis by imaging. The assay plate was evaluated on ArrayScan HCS Reader. The Cytoplasm to Nucleus Translocation BioApplication software was used to calculate the ratio of cytoplasmic and nuclear NF- $\kappa$ B intensity (Ding et al., 1998). The average intensity of 500 objects (cells) per well was quantified. The ratios were then compared among treated and untreated cells.

### *Preparation of whole cell lysates and cytoplasmic and nuclear fractions*

For whole cell lysate, the cells were harvested after the appropriate treatment and washed with ice-cold PBS for two times. Total cellular proteins were extracted by adding radio immunoprecipitation assay lysis buffer (RIPA buffer) (Sigma-Aldrich, St. Louis, MO) after addition of the protease inhibitor

cocktail (Roche Diagnostics, Mannheim, Germany). The lysate was centrifuged at  $10,000 \times g$  for 15 min at  $4^{\circ}\text{C}$ .

To separate the cytosolic proteins from the nuclear proteins, cells were collected by scraping in cold PBS. The cell pellet was then collected by centrifugation at  $450 \times g$  for 5 min, washed once with PBS and pelleted again at  $1,000 \times g$  for 5 min. The cell pellet was then lysed in hypotonic lysis buffer (100 mM KCl, 15 mM  $\text{MgCl}_2$ , 100 mM HEPES, pH 7.9) supplemented with 0.01 M DTT and protease inhibitors and kept on ice for 15 min. IGEPAL CA-630 solution (Sigma-Aldrich) (0.6% v/v final concentration) was then added to the cell suspension, followed by mixing for 10 s and centrifugation at  $10,000 \times g$  for 30 s. The supernatant was collected and designated the cytosolic fraction. Nuclear proteins were then extracted using a buffer containing 0.42 M NaCl, 1.5 mM  $\text{MgCl}_2$ , 0.2 mM EDTA, 20 mM HEPES, pH 7.9, and 25% (v/v) glycerol) supplemented with 0.01 M DTT and protease inhibitor. The nuclear suspension was mixed thoroughly for 30 min and centrifuged at  $12,000 \times g$  for 5 min. The supernatant, representing the nuclear fraction, was stored at  $-80^{\circ}\text{C}$ .

The protein concentration of the supernatant was measured with Pierce<sup>®</sup> BCA protein assay kit (Thermo Scientific, US) according to the manufacturer's instructions.

### ***Detection of protein expression***

Equal amounts of protein samples (30  $\mu\text{g}$ ) were loaded onto 10% sodium dodecyl sulfate-polyacrylamide gel electrophoresis (SDS-PAGE) and ran at 120 V for 2.5 h. Proteins were transferred to a polyvinylidene difluoride (PVDF) membrane (Bio-Rad Laboratories, Hercules, CA, US) for 1 h at 120 mA on Bio-Rad Cells (Bio-Rad Laboratories, Hercules, CA, US). The membranes were blocked with 5% nonfat milk in TBS-T (Tris-buffered saline with 0.1% Tween-20) for 1 h, washed, and then incubated with the primary antibody against p44/p42 MAPK (ERK1/2) (1:500), phospho-p44/p42 MAPK (ERK1/2) (1:500), p38 MAPK (1:500), phospho-p38 MAPK (Thr180/Thr182) (1:500),

SAPK/JNK (1:1000), phospho-SAPK/JNK(Thr183/Tyr185) (1:1000), NF- $\kappa$ B p65 (1:500), phospho-NF- $\kappa$ B p65 (1:500), GRP78 (1:500), HDAC1 (1:1000) or  $\beta$ -actin (1:1000) overnight at 4°C. The membranes were washed for ten times with 10 min with TBS-T and then incubated for 1 h with the horseradish peroxidase-conjugated secondary anti-IgG antibody using a dilution rate between 1:2000 and 1:5000 in 5% nonfat milk in TBS-T. The membranes were further washed for ten times with 10 min in TBS-T. Immunoreactive bands were visualized with an enhanced chemiluminescence HRP substrate (Millipore, Billerica, MA, USA) for 2–5 min. Images were captured with a LAS-4000 luminescent image analyzer (Bucher Biotec, Basel, Switzerland).  $\beta$ -actin was used as loading control for cytoplasmic and whole cell protein extracts. HDAC1 was used as loading control for nuclear fractions.

#### ***11 $\beta$ -HSD1 activity measurements in intact BV-2 cells***

11 $\beta$ -HSD1 activity was measured by the conversion of radioactively labeled [ $^3$ H]-cortisone to [ $^3$ H]-cortisol. After treatment, the medium was then removed and replaced by assay medium containing 50 nM cortisone with 10 nCi 1,2-[ $^3$ H]-cortisone at 37°C and 5% CO<sub>2</sub> for 12 h in serum-free DMEM. The medium supernatant was collected. The supernatant was mixed with 2–3 volumes of ethyl-acetate by shaking and the lower hydrophilic and the upper lipophilic phases were separated by centrifugation. The upper steroid containing phase was fully evaporated, resolved with methanol containing a mixture of 2 mM unlabeled cortisone and cortisol. Cortisone (E) and cortisol (F) separated by thin-layer chromatography using chloroform/methanol solvent system (9:1, v/v). [ $^3$ H]-labeled cortisone and cortisol were quantified by liquid scintillation analyzer (Packard Biosciences, Boston, MA, USA).

### *Statistical analysis of the data*

Data was expressed as mean  $\pm$  SD from at least 3 independent experiments (n), each experiment with triplicate determinations. Data were analyzed with Prism software package version 5 from GraphPad, San Diego, CA. Data were subjected to one-way ANOVA and post hoc analysis. Differences were considered statistically significant at  $p < 0.05$  and reported in each figure legend.

## **RESULTS**

### *Increased production of inflammatory cytokines and receptors in BV-2 cells*

We investigated whether TMT could induce the expression of neuroinflammatory mediators in BV-2 microglial cells. Several reports have recently indicated that TMT induced inflammatory response and reactive microglia marker expression in various cells (Fiedorowicz et al., 2008;Koda et al., 2009;McPherson et al., 2011;Ravanan et al., 2011). Thus, we investigated the effects of TMT on the expression of inflammatory related genes in BV-2 cells, including IL-6, iNOS, inflammatory related receptor, and the glucocorticoid-induced tumor necrosis factor receptor (GITR). BV-2 cells were exposed to TMT at concentrations between 0.1-2  $\mu$ M for 24 h, showed a concentration dependent manner to increase in IL-6, iNOS, and GITR mRNA levels at 24 h (Fig. 1A). Similarly, a concentration-dependent manner increase in the secretion of IL-6 induced by TMT was observed (Fig. 1B). The increase in IL-6 secretion correlates with an increase IL-6 mRNA expression.

In order to investigate IL-6 expression over a time course following TMT exposure, cells were treated with either 1  $\mu$ M TMT or 10 ng/ml LPS for 0.25, 0.5, 1, 6, 12, 18, 24, and 48 h. The levels of secreted IL-6 were measured by ELISA. TMT induced a time-dependent increase in IL-6 protein (Fig. 1C). Exposure to 1  $\mu$ M TMT resulted in the elevation of IL-6 protein levels in the medium which reached

statistical significance at 1 h post-TMT exposure, and reached maximum expression at 18 h post-TMT treatment, the levels of IL-6 mRNA was reached the maximum, which declined thereafter (Fig. 1C). Levels of IL-6 protein within the control media mildly increased from baseline after 24 h.

#### ***Activation of the NF- $\kappa$ B signaling pathway by TMT in BV-2 cells***

Since NF- $\kappa$ B is well known to play a critical role in the expression of pro-inflammatory molecules, we investigated whether TMT activates NF- $\kappa$ B in microglial cells. The importance of TMT induced IL-6 upregulation was investigated using the NF- $\kappa$ B inhibitor Cay10512. Pretreatment with Cay10512 (250 nM) for 1 h completely blocked TMT induced- IL-6 mRNA expression (Fig. 2A).

To elucidate whether TMT activates the NF- $\kappa$ B signaling pathway, we investigated the effect of TMT on NF- $\kappa$ B p65 subunit nuclear translocation in BV-2 cells. Cells were treated with 1  $\mu$ M TMT for 24 h or pre-incubated with Cay10512 (250 nM) for 1 h prior to treatment with 1 $\mu$ M TMT for 24 h. The translocation of the NF- $\kappa$ B p65 subunit and the NF- $\kappa$ B p65 subunit protein expression was detected by CellomicsArrayScan high-content imaging analysis and Western blotting, respectively. TMT significantly induced the translocation of NF- $\kappa$ B p65 subunit from the cytosol into the nucleus (Fig. 2B). This finding was confirmed by Western blot analysis of nuclear and cytosolic extracts (Fig. 2C). TMT treatment significantly increased NF- $\kappa$ B p65 subunit expression in nuclear extracts, which could be suppressed by pretreatment with Cay10512 (Fig. 2C). These results suggest that TMT induced the expression of neuroinflammatory molecules through the activation and nuclear translocation of NF- $\kappa$ B.

#### ***Activation of the MAPKs signaling pathway by TMT in BV-2 cells***

Mitogen-activated protein kinases (MAPKs) play an important role in the activation of inflammatory genes, which may involve crosstalk between MAPKs and NF- $\kappa$ B pathway. We next examined whether

inhibitors of MAPKs had any effects of the TMT-induced up-regulation of IL-6 and iNOS mRNA expression in BV-2 cells. We used PD98059 (50  $\mu$ M), SB202190 (20  $\mu$ M) and SP600125 (20  $\mu$ M) that are selective inhibitors of ERK1/2, p38, and JNK, respectively. Pre-incubation of cells for 1 h with PD98059 or SB202190 prior to stimulation with 1  $\mu$ M TMT for 24 h reduced the TMT-upregulated mRNA expression of IL-6 and iNOS (Fig. 3A). In contrast, no significant effect on TMT-induced IL-6 and iNOS expression was observed when cells were pretreated with SP600125. Similarly, treatment with any of three MAPK had no effect on the basal levels of IL-6 and iNOS mRNA expression.

To further explore the relationship between TMT-induced IL-6 and iNOS mRNA expression and MAPK activation, we determined a time course for ERK1/2, JNK, and p38 activation in BV-2 cells following TMT stimulation. TMT-induced a time-dependent activation of ERK1/2 and p38 as determined by Western blot analysis for phospho-ERK (p42/p44) and phospho-p38. However, TMT did not affect JNK phosphorylation (Fig. 3B). The degree of ERK1/2 activation following 1 h stimulation with 1  $\mu$ M TMT increased and continued to elevate until it reached a plateau at 2 h treatment (Fig. 3B). The phosphorylation of p38 induced by TMT was observed within 30 min of treatment (Fig. 3B). Additionally, cells were pre-treated with different MAPK inhibitors including PD98059 (ERK1/2 inhibitor, 50  $\mu$ M,) and SB202190 (p38 inhibitor, 20  $\mu$ M), and SP600125 (JNK inhibitor, 20  $\mu$ M) for 1 h and then stimulated with TMT for 2 h. Interestingly, the phosphorylation of ERK1/2 induced by TMT was inhibited by PD98059 pretreatment but was potentiated by SB202190 and SP600125 pretreatment (data not shown). The phosphorylation of p38 induced by TMT was inhibited by all the MAPK inhibitors (data not shown).

Cross-talk between MAPKs and the NF- $\kappa$ B pathways has been reported in microglia cells (Wilms et al., 2003;Gorina et al., 2011;Zheng et al., 2012). Therefore, the relationship between MAPKs and NF- $\kappa$ B in TMT induced inflammation was investigated. Cells were pre-treated with inhibitors for MAPKs for 1 h followed by TMT (1  $\mu$ M) treatment for 24 h. The expression of the NF- $\kappa$ B p65 subunit was confirmed

by Western blot analysis from nuclear and cytosolic extracts (Fig. 3C). Pretreatment with PD98059, SB202190, and SP600125 reversed the TMT-induced nuclear translocation of the NF- $\kappa$ B p65 subunit.

Taken together, the data suggests that the effect of TMT on the induction of the inflammatory response is associated with the activation of ERK1/2 and p38 MAPKs pathways in BV-2 microglial cells. In addition, MAPKs may disturb the activation of NF- $\kappa$ B induced by TMT.

#### ***Differential effect of RU-486 and spironolactone on the expression of pro-inflammatory mediators***

It has been demonstrated that corticosteroids such as corticosterone and dexamethasone disturb on MAPK and NF- $\kappa$ B activity (Auwardt et al., 1998;ten Hove et al., 2006;Armstrong et al., 2011;Manetsch et al., 2012;Mercado et al., 2012;Zhu et al., 2012) which result in an altered inflammatory response. Therefore, we want to investigate whether different glucocorticoids differentially influence TMT-induced inflammatory responses. In the present study we used a specific GR agonist, dexamethasone. In addition, both active form corticosterone and inactive form dehydrocorticosterone of the unselective corticosteroid receptor agonist were used. Pretreating cells with dexamethasone (100 nM) for 1 h followed by TMT treatment for 24 h completely blocked TMT-induced IL-6 and iNOS mRNA expression (Fig. 4A). Similarly, dexamethasone pretreatment markedly suppressed the release of IL-6 (Fig. 4C). Pretreating cells with either corticosterone (25 nM) or dehydrocorticosterone (50 nM) significantly enhanced TMT upregulation of IL-6 and iNOS mRNA expression and IL-6 secretion (Fig. 4A and Fig 4C).

To determine which receptor is involved in TMT induced inflammation in BV2 microglia cells, nuclear receptor blockers RU-486, a GR antagonist, and spironolactone, a MR antagonist were tested. Pretreatment with 1  $\mu$ M spironolactone completely abolished the effect of TMT on IL-6 and iNOS mRNA expression (Fig. 4B). In contrast, pretreatment with RU-486 (1  $\mu$ M) enhanced the action of TMT (Fig. 4B). Interestingly, the secretion of IL-6 stimulated by TMT was partially blocked by

spironolactone (Fig. 4D). These results suggest that the stimulatory effect of TMT on inflammation involves the MR.

MAPKs and NF- $\kappa$ B activity are differentially modulated by different steroid receptors including MR and GR (Auwardt et al., 1998;Fu et al., 2012;Zhu et al., 2012;Long et al., 2013). To further investigate which receptors modulate the potentiating effect of corticosterone on TMT actions, RU-486 and spironolactone were used. Pretreatment with 1  $\mu$ M spironolactone completely antagonized the stimulatory effect of 25 nM corticosterone to increase IL-6 expression but not RU-486 (Fig 4B and 4D).

### ***The potentiation of TMT induced inflammation by corticosterone on TMT acts through MAPKs***

Reports show glucocorticoid reamplification reinforces the inflammatory response was reported, this process is associated with MAPKs and 11 $\beta$ -HSD1 activity (Hu et al., 2009;Ishii-Yonemoto et al., 2010;Ahasan et al., 2012). Our studies found that 11 $\beta$ -HSD1 mediated the potentiation of the inflammatory action of corticosterone. Moreover, corticosterone also activated MAPKs (Nguyen Dinh Cat et al., 2011;Komatsuzaki et al., 2012). Therefore, we investigated the involvement of MAPKs on the potentiation of TMT-induced inflammation by corticosterone by measuring IL-6 mRNA expression and IL-6 release.

Preincubation of cells for 1 h with PD98059 or SB202190 prior to stimulation with 1  $\mu$ M TMT for 24 h reduced the TMT-upregulated mRNA expression of IL-6 and iNOS (data not shown). In contrast, no significant effect on the TMT-induced expression of IL-6 and iNOS was observed when cells were pretreated with SP600125. Similarly, treatment with any of three MAPK inhibitors did not affect the basal levels of IL-6 and iNOS mRNA expression. These results suggest that potentiation effect of corticosterone on TMT-induced inflammation is mediated by ERK1/2 and JNK.

### ***TMT induces inflammation by modulating 11 $\beta$ -HSD1***

It has been demonstrated that 11 $\beta$ -hydroxysteroid dehydrogenase type 1 (11 $\beta$ -HSD1) enhanced inflammation through local glucocorticoid activation (Hardy et al., 2006; Hardy et al., 2008; Kaur et al., 2010). 11 $\beta$ -HSD1 converts inactive steroids (such as cortisone and 11-dehydrocorticosterone) to their active counterparts (cortisol and corticosterone) (Tomlinson et al., 2004; Cooper and Stewart, 2009). According to the potentiation effect of corticosterone and 11-dehydrocorticosterone on TMT-induced inflammation, we hypothesized that the stimulatory effect of glucocorticoids on the inflammatory responses-induced by TMT is mediated by local glucocorticoid activation through 11 $\beta$ -HSD1.

Pretreatment with BNW-16, an 11 $\beta$ -HSD1 inhibitor, completely abolished the effect of 11-dehydrocorticosterone on TMT-induced IL-6 mRNA expression. Additionally, the stimulatory effect of corticosterone was also partially blocked by BNW-16 pretreatment. Similar results were obtained monitoring the levels of IL-6 release (data not shown).

### ***TMT induced 11 $\beta$ -HSD1 function***

We observed that the TMT induced inflammatory response in BV-2 cells was mediated through NF- $\kappa$ B, ERK1/2, p38 and MR. The potentiation effect of corticosterone and 11-dehydrocorticosterone on inflammation induced by TMT was reversed by an 11 $\beta$ -HSD1 inhibitor. Recently, several studies have shown that 11 $\beta$ -HSD1 expression is upregulated by NF- $\kappa$ B and ERK1/2 (Frey et al., 2004; Hu et al., 2009; Ishii-Yonemoto et al., 2010; Chantong et al., 2012; Lee et al., 2013). Therefore, we hypothesized that TMT may regulate the levels of 11 $\beta$ -HSD1. We investigated the direct effect of TMT on 11 $\beta$ -HSD1 mRNA and activity. Treatment with TMT for 24 h induced 11 $\beta$ -HSD1 mRNA expression and 11 $\beta$ -HSD1 activity in concentration-dependent manner (Fig 5A, 5B).

### *Pathways involving the induction of 11 $\beta$ -HSD1 by TMT*

To investigate the pathways involved in TMT induced upregulation of 11 $\beta$ -HSD1, we measured 11 $\beta$ -HSD1 mRNA induced by TMT following pretreatment of cells with specific inhibitors or antagonists for NF- $\kappa$ B, ERK1/2, p38, JNK, GR and MR with Cay10512, PD98059, SB203580, SP600125, RU486 and spironolactone, respectively. As shown in Fig. 6A, pretreatment cells with Cay10512 completely blocked TMT induced 11 $\beta$ -HSD1 expression. PD98059, SB203580, RU486 and spironolactone significantly blocked TMT-induced 11 $\beta$ -HSD1 expression. However, SP600125 had no effect. These results suggest that TMT induced 11 $\beta$ -HSD1 mRNA through NF- $\kappa$ B, ERK1/2, p38, MR and GR.

We found corticosterone potentiated the inflammatory response of TMT. Therefore, we investigated the action of corticosterone on TMT-induced 11 $\beta$ -HSD1 mRNA expression. Cells were pretreated with specific inhibitors or antagonists of NF- $\kappa$ B, ERK1/2, p38, JNK, GR and MR with Cay10512, PD98059, SB203580, SP600125, RU486 and spironolactone respectively and then stimulated with corticosterone and TMT. As shown in Fig. 6B, pretreatment cells with Cay10512, PD98059, SB203580, RU486, and spironolactone significantly blocked the TMT-induced 11 $\beta$ -HSD1. However, SP600125 had no effects. These results suggest that potentiation effect of corticosterone on TMT induced 11 $\beta$ -HSD1 mRNA is mediated by ERK1/2, p38, MR, and GR.

## **DISCUSSION**

In this study, we have demonstrated that TMT, at low concentrations, stimulates a concentration-dependent up-regulation of inflammatory related genes including IL-6, iNOS, and GITR in mouse microglial cells (Fig. 1A). The release of IL-6 stimulated by TMT was concentration- and time-dependent (Fig. 1C and Fig. 1D). TMT intoxication has been suggested to play a role in microglia

activation and subsequent neuroinflammation (Pompili et al., 2004;Koda et al., 2009). Microglia surrounding neurons were targeted by TMT and resulted in up-regulation of pro-inflammatory cytokines. It has been suggested that microglia are directly involved in TMT induced neurotoxicity (Geloso et al., 2011;Huong et al., 2011;Yang et al., 2012). The molecular mechanism of TMT induced inflammation in microglia is still not well-established. TMT induced cytotoxicity with an increase protease-activated receptor-1 (PAR-1) in rat primary microglia cells at the concentration of 10  $\mu$ M after 48 h exposure (Pompili et al., 2011). In human microglia cell cultures, TMT at concentration of  $5 \times 10^{-3}$  nM increased iNOS and TNF- $\alpha$  expression 1.5 and 2.5 fold, respectively, compared with control (Reali et al., 2005). However, our study showed that 0.1  $\mu$ M TMT could induce the expression of IL-6, iNOS and GTR mRNA with 1.25, 3.12, and 4.01 fold, respectively, in mouse microglia cells. This indicates that human microglia cells are more susceptibility to TMT toxicity than rodents. In addition to cytokine expression, GTR has been reported to play an important role in inflammatory diseases. GTR contributes to the *in vivo* development of the inflammatory response as well as the *in vitro* enhancement of dendritic cell activity (Ronchetti et al., 2011).

Activated NF- $\kappa$ B enters the nucleus and promotes the transcription of its target genes, including the pro-inflammatory cytokine IL-6 and iNOS (Cheng et al., 2009;Xu et al., 2011;Lukiw, 2012). An increase in IL-6 secretion was prevented by pretreating cells with Cay10512, an NF- $\kappa$ B inhibitor (Fig. 2A). An increase in nuclear translocation and protein levels of the NF- $\kappa$ B p65 subunit in nucleus was induced by TMT (Fig. 2B, 2C). These results are consistent with a previous observation showing that TMT at 5  $\mu$ M significantly increased translocation of NF- $\kappa$ B p65 subunit into nucleus in human neuroblastoma cells SY5Y. However, NF- $\kappa$ B inhibitors, MG132 and BAY11-7082, promoted TMT-induced cytotoxicity and early apoptosis (Qing et al., 2013). Bay 117082, a NF- $\kappa$ B inhibitor blocked the up-regulation of iNOS mRNA induced by TMT in human microglia cells (Reali et al., 2005).

MAPK kinases (ERK1/2, JNK and p38 MAPK) play important roles in mediating inflammatory responses in microglia cells through the relaying extracellular signals to various intracellular pathways and regulating stress-induced neurodegeneration (Katsuki et al., 2006;Choi et al., 2009;Wang et al., 2011b). We found that inhibitors of ERK and p38-MAPK significantly reduced the TMT-induced mRNA expression of IL-6 and iNOS (Fig. 3A). Immunoblotting analysis revealed that ERK1/2 and p38 but not JNK are intimately involved in the TMT stimulated mRNA expression of IL-6 and iNOS microglia (Figure 3A-3C). The earliest time point for TMT stimulation of ERK and p38 MAPK activation was 1 and 0.5 h, respectively (Fig. 3B). TMT activation of the ERK, p38, and JNK pathways was observed in primary cultures of cerebellar granule cells but only JNK and p38 inhibitors were able to protect TMT-induced apoptosis (Mundy and Freudenrich, 2006). Neuronal damage induced by TMT was dependent on the JNK cascades in primary cultures of cortical neurons which JNK inhibitor partially attenuated the TMT-induced nuclear condensation and accumulation of lactate dehydrogenase (Shuto et al., 2009b). In human neuroblastoma cells, an increase in the phosphorylation of ERK, p38, and JNK was observed during the 24-h exposure of TMT and pretreatment with ERK1/2 and JNK inhibitor reduced in TMT-induced cytotoxicity (Qing et al., 2013). TMT induced apoptosis via caspase activation, p38, and oxidative stress in PC12 cells (Jenkins and Barone, 2004). Our study showed the first evidence of the role of MAPKs pathways in the regulation of TMT-induced proinflammatory mediators in microglia cells.

An increasing amount of evidences *in vivo* implicates the role of corticosteroids including corticosterone and dexamethasone in TMT-induced toxicity and inflammation. For instance, treatment with dexamethasone almost prevented TMT-induced neuronal damage and behavioral abnormalities by attenuating oxidative stress (Shuto et al., 2009a). Both high and low levels of circulating corticosterone altered the rate of neuropathological and behavioral changes induced by TMT in rats (Tsutsumi et al., 2002). Corticosterone and dexamethasone administration partially reversed TMT-induced enhancement of IL-1 $\beta$  and IL-6 expressions in the reactive gliosis (Liu et al., 2005). Treatment with dexamethasone

prior to TMT potentiated the action of TMT on the elevation of TNF- $\alpha$ , TNF- $\beta$ , and IL-1 $\beta$  levels in rat hippocampus (Bruccoleri et al., 1999). Prolonged administration of corticosterone or dexamethasone but not aldosterone partially reversed the TMT-induced neuronal loss and reactive astrocytosis. (Imai et al., 2001). Furthermore, corticosteroids disturb the NF- $\kappa$ B and MAPKs pathways resulting in a change in cytokine release. (Auwardt et al., 1998;ten Hove et al., 2006;Armstrong et al., 2011;Manetsch et al., 2012;Mercado et al., 2012;Zhu et al., 2012). In the present study, corticosterone (25 nM) and inactive form, 11-dehydrocorticosterone (50 nM) potentiated TMT-induced IL-6 and iNOS mRNA expression as well as IL-6 release (Fig. 4A and 4C). A MR antagonist, spironolactone, blocked the action of TMT. On the contrary, a GR antagonist, RU486 enhanced TMT-induced cytokine expression (Fig. 4B and 4D). This result is consistent with previous evidences in animal studies indicating that neuronal degeneration-induced by TMT was prevented by dexamethasone treatment but was exacerbated by mifepristone, a GR antagonist (Shuto et al., 2009b). Neurotoxicity induced by TMT in the mouse hippocampus was enhanced by aldosterone which was reversed by spironolactone (Ogita et al., 2012). MR has been proposed to play a role in microglia activation and promotion of inflammation in brain during cerebral ischemia (Guo et al., 2008). The inhibitory effect on MKP-1-dependent MAPK pathways was induced by dexamethasone in activated microglia (Huo et al., 2011). The absence of GR in microglia induced the prolongation of NF- $\kappa$ B transcriptional activity and led to its persistent activation (Ros-Bernal et al., 2011).

Interestingly, the potentiation effect of corticosterone on TMT-induced cytokine expression was reversed by spironolactone but potentiated by RU486 (Fig. 4B and 4D). This result indicates that MR plays a role in corticosterone action. Corticosterone has a 10-fold higher affinity for the MR than the GR (De Kloet et al., 1984). Several studies have been shown that an increase in MAPKs phosphorylation was induced by corticosterone. For example, a release of corticosterone after stress leads to an activation of p38 and the p42/44 MAP kinases (Ahmed et al., 2006). Stress induced elevation of

corticosterone levels has been associated with MAPKs activation in rat hippocampus (Moosavi et al., 2011). The role of MR on MAPKs activation has also been investigated. Adosterone activated MAPKs resulted in ROS production which induced renal toxicity. The effects were reversed by a MR antagonist (Kiyomoto et al., 2008). An induction of adipocyte-derived factor mediated by MAPK activation in adipocytes was attenuated by MR antagonist (Nguyen Dinh Cat et al., 2011). However, no direct evidence indicating the involvement of MR on activation of MAPKs induced by corticosterone was reported. In the present study, the potentiation effect of corticosterone on TMT-induced IL-6 and iNOS mRNA expression was inhibited by inhibitors for ERK1/2 and p38.

11 $\beta$ -Hydroxysteroid dehydrogenase type 1 (11 $\beta$ -HSD1) is an intracellular enzyme that acts primarily as a reductase to convert inactive glucocorticoids into active form in tissues. It thus potentiates local glucocorticoid activity (Tomlinson et al., 2004; Cooper and Stewart, 2009). This enzyme has been suggested to increase inflammation (Hardy et al., 2006; Hardy et al., 2008; Kaur et al., 2010). The potentiation effect of 11-dehydrocorticosterone on TMT-induced cytokine expression was completely block by 11 $\beta$ -HSD1 inhibitor. Additionally, 11 $\beta$ -HSD1 inhibitor also blocked the stimulatory action of active corticosterone. These results indicate that the local concentration of corticosterone mediated by 11 $\beta$ -HSD1 may contribute to TMT action. Induction of 11 $\beta$ -HSD1 mRNA expression and 11 $\beta$ -HSD1 activity by TMT was observed in a concentration dependent manner (Fig. 5A, 5B). Several evidences have shown that TMT increased plasma corticosterone (Tsutsumi et al., 2002; Liu et al., 2005; Shirakawa et al., 2007; Little et al., 2012; Ogita et al., 2012). However, the role of TMT on local glucocorticoid regulation has not been reported. Our results suggest that TMT may disturb endogenous locally active corticosterone levels by increase of 11 $\beta$ -HSD1 mRNA expression and 11 $\beta$ -HSD1 activity.

11 $\beta$ -HSD1 is positively modulated by MR, NF- $\kappa$ B and ERK1/2 (Frey et al., 2004; Hu et al., 2009; Ishii-Yonemoto et al., 2010; Chantong et al., 2012; Lee et al., 2013) which are coincidentally the same pathways disturbed by TMT in microglia cells. In the present study, Cay10512, a NF- $\kappa$ B inhibitor, completely abolished TMT-induced 11 $\beta$ -HSD1 mRNA expression. Inhibitors for ERK1/2, JNK, GR, and MR

attenuated the action of TMT on 11 $\beta$ -HSD1 expression (Fig. 6A). These results confirm that the action of TMT on stimulation of inflammation may be related to 11 $\beta$ -HSD1. Furthermore, corticosterone also potentiated 11 $\beta$ -HSD1 expression induced by TMT. As expected, pretreating cells with inhibitors of NF- $\kappa$ B, ERK1/2, JNK, GR, and MR blocked the potentiation effect of corticosterone on TMT-induced 11 $\beta$ -HSD1 expression. Therefore, the inflammatory action of TMT might be related to 11 $\beta$ -HSD1 level and activity and local glucocorticoid concentrations. TMT induced 11 $\beta$ -HSD1 expression was mediated by NF- $\kappa$ B, ERK1/2, JNK, which are the same pathways which induce TMT regulated inflammation. However, there are differences in receptor regulation in the two pathways. Both MR and GR positively mediated TMT-induced 11 $\beta$ -HSD1 expression but TMT induced inflammation was mediated by the MR only. Classically glucocorticoids prevent inflammation but they act together with the pro-inflammatory cytokines to synergistically increase 11 $\beta$ -HSD1 expression in a variety of cell types (Sun and Myatt, 2003; Kaur et al., 2010). Inhibition of 11 $\beta$ -HSD1 emerges as a promising approach for the treatment of inflammatory-related diseases (Walker, 2006; Sun et al., 2011; Wang et al., 2011a). Furthermore, down-regulation of genes that play a role in humoral defense mechanisms, acute-phase response, and immune response was observed in mice treated with an 11 $\beta$ -HSD1 inhibitor (Luo et al., 2013).

In summary, microglia exposed to TMT (Fig. 7), in combination with glucocorticoids, including 11-dehydrocorticosterone and corticosterone, respond by enhancing the expression of proinflammatory cytokines and iNOS. The potentiation effects are regulated by local glucocorticoid levels which are balanced through NF- $\kappa$ B, ERK1/2, and JNK regulation. The MR is suggested to play a role in both controlling the action of TMT, and the stimulatory effect of glucocorticoid on the inflammatory response. The role of brain microglia in the mechanism of TMT induced neurotoxicity, especially within in the context of inflammation and endogenous glucocorticoids, should be further investigated in more detail.

## **ACKNOWLEDGMENTS**

This work was supported by the Swiss Center for Applied Human Toxicology. AO has a Chair for Molecular and Systems Toxicology by the Novartis Research Foundation.

**REFERENCES**

- Ahasan MM, Hardy R, Jones C, Kaur K, Nanus D, Juarez M, Morgan SA, Hassan-Smith Z, Benezech C, Caamano JH, Hewison M, Lavery G, Rabbitt EH, Clark AR, Filer A, Buckley CD, Raza K, Stewart PM, Cooper MS (2012) Inflammatory regulation of glucocorticoid metabolism in mesenchymal stromal cells. *Arthritis Rheum* 64:2404-2413.
- Ahmed T, Frey JU, Korz V (2006) Long-term effects of brief acute stress on cellular signaling and hippocampal LTP. *J Neurosci* 26:3951-3958.
- Armstrong J, Harbron C, Lea S, Booth G, Cadden P, Wreggett KA, Singh D (2011) Synergistic effects of p38 mitogen-activated protein kinase inhibition with a corticosteroid in alveolar macrophages from patients with chronic obstructive pulmonary disease. *J Pharmacol Exp Ther* 338:732-740.
- Auwardt RB, Mudge SJ, Chen CG, Power DA (1998) Regulation of nuclear factor kappaB by corticosteroids in rat mesangial cells. *J Am Soc Nephrol* 9:1620-1628.
- Barnes PJ, Karin M (1997) Nuclear factor-kappaB: a pivotal transcription factor in chronic inflammatory diseases. *N Engl J Med* 336:1066-1071.
- Blasi E, Barluzzi R, Bocchini V, Mazzolla R, Bistoni F (1990) Immortalization of murine microglial cells by a v-raf/v-myc carrying retrovirus. *J Neuroimmunol* 27:229-237.
- Brown GC, Neher JJ (2010) Inflammatory neurodegeneration and mechanisms of microglial killing of neurons. *Mol Neurobiol* 41:242-247.
- Brucoleri A, Pennypacker KR, Harry GJ (1999) Effect of dexamethasone on elevated cytokine mRNA levels in chemical-induced hippocampal injury. *J Neurosci Res* 57:916-926.
- Caso JR, Lizasoain I, Lorenzo P, Moro MA, Leza JC (2006) The role of tumor necrosis factor-alpha in stress-induced worsening of cerebral ischemia in rats. *Neuroscience* 142:59-69.
- Chantong B, Kratschmar DV, Nashev LG, Balazs Z, Odermatt A (2012) Mineralocorticoid and glucocorticoid receptors differentially regulate NF-kappaB activity and pro-inflammatory cytokine production in murine BV-2 microglial cells. *J Neuroinflammation* 9:260.
- Cheng YL, Wang CY, Huang WC, Tsai CC, Chen CL, Shen CF, Chi CY, Lin CF (2009) *Staphylococcus aureus* induces microglial inflammation via a glycogen synthase kinase 3beta-regulated pathway. *Infect Immun* 77:4002-4008.
- Choi Y, Lee MK, Lim SY, Sung SH, Kim YC (2009) Inhibition of inducible NO synthase, cyclooxygenase-2 and interleukin-1beta by torilin is mediated by mitogen-activated protein kinases in microglial BV2 cells. *Br J Pharmacol* 156:933-940.

- Cooper MS, Stewart PM (2009) 11Beta-hydroxysteroid dehydrogenase type 1 and its role in the hypothalamus-pituitary-adrenal axis, metabolic syndrome, and inflammation. *J Clin Endocrinol Metab* 94:4645-4654.
- Cuzzocrea S, Ronchetti S, Genovese T, Mazzon E, Agostini M, Di Paola R, Esposito E, Muia C, Nocentini G, Riccardi C (2007) Genetic and pharmacological inhibition of GITR-GITRL interaction reduces chronic lung injury induced by bleomycin instillation. *Faseb J* 21:117-129.
- De Kloet ER, Veldhuis HD, Wagenaars JL, Bergink EW (1984) Relative binding affinity of steroids for the corticosterone receptor system in rat hippocampus. *J Steroid Biochem* 21:173-178.
- Ding GJ, Fischer PA, Boltz RC, Schmidt JA, Colaianne JJ, Gough A, Rubin RA, Miller DK (1998) Characterization and quantitation of NF-kappaB nuclear translocation induced by interleukin-1 and tumor necrosis factor-alpha. Development and use of a high capacity fluorescence cytometric system. *J Biol Chem* 273:28897-28905.
- Evans MC, Couch Y, Sibson N, Turner MR (2013) Inflammation and neurovascular changes in amyotrophic lateral sclerosis. *Mol Cell Neurosci* 53:34-41.
- Fiedorowicz A, Figiel I, Zaremba M, Dzwonek K, Schliebs R, Oderfeld-Nowak B (2008) Trimethyltin-evoked apoptosis of murine hippocampal granule neurons is accompanied by the expression of interleukin-1beta and interleukin-1 receptor antagonist in cells of ameboid phenotype, the majority of which are NG2-positive. *Brain Res Bull* 77:19-26.
- Frank MG, Miguel ZD, Watkins LR, Maier SF (2010) Prior exposure to glucocorticoids sensitizes the neuroinflammatory and peripheral inflammatory responses to E. coli lipopolysaccharide. *Brain Behav Immun* 24:19-30.
- Frey FJ, Odermatt A, Frey BM (2004) Glucocorticoid-mediated mineralocorticoid receptor activation and hypertension. *Curr Opin Nephrol Hypertens* 13:451-458.
- Frieler RA, Meng H, Duan SZ, Berger S, Schutz G, He Y, Xi G, Wang MM, Mortensen RM (2011) Myeloid-specific deletion of the mineralocorticoid receptor reduces infarct volume and alters inflammation during cerebral ischemia. *Stroke* 42:179-185.
- Fu GX, Xu CC, Zhong Y, Zhu DL, Gao PJ (2012) Aldosterone-induced osteopontin expression in vascular smooth muscle cells involves MR, ERK, and p38 MAPK. *Endocrine* 42:676-683.
- Geloso MC, Corvino V, Michetti F (2011) Trimethyltin-induced hippocampal degeneration as a tool to investigate neurodegenerative processes. *Neurochem Int* 58:729-738.
- Ghosh S, Wu MD, Shaftel SS, Kyrkanides S, LaFerla FM, Olschowka JA, O'Banion MK (2013) Sustained interleukin-1beta overexpression exacerbates tau pathology despite reduced amyloid burden in an Alzheimer's mouse model. *J Neurosci* 33:5053-5064.

- Glass CK, Saijo K, Winner B, Marchetto MC, Gage FH (2010) Mechanisms underlying inflammation in neurodegeneration. *Cell* 140:918-934.
- Gorina R, Font-Nieves M, Marquez-Kisinousky L, Santalucia T, Planas AM (2011) Astrocyte TLR4 activation induces a proinflammatory environment through the interplay between MyD88-dependent NFkappaB signaling, MAPK, and Jak1/Stat1 pathways. *Glia* 59:242-255.
- Gottfried-Blackmore A, Sierra A, McEwen BS, Ge R, Bulloch K (2010) Microglia express functional 11 beta-hydroxysteroid dehydrogenase type 1. *Glia* 58:1257-1266.
- Grau JW, Washburn SN, Hook MA, Ferguson AR, Crown ED, Garcia G, Bolding KA, Miranda RC (2004) Uncontrollable stimulation undermines recovery after spinal cord injury. *J Neurotrauma* 21:1795-1817.
- Guo C, Ricchiuti V, Lian BQ, Yao TM, Coutinho P, Romero JR, Li J, Williams GH, Adler GK (2008) Mineralocorticoid receptor blockade reverses obesity-related changes in expression of adiponectin, peroxisome proliferator-activated receptor-gamma, and proinflammatory adipokines. *Circulation* 117:2253-2261.
- Hansen PR, Rieneck K, Bendtzen K (2004) Spironolactone inhibits production of proinflammatory cytokines by human mononuclear cells. *Immunol Lett* 91:87-91.
- Hardy R, Rabbitt EH, Filer A, Emery P, Hewison M, Stewart PM, Gittoes NJ, Buckley CD, Raza K, Cooper MS (2008) Local and systemic glucocorticoid metabolism in inflammatory arthritis. *Ann Rheum Dis* 67:1204-1210.
- Hardy RS, Filer A, Cooper MS, Parsonage G, Raza K, Hardie DL, Rabbitt EH, Stewart PM, Buckley CD, Hewison M (2006) Differential expression, function and response to inflammatory stimuli of 11beta-hydroxysteroid dehydrogenase type 1 in human fibroblasts: a mechanism for tissue-specific regulation of inflammation. *Arthritis Res Ther* 8:R108.
- Hu A, Fatma S, Cao J, Grunstein JS, Nino G, Grumbach Y, Grunstein MM (2009) Th2 cytokine-induced upregulation of 11beta-hydroxysteroid dehydrogenase-1 facilitates glucocorticoid suppression of proasthmatic airway smooth muscle function. *Am J Physiol Lung Cell Mol Physiol* 296:L790-803.
- Huo Y, Rangarajan P, Ling EA, Dheen ST (2011) Dexamethasone inhibits the Nox-dependent ROS production via suppression of MKP-1-dependent MAPK pathways in activated microglia. *BMC Neurosci* 12:49.

- Huong NQ, Nakamura Y, Kuramoto N, Yoneyama M, Nagashima R, Shiba T, Yamaguchi T, Hasebe S, Ogita K (2011) Indomethacin ameliorates trimethyltin-induced neuronal damage in vivo by attenuating oxidative stress in the dentate gyrus of mice. *Biol Pharm Bull* 34:1856-1863.
- Imai H, Kabuto M, Takita M, Kato N (1998) Interleukin-1 receptor antagonist inhibits transient increase of plasma corticosterone in the initial phase of trimethyltin-induced hippocampal necrosis. *Neurotoxicology* 19:163-166.
- Imai H, Nishimura T, Sadamatsu M, Liu Y, Kabuto M, Kato N (2001) Type II glucocorticoid receptors are involved in neuronal death and astrocyte activation induced by trimethyltin in the rat hippocampus. *Exp Neurol* 171:22-28.
- Ishii-Yonemoto T, Masuzaki H, Yasue S, Okada S, Kozuka C, Tanaka T, Noguchi M, Tomita T, Fujikura J, Yamamoto Y, Ebihara K, Hosoda K, Nakao K (2010) Glucocorticoid reamplification within cells intensifies NF-kappaB and MAPK signaling and reinforces inflammation in activated preadipocytes. *Am J Physiol Endocrinol Metab* 298:E930-940.
- Jenkins SM, Barone S (2004) The neurotoxicant trimethyltin induces apoptosis via caspase activation, p38 protein kinase, and oxidative stress in PC12 cells. *Toxicology letters* 147:63-72.
- Juknat A, Pietr M, Kozela E, Rimmerman N, Levy R, Coppola G, Geschwind D, Vogel Z (2012) Differential transcriptional profiles mediated by exposure to the cannabinoids cannabidiol and Delta9-tetrahydrocannabinol in BV-2 microglial cells. *Br J Pharmacol* 165:2512-2528.
- Katsuki H, Okawara M, Shibata H, Kume T, Akaike A (2006) Nitric oxide-producing microglia mediate thrombin-induced degeneration of dopaminergic neurons in rat midbrain slice culture. *J Neurochem* 97:1232-1242.
- Kaur K, Hardy R, Ahasan MM, Eijken M, van Leeuwen JP, Filer A, Thomas AM, Raza K, Buckley CD, Stewart PM, Rabbitt EH, Hewison M, Cooper MS (2010) Synergistic induction of local glucocorticoid generation by inflammatory cytokines and glucocorticoids: implications for inflammation associated bone loss. *Ann Rheum Dis* 69:1185-1190.
- Khasnavis S, Ghosh A, Roy A, Pahan K (2013) Castration Induces Parkinson Disease Pathologies in Young Male Mice via Inducible Nitric-oxide Synthase. *J Biol Chem* 288:20843-20855.
- Kiyomoto H, Rafiq K, Mostofa M, Nishiyama A (2008) Possible underlying mechanisms responsible for aldosterone and mineralocorticoid receptor-dependent renal injury. *J Pharmacol Sci* 108:399-405.

- Koda T, Kuroda Y, Imai H (2009) Rutin supplementation in the diet has protective effects against toxicant-induced hippocampal injury by suppression of microglial activation and pro-inflammatory cytokines: protective effect of rutin against toxicant-induced hippocampal injury. *Cell Mol Neurobiol* 29:523-531.
- Kolch W (2005) Coordinating ERK/MAPK signalling through scaffolds and inhibitors. *Nature reviews Molecular cell biology* 6:827-837.
- Komatsuzaki Y, Hatanaka Y, Murakami G, Mukai H, Hojo Y, Saito M, Kimoto T, Kawato S (2012) Corticosterone induces rapid spinogenesis via synaptic glucocorticoid receptors and kinase networks in hippocampus. *PLoS One* 7:e34124.
- Lee JA, Song HY, Ju SM, Lee SJ, Seo WY, Sin DH, Goh AR, Choi SY, Park J (2010) Suppression of inducible nitric oxide synthase and cyclooxygenase-2 by cell-permeable superoxide dismutase in lipopolysaccharide-stimulated BV-2 microglial cells. *Mol Cells* 29:245-250.
- Lee JH, Gao Z, Ye J (2013) Regulation of 11beta-HSD1 expression during adipose tissue expansion by hypoxia through different activities of NF-kappaB and HIF-1alpha. *Am J Physiol Endocrinol Metab* 304:E1035-1041.
- Li M, Dai FR, Du XP, Yang QD, Chen Y (2012) Neuroprotection by silencing iNOS expression in a 6-OHDA model of Parkinson's disease. *J Mol Neurosci* 48:225-233.
- Lin LC, Ho FM, Yen SJ, Wu PY, Hung LF, Huang WJ, Liang YC (2010) Carbon monoxide induces cyclooxygenase-2 expression through MAPKs and PKG in phagocytes. *Int Immunopharmacol* 10:1520-1525.
- Little JP, Madeira JM, Klegeris A (2012) The saturated fatty acid palmitate induces human monocytic cell toxicity toward neuronal cells: exploring a possible link between obesity-related metabolic impairments and neuroinflammation. *Journal of Alzheimer's disease : JAD* 30 Suppl 2:S179-183.
- Liu Y, Imai H, Sadamatsu M, Tsunashima K, Kato N (2005) Cytokines participate in neuronal death induced by trimethyltin in the rat hippocampus via type II glucocorticoid receptors. *Neuroscience Research* 51:319-327.
- Livak KJ, Schmittgen TD (2001) Analysis of relative gene expression data using real-time quantitative PCR and the 2(-Delta Delta C(T)) Method. *Methods* 25:402-408.
- Long HD, Lin YE, Liu MJ, Liang LY, Zeng ZH (2013) Spironolactone Prevents Dietary-Induced Metabolic Syndrome by Inhibiting PI3-K/Akt and p38MAPK Signaling Pathways. *J Endocrinol Invest*.

- Loram LC, Taylor FR, Strand KA, Frank MG, Sholar P, Harrison JA, Maier SF, Watkins LR (2011) Prior exposure to glucocorticoids potentiates lipopolysaccharide induced mechanical allodynia and spinal neuroinflammation. *Brain Behav Immun* 25:1408-1415.
- Lukiw WJ (2012) NF-kappaB-regulated, proinflammatory miRNAs in Alzheimer's disease. *Alzheimers Res Ther* 4:47.
- Luo MJ, Thieringer R, Springer MS, Wright SD, Hermanowski-Vosatka A, Plump A, Balkovec JM, Cheng K, Ding GJ, Kawka DW, Koo GC, Grand CB, Luo Q, Maletic MM, Malkowitz L, Shah K, Singer I, Waddell ST, Wu KK, Yuan J, Zhu J, Stepaniants S, Yang X, Lum PY, Wang IM (2013) 11beta-HSD1 inhibition reduces atherosclerosis in mice by altering proinflammatory gene expression in the vasculature. *Physiological genomics* 45:47-57.
- Manetsch M, Ramsay EE, King EM, Seidel P, Che W, Ge Q, Hibbs DE, Newton R, Ammit AJ (2012) Corticosteroids and beta(2)-agonists upregulate mitogen-activated protein kinase phosphatase 1: in vitro mechanisms. *Br J Pharmacol* 166:2049-2059.
- McPherson CA, Aoyama M, Harry GJ (2011) Interleukin (IL)-1 and IL-6 regulation of neural progenitor cell proliferation with hippocampal injury: differential regulatory pathways in the subgranular zone (SGZ) of the adolescent and mature mouse brain. *Brain Behav Immun* 25:850-862.
- Mercado N, Hakim A, Kobayashi Y, Meah S, Usmani OS, Chung KF, Barnes PJ, Ito K (2012) Restoration of corticosteroid sensitivity by p38 mitogen activated protein kinase inhibition in peripheral blood mononuclear cells from severe asthma. *PLoS One* 7:e41582.
- Miura R, Nakamura K, Miura D, Miura A, Hisamatsu K, Kajiya M, Nagase S, Morita H, Fukushima Kusano K, Ohe T, Ishihara K (2006) Anti-inflammatory effect of spironolactone on human peripheral blood mononuclear cells. *J Pharmacol Sci* 101:256-259.
- Moisan MP, Seckl JR, Edwards CR (1990) 11 beta-hydroxysteroid dehydrogenase bioactivity and messenger RNA expression in rat forebrain: localization in hypothalamus, hippocampus, and cortex. *Endocrinology* 127:1450-1455.
- Moosavi M, Ghasemi R, Maghsoudi N, Rastegar K, Zarifkar A (2011) The relation between pregnancy and stress in rats: considering corticosterone level, hippocampal caspase-3 and MAPK activation. *Eur J Obstet Gynecol Reprod Biol* 158:199-203.
- Motta AC, Vissers JL, Gras R, Van Esch BC, Van Oosterhout AJ, Nawijn MC (2009) GITR signaling potentiates airway hyperresponsiveness by enhancing Th2 cell activity in a mouse model of asthma. *Respiratory research* 10:93.
- Mundy WR, Freudenrich TM (2006) Apoptosis of cerebellar granule cells induced by organotin compounds found in drinking water: involvement of MAP kinases. *Neurotoxicology* 27:71-81.

- Munhoz CD, Sorrells SF, Caso JR, Scavone C, Sapolsky RM (2010) Glucocorticoids exacerbate lipopolysaccharide-induced signaling in the frontal cortex and hippocampus in a dose-dependent manner. *J Neurosci* 30:13690-13698.
- Nakatani Y, Amano T, Tsuji M, Takeda H (2012) Corticosterone suppresses the proliferation of BV2 microglia cells via glucocorticoid, but not mineralocorticoid receptor. *Life Sci* 91:761-770.
- Nguyen Dinh Cat A, Briones AM, Callera GE, Yogi A, He Y, Montezano AC, Touyz RM (2011) Adipocyte-derived factors regulate vascular smooth muscle cells through mineralocorticoid and glucocorticoid receptors. *Hypertension* 58:479-488.
- Niranjan R (2013) The Role of Inflammatory and Oxidative Stress Mechanisms in the Pathogenesis of Parkinson's Disease: Focus on Astrocytes. *Mol Neurobiol*.
- Ogita K, Sugiyama C, Acosta GB, Kuramoto N, Shuto M, Yoneyama M, Nakamura Y, Shiba T, Yamaguchi T (2012) Opposing roles of glucocorticoid receptor and mineralocorticoid receptor in trimethyltin-induced cytotoxicity in the mouse hippocampus. *Neuroscience letters* 511:116-119.
- Orre M, Kamphuis W, Dooves S, Kooijman L, Chan ET, Kirk CJ, Dimayuga Smith V, Koot S, Mamber C, Jansen AH, Ovaas H, Hol EM (2013) Reactive glia show increased immunoproteasome activity in Alzheimer's disease. *Brain* 136:1415-1431.
- Pompili E, Fabrizi C, Nori SL, Panetta B, Geloso MC, Corvino V, Michetti F, Fumagalli L (2011) Protease-activated receptor-1 expression in rat microglia after trimethyltin treatment. *J Histochem Cytochem* 59:302-311.
- Pompili E, Nori SL, Geloso MC, Guadagni E, Corvino V, Michetti F, Fumagalli L (2004) Trimethyltin-induced differential expression of PAR subtypes in reactive astrocytes of the rat hippocampus. *Brain Res Mol Brain Res* 122:93-98.
- Qin L, Liu Y, Hong JS, Crews FT (2013) NADPH oxidase and aging drive microglial activation, oxidative stress, and dopaminergic neurodegeneration following systemic LPS administration. *Glia* 61:855-868.
- Qing Y, Liang Y, Du Q, Fan P, Xu H, Xu Y, Shi N (2013) Apoptosis induced by Trimethyltin chloride in human neuroblastoma cells SY5Y is regulated by a balance and cross-talk between NF-kappaB and MAPKs signaling pathways. *Archives of toxicology* 87:1273-1285.
- Queisser N, Amann K, Hey V, Habib SL, Schupp N (2013) Blood pressure has only minor influence on aldosterone-induced oxidative stress and DNA damage in vivo. *Free Radic Biol Med* 54:17-25.

- Ravanan P, Harry GJ, Awada R, Hoareau L, Tallet F, Roche R, Lefebvre d'Hellencourt C (2011) Exposure to an organometal compound stimulates adipokine and cytokine expression in white adipose tissue. *Cytokine* 53:355-362.
- Reali C, Scintu F, Pillai R, Donato R, Michetti F, Sogos V (2005) S100b counteracts effects of the neurotoxicant trimethyltin on astrocytes and microglia. *J Neurosci Res* 81:677-686.
- Ronchetti S, Nocentini G, Petrillo MG, Bianchini R, Sportoletti P, Bastianelli A, Ayroldi EM, Riccardi C (2011) Glucocorticoid-Induced TNFR family Related gene (GITR) enhances dendritic cell activity. *Immunol Lett* 135:24-33.
- Ros-Bernal F, Hunot S, Herrero MT, Parnadeau S, Corvol JC, Lu L, Alvarez-Fischer D, Carrillo-de Sauvage MA, Saurini F, Coussieu C, Kinugawa K, Prigent A, Hoglinger G, Hamon M, Tronche F, Hirsch EC, Vyas S (2011) Microglial glucocorticoid receptors play a pivotal role in regulating dopaminergic neurodegeneration in parkinsonism. *Proc Natl Acad Sci U S A* 108:6632-6637.
- Santucci L, Agostini M, Bruscoli S, Mencarelli A, Ronchetti S, Ayroldi E, Morelli A, Baldoni M, Riccardi C (2007) GITR modulates innate and adaptive mucosal immunity during the development of experimental colitis in mice. *Gut* 56:52-60.
- Shirakawa T, Nakano K, Hachiya NS, Kato N, Kaneko K (2007) Temporospatial patterns of COX-2 expression and pyramidal cell degeneration in the rat hippocampus after trimethyltin administration. *Neuroscience Research* 59:117-123.
- Shuto M, Higuchi K, Sugiyama C, Yoneyama M, Kuramoto N, Nagashima R, Kawada K, Ogita K (2009a) Endogenous and exogenous glucocorticoids prevent trimethyltin from causing neuronal degeneration of the mouse brain in vivo: involvement of oxidative stress pathways. *J Pharmacol Sci* 110:424-436.
- Shuto M, Seko K, Kuramoto N, Sugiyama C, Kawada K, Yoneyama M, Nagashima R, Ogita K (2009b) Activation of c-Jun N-terminal kinase cascades is involved in part of the neuronal degeneration induced by trimethyltin in cortical neurons of mice. *J Pharmacol Sci* 109:60-70.
- Smith JA, Das A, Ray SK, Banik NL (2012) Role of pro-inflammatory cytokines released from microglia in neurodegenerative diseases. *Brain Res Bull* 87:10-20.
- Sun D, Wang Z, Caille S, DeGraffenreid M, Gonzalez-Lopez de Turiso F, Hungate R, Jaen JC, Jiang B, Julian LD, Kelly R, McMinn DL, Kaizerman J, Rew Y, Sudom A, Tu H, Ursu S, Walker N, Willcockson M, Yan X, Ye Q, Powers JP (2011) Synthesis and optimization of novel 4,4-disubstituted cyclohexylbenzamide derivatives as potent 11beta-HSD1 inhibitors. *Bioorganic & medicinal chemistry letters* 21:405-410.

- Sun K, Myatt L (2003) Enhancement of glucocorticoid-induced 11beta-hydroxysteroid dehydrogenase type 1 expression by proinflammatory cytokines in cultured human amnion fibroblasts. *Endocrinology* 144:5568-5577.
- Syngle A, Vohra K, Khichi D, Garg N, Verma I, Kaur L (2013) Spironolactone improves endothelial dysfunction in ankylosing spondylitis. *Clin Rheumatol* 32:1029-1036.
- Tanaka J, Fujita H, Matsuda S, Toku K, Sakanaka M, Maeda N (1997) Glucocorticoid- and mineralocorticoid receptors in microglial cells: the two receptors mediate differential effects of corticosteroids. *Glia* 20:23-37.
- Tang X, Wu X, Dubois AM, Sui G, Wu B, Lai G, Gong Z, Gao H, Liu S, Zhong Z, Lin Z, Olson J, Ren X (2013) Toxicity of trimethyltin and dimethyltin in rats and mice. *Bulletin of environmental contamination and toxicology* 90:626-633.
- ten Hove W, Houben LA, Raaijmakers JA, Koenderman L, Bracke M (2006) Rapid selective priming of FcalphaR on eosinophils by corticosteroids. *J Immunol* 177:6108-6114.
- Tomlinson JW, Walker EA, Bujalska IJ, Draper N, Lavery GG, Cooper MS, Hewison M, Stewart PM (2004) 11beta-hydroxysteroid dehydrogenase type 1: a tissue-specific regulator of glucocorticoid response. *Endocr Rev* 25:831-866.
- Tsutsumi S, Akaike M, Arimitsu H, Imai H, Kato N (2002) Circulating corticosterone alters the rate of neuropathological and behavioral changes induced by trimethyltin in rats. *Exp Neurol* 173:86-94.
- Walker BR (2006) Cortisol--cause and cure for metabolic syndrome? *Diabetic medicine : a journal of the British Diabetic Association* 23:1281-1288.
- Wang M, Tian X, Leung L, Wang J, Houvig N, Xiang J, Wan ZK, Saiah E, Hahm S, Suri V, Xu X (2011a) Comparative pharmacokinetics and metabolism studies in lean and diet- induced obese mice: an animal efficacy model for 11beta-hydroxysteroid dehydrogenase type 1 (11beta-HSD1) inhibitors. *Drug metabolism letters* 5:55-63.
- Wang YP, Wu Y, Li LY, Zheng J, Liu RG, Zhou JP, Yuan SY, Shang Y, Yao SL (2011b) Aspirin-triggered lipoxin A4 attenuates LPS-induced pro-inflammatory responses by inhibiting activation of NF-kappaB and MAPKs in BV-2 microglial cells. *J Neuroinflammation* 8:95.
- Waskiewicz AJ, Cooper JA (1995) Mitogen and stress response pathways: MAP kinase cascades and phosphatase regulation in mammals and yeast. *Curr Opin Cell Biol* 7:798-805.
- Wilms H, Rosenstiel P, Sievers J, Deuschl G, Zecca L, Lucius R (2003) Activation of microglia by human neuromelanin is NF-kappaB dependent and involves p38 mitogen-activated protein kinase: implications for Parkinson's disease. *Faseb J* 17:500-502.

- Wongchana W, Palaga T (2012) Direct regulation of interleukin-6 expression by Notch signaling in macrophages. *Cell Mol Immunol* 9:155-162.
- Xu Z, Xiao SB, Xu P, Xie Q, Cao L, Wang D, Luo R, Zhong Y, Chen HC, Fang LR (2011) miR-365, a novel negative regulator of interleukin-6 gene expression, is cooperatively regulated by Sp1 and NF-kappaB. *J Biol Chem* 286:21401-21412.
- Yang M, Kim J, Kim T, Kim SH, Kim JC, Takayama C, Hayashi A, Joo HG, Shin T, Moon C (2012) Possible involvement of galectin-3 in microglial activation in the hippocampus with trimethyltin treatment. *Neurochem Int* 61:955-962.
- Yeager MP, Rassias AJ, Pioli PA, Beach ML, Wardwell K, Collins JE, Lee HK, Guyre PM (2009) Pretreatment with stress cortisol enhances the human systemic inflammatory response to bacterial endotoxin. *Crit Care Med* 37:2727-2732.
- You S, Poulton L, Cobbold S, Liu CP, Rosenzweig M, Ringler D, Lee WH, Segovia B, Bach JF, Waldmann H, Chatenoud L (2009) Key role of the GITR/GITRLigand pathway in the development of murine autoimmune diabetes: a potential therapeutic target. *PLoS One* 4:e7848.
- Zheng X, Zheng W, Liu S, Patel HM, Xia X, Ouyang H, Levitt RC, Candiotti KA, Hao S (2012) Crosstalk between JNK and NF-kappaB in the KDO2-mediated production of TNFalpha in HAPI cells. *Cell Mol Neurobiol* 32:1375-1383.
- Zhu CJ, Wang QQ, Zhou JL, Liu HZ, Hua F, Yang HZ, Hu ZW (2012) The mineralocorticoid receptor-p38MAPK-NFkappaB or ERK-Sp1 signal pathways mediate aldosterone-stimulated inflammatory and profibrotic responses in rat vascular smooth muscle cells. *Acta Pharmacol Sin* 33:873-878.

## Figures and Figure Legend

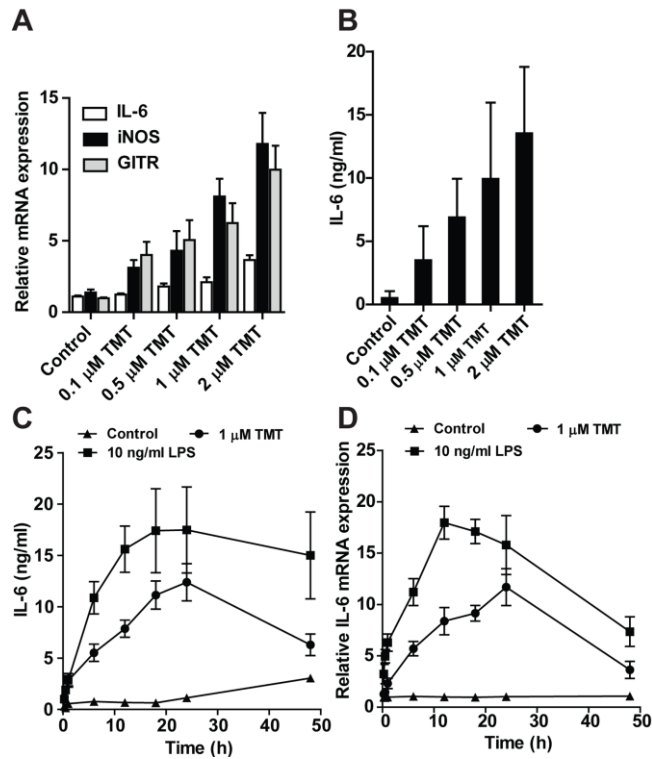


**Fig.1.** TMT stimulated inflammatory response in BV-2 cells. (A) Concentration dependent effect of TMT on IL-6, iNOS, and GITR mRNA expression. Cells were treated with TMT at the concentrations range 0.1-2  $\mu$ M. The mRNA levels were quantified and normalized to the level of GAPDH by real-time RT-PCR analysis. (B) Concentration dependence of TMT on IL-6 release. Cells were treated with TMT at the concentrations range of 0.1-2  $\mu$ M. Levels of IL-6 in the culture medium of BV-2 treated cells were detected by ELISA. (C) Time course for TMT-stimulated IL-6 release. Levels of IL-6 in the culture medium of BV-2 cells treated with either 1  $\mu$ M TMT or 10 ng/ml LPS were detected by ELISA. Results were expressed as the mean  $\pm$  SD of at least 3 independent experiments and significant was determined by one-way ANOVA followed by Turkey's tests, \* $p$  < 0.05, \*\* $p$  < 0.01; \*\*\* $p$  < 0.005.

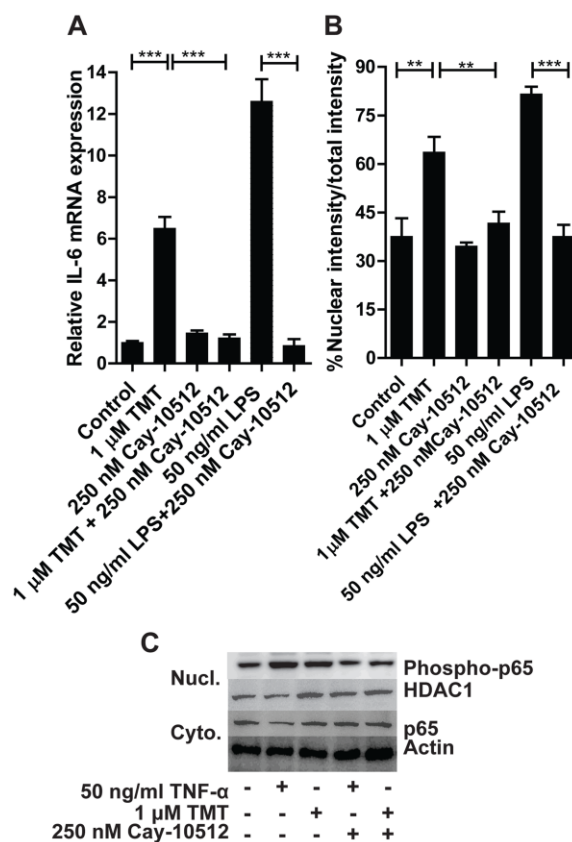


**Fig. 2.** NF- $\kappa$ B is involved in the induction of IL-6 by TMT. Cells were treated with TMT (1  $\mu$ M) or 0.1% DMSO for 24 h after pre-incubation without or with 250 nM Cay10512 for 1 h. (A) IL-6 mRNA levels were measured by RT-PCR and were quantified and normalized to the level of GAPDH. (B) Analysis of the intracellular localization of the p65 subunit of NF- $\kappa$ B by Cellomics ArrayScan HCS imaging system. The ratio between the intensity of nuclear p65 fluorescence and total cellular p65 fluorescence was quantitated. (C) Western blot analysis using antibodies against phospho-p65 and p65 subunit of NF- $\kappa$ B in nuclear and cytoplasmic fractions. Representative blots from 3 independent experiments. Results were expressed as the mean  $\pm$  SD of at least 3 independent experiments and significance was determined by one-way ANOVA followed by Turkey's tests, \* $p$  < 0.05, \*\* $p$  < 0.01;

\*\*\* $p$  < 0.005.

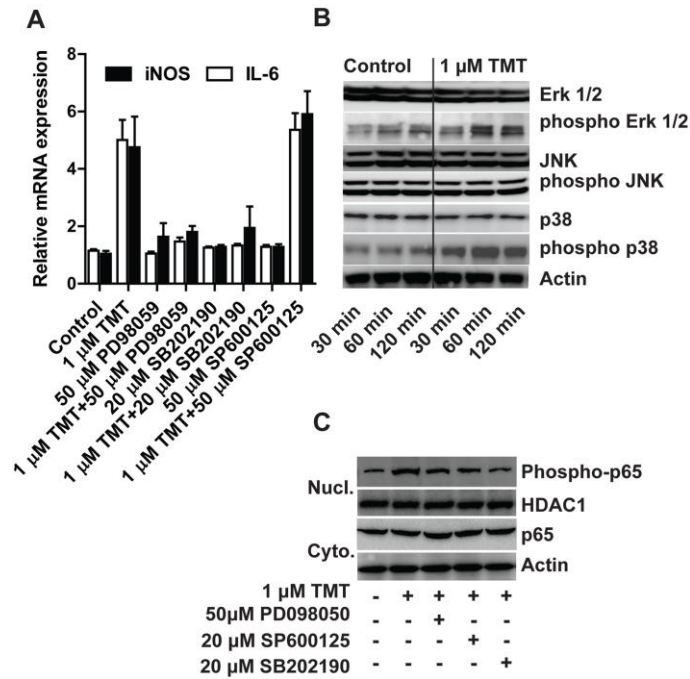


**Fig 3.** Activation of the MAPKs signaling pathway by TMT in BV-2 cells. (A) The effects of MAPK inhibitors on TMT-induced IL-6 and iNOS mRNA expression. Cells were pre-treated with specific MAPK inhibitors (PD98059 for ERK1/2, SP600125 for JNK, and SB203580 for p38) at the concentrations of 50, 20 and 20  $\mu$ M respectively, for 1 h and then stimulated with TMT (1  $\mu$ M) for 24 h. mRNA levels were measured by RT-PCR and were quantified and normalized to the level of GAPDH. (B) Time course of the effect of TMT on the phosphorylation of MAPKs. BV-2 cells were treated with TMT (1  $\mu$ M) for 0.5, 1, and 2 h. (D) MAPKs inhibitors and the effect on TMT-induced p65 phosphorylation. Cells were pre-treated with specific MAPK inhibitors for 1 h and then stimulated with TMT (1  $\mu$ M) for 24 h. Western blot analysis using antibodies against phospho-p65 and p65 subunit of NF- $\kappa$ B in nuclear and cytoplasmic fractions. Representative blots from 3 independent experiments. Results were expressed as the mean  $\pm$  SD of at least 3 independent experiments and significance was determined by one-way ANOVA followed by Turkey's tests, \* $p$  < 0.05, \*\* $p$  < 0.01; \*\*\* $p$  < 0.005.

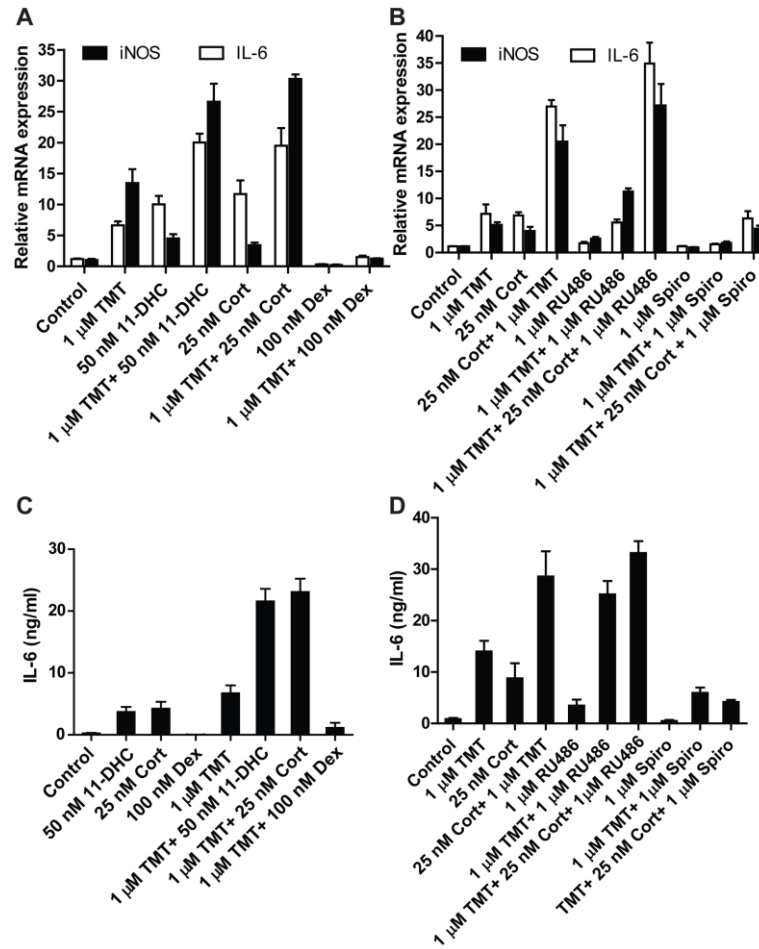


**Fig. 4.** The effect of GR and MR antagonists on TMT-induced inflammatory responses. Cells were pre-treated with corticosterone, dehydrocorticosterone and dexamethasone at the concentrations of 25, 50, and 100 nM respectively for 24 h and then stimulated with TMT (1  $\mu$ M) for 24 h. (A) IL-6 and iNOS mRNA levels were measured by RT-PCR and were quantified and normalized to the level of GAPDH. (C) The levels of IL-6 in the culture medium were detected by ELISA. Cells were pre-treated with RU486 (1  $\mu$ M) and spironolactone (1  $\mu$ M) for 1 h, followed by incubation with 25 nM corticosterone for 24 h and continued stimulating with 1  $\mu$ M TMT for 24 h. (B) IL-6 and iNOS mRNA levels were measured by RT-PCR and were quantified and normalized to the level of GAPDH. (D) The levels of IL-6 in the culture medium were detected by ELISA. Results were expressed as the mean  $\pm$  SD of at least 3 independent experiments and significance was determined by one-way ANOVA followed by Turkey's tests, \* $p$  < 0.05, \*\* $p$  < 0.01; \*\*\* $p$  < 0.005.

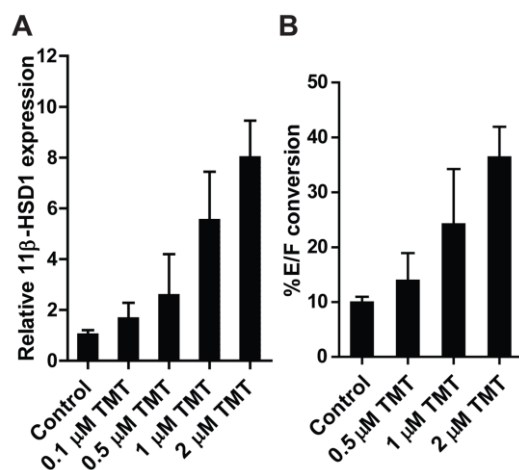


**Fig. 5.** TMT induced 11β-HSD1 in concentration dependent manner. (A) TMT induced 11β-HSD1 mRNA expression. Cells were treated with TMT at the concentration range 0.1-2 μM for 24 h. 11β-HSD1 mRNA levels were quantified and normalized to the level of GAPDH by real-time RT-PCR analysis. (B) TMT induced 11β-HSD1 activity. Cells were treated with TMT at the concentrations range 0.5-2 μM for 24 h. 11β-HSD1 activity was determined by the conversion of cortisone to cortisol. Results were expressed as the mean ± SD of at least 3 independent experiments and significance was determined by one-way ANOVA followed by Turkey's tests, \* $p < 0.05$ , \*\* $p < 0.01$ ; \*\*\* $p < 0.005$ .

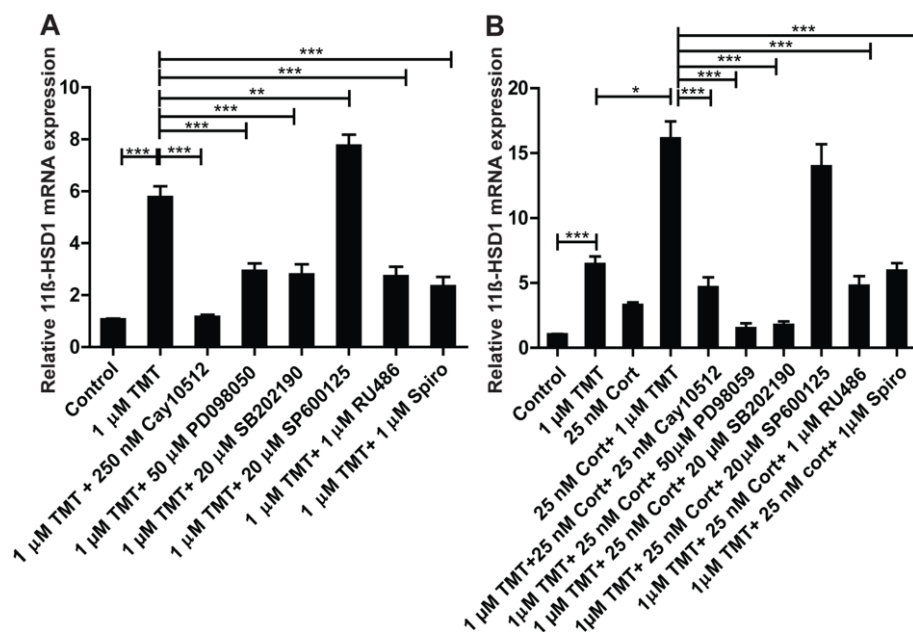


**Fig. 6.** TMT induction of 11β-HSD1 is mediated through NF-κB, ERK1/2, p38, and MR. (A) Cells were pre-treated with Cay10512 (250 nM), PD98059 (50 μM), SP600125 (50 μM), SB203580 (20 μM), RU486 (1 μM) and spironolactone (1 μM) for 1 h and then stimulated with TMT (1 μM) for 24 h. (B) Cells were pre-treated with Cay10512 (250 nM), PD98059 (50 μM), SP600125 (50 μM), SB203580 (20 μM), RU486 (1 μM) and spironolactone (1 μM) for 1 h and followed by incubation with 25 nM corticosterone 24 h and continued stimulating with 1 μM TMT for 24 h. 11β-HSD1 mRNA levels were measured by RT-PCR and were quantified and normalized to the level of GAPDH. Results were expressed as the mean ± SD of at least 3 independent experiments and significance was determined by one-way ANOVA followed by Turkey's tests, \* $p < 0.05$ , \*\* $p < 0.01$ ; \*\*\* $p < 0.005$ .

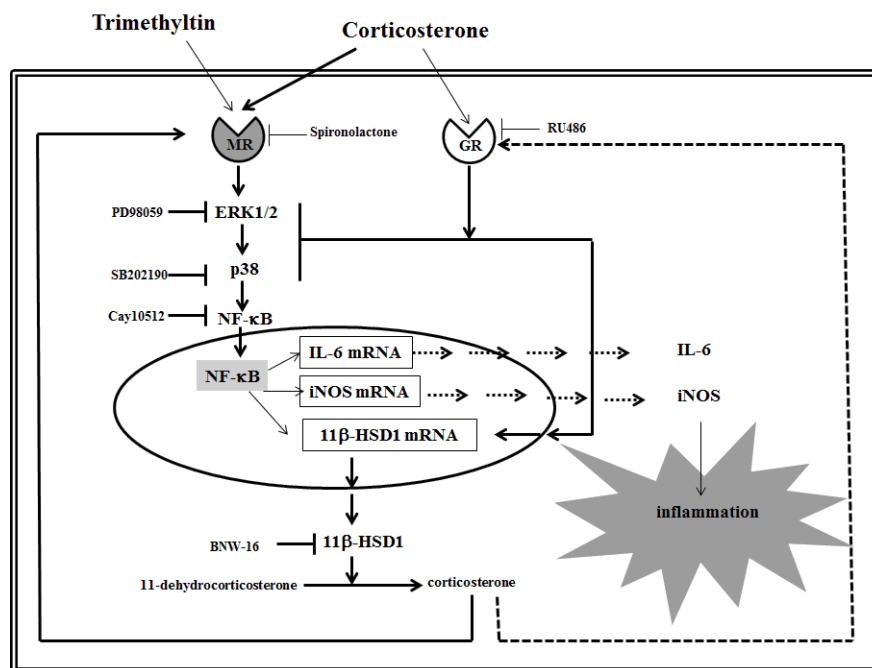


**Fig. 7** Proposed model of the inflammatory mechanism of trimethyltin (TMT) in BV-2 cells. This study suggests that TMT activates MR which activates ERK1/2, p38 MAPKs, and NF- $\kappa$ B to increase IL-6 and iNOS expression. Corticosterone potentiates the action of TMT by stimulating the same receptor, MR. TMT directly activates 11 $\beta$ -HSD1 activity. An up-regulation of 11 $\beta$ -HSD1 mRNA is also induced by TMT through MR-mediated pathway. Activation of GR by dexamethasone or high concentration of corticosterone suppresses MAPKs and inflammation but increased 11 $\beta$ -HSD1 mRNA leading to increased local concentration of corticosterone.

## CHAPTER 7

### Conclusion and outlook

Neuroinflammation is an important contribution to neurodegenerative diseases such as Alzheimer's disease (AD), Parkinson's disease (PD), and amyotrophic lateral sclerosis. Microglia activation results in an increased expression of cytokines and ultimately leads to oxidative and ER stress that cause neuronal damage and neurodegenerative diseases (4,12,100,204,205). Among the mechanisms involved our research focused on microglia activation and observe the cellular and molecular inflammatory signaling that leads to oxidative stress and ER stress. Activated microglia become highly pro-inflammatory cells through their production of cytokines, chemokines and free radicals.

Corticosteroids regulate the function of microglia through mineralocorticoid receptors (MR) and glucocorticoid receptors (GR) (41,50,52). The function of MR in microglia cells is suggested to increase microglia activity (46,50). In contrast, the GR exerts inhibitory effects (51,52). Although corticosteroids including corticosterone have a potent anti-inflammatory effects at pharmacological concentrations (31,57-59), many studies have shown that corticosterone also has a proinflammatory potential in microglia (29-31,34). Based on our observations (**Figure 2**), we propose that activation of MR results in an increased cytokine expression and release. MR activation stimulates the NF- $\kappa$ B pathway. In contrast, activation of GR inhibits NF- $\kappa$ B activity, resulting in suppression of inflammation. 11 $\beta$ -hydroxysteroid dehydrogenase 1 (11 $\beta$ -HSD1) modulates local glucocorticoid availability by converting inactive to active glucocorticoids. Corticosterone at low concentrations acts through MR to activate NF- $\kappa$ B and stimulates production of proinflammatory cytokines such as IL-6 and TNF- $\alpha$ . At high concentrations, corticosterone binds to GR to inhibit NF- $\kappa$ B and proinflammatory mediators. Pro-inflammatory cytokines, like IL-6 and TNF- $\alpha$  induce 11 $\beta$ -HSD1 expression. This leads to increased active glucocorticoid concentrations resulting in the activation of GR and suppression of NF- $\kappa$ B. Thus a precise control of the balance of MR and GR activity is essential for the resolution of inflammation.

Additional to corticosteroid receptors, microglia function is also regulated by metabotropic glutamate receptors (mGluRs), which have eight subtypes based on their signal transduction pathways and pharmacological profiles (67,69). Metabotropic glutamate receptor subtype 5 (mGluR5) mediates their signaling through G $\alpha$ q-proteins which activate PLC, leading to phosphoinositide hydrolysis and intracellular Ca<sup>2+</sup> mobilization and also activation of ERK1 and ERK2 downstream signaling pathways

(67). mGluR5 is expressed in microglia (66,70) and activation of mGluR5 inhibits microglia activation, oxidative stress, and the release of inflammatory mediators both *in vitro* and *in vivo* (71-76). The present study indicates that antagonism of mGluR5 by MPEP results in an elevation of  $[Ca^{2+}]_i$  from the ER, probably through  $IP_3$  receptor activation, leading to induction of ER stress, oxidative stress and inflammation in microglia cells (**Figure 3**). The results propose that mGluR5 has at least two independent pathways to regulate the stress and inflammatory responses. First, mGluR5 may suppress  $G_i/\alpha$  pathway resulting in a decrease in PLC activity and  $Ca^{2+}$  release from the ER. However, mGluR5 has been documented to activate the  $G_{\alpha q}$ -protein leading to activation of PLC, PKC and  $Ca^{2+}$  release (72). Therefore, it could be postulated that mGluR5 may cross-regulate  $G_i$ -couple receptors or mGluR5 has a direct modulatory effect on  $G_i$  (PTX-sensitive protein) protein so it needs further investigation. Second, mGluR5 may regulate the AMPK pathway that influences mitochondrial function. Inhibition of mGluR5 results in ATP depletion which was reversed by AMPK activation. Decreased ATP production leads to not only an increased ROS production in mitochondria and oxidative stress but also an activation of AMPK to maintain energy homeostasis. Prolonged AMPK activation can induce ER stress. We propose suggest a model of a direct effect of mGluR5 antagonism in microglia on oxidative stress, inflammation and ER stress mediated by  $Ca^{2+}$  homeostasis. In addition, AMPK is also involved in mGluR5 receptor regulation.

Chronic exposure or acute exposure of xenobiotics such as organotin compounds causes a progressive neurodegenerative disorder (194,198,206). However, the mechanisms of organotin action in microglia have not been well characterized. In the present studies, we focused on two structurally different organotins. DBT is a diorganotins found in the environment and in dietary sources (175-177,179). It has been shown to be a neurotoxicin various models (179,194-197). In the present studies, we investigated the signaling involved in DBT-induced microglia dysfunctions, including inflammatory response and oxidative stress (**Figure 4**). DBT increased cytokine expression and release such as IL-6 and TNF- $\alpha$  through NF- $\kappa$ B activation. Oxidative stress was induced by DBT, which is suggested to be mediated by NOX-2, AMPK and  $Ca^{+2}$  dysregulation. The results indicate that MAPKs may play a role in DBT-induced inflammation but it remains unclear whether DBT directly affects on MAPKs or whether it acts through PKC and PLC. PI3K/Akt pathway is suggested to be involved in DBT action on inflammation.  $Ca^{+2}$  seems to be a central regulator of DBT action because BAPTA-AM could completely block the action of DBT on inflammatory response and oxidative stress.

TMT is an organotin compound with potent neurotoxic effects characterized by neuroinflammation and microglia activation (167,169,207,208). TMT also disturbed the balance of endogenous corticosterone regulation, resulting in enhanced neurotoxicity (170-173). Although TMT neurotoxicity is generally well documented there are few studies on disturbance of endogenous corticosteroids in microglia cells. In the present studies, TMT increased inflammation with activation of iNOS and IL-6 (**Figure 5**). The activation of MR is proposed to be the target of TMT action that activates ERK1/2, p38 MAPKs, followed by NF- $\kappa$ B activation. Corticosterone binds to MR and potentiates the action of TMT on inflammation. TMT disturbs local availability of corticosterone by activation of 11 $\beta$ -HSD1 activity and expression. When the concentration of corticosterone exceeds the affinity of GR for this hormone, it leads to inhibition of MAPKs and inflammation. These results partly explain the increased severity of TMT neurotoxicity during stress.

Collectively, the present research contributes to the understanding that

1. GR and MR activity differentially regulate inflammatory response in microglia cells. Feed-forward and feedback regulation between MR and GR is adjusted by 11 $\beta$ -HSD1 to maintain cellular homeostasis.
2. Factors influencing 11 $\beta$ -HSD1 such as stress, infection, and xenobiotic compounds affect the susceptibility of microglia cell activity and neuroinflammation.
3. Metabotropic glutamate receptor 5 (mGluR5) has protective effects on microglia by modulating calcium-mediated pathways and AMPK-mediated pathways.
4. Xenobiotics such as silane, DBT and TMT activate microglia and increase inflammation by disturbing MR activity

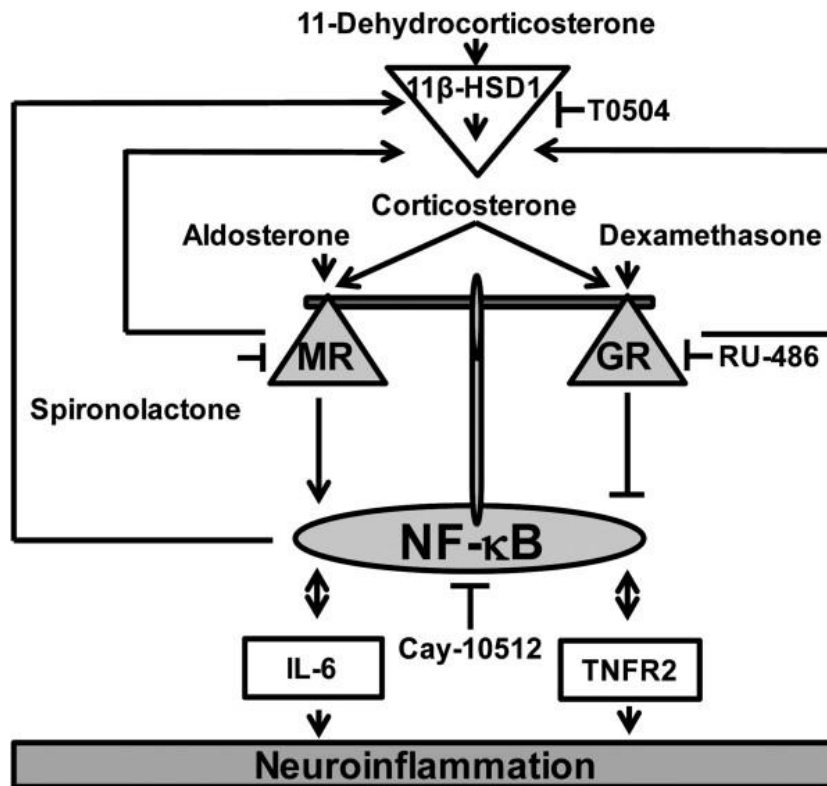


**Figure 2** : Model for the role of MR and GR in regulating neuroinflammation in BV-2 cells. This study suggests that MR promotes a neuroinflammatory response mediated through NF-κB activation, which can be blocked by activation GR. The control of local glucocorticoid availability by 11β-HSD1 is important in regulating the fine-tuning of the balance between MR and GR activity. Corticosterone binds with high affinity to MR, followed by binding to GR with lower affinity. 11β-HSD1 inhibitors (such as T0504) block the differential effects of 11-dehydrocorticosterone on MR and GR. IL-6 stimulated 11β-HSD1 expression, suggesting that IL-6 is involved in a regulatory feed-forward mechanism to adjust the local levels of active glucocorticoids and therefore the balance between MR and GR. IL-6 and TNFR2 activation both lead to the activation of NF-κB, and their own expression is upregulated upon NF-κB activation.

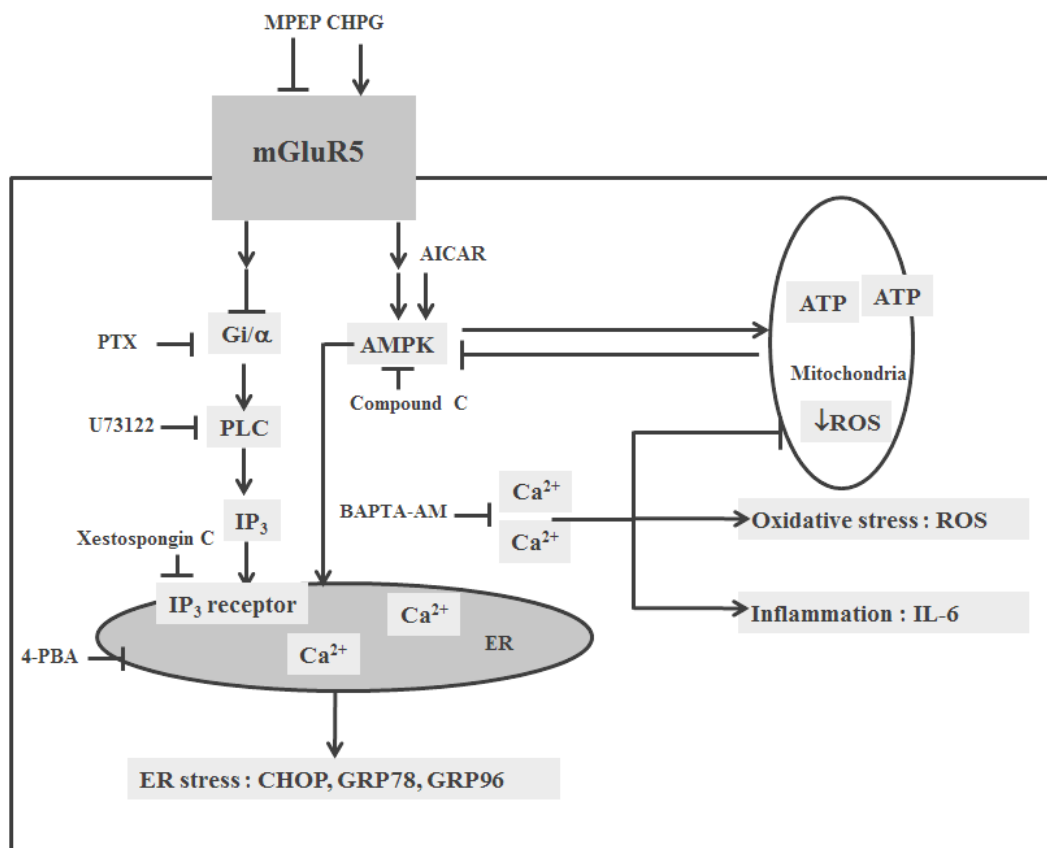


**Figure 3** : Proposed model of signaling pathway of mGluR5 regulation in BV-2 cells. Our results suggest that blockage of mGluR5 may activate PTX-sensitive G-protein (Gi-protein) leading to increased IP<sub>3</sub> through PLC activation. An increased Ca<sup>2+</sup> release from the ER induces ER stress, oxidative stress and inflammatory response of the cell. mGluR5 may also directly modulate AMPK, which contributes to the maintenance of mitochondrial functions. Disturbance of energy homeostasis induces AMPK activation and prolonged ATP depletion and elevated calcium can cause ER stress.

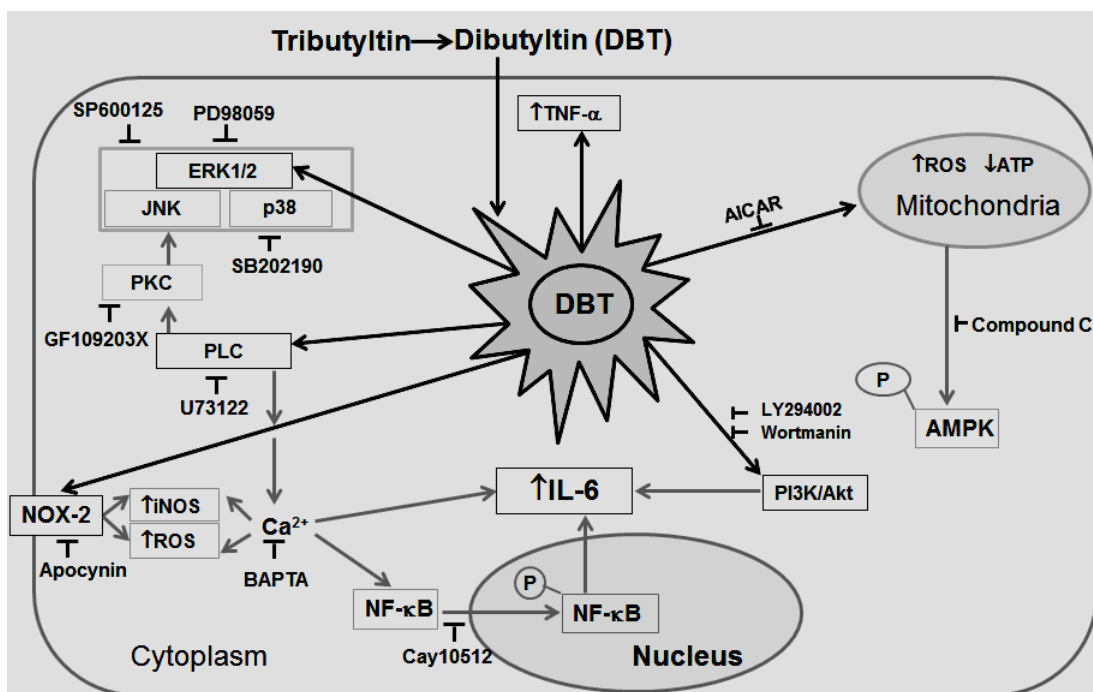


**Figure 4 :** Model of the inflammatory mechanism of dibutyltin (DBT) in BV-2 cells. This study suggests that DBT increases inflammation via activation of MAPKs, which is mediated by PLC and PKC. DBT activates NF-κB activity, leading to enhanced inflammation, which may be regulated by Ca<sup>2+</sup>. DBT induced mitochondrial dysfunction, resulting in a decrease ATP production and increased oxidative stress through AMPK pathway. An induction of oxidative stress by DBT promotes the inflammatory response involving NOX-2. The loss of calcium homeostasis is postulated to be a main target of DBT action.

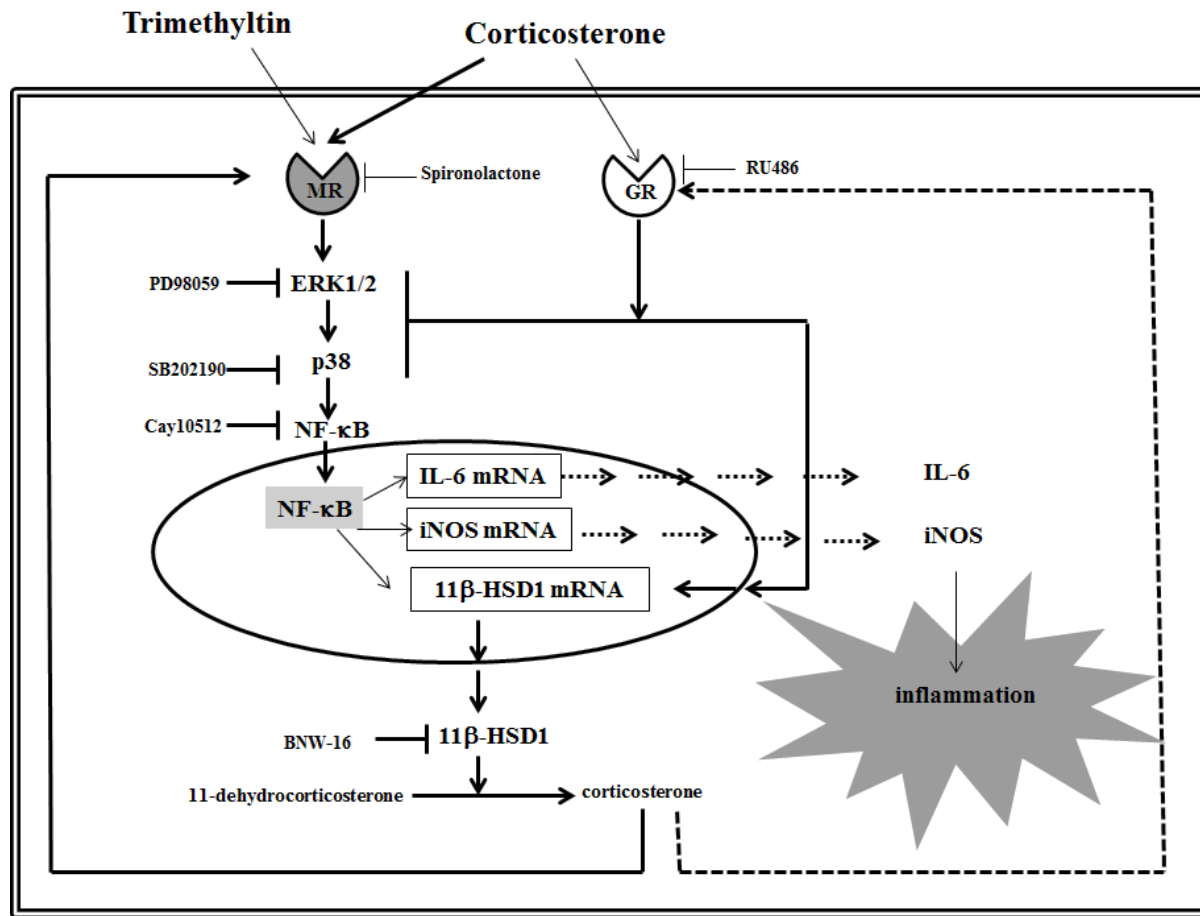


**Figure 5** : Model of the inflammatory mechanism of trimethyltin (TMT) in BV-2 cells. This study suggests that TMT activates MR that activates ERK1/2, p38 MAPKs, and NF-κB to increase IL-6 and iNOS expression. Corticosterone potentiates the action of TMT by stimulating the same receptor, MR. TMT directly activates 11β-HSD1 activity. An up-regulation of 11β-HSD1 mRNA also is induced by TMT through MR-mediated pathway. Activation of GR by dexamethasone or high concentration of corticosterone suppresses MAPKs and inflammation but increased 11β-HSD1 mRNA leading to increased local concentration of corticosterone.

## REFERENCES

1. Graeber, M. B. (2010) *Science* **330**, 783-788
2. Ransohoff, R. M., and Cardona, A. E. (2010) *Nature* **468**, 253-262
3. Tynan, R. J., Naicker, S., Hinwood, M., Nalivaiko, E., Buller, K. M., Pow, D. V., Day, T. A., and Walker, F. R. (2010) *Brain Behav Immun* **24**, 1058-1068
4. Sugama, S., Fujita, M., Hashimoto, M., and Conti, B. (2007) *Neuroscience* **146**, 1388-1399
5. Niranjana, R. (2013) *Mol Neurobiol*
6. Orre, M., Kamphuis, W., Dooves, S., Kooijman, L., Chan, E. T., Kirk, C. J., Dimayuga Smith, V., Koot, S., Mamber, C., Jansen, A. H., Ovaas, H., and Hol, E. M. (2013) *Brain* **136**, 1415-1431
7. Evans, M. C., Couch, Y., Sibson, N., and Turner, M. R. (2013) *Mol Cell Neurosci* **53**, 34-41
8. Glass, C. K., Saijo, K., Winner, B., Marchetto, M. C., and Gage, F. H. (2010) *Cell* **140**, 918-934
9. Morales, I., Farias, G., and Maccioni, R. B. (2010) *Neuroimmunomodulation* **17**, 202-204
10. Collins, L. M., Toulouse, A., Connor, T. J., and Nolan, Y. M. (2012) *Neuropharmacology* **62**, 2154-2168
11. Koziarowski, D., Tomasiuk, R., Szlufik, S., and Friedman, A. (2012) *Cytokine* **60**, 762-766
12. Rubio-Perez, J. M., and Morillas-Ruiz, J. M. (2012) *TheScientificWorldJournal* **2012**, 756357
13. Sorenson, M., Janusek, L., and Mathews, H. (2013) *Biol Res Nurs* **15**, 226-233
14. Qin, L., Liu, Y., Hong, J. S., and Crews, F. T. (2013) *Glia* **61**, 855-868
15. Ghosh, S., Wu, M. D., Shaftel, S. S., Kyrkanides, S., LaFerla, F. M., Olschowka, J. A., and O'Banion, M. K. (2013) *J Neurosci* **33**, 5053-5064
16. Smith, J. A., Das, A., Ray, S. K., and Banik, N. L. (2012) *Brain Res Bull* **87**, 10-20
17. Clark, K. H., Wiley, C. A., and Bradberry, C. W. (2013) *Neurotox Res* **23**, 174-188
18. Woodcock, T., and Morganti-Kossmann, M. C. (2013) *Front Neurol* **4**, 18
19. Khasnavis, S., Ghosh, A., Roy, A., and Pahan, K. (2013) *J Biol Chem* **288**, 20843-20855
20. Li, M., Dai, F. R., Du, X. P., Yang, Q. D., and Chen, Y. (2012) *J Mol Neurosci* **48**, 225-233
21. Brown, G. C., and Neher, J. J. (2010) *Mol Neurobiol* **41**, 242-247
22. You, S., Poulton, L., Cobbold, S., Liu, C. P., Rosenzweig, M., Ringler, D., Lee, W. H., Segovia, B., Bach, J. F., Waldmann, H., and Chatenoud, L. (2009) *PLoS One* **4**, e7848
23. Motta, A. C., Vissers, J. L., Gras, R., Van Esch, B. C., Van Oosterhout, A. J., and Nawijn, M. C. (2009) *Respiratory research* **10**, 93
24. Cuzzocrea, S., Ronchetti, S., Genovese, T., Mazzon, E., Agostini, M., Di Paola, R., Esposito, E., Muia, C., Nocentini, G., and Riccardi, C. (2007) *Faseb J* **21**, 117-129
25. Santucci, L., Agostini, M., Bruscoli, S., Mencarelli, A., Ronchetti, S., Ayroldi, E., Morelli, A., Baldoni, M., and Riccardi, C. (2007) *Gut* **56**, 52-60
26. Veroni, C., Gabriele, L., Canini, I., Castiello, L., Coccia, E., Remoli, M. E., Columba-Cabezas, S., Arico, E., Aloisi, F., and Agresti, C. (2010) *Mol Cell Neurosci* **45**, 234-244
27. Dinkel, K., MacPherson, A., and Sapolsky, R. M. (2003) *J Neurochem* **84**, 705-716
28. Munhoz, C. D., Lepsch, L. B., Kawamoto, E. M., Malta, M. B., Lima Lde, S., Avellar, M. C., Sapolsky, R. M., and Scavone, C. (2006) *J Neurosci* **26**, 3813-3820
29. Sorrells, S. F., Caso, J. R., Munhoz, C. D., and Sapolsky, R. M. (2009) *Neuron* **64**, 33-39
30. Sorrells, S. F., and Sapolsky, R. M. (2007) *Brain Behav Immun* **21**, 259-272
31. MacPherson, A., Dinkel, K., and Sapolsky, R. (2005) *Exp Neurol* **194**, 376-383
32. Franko, K. L., Forhead, A. J., and Fowden, A. L. (2010) *J Endocrinol* **204**, 319-329
33. Loram, L. C., Taylor, F. R., Strand, K. A., Frank, M. G., Sholar, P., Harrison, J. A., Maier, S. F., and Watkins, L. R. (2011) *Brain Behav Immun* **25**, 1408-1415
34. Frank, M. G., Thompson, B. M., Watkins, L. R., and Maier, S. F. (2012) *Brain Behav Immun* **26**, 337-345
35. Espinosa-Oliva, A. M., de Pablos, R. M., Villaran, R. F., Arguelles, S., Venero, J. L., Machado, A., and Cano, J. (2011) *Neurobiol Aging* **32**, 85-102
36. Vedder, H., Weiss, I., Holsboer, F., and Reul, J. M. (1993) *Brain Res* **605**, 18-24

37. Rupprecht, R., Arriza, J. L., Spengler, D., Reul, J. M., Evans, R. M., Holsboer, F., and Damm, K. (1993) *Mol Endocrinol* **7**, 597-603
38. De Kloet, E. R., Vreugdenhil, E., Oitzl, M. S., and Joels, M. (1998) *Endocr Rev* **19**, 269-301
39. Kitchener, P., Di Blasi, F., Borrelli, E., and Piazza, P. V. (2004) *Eur J Neurosci* **19**, 1837-1846
40. Sapolsky, R. M., Romero, L. M., and Munck, A. U. (2000) *Endocr Rev* **21**, 55-89
41. Sierra, A., Gottfried-Blackmore, A., Milner, T. A., McEwen, B. S., and Bulloch, K. (2008) *Glia* **56**, 659-674
42. Ahima, R., Krozowski, Z., and Harlan, R. (1991) *J Comp Neurol* **313**, 522-538
43. Cintra, A., Bhatnagar, M., Chadi, G., Tinner, B., Lindberg, J., Gustafsson, J. A., Agnati, L. F., and Fuxe, K. (1994) *Ann N Y Acad Sci* **746**, 42-61; discussion 61-43
44. Herman, J. P., Figueiredo, H., Mueller, N. K., Ulrich-Lai, Y., Ostrander, M. M., Choi, D. C., and Cullinan, W. E. (2003) *Front Neuroendocrinol* **24**, 151-180
45. Patel, P. D., Lopez, J. F., Lyons, D. M., Burke, S., Wallace, M., and Schatzberg, A. F. (2000) *J Psychiatr Res* **34**, 383-392
46. Frieler, R. A., Meng, H., Duan, S. Z., Berger, S., Schutz, G., He, Y., Xi, G., Wang, M. M., and Mortensen, R. M. (2011) *Stroke* **42**, 179-185
47. Syngle, A., Vohra, K., Khichi, D., Garg, N., Verma, I., and Kaur, L. (2013) *Clin Rheumatol* **32**, 1029-1036
48. Hansen, P. R., Rieneck, K., and Bendtzen, K. (2004) *Immunol Lett* **91**, 87-91
49. Miura, R., Nakamura, K., Miura, D., Miura, A., Hisamatsu, K., Kajiya, M., Nagase, S., Morita, H., Fukushima Kusano, K., Ohe, T., and Ishihara, K. (2006) *J Pharmacol Sci* **101**, 256-259
50. Tanaka, J., Fujita, H., Matsuda, S., Toku, K., Sakanaka, M., and Maeda, N. (1997) *Glia* **20**, 23-37
51. Nakatani, Y., Amano, T., Tsuji, M., and Takeda, H. (2012) *Life sciences* **91**, 761-770
52. Ros-Bernal, F., Hunot, S., Herrero, M. T., Parnadeau, S., Corvol, J. C., Lu, L., Alvarez-Fischer, D., Carrillo-de Sauvage, M. A., Saurini, F., Coussieu, C., Kinugawa, K., Prigent, A., Hoglinger, G., Hamon, M., Tronche, F., Hirsch, E. C., and Vyas, S. (2011) *Proceedings of the National Academy of Sciences of the United States of America* **108**, 6632-6637
53. Nguyen Dinh Cat, A., Briones, A. M., Callera, G. E., Yogi, A., He, Y., Montezano, A. C., and Touyz, R. M. (2011) *Hypertension* **58**, 479-488
54. Kiyomoto, H., Rafiq, K., Mostofa, M., and Nishiyama, A. (2008) *J Pharmacol Sci* **108**, 399-405
55. Queisser, N., Amann, K., Hey, V., Habib, S. L., and Schupp, N. (2013) *Free Radic Biol Med* **54**, 17-25
56. Chantong, B., Kratschmar, D. V., Nashev, L. G., Balazs, Z., and Odermatt, A. (2012) *J Neuroinflammation* **9**, 260
57. Sugama, S., Takenouchi, T., Kitani, H., Fujita, M., and Hashimoto, M. (2009) *Journal of Neuroimmunology* **208**, 104-114
58. Morale, M. C., Serra, P. A., Delogu, M. R., Migheli, R., Rocchitta, G., Tirolo, C., Caniglia, S., Testa, N., L'Episcopo, F., Gennuso, F., Scoto, G. M., Barden, N., Miele, E., Desole, M. S., and Marchetti, B. (2004) *Faseb J* **18**, 164-166
59. Sugama, S., Takenouchi, T., Fujita, M., Kitani, H., Conti, B., and Hashimoto, M. (2012) *Neuroscience* **232C**, 13-20
60. Hong, J., Kim, B. K., Lim, H., Lee, S., and Lee, S. J. (2012) *Immunopharmacol Immunotoxicol* **34**, 912-918
61. Ganter, S., Northoff, H., Mannel, D., and Gebicke-Harter, P. J. (1992) *J Neurosci Res* **33**, 218-230
62. Kaur, C., Wu, C. H., Wen, C. Y., and Ling, E. A. (1994) *Arch Histol Cytol* **57**, 449-459
63. Seckl, J. R. (2004) *Curr Opin Pharmacol* **4**, 597-602
64. Seckl, J. R., and Walker, B. R. (2004) *Trends Endocrinol Metab* **15**, 418-424
65. Gottfried-Blackmore, A., Sierra, A., McEwen, B. S., Ge, R., and Bulloch, K. (2010) *Glia* **58**, 1257-1266
66. Ferraguti, F., and Shigemoto, R. (2006) *Cell Tissue Res* **326**, 483-504
67. Byrnes, K. R., Loane, D. J., and Faden, A. I. (2009) *Neurotherapeutics* **6**, 94-107
68. Pajooohesh-Ganji, A., and Byrnes, K. R. (2011) *Neurotherapeutics* **8**, 195-205
69. Conn, P. J., and Pin, J. P. (1997) *Annu Rev Pharmacol Toxicol* **37**, 205-237
70. Biber, K., Laurie, D. J., Berthele, A., Sommer, B., Tolle, T. R., Gebicke-Harter, P. J., van Calker, D., and Boddeke, H. W. (1999) *J Neurochem* **72**, 1671-1680

71. Byrnes, K. R., Loane, D. J., Stoica, B. A., Zhang, J., and Faden, A. I. (2012) *J Neuroinflammation* **9**, 43
72. Byrnes, K. R., Stoica, B., Loane, D. J., Riccio, A., Davis, M. I., and Faden, A. I. (2009) *Glia* **57**, 550-560
73. Byrnes, K. R., Stoica, B., Riccio, A., Pajoohesh-Ganji, A., Loane, D. J., and Faden, A. I. (2009) *Ann Neurol* **66**, 63-74
74. Loane, D. J., Stoica, B. A., Byrnes, K. R., Jeong, W., and Faden, A. I. (2013) *J Neurotrauma* **30**, 403-412
75. Loane, D. J., Stoica, B. A., Pajoohesh-Ganji, A., Byrnes, K. R., and Faden, A. I. (2009) *J Biol Chem* **284**, 15629-15639
76. Mead, E. L., Mosley, A., Eaton, S., Dobson, L., Heales, S. J., and Pocock, J. M. (2012) *J Neurochem* **121**, 287-301
77. Piers, T. M., Heales, S. J., and Pocock, J. M. (2011) *Neurosci Lett* **505**, 140-145
78. Movsesyan, V. A., Stoica, B. A., and Faden, A. I. (2004) *J Neurochem* **89**, 1528-1536
79. Wang, J. W., Wang, H. D., Zhong, W. Z., Li, N., and Cong, Z. X. (2012) *Brain Res* **1464**, 73-81
80. Wang, J. W., Wang, H. D., Cong, Z. X., Zhang, X. S., Zhou, X. M., and Zhang, D. D. (2013) *Biochem Biophys Res Commun* **430**, 1016-1021
81. Jang, B. C., Paik, J. H., Kim, S. P., Shin, D. H., Song, D. K., Park, J. G., Suh, M. H., Park, J. W., and Suh, S. I. (2005) *Cell Signal* **17**, 625-633
82. Lee, J. Y., Jhun, B. S., Oh, Y. T., Lee, J. H., Choe, W., Baik, H. H., Ha, J., Yoon, K. S., Kim, S. S., and Kang, I. (2006) *Neurosci Lett* **396**, 1-6
83. Crews, F. T., Zou, J., and Qin, L. (2011) *Brain Behav Immun* **25 Suppl 1**, S4-S12
84. Xing, B., Xin, T., Hunter, R. L., and Bing, G. (2008) *J Neuroinflammation* **5**, 4
85. Hu, X., Zhou, H., Zhang, D., Yang, S., Qian, L., Wu, H. M., Chen, P. S., Wilson, B., Gao, H. M., Lu, R. B., and Hong, J. S. (2012) *J Neuroimmune Pharmacol* **7**, 187-201
86. Wang, Y. P., Wu, Y., Li, L. Y., Zheng, J., Liu, R. G., Zhou, J. P., Yuan, S. Y., Shang, Y., and Yao, S. L. (2011) *J Neuroinflammation* **8**, 95
87. Yang, C. M., Luo, S. F., Wang, C. C., Chiu, C. T., Chien, C. S., Lin, C. C., and Hsiao, L. D. (2000) *Br J Pharmacol* **130**, 891-899
88. Lee, C. W., Chien, C. S., and Yang, C. M. (2004) *Am J Physiol Lung Cell Mol Physiol* **286**, L921-930
89. Zhou, X., Yang, W., and Li, J. (2006) *J Biol Chem* **281**, 31337-31347
90. Li, X. Q., Cao, W., Li, T., Zeng, A. G., Hao, L. L., Zhang, X. N., and Mei, Q. B. (2009) *Int Immunopharmacol* **9**, 1032-1041
91. Yamashiro, K., Sasano, T., Tojo, K., Namekata, I., Kurokawa, J., Sawada, N., Suganami, T., Kamei, Y., Tanaka, H., Tajima, N., Utsunomiya, K., Ogawa, Y., and Furukawa, T. (2010) *Biochem Biophys Res Commun* **398**, 284-289
92. Zhou, S., Yuan, X., Liu, Q., Zhang, X., Pan, X., Zang, L., and Xu, L. (2010) *Cytokine* **52**, 210-214
93. Fukuno, N., Matsui, H., Kanda, Y., Suzuki, O., Matsumoto, K., Sasaki, K., Kobayashi, T., and Tamura, S. (2011) *Biochem Biophys Res Commun* **408**, 202-207
94. Katz, S., Boland, R., and Santillan, G. (2006) *Int J Biochem Cell Biol* **38**, 2082-2091
95. Lee, I. T., Lin, C. C., Lin, W. N., Wu, W. L., Hsiao, L. D., and Yang, C. M. (2013) *Int J Biochem Cell Biol* **45**, 1657-1668
96. Butterfield, D. A., Perluigi, M., and Sultana, R. (2006) *Eur J Pharmacol* **545**, 39-50
97. Agostinho, P., Cunha, R. A., and Oliveira, C. (2010) *Curr Pharm Des* **16**, 2766-2778
98. Kovacic, P., and Somanathan, R. (2012) *Curr Neuropharmacol* **10**, 289-302
99. Domercq, M., Vazquez-Villoldo, N., and Matute, C. (2013) *Front Cell Neurosci* **7**, 49
100. Wong, W. T. (2013) *Frontiers in cellular neuroscience* **7**, 22
101. Kettenmann, H., Hanisch, U. K., Noda, M., and Verkhratsky, A. (2011) *Physiol Rev* **91**, 461-553
102. Beraud, D., Hathaway, H. A., Trecki, J., Chasovskikh, S., Johnson, D. A., Johnson, J. A., Federoff, H. J., Shimoji, M., Mhyre, T. R., and Maguire-Zeiss, K. A. (2013) *J Neuroimmune Pharmacol* **8**, 94-117
103. Hu, S., Sheng, W. S., Schachtele, S. J., and Lokensgard, J. R. (2011) *J Neuroinflammation* **8**, 123
104. Kacimi, R., Giffard, R. G., and Yenari, M. A. (2011) *J Inflamm (Lond)* **8**, 7
105. Ibrahim, A. S., El-Remessy, A. B., Matragoon, S., Zhang, W., Patel, Y., Khan, S., Al-Gayyar, M. M., El-Shishtawy, M. M., and Liou, G. I. (2011) *Diabetes* **60**, 1122-1133
106. Peterson, L. J., and Flood, P. M. (2012) *Mediators Inflamm* **2012**, 401264

107. Filosto, M., Scarpelli, M., Cotelli, M. S., Vielmi, V., Todeschini, A., Gregorelli, V., Tonin, P., Tomelleri, G., and Padovani, A. (2011) *J Neurol* **258**, 1763-1774
108. Federico, A., Cardaioli, E., Da Pozzo, P., Formichi, P., Gallus, G. N., and Radi, E. (2012) *J Neurol Sci* **322**, 254-262
109. Hardie, D. G. (2007) *Nat Rev Mol Cell Biol* **8**, 774-785
110. Hardie, D. G. (2011) *Genes Dev* **25**, 1895-1908
111. Hardie, D. G. (2011) *Proc Nutr Soc* **70**, 92-99
112. Zhang, J., Xie, Z., Dong, Y., Wang, S., Liu, C., and Zou, M. H. (2008) *J Biol Chem* **283**, 27452-27461
113. Cardaci, S., Filomeni, G., and Ciriolo, M. R. (2012) *J Cell Sci* **125**, 2115-2125
114. Ronnett, G. V., Ramamurthy, S., Kleman, A. M., Landree, L. E., and Aja, S. (2009) *J Neurochem* **109 Suppl 1**, 17-23
115. Garcia-Gil, M., Pesi, R., Perna, S., Allegrini, S., Giannecchini, M., Camici, M., and Tozzi, M. G. (2003) *Neuroscience* **117**, 811-820
116. Kuznetsov, J. N., Leclerc, G. J., Leclerc, G. M., and Barredo, J. C. (2011) *Mol Cancer Ther* **10**, 437-447
117. Yao, J., Bi, H. E., Sheng, Y., Cheng, L. B., Wendu, R. L., Wang, C. H., Cao, G. F., and Jiang, Q. (2013) *Int J Mol Sci* **14**, 10355-10368
118. Park, L. C., Zhang, H., Sheu, K. F., Calingasan, N. Y., Kristal, B. S., Lindsay, J. G., and Gibson, G. E. (1999) *J Neurochem* **72**, 1948-1958
119. Kraft, A. D., and Harry, G. J. (2011) *International Journal of Environmental Research and Public Health* **8**, 2980-3018
120. Lassmann, H., and van Horssen, J. (2011) *FEBS Lett* **585**, 3715-3723
121. Tapia-Gonzalez, S., Garcia-Segura, L. M., Tena-Sempere, M., Frago, L. M., Castellano, J. M., Fuente-Martin, E., Garcia-Caceres, C., Argente, J., and Chowen, J. A. (2011) *J Neuroendocrinol* **23**, 365-370
122. Lu, D. Y., Tang, C. H., Chen, Y. H., and Wei, I. H. (2010) *J Cell Biochem* **110**, 697-705
123. Meares, G. P., Qin, H., Liu, Y., Holdbrooks, A. T., and Benveniste, E. N. (2013) *J Immunol* **190**, 372-380
124. Yoon, S. O., Park, D. J., Ryu, J. C., Ozer, H. G., Tep, C., Shin, Y. J., Lim, T. H., Pastorino, L., Kunwar, A. J., Walton, J. C., Nagahara, A. H., Lu, K. P., Nelson, R. J., Tuszynski, M. H., and Huang, K. (2012) *Neuron* **75**, 824-837
125. Chiang, M. C., Cheng, Y. C., Lin, K. H., and Yen, C. H. (2013) *Neuroscience* **229**, 118-129
126. Hayashi, A., Matsunaga, N., Okazaki, H., Kakimoto, K., Kimura, Y., Azuma, H., Ikeda, E., Shiba, T., Yamato, M., Yamada, K., Koyanagi, S., and Ohdo, S. (2013) *Neuromolecular Med* **15**, 238-251
127. Ng, C. H., Guan, M. S., Koh, C., Ouyang, X., Yu, F., Tan, E. K., O'Neill, S. P., Zhang, X., Chung, J., and Lim, K. L. (2012) *J Neurosci* **32**, 14311-14317
128. Ikeda, M., Tsuno, S., Sugiyama, T., Hashimoto, A., Yamoto, K., Takeuchi, K., Kishi, H., Mizuguchi, H., Kohsaka, S. I., and Yoshioka, T. (2013) *Biochim Biophys Acta*
129. Noda, M., Ifuku, M., Mori, Y., and Verkhatsky, A. (2013) *Adv Exp Med Biol* **961**, 289-294
130. Zou, J., Vetreno, R. P., and Crews, F. T. (2012) *Glia* **60**, 661-673
131. Eichhoff, G., Brawek, B., and Garaschuk, O. (2011) *Biochim Biophys Acta* **1813**, 1014-1024
132. Cuchillo-Ibanez, I., Albillos, A., Aldea, M., Arroyo, G., Fuentealba, J., and Garcia, A. G. (2002) *Ann N Y Acad Sci* **971**, 108-116
133. Brawek, B., and Garaschuk, O. (2013) *Cell Calcium* **53**, 159-169
134. Foskett, J. K., White, C., Cheung, K. H., and Mak, D. O. (2007) *Physiol Rev* **87**, 593-658
135. Sammels, E., Parys, J. B., Missiaen, L., De Smedt, H., and Bultynck, G. (2010) *Cell Calcium* **47**, 297-314
136. Hacki, J., Egger, L., Monney, L., Conus, S., Rosse, T., Fellay, I., and Borner, C. (2000) *Oncogene* **19**, 2286-2295
137. Xu, H., Xu, W., Xi, H., Ma, W., He, Z., and Ma, M. (2013) *J Plant Physiol*
138. Sano, R., and Reed, J. C. (2013) *Biochim Biophys Acta*
139. Hotamisligil, G. S. (2007) *Novartis Found Symp* **286**, 86-94; discussion 94-88, 162-163, 196-203
140. Malhotra, J. D., Miao, H., Zhang, K., Wolfson, A., Pennathur, S., Pipe, S. W., and Kaufman, R. J. (2008) *Proc Natl Acad Sci U S A* **105**, 18525-18530
141. Park, Y. J., Ko, J. W., Jang, Y., and Kwon, Y. H. (2013) *Neurochem Res* **38**, 1561-1571
142. Zhuo, X. Z., Wu, Y., Ni, Y. J., Liu, J. H., Gong, M., Wang, X. H., Wei, F., Wang, T. Z., Yuan, Z., Ma, A. Q., and Song, P. (2013) *Apoptosis* **18**, 800-810

143. W., A. J., Kim, W. H., Yeo, J., and Jung, M. H. (2010) *Mol Cells* **30**, 545-549
144. Maria, D. A., de Souza, J. G., Morais, K. L., Berra, C. M., Zampolli Hde, C., Demasi, M., Simons, S. M., de Freitas Saito, R., Chammas, R., and Chudzinski-Tavassi, A. M. (2013) *Invest New Drugs* **31**, 493-505
145. Yang, L., Sha, H., Davisson, R. L., and Qi, L. (2013) *J Biol Chem* **288**, 13631-13638
146. Rhee, S. G. (2001) *Annu Rev Biochem* **70**, 281-312
147. Ethier, M. F., and Madison, J. M. (2006) *Am J Respir Cell Mol Biol* **35**, 496-502
148. Mizuta, K., Mizuta, F., Xu, D., Masaki, E., Panettieri, R. A., Jr., and Emala, C. W. (2011) *Am J Respir Cell Mol Biol* **45**, 1232-1238
149. Sundstrom, L., Greasley, P. J., Engberg, S., Wallander, M., and Ryberg, E. (2013) *FEBS Lett*
150. Rolin, J., Al-Jaderi, Z., and Maghazachi, A. A. (2013) *Immunobiology* **218**, 875-883
151. Werry, T. D., Wilkinson, G. F., and Willars, G. B. (2003) *Biochem J* **374**, 281-296
152. Roach, T. I., Rebres, R. A., Fraser, I. D., Decamp, D. L., Lin, K. M., Sternweis, P. C., Simon, M. I., and Seaman, W. E. (2008) *J Biol Chem* **283**, 17351-17361
153. Flaherty, P., Radhakrishnan, M. L., Dinh, T., Rebres, R. A., Roach, T. I., Jordan, M. I., and Arkin, A. P. (2008) *PLoS Comput Biol* **4**, e1000185
154. de Carvalho Oliveira, R., and Santelli, R. E. (2010) *Talanta* **82**, 9-24
155. Harino, H., Fukushima, M., and Kawai, S. (2000) *Arch Environ Contam Toxicol* **39**, 13-19
156. Hu, J., Zhen, H., Wan, Y., Gao, J., An, W., An, L., Jin, F., and Jin, X. (2006) *Environ Sci Technol* **40**, 3142-3147
157. Okoro, H. K., Fatoki, O. S., Adekola, F. A., Ximba, B. J., Snyman, R. G., and Opeolu, B. (2011) *Rev Environ Contam Toxicol* **213**, 27-54
158. Graceli, J. B., Sena, G. C., Lopes, P. F., Zamprogno, G. C., da Costa, M. B., Godoi, A. F., Dos Santos, D. M., de Marchi, M. R., and Dos Santos Fernandez, M. A. (2013) *Reprod Toxicol* **36**, 40-52
159. Kotake, Y. (2012) *Biol Pharm Bull* **35**, 1876-1880
160. Mignini, F., Nasuti, C., Artico, M., Giovannetti, F., Fabrizi, C., Fumagalli, L., Iannetti, G., and Pompili, E. (2012) *Int J Immunopathol Pharmacol* **25**, 1107-1119
161. Delgado Filho, V. S., Lopes, P. F., Podratz, P. L., and Graceli, J. B. (2011) *Braz J Med Biol Res* **44**, 958-965
162. Koczyk, D., Skup, M., Zaremba, M., and Oderfeld-Nowak, B. (1996) *Acta Neurobiol Exp (Wars)* **56**, 237-241
163. Ishida, N., Akaike, M., Tsutsumi, S., Kanai, H., Masui, A., Sadamatsu, M., Kuroda, Y., Watanabe, Y., McEwen, B. S., and Kato, N. (1997) *Neuroscience* **81**, 1183-1191
164. Gui-bin, J., Qun-fang, Z., and Bin, H. (2000) *Bull Environ Contam Toxicol* **65**, 277-284
165. Tang, X., Wu, X., Dubois, A. M., Sui, G., Wu, B., Lai, G., Gong, Z., Gao, H., Liu, S., Zhong, Z., Lin, Z., Olson, J., and Ren, X. (2013) *Bulletin of environmental contamination and toxicology* **90**, 626-633
166. Little, J. P., Madeira, J. M., and Klegeris, A. (2012) *Journal of Alzheimer's disease : JAD* **30 Suppl 2**, S179-183
167. Koda, T., Kuroda, Y., and Imai, H. (2009) *Cell Mol Neurobiol* **29**, 523-531
168. Ravanan, P., Harry, G. J., Awada, R., Hoareau, L., Tallet, F., Roche, R., and Lefebvre d'Hellencourt, C. (2011) *Cytokine* **53**, 355-362
169. Qing, Y., Liang, Y., Du, Q., Fan, P., Xu, H., Xu, Y., and Shi, N. (2013) *Archives of toxicology* **87**, 1273-1285
170. Shirakawa, T., Nakano, K., Hachiya, N. S., Kato, N., and Kaneko, K. (2007) *Neuroscience Research* **59**, 117-123
171. Tsutsumi, S., Akaike, M., Arimitsu, H., Imai, H., and Kato, N. (2002) *Exp Neurol* **173**, 86-94
172. Imai, H., Kabuto, M., Takita, M., and Kato, N. (1998) *Neurotoxicology* **19**, 163-166
173. Ogita, K., Sugiyama, C., Acosta, G. B., Kuramoto, N., Shuto, M., Yoneyama, M., Nakamura, Y., Shiba, T., and Yamaguchi, T. (2012) *Neuroscience letters* **511**, 116-119
174. Shuto, M., Higuchi, K., Sugiyama, C., Yoneyama, M., Kuramoto, N., Nagashima, R., Kawada, K., and Ogita, K. (2009) *J Pharmacol Sci* **110**, 424-436
175. Nath, M. (2008) *Appl Organomet Chem* **22**, 598-612
176. Choi, M., Moon, H. B., and Choi, H. G. (2012) *Arch Environ Contam Toxicol* **62**, 333-340

177. Rastkari, N., Mesdaghinia, A., Yunesian, M., and Ahmadkhaniha, R. (2012) *Bull Environ Contam Toxicol* **88**, 74-77
178. Fent, K. (1996) *Crit Rev Toxicol* **26**, 1-117
179. Mundy, W. R., and Freudenrich, T. M. (2006) *Neurotoxicology* **27**, 71-81
180. Gipperth, L. (2009) *J Environ Manage* **90**, S86-S95
181. Takahashi, S., Mukai, H., Tanabe, S., Sakayama, K., Miyazaki, T., and Masuno, H. (1999) *Environ Pollut* **106**, 213-218
182. Appel, K. E. (2004) *Drug Metab Rev* **36**, 763-786
183. Omura, M., Shimasaki, Y., Oshima, Y., Nakayama, K., Kubo, K., Aou, S., Ogata, R., Hirata, M., and Inoue, N. (2004) *Environ Sci* **11**, 123-132
184. Kannan, K., Senthilkumar, K., and Giesy, J. P. (1999) *Environ Sci Technol* **33**, 1776-1779
185. Nielsen, J. B., and Strand, J. (2002) *Environ Res* **88**, 129-133
186. Whalen, M. M., Loganathan, B. G., and Kannan, K. (1999) *Environ Res* **81**, 108-116
187. Nakatsu, Y., Kotake, Y., Hino, A., and Ohta, S. (2008) *Toxicol Appl Pharmacol* **230**, 358-363
188. Yamada, J., Inoue, K., Furukawa, T., and Fukuda, A. (2010) *Toxicol Lett* **198**, 282-288
189. Ishihara, Y., Kawami, T., Ishida, A., and Yamazaki, T. (2012) *Neurochem Int* **60**, 782-790
190. Ueno, S., Kashimoto, T., Susa, N., Shiota, Y., Okuda, M., Mutoh, K., Hoshi, F., Watanabe, K., Tsuda, S., Kawazoe, S., Suzuki, T., and Sugiyama, M. (2003) *Toxicol Sci* **75**, 201-207
191. Jurkiewicz, M., Averill-Bates, D. A., Marion, M., and DenizEAU, F. (2004) *Biochim Biophys Acta* **1693**, 15-27
192. Tomiyama, K., Yamaguchi, A., Kuriyama, T., and Arakawa, Y. (2009) *J Immunotoxicol* **6**, 184-193
193. Koskela, A., Viluksela, M., Keinanen, M., Tuukkanen, J., and Korkalainen, M. (2012) *Toxicol Appl Pharmacol* **263**, 210-217
194. Jenkins, S. M., Ehman, K., and Barone, S., Jr. (2004) *Brain Res Dev Brain Res* **151**, 1-12
195. Eskes, C., Honegger, P., Jones-Lepp, T., Varner, K., Matthieu, J. M., and Monnet-Tschudi, F. (1999) *Toxicol In Vitro* **13**, 555-560
196. Ferreira, M., Blanco, L., Garrido, A., Vieites, J. M., and Cabado, A. G. (2013) *Journal of agricultural and food chemistry*
197. Liu, E., Du, X., Ge, R., Liang, T., Niu, Q., and Li, Q. (2013) *Food Chem Toxicol*
198. Moser, V. C., McGee, J. K., and Ehman, K. D. (2009) *Journal of toxicology and environmental health. Part A* **72**, 47-52
199. Hurt, K., Hurd-Brown, T., and Whalen, M. (2013) *J Appl Toxicol* **33**, 503-510
200. Odman-Ghazi, S. O., Abraha, A., Isom, E. T., and Whalen, M. M. (2010) *Cell Biol Toxicol* **26**, 469-479
201. Person, R. J., and Whalen, M. M. (2010) *Toxicol Mech Methods* **20**, 227-233
202. Jin, M., Kim, B. W., Koppula, S., Kim, I. S., Park, J. H., Kumar, H., and Choi, D. K. (2012) *Neurotoxicology* **33**, 147-155
203. Henn, A., Lund, S., Hedtjarn, M., Schratzenholz, A., Porzgen, P., and Leist, M. (2009) *Altex* **26**, 83-94
204. McMahon, J. M., McQuaid, S., Reynolds, R., and FitzGerald, U. F. (2012) *Mult Scler* **18**, 1437-1447
205. Kyuhou, S., Kato, N., and Gemba, H. (2006) *Neurosci Lett* **396**, 91-96
206. Martin, F., Corrigan, F. M., Donard, O. F., Kelly, J., Besson, J. A., and Horrobin, D. F. (1997) *Hum Exp Toxicol* **16**, 512-515
207. McPherson, C. A., Kraft, A. D., and Harry, G. J. (2011) *Neurotox Res* **19**, 341-352
208. Harry, G. J., Funk, J. A., Lefebvre d'Hellencourt, C., McPherson, C. A., and Aoyama, M. (2008) *Brain Res* **1194**, 8-20



## BOONRAT CHANTONG

### PERSONAL INFORMATION

**Name:** BoonratChantong

**Gender:** Female

**Nationality:** Thai

**Date of Birth:** 20<sup>th</sup> Feb, 1976

**Occupation:** Lecturer

#### **Correspondence Address:**

(1) Molecular & Systems Toxicology

Universität Basel

Pharmacenter

Klingelbergstrasse 50

CH-4056 Basel

Switzerland

**Tel:** +41 (0)61 267 15 30

**E-mail:** [boonrat.chantong@unibas.ch](mailto:boonrat.chantong@unibas.ch)

(2) Faculty of Veterinary Sciences

999 Phuttamonthon 4 Road, Salaya

Nakhon Pathom 73170

Thailand

**Tel:** +66 (0)81 684 88 82

**E-mail:** [boonrat.cha@mahidol.ac.th](mailto:boonrat.cha@mahidol.ac.th)

## **EDUCATION**

- 1998** Bachelor of Science (Pharmacy), Faculty of Pharmaceutical Sciences,  
Chulalongkorn University, Bangkok, Thailand
- 2004** Master of Science (Pharmacy), Faculty of Pharmaceutical Sciences,  
Chulalongkorn University, Bangkok, Thailand
- 2008** Start PhD program, Molecular & Systems Toxicology, Universität Basel, Basel, Switzerland

## **RESEARCH PUBLICATIONS**

1. **Chantong B**, Kampeera T, Sirimanapong W, Wongtongtair S, Hutamekalin P and Meksuriyen D. 2008. Antioxidant activity and cytotoxicity of plants commonly used in veterinary medicine. *Acta Hort. (ISHS)* 786:91-98.
2. **Chantong B**, Wongtongtair S, Nusuetrong P, Sotanaphun U, Chaichantipyuth C, Meksuriyen D. 2009. Stability of barakol under hydrolytic stress conditions and its major degradation product. *Planta Med.* 75(4):346-350.
3. Nashev LG, Vuorinen A, Praxmarer L, **Chantong B**, Cereghetti D, Winiger R., Schuster D, Odermatt A. 2012 Virtual Screening as a Strategy for the Identification of Xenobiotics Disrupting Corticosteroid Action. *PLoS ONE* 7(10):e46958
4. **Chantong B**, Kratschmar D, Lyubomir LG, Zoltan B, Odermatt A. 2012 Mineralocorticoid and glucocorticoid receptors differentially regulate NF-kappaB activity and pro-inflammatory cytokine production in murine BV-2 microglial cells. *J. Neuroinflammation* 9:260